MASS TRANSFER IN HAEMOPERFUSION COLUMNS AND OTHER SORBENT-BASED DEVICES FOR BLOOD DETOXIFICATION

A thesis submitted to the University of Strathclyde in part fulfilment of requirements for the degree

of

Doctor of Philosophy

DAVID F. RADCLIFFE, B.E., M. Eng. Sc.

Bioengineering Unit
University of Strathclyde
Wolfson Centre
106 Rottenrow
Glasgow G4 ONW

June, 1978

ABSTRACT

Haemoperfusion columns and other devices containing sorbents, such as activated carbon and polymeric resins, have been developed over the last decade for removing toxic substances from the blood. The design of these perfusion devices has been largely empirical. This thesis investigates the controlling mass transfer processes in perfusion devices (in particular on haemoperfusion columns), thereby facilitating the rational design and evaluation of such devices.

A lumped parameter model of a packed bed, haemoperfusion column was developed, based on a mixing cell description of the column hydrodynamics. It incorporates intraparticle diffusion (described by a quadratic driving force equation), a nonlinear sorption isotherm and a finite external diffusion resistance. The model was validated using in vitro data from two types of perfusion column containing activated carbon and simulations based on parameter values estimated in independent stirred batch experiments. Two sorbates (sodium salicylate and sodium phenobarbitone) and a variety of flow rates and inlet concentrations were used in the validation experiments. The model was simulated using the CSMP package.

Simulations of the validated model were used to investigate the contribution of each of the basic parameters to the performance of a perfusion column. These simulations were complemented by in vitro data. The fundamental mass transfer process in a haemoperfusion column is dialytic. Hence the concept of the equivalent haemodialyser (i.e. the haemodialyser with the same number of mass transfer units as the particular haemoperfusion column) is introduced for the interpretation of haemoperfusion column performance.

Mass transfer in other blood detoxification devices which incorporate sorbents (e.g. haemodialysers with dialysate regeneration or sorbent augmented dialysate) were investigated briefly. In general, the sorbent does not radically alter the performance of the basic device; rather it complements this performance by simplifying the mode of operation of the device.

ACKNOWLEDGMENTS

I wish to thank the following for their various contributions to this thesis.

My Supervisor, Dr. John Gaylor, for the patience he has shown during the often turbulent passage of my endeavours over the past three years and for the helpful advice and suggestions he offered regarding my thesis. Professor Robert Kenedi for his support and active encouragement and for the facilities provided by the Bio--engineering Unit, and Professor John Paul for handling of the academic and administrative problems that arose. The University of Strathclyde for the Open Studentship which supported me during my studies.

Mr. J. Fennimore of Smith and Nephew Research Limited for donating 12 Haemocol haemoperfusion columns and samples of activated carbon. The Scottish Universities Research Reactor Centre for providing the facilities for the hydrodynamics experiments and Thien How for his assistance in performing these experiments.

My wife, Vicki, for typing this manuscript, for her financial support, and, most especially, for having the patience of Job. Our parents for encouraging us to leave the antipodes and to see how the 'other half' lives, and for their moral support from afar.

All the students and staff of the Bioengineering Unit who have helped me. In particular, Bill Greer, for stimulating exchanges on modelling, simulation and computing; also my other colleagues from the M.Sc. course and in the Artificial Organs Division, Mario D'Angelo, Jack Ferguson, Sue Gerrard, Terry Hanson, Thien How, Dave McClure, Chris McLeod, Roshan Maini, Bobby Naismith, Pete Sharrock and Liz Smith, who supported Vicki and myself and assisted the work in many ways.

TABLE OF CONTENTS

INTRODUCTION

There are several clinical conditions in which toxic substances need to be removed rapidly from the body, i.e. acute poisoning, acute and chronic kidney (renal) failure and acute liver (hepatic) failure. The techniques devised to fulfil this need fall into three categories- (a) those that increase natural excretion or detoxification of the toxin, (b) those that remove the toxin from the body via the gastro-intestinal (GI) tract and (c) those that remove the toxin via the blood using an extracorporeal detoxification circuit. This thesis is concerned with the last type of therapy; in particular with quantitative aspects of mass transfer in extracorporeal devices that employ sorbents. For convenience, these sorbent-based, blood detoxification devices are termed perfusion devices throughout this thesis.

The first extracorporeal detoxification devices, haemodialysers, utilized a membrane separation technique, dialysis to remove toxins from the blood. The haemodialyser or 'artificial kidney' remains the single most important detoxification device, providing the theraputic mainstay for chronic renal failure. In recent years 'artificial kidneys' based on a second membrane technique, ultrafiltration, have had limited clinical success.

The first clinical trials of perfusion devices were conducted by Yatzidis and colleagues in 1964, using haemoperfusion columns to treat patients with chronic renal failure. The most intense period of development, however, did not occur until the late 1960's and early 1970's, culminating in 1973 with the first commercially available devices; the Haemocol haemoperfusion column and the Redy, dialysate regeneration system. Wide--spread use of these and subsequent commercial devices is only just beginning.

Despite the upsurge in interest in perfusion devices over the past decade, the literature contains scant informed discussion on the mass

transfer processes involved. Statements on the role of the sorbent in the device are often imprecise or in some cases completely incorrect. If perfusion devices are to be rationally compared to one another, and to other detoxification systems such as haemodialysers, it is essential that the controlling mass transfer processes be thoroughly delineated and understood.

The principal aim of the thesis is to improve our understanding of the mass transfer processes controlling perfusion devices, with particular emphasis on haemoperfusion columns. As a preliminary step towards this aim Chapter 1 reviews the wide variety of perfusion devices currently in use or under development. Devices are grouped according to the way in which the sorbent is utilized. The review includes an outline of the three areas of clinical application of perfusion devices with respect to the toxins, the problems and the alternative therapies. Chapter 2 outlines methods of expressing the mass transfer performance of extracorporeal detoxification devices in general, and perfusion devices in particular. Previous studies of the performance of perfusion devices, all of which failed to elucidate the controlling mass transfer processes, are also reviewed. These two chapters culminate in the development of a rational methodology (Section 2.5) for the achievement of the thesis aim. The work in subsequent chapters stems directly from the detailed objectives outlined in the thesis methodology.

CHAPTER 1

PERFUSION DEVICES AND THERAPUTIC MEDICINE

CHAPTER 1

PERFUSION DEVICES AND THERAPUTIC MEDICINE

Perfusion devices and their clinical applications are reviewed in this chapter.

1.1 Introduction

Sorption involves contacting a free fluid phase with a rigid and durable particulate phase (the sorbent) which has the property of selectively taking up and storing one or more solute species(the sorbate) originally contained in the fluid. (Perry et al., 1973). Two types of sorbent have been incorporated into blood detoxification devices; i.e. adsorbents and ion exchange resins. Adsorbents utilize two different types of sorption mechanism, physical adsorption and chemisorption. Weak electrostatic (van der Waal) forces bind the sorbate in physical adsorption whereas stronger chemical forces (covalent bonds) bind the sorbate in chemisorption. A range of binding strengths exist between these extremes. Ion exchange, as the name implies, involves ionic binding forces; sorbate ions displace existing ions, of like charge, from exchange sites on the sorbent resin. Adsorbents have a limited capacity to act as ion exchangers and visa versa. Most perfusion devices employ adsorbents such as activated carbon and uncharged macroreticular resins.

Perfusion devices can be classified into two groups on the basis of how they operate rather than the type of sorbent employed: i.e. Haemoperfusion Devices (Section 1.2) and Dialysate and Ultrafiltrate Perfusion Devices (Section 1.3). In the former, blood is perfused directly over the sorbent to remove the toxin. In the latter, the toxin is first transferred by a membrane separation process to an intermediate fluid (e.g. dialysate). This intermediate fluid is then perfused over the sorbent to remove the toxin. In both cases the sorbent acts as a storage element in the device while the various mass transfer processes control the rate of removal.

Perfusion devices, in common with other extracorporeal detoxification

systems, have had a range of clinical applications, i.e. in acute poisoning, acute hepatic failure and chronic renal failure. Each of these applications in turn involves a wide variety of 'possible' toxins. Uncertainty exists regarding the identity and action of some of the 'possible' toxins. This uncertainty together with the sheer variety of toxins requires blood detoxification therapies to be relatively non-specific, i.e. to remove toxins over a broad molecular weight spectrum. Consequently, the emphasis throughout is on perfusion devices employing non-specific sorbents e.g. activated carbon and uncharged polymeric resins. Those employing more specific sorbents such as ion exchange resins are only discussed briefly.

The variety of 'possible' toxins and role of perfusion devices relative to other theraputic techniques is reviewed in Section 1.4 with respect to the three clinical applications mentioned above.

1.2 Haemoperfusion Columns

The most widespread application of sorbents in extracorporeal systems has been that of haemoperfusion.

Haemoperfusion is a detoxification process whereby a patient's blood is perfused continuously through a cartridge containing sorbents. The blood leaves the body from an artery in the forearm (or leg), passes through a small bore plastic tube (a blood line) to the sorbent cartridge and returns via another blood line to the corresponding vein in the forearm (or leg). Flow through the circuit is usually maintained by a peristaltic, blood pump. Typical flow rates are 200 to 300 ml/min. The pressure drop across some devices is such that a pump is not always essential. Heparin is administered before and during therapy to avoid clotting in the extracorporeal circuit. Any small clots or air bubbles that should form in the circuit are collected in the bubble trap and filter inserted in the venous blood line. (Figure 1.2.1).

The vast majority of haemoperfusion columns employ activated carbon as the sorbent although a few contain uncharged resins, and even fewer, ion exchange resins. Not all the columns mentioned in the literature have had clinical trials. Those that have can be grouped according to their commercial availability. Tables 1.2.1 and Table 1.2.2 list the physical features of the non-commercial and commercial columns respectively. (The rationale for the membrane coating, as listed in these tables, is discussed in Section 1.2.2.)

The commercial and non-commercial columns are not entirely unrelated. For example, the resin system used by Rosenbaum was the prototype for the DX-60 column and the Strathclyde column(s) was involved in development of the Adsorba 300C. The King's College Hospital column used coated carbon supplied by Smith and Nephew - the same type as in the Haemocol column.

1.2.1 Column construction

Most haemoperfusion columns consist of a packed bed of sorbent

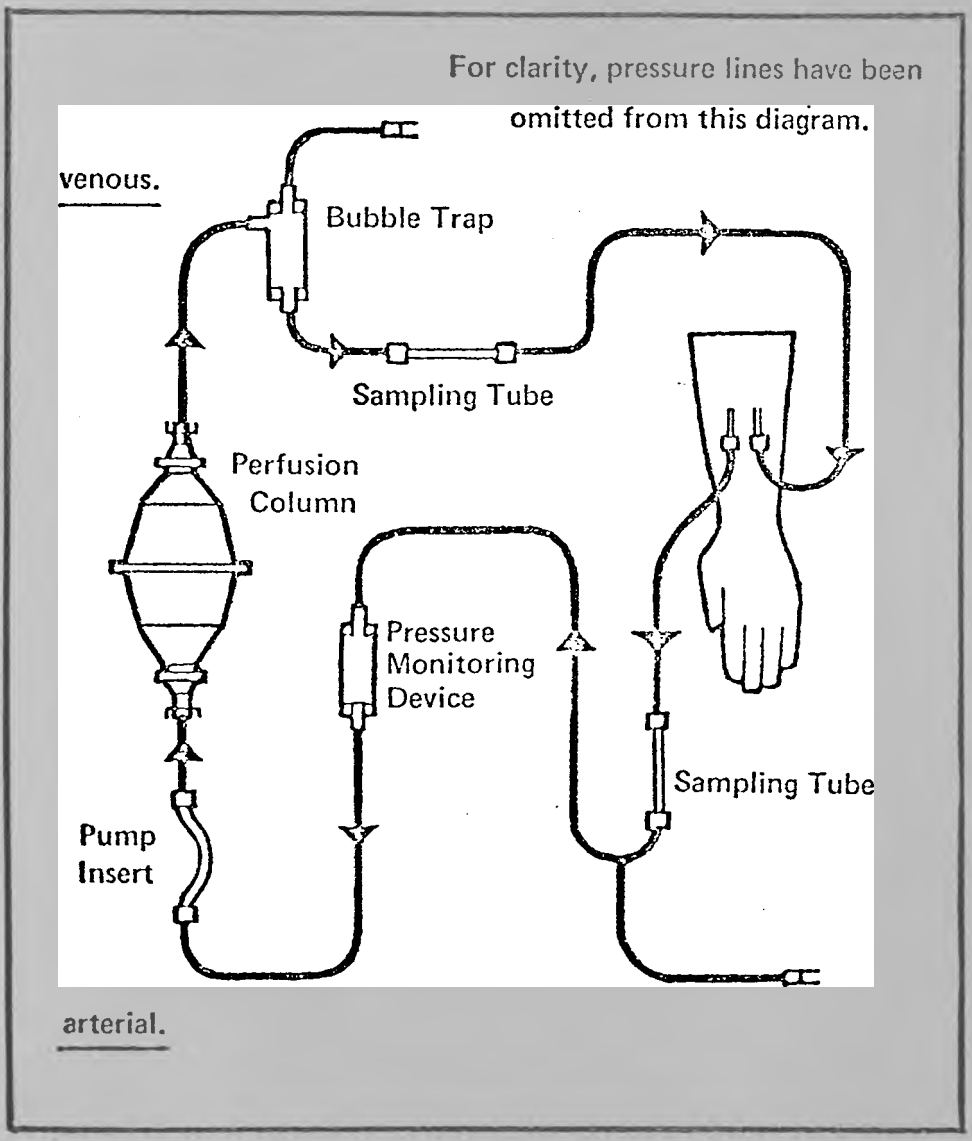

Figure 1.2.1 Extracorporeal Haemoperfusion Circuit (after Haemocol Brochure)

Author/ Institute	Sorbent		Membrane Coating	Weight of Sorbent	Reference
	Type	Size			
Yatzidis	Merck N 9624 a.c.	Granules 0.5 - 0.75mm	none/ cellulose acetate	200 gm	Yatzidis et al. (1965) Yatzidis et al.(1976)
Chang	Fisher a.c.	Granules 6/14 mesh 1.4 - 3.3 mm	none/ collodion plus albumin or heparin	300 gm	Chang et al. (1977)
Strathclyde	Norit Clydesdale RBX a.c.	Extruded Pellets 1mm ϕ x 2.5mm	acrylic copolymer 0.25% - 1% w/w	100 gm to 400 gm	Edwards (1975) Martin et al. (1977)
Kings' College Hospital	Sutcliffe & Speakman a.c.	Granules 6/10 mesh 2. - 3.3 mm	acrylic hydrogel 4% w/w	200 gm	Gazzard et al. (1974)
Amano	a.c.	Spherical Beads 0.3 - 0.4 mm	collodion 0.5μ thick	150 gm	Amano et al. (1976)
Rosenbaum	Amberlite XAD2, XAD 4 & XAD 7 resin	Spherical Beads	none	312 gm 650 gm net	Rosenbaum (1975) Rosenbaum et al. (1977)

* a.c. - Activated carbon

Table 1.2.1 Non-Commercial Haemoperfusion Columns

Name and Supplier	Sorbent		Membrane Coating	Weight of Sorbent	Reference (s)
	Type	Size			
Haemocol (Smith and Nephew)	Sutcliffe & Speakman 610 a.c.	Granules 6/10 mesh (1.65 -3.3mm)	acrylic hydrogel 2% w/w	300 gm	Brochure Fennimore et al. (1974)
Adsorba 300C (ab Gambro)	Norit Clydesdale RBX a.c.	Extruded Pellets 1.0 mm ϕ x 2.5 long	cellulose acetate 3 - 5 μ thick	300 gm	Brochure Thysell et al. (1975)
Haemodetoxifier (Becton & Dickenson)	a.c.	Granules 20/50 mesh (0.3 - 0.8 mm)	none granules immobilized by polyester sheet	95 gm	Brochure Hill et al. (1977)
DX-60 (Extracorporeal Inc.)	Amberlite XAD-4 Uncharged resin	Spherical Beads 20/50 mesh (0.3 - 0.8mm)	none	310 gm (dry)	Brochure Rosenbaum (1975)
Detoxyl-1 (Sorin Biomedica)	Del Monogo K 400 L a.c.	Granules 16/30 mesh (0.58-1.19 mm)	cellulose acetate	80 $\pm$ 5 gm	Brochure Denti et al. (1975)

* a.c. - Activated Carbon

Table 1.2.2 Commercial Haemoperfusion Columns

granules encased in a rigid plastic housing. Prior to column assembly the granules are thoroughly washed to remove dust and water soluble debris. In the case of activated carbon, the granules are then coated with a semipermeable membrane. (Section 1.2.2.) The column is assembled and primed with isotonic saline, such that the air in both the inter-particle and intra-particle voids is expelled and replaced with fluid. Fine mesh plates at both ends of the bed retain the granules within the cartridge. Gross movement of the particles is impossible although local attrition can occur. The column is sterilized prior to clinical use. In the Haemocol, the membrane coating softens during steam sterilization, allowing adjacent granules to adhere and thereby reduces granule attrition (Fennimore and Munro, 1975).

The majority of columns are cylindrical, with a length to diameter ratio of 3 to 5. The Adsorba 300C, the DX-60 and the Detoxyl-1 (Table 1.2.2.) and columns developed at the University of Strathclyde, King's College Hospital and by Rosenbaum (Table 1.2.1) are typical examples. There are exceptions however. Chang (1966-1977) has consistently employed a 'stout' cylinder; length to diameter ratio less than one while Yatzidis et al. (1965) used a cylinder with tapered ends. Another example is the Haemocol (Table 1.2.2) which is biconical, i.e. widest at the middle, with a double taper towards each end. (See Figure1.2.1).

Several haemoperfusion columns differ from the packed bed design. For example, the Becton and Dickinson Haemodetoxifier (Table 1.2.2) consists of a 'fixed' bed. Uncoated activated carbon granules are attached to one side of a polyester strip. The strip is wound in a tight spiral coil around a central spool and the coil encased in a cylindrical housing. Blood enters at one end of the housing and passes along the channels between the successive turns of the coil, and exits at the other end.

The Film Adsorber (van Zutphen, 1975) has certain similarities with the B & D cartridge. Uncoated activated carbon with a small particle size (0.4 mm diameter) is cast into a thin collodion film (0.150 mm thick).

Glass beads (0.2 to 0.225 mm diameter) are placed in the film while it is still liquid. When dry, the film is wound into a spiral, around a central spool with the beads acting as spacers. This coil is placed in a cylindrical housing. The blood passes through the 0.05 mm channels between successive turns of the film. To date no clinical trials have been reported.

A third haemoperfusion column not based on a packed bed of sorbents is that developed at the Southern Research Institute (Davis et al., 1974 and 1977). Powdered activated carbon is cast into a polymeric filament which is cross-wound onto a central mandrel. Blood enters down the perforated central core of the coil, passes radially through the coil and is collected in grooves in the outer casing. Preclinical trials have been conducted and the in vitro performance has been reported by Holland et al. (1977).

A comparable perfusion device has been developed by Malchesky et al. (1976 and 1977). Small sorbent particles are placed inside hollow fibres made of Cuprophan. These fibres are similar to conventional hollow fibres employed in some haemodialysers. Unlike a conventional hollow dialyser however, the blood passes over the outside of the fibres. The fibres are 300 to 330 μM outside diameter and 200 μM inside diameter. The wall of the fibre has two distinct sections, a thin inner wall (adjacent to the sorbent) which consists of Cuprophan membrane and a thicker, outer layer which is an open Cuprophan matrix. These sorbent fibres have been incorporated in prototype devices with conventional dialysis and ultrafiltration hollow fibres with dialysate or ultrafiltrate passing through the lumen of the hollow fibres.

1.2.2 Micro-emboli and blood compatibility

A major problem encountered in the early attempts to haemo-perfuse with activated carbon was the formation of carbon emboli. These minute particles of carbon were generated by attrition between granules of carbon. Hagstam et al. (1966) showed that these micro-emboli accumulated in the lungs, spleen, liver and kidneys.

Perfusion also produced drops in the number of platelets circulating through the extracorporeal circuit (Yatzidis, 1964; Dunea and Kolff, 1965 and De Myttenaere, 1967). (Platelets or thrombocytes are cellular elements essential to coagulation and clotting in blood.)

To reduce these two effects the activated carbon granules were encapsulated with biocompatible, semipermeable membranes. The membranes allow toxins to pass into the carbon while preventing direct granular attrition and emboli generation. The membranes are also more blood compatible than the carbon and thereby reduce the platelet drop.

Yatzidis et al. (1966) applied a cellulose acetate coating and could not detect carbon emboli when a column of granules was rinsed with saline. However, with a similar coating, Rosenbaum et al. (1968) found that significant carbon emboli and platelet drops still occurred in vivo. A thorough study of coating has been carried out by Chang (1966-1977). Five different materials were tried- nylon, cellulose acetate, collodion (cellulose nitrate), heparin complexed collodion and albumin complexed collodion. A summary of results (Chang, 1977) shows that both uncoated and collodion coated carbon caused 50 to 60% platelet drops and albumin-collodion coating 10-20% drops while heparin-collodion coating produced no significant drops (in dogs). The albumin-collodion coating was chosen for clinical use, as a compromise between bio--compatibility and membrane permeability. Carbon emboli were eliminated by all five coating systems. Andrade et al. (1972) experimented with three types of coating (in sheep) : albumin, Hydron (hydrogel) and Poly-HEMA (polyhydroxyethylmethacrylate). Provided the carbon was properly washed prior to coating, no emboli were detected. Platelet drops were : uncoated, 50- 70%; albumin coated, 20-50%; poly-HEMA and Hydron coated, 20% or less.

From these and other investigations it appears that all haemo--perfusion systems can produce significant platelet drops - up to 50% for coated carbon and from 30 to 80% for uncoated carbon. Uncoated resins have drops

of 40 to 80% (Winchester, 1977 and Hill et al., 1977). Tremendous variations can occur from subject to subject (Winchester, 1977).

The significance of platelet drops, per se, an an indicator of blood compatibility has been questioned recently. (De Jong et al., 1975 and 1977 and Lindsay, R.M., 1977). In fact, the whole question of blood compatibility, with respect to extracorporeal circuits, is presently in a state of flux. (Kenedi et al., 1977). This position will prevail until the clinical significance and pathogenesis of specific blood/device reactions are elucidated. The non-specific nature of terms such a biocompatibility and blood compatibility is one major obstacle. The wide range of clinical applications of extracorporeal circuits is another. In some applications, e.g. acute poisoning cases, adverse blood reactions are secondary to the theraputic benefits whereas in others, e.g. acute hepatic coma, platelet drops and hypotension are still considered to be significant problems (Langley, P.G. et al., 1977 and Hughes, R.D. et al., 1977).

1.3 Dialysate and Ultrafiltrate Perfusion Devices

In dialysate perfusion, the toxin is first transferred from the patient's blood to the dialysate via a haemodialyser. It is then removed by perfusion of the dialysate over a sorbent.

A haemodialyser utilizes the membrane separation process, dialysis. Thus solutes (toxins) in the blood are transferred across a semipermeable membrane into a dialysate solution at rates proportional to their respective concentration gradients between the two fluids. The membrane, usually cellulosic in origin, acts as a sieve with a molecular weight cut off in the region of 5000 A. Blood formed elements and proteins are therefore prevented from entering the dialysate phase. The dialysate consists of isotonic saline plus certain blood electrolytes and organic solutes. Ions and organic molecules of the type added to the dialysate are not transferred thus preventing loss of these 'essential' solutes. A secondary mass transfer process, ultrafiltration, operates in haemodialysers. Hydrostatic and osmotic pressure differential across the semipermeable membrane cause fluid to pass from the blood to the dialysate. This flux brings with it toxins dissolved in the fluid. The haemodialyser is attached to the patient in a similar manner to that in haemoperfusion. In addition, however, a complex and cumber-
-some dialysate supply and control system must be provided.

Haemodialysis is, of course, a blood detoxification technique in its own right. The addition of dialysate perfusion merely simplifies the dialysate supply system by reducing the volume of dialysate and in some cases improves the dialyser performance.

Ultrafiltrate perfusion is closely related to dialysate perfusion. Large volumes of plasma water are separated from the blood through an ultra-
-filter. The ultrafiltrate containing dissolved toxins (in the same concentrations as in the blood) is passed over a sorbent, 'cleansed' and then returned to the blood. An ultrafilter (a haemodiafilter) is physically similar to a haemodialyser, except that the membrane is more porous and there is no dialysate. By applying

a pressure gradient across the ultrafiltration membrane, the ultrafiltrate is transferred into what would be the dialysate path. Ultrafiltration has been used clinically without the sorbent perfusion stage. The ultrafiltrate is, in this case, discarded and a similar volume of sterile, isotonic (toxin free) saline returned, in its place, to the patient.

1.3.1 Dialysate perfusion devices

Several methods of dialysate perfusion have been reported. They are characterized by the method of incorporating the sorbent into the system. i.e. dialysate regeneration, sorbent/dialysate slurry, hollow fibre containment and the integral sorbent membrane. The first two techniques are the only ones to have been applied clinically.

Dialysate regeneration. In dialysate regeneration a small volume of dialysate is recirculated through the dialyser via a packed bed containing suitable sorbents. As a dialysate regeneration cartridge is not in the blood circuit there are fewer restrictions on its design and construction. Firstly emboli are not a potential problem, so no coating or immobilization is required. Smaller granules can be used as high pressure drops and flow rates can be tolerated. Air bubble formation in the bed would only reduce performance and not directly threaten the patient. There are two commercially available regeneration cartridges; the Redy and the Takeda TM101. The Redy cartridge contains three sorbents (activated carbon; hydrated zirconium oxide and sodium zirconium phosphate) and one enzyme (urease), specifically developed for the removal of suspected toxins and for control of blood electrolytes in chronic renal failure. (Stevens, 1974). Its purpose was to reduce the volume of dialysate required per treatment from 300 or 400 litres down to just 5 litres. (Gordon et al., 1969). This simplifies the dialysis procedure particularly for mobile or home applications. (Mitchell, 1975). The Takeda cartridge contains only activated carbon and alumina. (Maeda et al., 1973). Like the Redy it was developed for use in chronic renal failure, but operating on 30 litres of dialysate it is less compact. More recently, the Takeda cartridge has been used clinically with only 10 litres of dialysate (Maeda et al., 1974 and

Saito, 1975).

Other, non commercial, regeneration systems have been evaluated clinically. Petrella et al. (1974) reported a cartridge similar to the Redy; the principal difference being the choice of urea sorbent. Whereas the Redy converts urea to ammonia ions by enzymatic action and then removes these by ion exchange, Petrella's system uses oxystarch to adsorb the urea directly. Denti and Biagini (1977) designed a cartridge based on activated carbon alone, with a 50 litre dialysate volume. The ultimate application of dialysate regeneration is for the Wearable Artificial Kidney (WAK). (Stephen et al., 1975). If a compact urea sorbent is produced it is expected that the WAK will operate on 0.5 litres of dialysate. Pending a suitable urea sorbent, 20 litres of dialysate must be used for two thirds of the treatment time (Walker et al., 1974).

Sorbent augmented dialysate. In an attempt to improve the mass transfer of protein bound and lipid soluble toxins in dialysers, sorbents have been added to conventional aqueous dialysate. Following the early work of Twiss and Paulsen (1966) and Kolobow and Dedrick (1966) some interest has been shown in replacing the dialysate by activated carbon slurries. Decker et al. (1971) studied barbiturate removal in vitro and more recently Merino et al. (1977) treated acute hepatic coma induced in dogs using activated carbon slurries. Other 'sorbents' have been slurried with, or used in place of, conventional dialysate.

Lipids (cottonseed and olive oil) have been used in place of aqueous dialysate for the removal of highly lipid soluble toxins such as gluthethimide by both haemo- and peritoneal dialysis. (Shinaberger et al., 1965 and von Hartitzsch et al., 1973). Human serum albumin and tromethamine (THAM) have been added to dialysate for peritoneal dialysis. (Winchester et al., 1977). (In peritoneal dialysis the membrane that encases the gut, the peritoneum, replaces the semi--permeable membrane of the haemodialyser. Sterile, isotonic dialysate is infused into the gut cavity. Toxins pass from the many blood vessels in the gut across the peritoneum and into the dialysate. Fresh dialysate is regularly infused into the gut to replace the 'spent' dialysate.)

Integral sorbent/membrane. Sorbents have been incorporated into conventional haemodialysers by casting powdered sorbent into the membrane, i.e. an integral sorbent membrane. Two forms of dialysis membrane have been modified in this way. Malchesky et al. (1977) tested a conventional Cuprophan hollow fibre in which the outer, matrix of the fibre wall was impregnated with sorbents (activated carbon and aluminum oxide). Unlike a conventional hollow fibre dialyser however, the blood passes over the outside of the fibre and dialysate and/or ultrafiltrate passes along the lumen. They also experimented with a conventional, tubular Cuprophan membrane, of the type used in coil dialysers. The membrane has a structure similar to that of a hollow fibre i.e. a thin, inner layer of Cuprophan membrane with a spongy, outer matrix in which the sorbent is impregnated. The integral sorbent/membrane is wound into a coil dialyser with blood passing through the lumen and dialysate perfusing over the outside in the conventional manner. The haemocarbodialyser developed by Denti et al. (1977) has a similar design.

1.3.2 Ultrafiltrate perfusion systems

Ultrafiltrate perfusion systems can be classified according to the degree of porosity of the ultrafilter membrane; in particular whether it passes or retains plasma proteins.

Membranes that retain proteins have been used for haemodiafiltration since 1967 (Henderson et al., 1967). Interest has been developing in the use of sorbents to purify the ultrafiltrate so that it may be returned to the body. (Henderson, 1977 and Franz, 1977). This overcomes the need to infuse large volumes of sterile saline into the patient, thereby greatly simplifying haemodialfiltration.

Two ultrafilters are being developed that can pass all molecules up to and including proteins, i.e. plasma filtration. Formed blood elements such as platelets and blood cells are retained on the blood side. Maini (1975) and Maini et al. (1977) fitted a conventional flat bed haemodialyser with a high porosity membrane. Dialysate composed of banked human plasma is recirculated through a column, containing activated carbon and ion exchange

resins, and back to the dialyser. A flow diagram is shown in Figure 7.3.1. Toxins pass into the dialysate by means of both ultrafiltration and dialysis. (i.e. convective and diffusive transport). The toxins are removed by the sorbents and the remainder of the ultrafiltrate is withdrawn from the recirculating dialysate and returned to the blood entering the dialyser. The ultrafiltration rate is equal to the flow in the ultrafiltrate feedback loop. To date it has only been tested in vitro .

Nose et al. (1975; 1977) employed a macroporous membrane with a completely different design. The sorbent was sandwiched between two layers of porous membrane and blood was passed along the upper layer of membrane (See Figure 7.3.1). Plasma filters across this membrane, perfuses through the sorbent and out through the lower membrane. This purified plasma is collected in a channel and is reunited with the blood that has passed across the upper membrane. A flow restriction in the blood path maintains the appropriate pressure differential for the system to operate. A series of these units are linked to form a complete device. Details of both of the devices are given in Chapter 7.

1.4 Clinical Applications

Perfusion devices have been applied in three main areas of therapeutic medicine : acute poisoning, chronic renal failure and acute (fulminant) hepatic failure.

1.4.1 Acute poisoning

Hospital admissions due to poisoning have risen dramatically over the last two decades. The majority of cases (80%) are self poisoning. ("Self poisoning is a conscious, often impulsive, manipulative act, undertaken to secure redress of an intolerable situation.....thoughts of self-destruction are not prominent.") Accidental and suicidal poisoning each account for about 10% and there are a small number of homicidal. (Matthew and Lawson, 1975). Altogether they account for about 10% of all acute adult medical admissions.

These dramatic statistics should be tempered by the knowledge that the vast majority of patients recover physically with, at most, supportive treatment of the type outlined by Clemesen and Nilsson (1961) - the so called Scandinavian Method. For example in the Edinburgh Royal Infirmary (Regional Poisoning Centre) between 1967 and 1973 only 325 (3%) of the 10,134 cases required specialized techniques. Of those, 308 received forced diuresis, seven had peritoneal dialysis and ten had haemodialysis. (Matthew and Lawson, 1975). In addition many of those who die, do so either before admission or their health has deteriorated so much before admission that even the most aggressive therapy is of no avail. This is not to say that haemoperfusion and other extracorporeal procedures do not have a life saving role in acute poisoning. Nevertheless the main role of aggressive therapies is the reduction in length and severity of coma and/or drug related complications, thereby reducing the chances of mortality in severely poisoned patients. They are used in conjunction with supportive therapy.

A wide spectrum of substances are involved in acute poisoning. The vast majority of self poisoning cases involve therapeutic drugs, of which

three groups are particularly important; the CNS depressants or hypnotics (e.g. barbiturates, gluthethimide, methaqualone); The analgesics (e.g. salicylates and paracetamol) and the tricyclic antidepressants. (Matthew and Lawson, 1975). Most applications of haemoperfusion and haemodialysis have involved drugs of the first two types. (Volans et al., 1977). It is quite common for several drugs to be taken simultaneously. This often occurs simply because a proprietary brand drug contains two or more agents (e.g. Tuinal contains amylobarbitone and quinalbarbitone). The presence of alcohol further complicates many cases. Household, industrial and agricultural chemicals are involved in many accidental poisonings (e.g. kerosene, carbon tetrachloride, other organic solvents and paraquat). Haemoperfusion has been used for paraquat poisoning (Maini and Winchester, 1975 and Widdop et al., 1975). Metals such as copper, lead, mercury and arsenic can also be toxic in sufficient concentrations; such cases are often chronic rather than acute.

As mentioned previously the mainstay of acute poisoning therapy is the Scandinavian Method of intensive supportive care. It is simply a logical approach in four parts; (a) assessment of the patient, (b) emergency measures, (c) general care and (d) special care. Assessment normally involves either defining the degree of coma or measuring the level of drug in the plasma or both, depending upon the particular poison. Emergency measures, such as restoration of respiratory function where sedative drugs are involved and shock therapy for cardiovascular complications, are often necessary to maintain life. Prevention of further adsorption of the poison from the gut may also be important. To this end the stomach contents can be washed out (gastric lavage) or oral adsorbents may be given. Once the life threatening complications have been controlled a high standard of general nursing care is required. This is to keep the patient's condition stable and to avoid secondary complications such as dehydration, hypothermia and even bed sores. In severely poisoned patients special methods of care (aggressive therapies) are called for.

Aggressive therapies are all designed to increase the elimination of the poison from the body, and thereby reduce the period of maximum risk.

The most common therapy is forced diuresis. This works on the principal that by infusing saline into the patient, urine output is increased and with it the natural excretion of the poison. It is obviously of most use with poisons readily removed by the kidneys and it is contra-indicated if renal function is impaired. For example, forced diuresis is more effective with 'long acting' barbiturates as compared to the less water soluble 'short acting' barbiturates. Peritoneal dialysis, haemodialysis and haemoperfusion are less common forms of aggressive therapy. Although peritoneal dialysis is quite a simple procedure it is usually less effective than haemodialysis. However, the decision as to which is employed is often dictated by availability of equipment and appropriate expertise and not by effectiveness. Dialysate perfusion has been used in conjunction with both haemo- and peritoneal dialysis, with mixed success. (Knepshield et al., 1973).

Until recently haemoperfusion had only been used spasmodically in acute poisoning. However, the current commercial availability of haemoperfusion columns has given this technique a timely boost. Haemoperfusion is at least as effective as haemodialysis for the removal of most poisons. The technique is extremely simple compared to both types of dialysis and requires far less set-up time. However, Volans et al. (1977) have recommended that it be carried out only in specialist centres with adequate laboratory facilities.

1.4.2 Chronic renal failure

The kidneys fulfil a number of metabolic roles. (Ganong, 1973).

(a) Regulation of extracellular fluid composition

This involves three processes : the regulation of electrolyte concentrations, the excretion of excess water and maintenance of the acid-base balance in the bicarbonate buffer system.

(b) Excretion of waste metabolites

The end products of nitrogen metabolism are excreted by the kidney, in the urine. (e.g. urea, creatinine and uric acid). Other endogenous wastes and exogenous toxins are excreted in the same way. (Endogenous toxins are those that are generated within the body as the end products of metabolism

and exogenous toxins are those that are introduced into the body from without.)

(c) Endocrine Gland

The hormone, erythopoietin, and the enzyme, renin, are secreted by the kidney. The former stimulates red blood cell production while the latter helps to regulate blood pressure.

(d) Activation of Vitamin D

Vitamin D, which plays a vital role in calcium metabolism (including bone growth), is activated in the kidney under parathyroid control.

Kidney failure can be either acute (temporary) or chronic (permanent and worsening). In acute failure, supportive therapy is applied until kidney function returns. In chronic failure, dietary restrictions are imposed until such time as the deteriorating kidney function is insufficient to remove metabolic wastes and to regulate fluid composition. This usually occurs when kidney function falls below 5% of full capacity. Regular or maintenance dialysis and/or transplantation is then required, in addition to dietary control, to sustain life. The vast majority of dialysis patients have haemodialysis as opposed to peritoneal dialysis. Neither process completely replaces kidney function, however they stabilize the patient's condition and ensure a moderate life expectancy (Brunner et al., 1975). Transplantation offers the patient a near normal life, free from the thrice weekly dialysis period. However, it will only have a limited role to play until the immunological (rejection) problems are solved. Even then dialysis will still be needed to stabilize and maintain patients while awaiting a donor kidney.

The total body disease state that develops after kidney failure is known as uraemia; literally urine in the blood.

Substantial numbers of people are involved in chronic renal failure. In Europe it is predicted that between 75 and 95 people per million of population will be under treatment by 1980. (Brunner et al., 1975). The numbers vary widely according to country. For example. Switzerland will

have between 203 and 236 per million while Poland is expected to have only 4.8 to 7.6 per million. This disparity reflects the treatment policies of individual nations as much as different incidences of chronic renal failure. At the beginning of 1975, 45.9 people per million were being treated in Europe; 79% on haemodialysis, 20% with functioning transplants and the other 1% on peritoneal dialysis. (Brunner et al., 1975). Similar numbers are under treatment in the other industrialized nations. As each dialysis patient is treated two or three times per week, the number of dialysers used (even allowing for several re-uses) is vast.

Although dialysis is capable of stabilizing and sustaining a uraemic patient, great uncertainty exists as to the identity of toxic substances that need to be removed. (Bergstrom, 1975). At least three major symposia have been held to discuss uraemic toxins. (Welt et al., 1970, Giordano, 1975 and Gotch and Krueger, 1975). Table 1.4.1 is a list of 'established' and 'suspected' toxins quoted by Bergstrom. Interestingly urea, creatinine and uric acid, the very solutes whose toxicity is implicit in every discussion on uraemia, are only 'suspected' of being toxic. While other authors may disagree with this characterization, it does highlight the uncertain nature of uraemic toxicity. The search was at one time dominated by the elusive middle molecules. The middle molecule hypothesis was developed by Babb et al. (1971 and 1972) from observed differences in the condition of patients on peritoneal dialysis compared to those on haemodialysis. Unidentified molecules in the middle molecular weight range (500 to 5000 MW) were suspected of causing uraemic neuropathy. Although the search for middle molecules continues (Bergstrom et al., 1977), general interest appears to be waning.

The rush to find uraemic toxins, in particular middle molecules, has obscured the fact that the biochemical nature of uraemia is very complex and involves many body systems. No simple relationship is likely to exist between any toxin (or group of toxins) and uraemic pathology. The indirect consequences of dialysis therapy such as depletion of essential solutes, should not be overlooked either. (Bergstrom, 1975).

Established Toxins	Suspected Toxins	
Water	Urea	Aromatic oxyacids
Sodium	Creatinine	Pseudouridine
Potassium	Uric acid	Oxalic acid
Hydrogen ions	Methylguanidine	Magnesium
Inorganic phosphate	Guanidinosuccinic acid	Arsenic
Parathyroid hormone	Other guanidines	Myoinositol
Renin	Amino acids	Middle molecules
	Amines (aliphatic and aromatic)	Glucagon
	Phenols	Growth hormone
	Indoles	Natriuretic hormone

Table 1.4.1. Uraemic Toxins (from Bergstrom, 1975)

The first rational and thorough comparison of various haemodialysis treatment regimes is underway in the United States of America. (Wineman, 1977). It is hoped that this study will give unbiased correlations between the type of therapy and the biochemical, neurological and clinical indicators of adequacy of treatment.

Until the biochemical etiology of uraemia is better understood new techniques, such as haemoperfusion, can only be evaluated against the existing ones. Paradoxically a better understanding of uraemia, with its possible complexity, may cause more problems for treatment design than do the present uncertainties.

Haemoperfusion and dialysate regeneration have been used in uraemia and several ultrafiltrate perfusion systems have been proposed. (Winchester, 1977; Henderson, 1977 and Denti and Biagini, 1977). Dialysate regeneration greatly simplifies haemo- and peritoneal dialysis, by reducing the volume of dialysate. Provided sufficient quantities of sorbents are used, dialyser performance is not limited by the regeneration cartridge, i.e. the dialyser acts as if a continuous supply of fresh dialysate was being fed into it. This application of sorbents has an important place in home and mobile (holiday) dialysis.

The role of haemoperfusion is not so clear. In a dialyser a continuous molecular weight spectrum of solutes is removed. This spectrum depends directly on the size of the molecule relative to the porosity of the membrane. In haemo--perfusion, however, this solute spectrum can be discontinuous as it depends not only on the molecular size but also on the relative binding affinities of the solutes on the sorbent. i.e. two solutes of similar molecular weight may be removed at vastly different rates, whereas in dialysis the rates would be similar. It is, therefore, difficult to directly compare the performance of a dialyser and a haemoperfusion column. In addition adsorbents, such as activated carbon, have very little capacity for either ion exchange or urea and water adsorption. Accordingly these solutes must be controlled by other means. Winchester et al. (1975), Chang et al. (1974) and Dunea et al. (1976) have used haemoperfusion

in conjunction with haemodialysis for uraemic patients. Chang also tried ultrafiltration for control of water, electrolytes and urea. Such arrangements are more complex than simple haemodialysis yet they offer no clear advantages. We know that maintenance dialysis is an adequate technique for the treatment of uraemia caused by chronic renal failure. Therefore, given our limited knowledge of uraemic etiology and the difficulties in comparing therapies, it is difficult to justify the use of haemoperfusion in chronic renal failure. Not all authors share this point of view. (Winchester, 1977).

1.4.3 Acute hepatic support

The liver is the major metabolic 'factory' of the body. Food absorbed in the intestines is transported, via the portal vein, to the liver. Here, many types of carbohydrate, fat and protein degradation and synthesis take place. Some of the products of these processes are then stored in the liver pending distribution to various parts of the body. Substances synthesised include glycogen (later converted into glucose), blood proteins (albumin, globulins and blood clotting factors), cholesterol and vitamin A. End products of protein metabolism such as urea and uric acid are formed in the liver for excretion by the kidney. Iron from the degradation of dead red blood cells is stored for inclusion in the haemoglobin of new red cells. Bilirubin, a red cell pigment, is conjugated with glucuronic acid and excreted into the intestine. The liver is also an important gland. It secretes bile, which is concentrated in the gall bladder, and released into the intestine to aid digestion and adsorption of fats. Detoxification of many exogenous and endogenous substances occurs in the liver. This often involves making the toxins more water soluble, thus increasing their excretion by the kidneys. (Ganong, 1973).

Hepatic failure results from several diseases and certain forms of acute poisoning. Naturally, major complications follow loss of the metabolic capabilities of the liver. Failure can be acute or chronic. An important difference between kidney and liver failure is that in the latter damage to the organ can be repaired by tissue regeneration. Hepatic therapy is therefore aimed very much at supporting the patient over the acute crisis. Even so, not all chronic

liver failure is potentially reversible. Most interest in hepatic support has been for the acute (fulminant) failure that results from viral hepatitis or poisoning by hepatotoxic drugs (e.g. paracetamol). These failures are characterized by a progressive deterioration in the patient's mental state culminating in coma and death. Only 10-20% of those who develop severe coma survive. (Benhamou et al., 1972). Although the world-wide death rate due to chronic cirrohsis of the liver has been presented (Williams et al., 1975), similar statistics for acute failure were not available.

The biochemical nature of hepatic encephalopathy (coma) in acute failure is exceedingly complex (Williams, 1977). A number of substances accumulated after failure have been implicated, e.g. ammonia, free fatty acids, mercaptans and free phenols. (Brunner et al., 1975). The toxic potential of each substance taken alone is magnified when several are present. (Zieve et al., 1975). Possible relationships between amino acid concentrations and coma have been studied recently. (Abouna et al., 1977 and Williams, 1977). Middle molecules that may alter the permeability of the blood-brain barrier have also been implicated. (Delorme et al., 1976).

Many techniques have been suggested for acute hepatic support, and in particular for reversal of hepatic coma (Maini, 1975). There are two broad types (a) those that remove hepatic toxins and (b) those that attempt to replace liver function.

Methods of hepatic toxin removal include peritoneal dialysis, haemodialysis, exchange transfusion, plasma exchange (plasmapheresis), oral adsorbents and haemoperfusion. All have only met with limited success. The first large trial of haemoperfusion over activated carbon gave excellent results - 39% survival out of 31 patients compared with 13% in the previous 96 patients, who had only received standard supportive therapy. (Gazzard et al., 1974 and Williams, 1977). Subsequent trials were less effective. In fact none of a group of 18 patients treated by haemoperfusion survived. (Williams, 1977). Conversely recent trials with haemodialysis has been more promising than the earlier ones. (Delorme et al., 1976). This change may be related to changes in the mass

transfer properties of dialysis membranes in the intervening time. Six out of 16 patients (or 37.5%) recovered consciousness in a study by Silk et al. (1976). The ultrafiltrate perfusion techniques developed by Maini (1975) and Nose et al. (1975) and discussed in Sections 1.3 and 7.3 are intended for hepatic support although no clinical trials have been conducted.

Techniques that attempt to replace liver function include cross circulation and cross dialysis (both between the patient and a living'donor'), haemoperfusion through a whole cadaveric liver, haemoperfusion over liver tissue (slices, fresh, frozen or dried), haemoperfusion over liver enzymes (bonded to polymeric resins) and liver transplantations. (Maini, 1975 and Nose et al., 1977a). Clearly all these techniques are aimed at producing some degree of normal liver metabolism. Although this approach to hepatic support has its attractions, there are still many problems to be overcome, especially immunological ones.

The role of all hepatic support techniques, including haemoperfusion and ultrafiltrate perfusion, will remain limited and uncertain so long as uncertainties remain regarding the etiology of hepatic coma and the other symptoms of acute hepatic coma and the other symptoms of acute hepatic failure.

1.5 Summary (State of Art)

Although many extracorporeal, blood detoxification systems have incorporated sorbents, haemoperfusion and dialysate regeneration are the only two techniques to have achieved extensive clinical application and commercial availability. Of these, haemoperfusion has received the most widespread use. In fact, the state of the art of perfusion devices in theraputic medicine is very much the state of the art of haemoperfusion.

Haemoperfusion is one of three extracorporeal techniques suitable for removing toxins in severe cases of acute poisoning. It is quick to set up, easy to use and very efficient, compared to the other two, haemo- and peritoneal dialysis. Now that haemoperfusion columns are available commercially their relative importance, as an extreme measure in acute poisoning, will increase.

Haemodialysis remains the mainstay of uraemic therapy following chronic renal failure. Haemoperfusion offers no clear advantages over dialysis. In fact, it has several disadvantages e.g. no water removal. Its use in conjunction with dialysis and/or ultrafiltration is speculative and has no place as yet in regular maintenance dialysis programmes. Dialysate regeneration, on the other hand, has a very clear and important place in uraemic therapy. By reducing the volume of dialysate required per treatment it greatly simplifies haemodialysis, especially when carried out in the home or on holidays.

The role of all extracorporeal blood detoxification systems, including sorbent-based ones, is very uncertain in acute hepatic failure. Until more is known of the etiology of the symptoms of acute hepatic failure, e.g. coma, this uncertainty will persist.

CHAPTER 2

PERFORMANCE ASSESSMENT OF PERFUSION DEVICES

CHAPTER 2

PERFORMANCE ASSESSMENT OF PERFUSION DEVICES

2.1 Introduction

For the purposes of this thesis performance assessment is restricted to mass transfer performance. There are, of course, other aspects to performance assessment, e.g. biocompatibility. Biocompatibility, in this instance, refers to blood/device interactions, i.e. blood loss, damage of blood elements, elution of toxic substances from the device into the blood etc. Section 1.2 contained a brief account of the early problems of biocompatibility encountered in adsorbent based devices. Non-medical considerations such as cost, availability, preparation time and ease of use are also important. Surprisingly, perhaps, one or more of these features can be almost as significant as mass transfer performance in relation to the clinical decision as to which detoxification device to use. Therefore although the thesis is concerned with the mass transfer performance, it is important that these other aspects of performance assessment are not forgotten.

The operating conditions for a perfusion device vary significantly from those of sorbent-based devices in the chemical industry. Although the mass transfer principles are the same for both applications, the relative importance of the system parameters to the mass transfer performance is usually quite different. Therefore, analyses specific to perfusion devices are required. However, investigations into the controlling mass transfer processes in perfusion devices are limited both in number and depth. Those papers that have addressed this problem are critically reviewed in Section 2.4.

Because our understanding of the controlling mass transfer processes is so limited, rational methods of performance assessment have not been devised. In the absence of such methods the obvious alternative techniques are employed. These techniques are of two types:- those designed for other blood detoxification devices such as haemodialysers and those designed for sorbent-based devices with industrial applications. These two approaches are

reviewed in Section 2.2 with reference to their applicability to perfusion devices. Indentification of the controlling mass transfer processes will permit more rational performance assessment based either on these or other techniques.

Although the crucial test of every blood detoxification device is its performance clinically, investigations into the mass transfer processes are most easily performed on the basis of in vitro experimentation. The design and clinical interpretation of in vitro experiments requires an understanding of the clinical pharmacokinetics, i.e. the distribution and movement of the toxin within the body during treatment. The different types of pharmacokinetic models are introduced in Section 2.3 together with a discussion on their role in performance assessment.

Based on the background presented in Sections 2.2 to 2.4 and in Chapter 1, a rational methodology for achieving the thesis aim is outlined in Section 2.5. It includes several general assumptions on which the work in subsequent chapters is based.

2.2 Methods of Mass Transfer Assessment

2.2.1 Dialysance and clearance

Because the mass transfer processes are not thoroughly understood, no generally accepted methodology or testing standards exist for the direct assessment of mass transfer of perfusion devices. This is in contrast to haemodialysers for which a manual, produced by the National Institute of Arthritis and Metabolic Diseases in the USA (Klein et al., 1976) entitled "Evaluation of Haemodialysers", has received general acceptance. As haemodialysis was the first, and the most widely used extracorporeal, detoxification technique, the concepts of mass transfer measurement developed for it have been applied to perfusion devices; whether applicable or not. The keys to haemodialyser performance are dialysance and clearance.

Wolf et al. (1951) compared the performance of the haemodialyser or 'artificial kidney' to that of the human kidney. Toxin excretion from the human kidney is traditionally measured by the clearance, i.e. the volume of blood 'cleared' of toxin per unit time.

$$\text{Clearance (Cl)} = \frac{\text{rate of excretion of toxin}}{\text{conc. of toxin in arterial blood}}$$

Clearance is constant for a given toxin irrespective of blood concentration and hence can be considered as a fundamental characteristic of the kidney. Wolf and co-workers coined the term dialysance as the comparable characteristic for the artificial kidney. The rate of toxin removal in a haemodialyser was found to be proportional to the toxin concentration in the inlet blood line minus the concentration in the dialysate entering the dialyser. The proportionality constant was termed the dialysance, i.e.

$$\text{Dialysance (Dl)} = \frac{\text{rate of toxin removal by dialyser}}{\text{(blood inlet conc.} - \text{dialysate inlet conc.)}}$$

The clearance of a haemodialyser can be defined analogous to that in the human kidney. If the dialysate concentration entering a haemodialyser

is zero then the dialysance is equal to the clearance. Dialysance is a fundamental, steady state property of the haemodialyser. It summarizes the mass transfer characteristics of the device at given blood and dialysate flow rates.

Dialysance and clearance can be expressed as functions of either the external, input/output parameters of the haemodialyser or the internal, mass transfer characteristics. Using the four part, 'black box' representation of a haemodialyser, illustrated in Figure 2.2.1, the expressions for dialysance and clearance are;

$$DI = Q_b \frac{(C_{bi} - C_{bo})}{(C_{bi} - C_{di})} = Q_d \frac{(C_{do} - C_{di})}{(C_{bi} - C_{di})}$$

and

$$CI = Q_b \frac{(C_{bi} - C_{bo})}{C_{bi}} = Q_d \frac{(C_{do} - C_{di})}{C_{bi}}$$

where: C = concentration of toxin, Q = volumetric flow rate
subscripts: b = blood, d = dialysate, i = inlet, o = outlet.

Dialysance formulae based on the mass transfer characteristics are quoted in Figure 2.2.1, for three different flow geometries. The clearance depends upon the inlet concentration in the dialysate and it can only be expressed in terms of the mass transfer characteristics if C_{di} is known.

All the above formulae assume there is no convective contribution to the mass flux due to solvent flow between the blood and dialysate compartments. In clinical practice water is removed from the blood by ultrafiltration. This is taken into account by modifying the formulae in these cases. In vitro mass transfer experiments with haemodialysers are designed to produce zero ultra-filtration, thereby avoiding this modification. These formulae provide the basis on which the performance of conventional haemodialysers can be compared to that of haemoperfusion columns and other perfusion devices. (See Chapters 6 and 7).

Flow Geometry	Calculations of Dl from K_o data**	Calculation of K_o from clearance data
Cocurrent 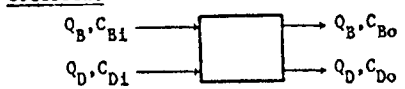	$Dl = Q_B\left[\frac{1-\exp[-N_T(1+Z)]}{1+Z}\right]$	$K_o = \left[\frac{-Q_B \ln[1-\frac{Dl}{Q_B}(1+Z)]}{A(1+Z)}\right]$
Countercurrent 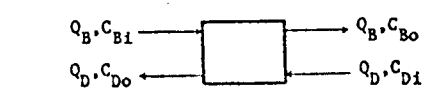	$Dl = Q_B\left[\frac{\exp[N_T(1-Z)]-1}{\exp[N_T(1-Z)]-Z}\right]$ If $Z = 1$, $Dl = Q_B[\frac{N_T}{1+N_T}]$	$K_o = \frac{Q_B}{A(1-Z)}\ln\left[\frac{1-Dl/Q_D}{1-Dl/Q_B}\right]$ If $Z = 1$, $K_o = \frac{Dl}{A(1-Dl/Q_B)}$
Well-mixed 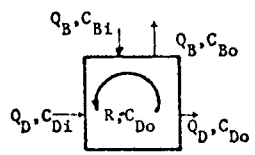 Recirculation (R) >> Q_D	$Dl = Q_B\left[\frac{1-\exp(-N_T)}{1+Z[1-\exp(-N_T)]}\right]$	$K_o = \frac{Q_B}{A}\ln\left[\frac{1-Dl/Q_D}{1-Dl/Q_B(1+Z)}\right]$
		$N_T = K_o A/Q_B$ $Z = Q_B/Q_D$

**For $Q_B << Q_D$, $Dl = Q_B[1-\exp(-N_T)]$ and $K_o = \frac{Q_B}{A}\ln[1-Dl/Q_B]$.

Figure 2.2.1 Formulae for Dialysance and Overall Mass Transfer Coefficient in Haemodialysers in the Absence of Ultrafiltration (after Klein et al. 1976)

Dialysance and clearance are expressed more fundamentally as fractional dialysance and fractional clearance. These terms are defined below. By analogy with heat exchanger design the fractional dialysance could be termed the effectiveness. Likewise the fractional clearance may be termed the efficiency.

$$\text{Fractional Dialysance or Effectiveness} = \frac{\text{actual mass transfer in device}}{\text{max. possible mass transfer}}$$

$$= \frac{Q_d\ (C_{do} - C_{di}\ )}{Q_b\ (C_{bi} - C_{do}\ )} = \frac{C_{bi} - C_{bo}}{C_{bi} - C_{di}}$$

$$\text{Fractional Clearance or Efficiency} = \frac{\text{actual mass transfer in device}}{\text{rate of mass entering device}}$$

$$= Q_d\ \frac{(C_{do} - C_{di}\ )}{Q_b\ C_{bi}} = \frac{C_{bi} - C_{bo}}{C_{bi}}$$

The effectiveness is the efficiency of the device with respect to its theoretical limitations. For example, a dialyser can be 100% effective but less than 100% efficient. If a dialyser has a finite inlet dialysate concentration then the outlet blood concentration has a theoretical lower limit equal to this value. Therefore, the dialyser can not be 100% efficient. However, if the outlet blood concentration reaches this lower limit then the dialyser is 100% effective.

The concepts of clearance and dialysance are relatively simple yet their implementation is often fraught with problems. The expressions in Figure 2.2.1 refer to steady-state mass transfer, i.e. the initial transients have ceased. This implies that both the blood and the dialysate inlet concentrations must be constant. In clinical practice, of course, the inlet blood concentration is steadily falling. Fortunately, the transients in a haemodialyser caused by a decreasing inlet blood concentration are negligible and a quasi-steady state can be assumed. As the steady state dialysance is independent of blood concentration, so the clinical dialysance remains constant - at least in theory.

Another implicit assumption of the dialysance and clearance formulae is the use of 'mixing cup' concentration values, i e. the total amount

of toxin in a given volume of fluid divided by that volume. This presents no problems with dialysance concentrations as the dialysate is homogeneous fluid. However, the concentration in blood are easily misinterpreted.

Blood is a heterogeneous fluid comprising formed elements (cells) suspended in an aqueous phase, the plasma. Another aqueous phase, the intracellular fluid, is enclosed by the semipermeable membranes of the formed elements, the majority of which are red blood cells (RBC's). Both aqueous phases contain proteins. Toxins in whole blood can be in simple solution or bound to the proteins in either of the aqueous phases, i.e. free or bound, intracellular or extracellular. Therefore, it is critical that any technique used to measure a toxin concentration takes account of its distribution in the blood. Often this is not achieved in clinical practice. For convenience, the whole blood concentration is frequently represented by the free concentration in the plasma. This is only a reasonable approximation if a negligible amount of toxin is bound (intra- and extracellularly) and if the free plasma concentration and the intracellular concentration are in equilibrium (with an equilibrium constant of one). Although the first restriction holds for some possible toxins in chronic renal failure, i.e. urea, creatinine and uric acid, the free plasma and intracellular concentrations are not always in equilibrium at the outlet of a haemodialyser. This was shown theoretically by Gaylor et al. (1970) and verified in vitro by Gaylor (1974). Equilibration is very rapid for urea so the outlet free plasma concentration equals the whole blood concentration. Therefore no error occurs if plasma concentration is substituted for whole blood value. This is not the case for uric acid and creatinine. The plasma concentration at the outlet is lower than the whole blood concentration, hence the dialysance is over--estimated if the plasma concentration is used instead of the whole blood value. A clinical study by Bass et al. (1975) showed both urea and creatinine dialysance were overestimated if the free plasma and not the whole blood concentrations were used. Doubts were expressed over the validity of the urea results.

The necessity for precision when measuring blood concentration for inclusion in mass transfer formulae applies equally to perfusion devices as to haemodialysers.

The applicability of dialysance and clearance as concepts for the measurement of mass transfer in perfusion devices is limited compared to that in haemodialysers. As there is no equivalent to the inlet dialysate concentration in a haemoperfusion column, dialysance has no meaning. Only clearance can be applied to such devices. Unlike haemodialysers, haemoperfusion columns have no net outflow of toxin. Instead of leaving the system in a dialysate solution it accumulates in the sorbent. With no net outflow to balance the inflow in the blood it is impossible for a steady state operating point to be achieved. Therefore, the clearance must be time dependent. In haemoperfusion columns this time dependence is exaggerated by the fall in the inlet blood concentration that occurs clinically. Hence clearance ceases to be a single, convenient parameter that summarizes the mass transfer performance. By studying the controlling mass transfer processes in haemoperfusion columns it is possible to understand this time dependence and thereby assign some meaning to the clearance performance of such devices.

For dialysate and ultrafiltrate perfusion devices it is essential to differentiate between the performance of the haemodialyser or ultrafilter and the performance of the sorbent element. Toxin removal is primarily controlled by the haemodialyser (or ultrafilter). The perfusion element does not augment this basic performance. Hence dialysance and clearance are useful for describing the clinical performance of haemodialysers (or ultrafilters) that incorporate perfusion elements. In cases where the sorbent is physically independent of the haemodialyser (or ultrafilter), i.e. dialysate regeneration cartridges, the performance of the perfusion element can be considered separately. For reasons similar to those given above with respect to haemoperfusion columns, clearance is not a suitable method for describing the mass transfer in dialysate (or ultrafiltrate) regeneration devices. The fundamental design criterion for such devices is that the outlet concentration be zero. This is a similar specification to that of sorbent columns used in the chemical industry. Therefore the techniques employed in that industry may be suitable for describing the performance of, and designing, certain dialysate and ultrafiltrate perfusion devices.

2.2.2 Breakthrough curves

Sorbents have been used for decolouration and effluent purification in the chemical industry for half a century or more. In common with most perfusion devices, industrial types normally consist of packed beds of granular sorbents. The solution to be decoloured or purified passes through the packed bed only once, i.e. a single pass operation. For design purposes it is assumed that the concentration of impurity entering the bed is constant. The performance of the bed is judged by the concentration-time curve at the outlet, i.e. the breakthrough curve. Once the concentration rises above an arbitrary threshold value, say 5% of the inlet concentration, the bed is assumed to be exhausted and it must be replaced or regenerated. A typical breakthrough curve is shown in Figure 2.2.2, Curve (a). As the effluent flow rate is assumed constant the dependent variable in the breakthrough curve can be changed to the throughput volume, i.e. the total volume of effluent to pass through the column up to a given time.

If the flow rate is infinitely slow or the mass transfer rate between the effluent and the adsorbent is infinitely fast, then the breakthrough is a step rather than a sigmoid shaped curve. (Figure 2.2.2, Curve (b)). The area above a breakthrough curve equals the amount of impurity adsorbed up to a given throughput volume. Hence, the area up to the step (curve (b)) represents the capacity of the bed. Therefore breakthrough occurs on curve (a) when only about 80% of the capacity has been utilized. Design of industrial devices centres upon minimizing this loss of capacity. To find the breakthrough point (and hence the functional capacity of the system) one needs the shape of the breakthrough curve and total capacity of the bed.

If the length of the bed exceeds a particular minimum value then the shape of the breakthrough curve becomes independent of the length of the bed. This so called constant pattern, breakthrough curve merely undergoes a time shift to account for the changes in capacity with changes in bed length. This phenomena is illustrated in Figure 2.2.3. Values of the minimum length required to achieve a constant pattern are given by Vermeulen (1958) and Hashimoto et al. (1977).

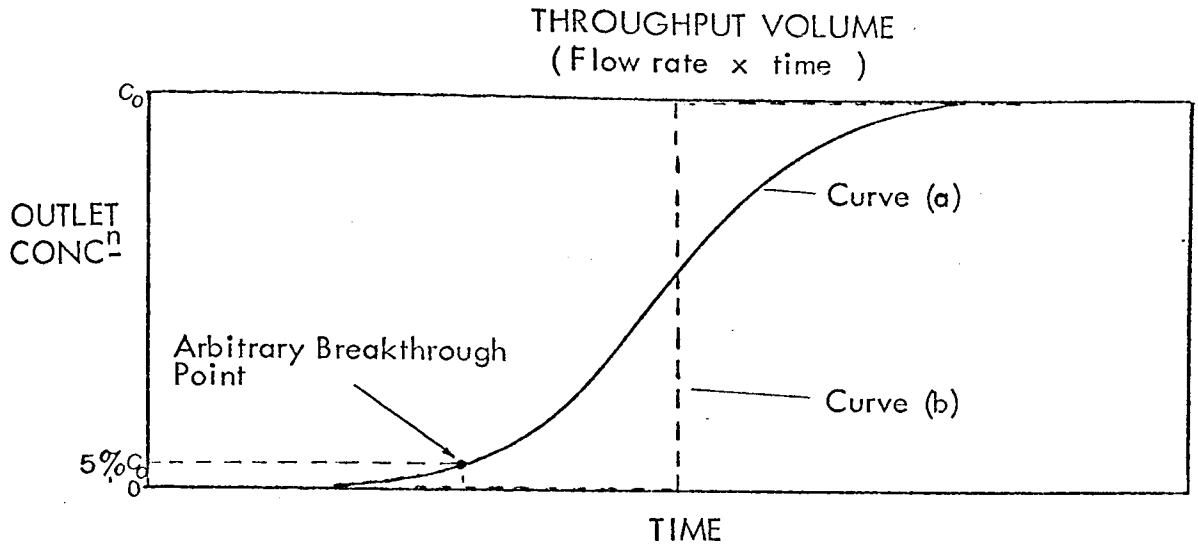

Figure 2.2.2 General Breakthrough Curve

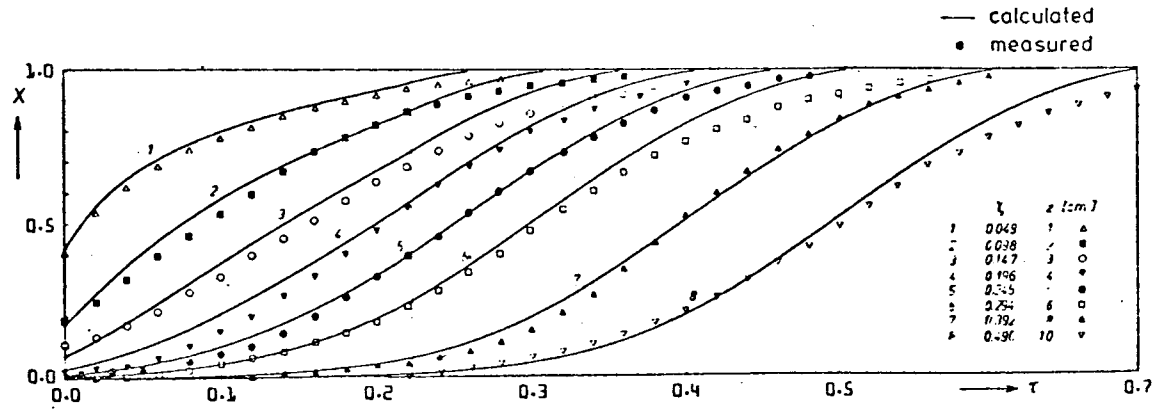

Figure 2.2.3 Development of Constant Pattern Breakthrough Curve with Increasing Column Length (after Spahn and Schlunder, 1976)

The shape of the constant pattern curve depends upon the flow, sorption and mass transfer properties of the bed. The complete family of such curves is produced by combining these system parameters into dimensionless groups and solving the bed equations under the constant pattern assumption. Hall et al. (1966) and Fleck et al. (1973) tabulate these normalized, constant pattern breakthrough curves for various types of mass transfer within the bed. The constant pattern assumption applies for most industrial packed beds, hence the above solutions are sufficient to design these devices.

Constant pattern curves are potentially useful for designing certain dialysate and ultrafiltrate regeneration cartridges. Unfortunately, the constant pattern results are based on a constant inlet concentration, whereas, in practice, the inlet concentration decreases with time. This restricts the scope of quantitative design by this method. Nevertheless, it provides a framework in which semiquantitative rather than the present empirical design is possible. Van Zutphen (1975) used constant pattern curves to interpret the mass transfer in the film adsorber, haemoperfusion column (Section 1.3). However, this technique is not generally applicable for constant inlet concentration experiments on haemoperfusion columns as constant pattern conditions are not usually achieved.

2.3 Pharmacokinetic Considerations

Experiments to investigate the basic mass transfer processes in blood detoxification devices are conducted *in vitro*. For obvious reasons such experiments can not be performed clinically, and it is difficult to justify animal experiments. In addition the *in vitro* format facilitates simple experiments where the variables are both limited in number and easily controlled. Normally this entails using an aqueous solution as a blood substitute. Bovine blood is employed in more advanced experiments. Having measured the mass transfer *in vitro*, the results are extrapolated by *apriori* argument to predict what happens clinically. This extrapolation centres on the toxin pharmacokinetics in the patient.

"Pharmacokinetics constitutes the study of all processes involved in time-dependent concentration changes of drug, poison, other foreign substance or their metabolites in human or animal bodies and isolated tissues and their description in mathematical equations." Kruger-Thiemer (1977).

The clinical performance of a perfusion device is affected by the pharmacokinetics in two ways. Firstly, the pharmacokinetics control the inlet concentration to the device. The toxin kinetics in the device and the body are coupled to form a closed-loop, with the outlet concentration of the one being related to the inlet concentration of the other. This is critical since the performance of perfusion devices is dependent upon the inlet concentration. For haemoperfusion columns the inlet concentration equals the arterial concentration in the patient whereas for a dialysate (or ultrafiltrate) regeneration cartridge the inlet concentration equals the outlet dialysate (or ultrafiltrate) concentration. This concentration is in turn related to the arterial concentration in the patient via the clearance in the haemodialyser (or ultrafilter).

Secondly, the pharmacokinetics of the blood affect the mass transfer in the device. Section 2.2 stated that blood was a heterogeneous fluid with potential toxin distribution in four phases; free or bound in either the extracellular or intracellular fluid. Perfusion devices usually have access only to the free toxin in the plasma (extracellular fluid). Hence, the clinical

performance of the device may be reduced in comparison with the in vitro results where the toxin is in simple aqueous solution in the blood substitute. Uncoated haemoperfusion and ultrafiltrate perfusion devices can remove toxin by adsorbing the plasma protein to which the toxin is bound. However this involves only a small fraction of the bound toxin and is therefore insignificant. (Chapter 6 and 7).

The effects of pharmacokinetics are frequently overlooked in the design and interpretation of in vitro experiments and in clinical evaluations. In particular, the distribution of toxin in the blood is seldom discussed in clinical papers. Rosenbaum (1977) is one of the few exceptions.

2.3.1 Pharmacokinetic models

Toxins exist in the body fluids and tissues in several forms; in free solution, as either ionized or neutral molecules, or bound to plasma or tissue proteins. The degree of ionization depends upon the relative magnitude of the pH in the fluid and the pK_a of the molecule. Transport across biological membranes, such as those lining the GI tract or those surrounding cells or sections of tissue, is usually by simple Fickian diffusion. The rate of diffusion depends upon the lipid/water partition coefficient of the membrane. The more lipid soluble the toxin is the higher the membrane permeability. The concen--tration driving force for this diffusion is provided by the unionized portion of the toxin in free solution. Although the unionized toxin concentration might reach an equilibrium across a membrane, a gradient may still exist between the total (free plus bound) toxin concentrations on either side of the membrane. Protein binding is normally reversible. If the concentration of free, unionized toxin falls, some of the bound toxin is released into solution and visa versa. Likewise, the ionization is reversible in that is is controlled by a mass action law. Therefore all the toxin in a given cell or section of tissue is ultimately accessible via the cell or tissue membrane. Toxins are removed from the body by either excretion or biotransformation. (If biotransformation renders a toxin harmless then effectively it has been excreted.) Most biotransformation occurs in the liver although some takes place in the kidneys and the other organs.

The kidney excretes toxins and/or their metabolites into the urine. (Brodie, 1964 and Curry, 1974).

The pharmacokinetics are modelled by considering the body as a series of well mixed, fluid and tissue compartments. Toxins are transported between these compartments either by diffusion through separating membranes or by convection in the blood as it passes between compartments. The compartments have a variable degree of anatomical significance dependent upon the type of model employed. From the engineering view point pharmacokinetic models of the body can be classified as structural, functional and a combination of both.

Structural models are built up from known anatomical, physiological and pharmacological data relating to the distribution and move--ment of the toxin in question. Bischoff and Brown (1966) developed this type of model, a typical example of which is shown in Figure 2.3.1. Cooney (1976) refers to them as fluid/tissue models because individual regions of the body are visualized as having two sections, a fluid section and a tissue section. The whole body model is based on the arterio-venous system with each of the fluid sections representing the capillary bed associated with a particular region of the body. Toxins diffuse between the adjacent tissue and fluid sections. Dedrick and Bischoff (1967) modelled the pharmacokinetics of barbiturate drugs based on three body regions, viz. the visera, adipose tissue and lean tissue. The model included the effects of protein binding in the plasma and the tissues. Chen and Andrade (1976) extended this model to include the liver, the gastrointestinal tract and the brain. Chen et al. (1977) applied a similar model to salicylate pharmacokinetics. Dedrick et al. (1971) described urea pharmacokinetics based on the visera, lean tissue and the brain. All the above models were validated using animal data.

Functional models are the pharmacokinetic transfer functions of the body i.e. the functional relationship between a stimulus (e.g. intravenous injection of drug) and the pharmacokinetic response. These linear models are

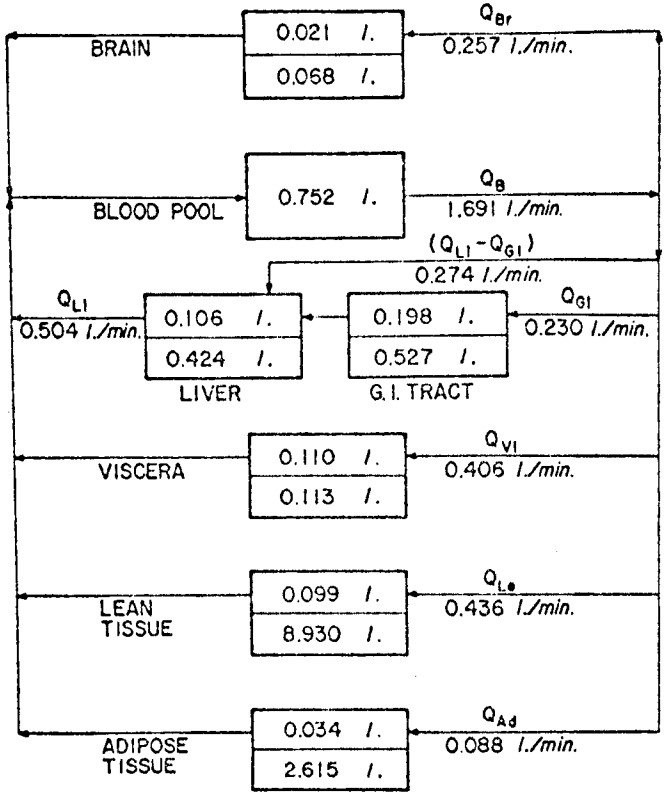

Figure 2.3.1 Typical Structural (Fluid/Tissue) Pharmacokinetic Model (after Chen and Andrade, 1976)

The mathematical equation of transient mass balance for body region Y (Fig. 4) is:

$$(F_{W,B}V_{YB}+F_{W,YT}V_{YT})\frac{dC_Y}{dt}+(C_{M,B}V_{YB})\frac{dX_{YB}}{dt}+(C_{M,YT}V_{YT})\frac{dX_{YT}}{dt}=Q_Y(F_{W,B}C_B+C_{M,B}X_B)-Q_Y(F_{W,B}C_Y+C_{M,B}X_{YB}) \quad \text{(Eq. 4)}$$

where:

$$C_{M,B}=F_{Pl,B}C_{M,Pl}+(1-F_{Pl,B})C_{M,RBC}$$

and:

C_B = free drug concentration in blood water from the blood pool (micromoles per liter)
C_Y = free drug concentration in blood water or tissue water of body region Y (micromoles per liter)
$C_{M,B}$ = effective binding macromolecule concentration in blood (kilograms per liter)
$C_{M,Pl}$ = effective binding macromolecule concentration in plasma (kilograms per liter)
$C_{M,RBC}$ = effective binding macromolecule concentration in red blood cells (kilograms per liter)
$C_{M,YT}$ = effective binding macromolecule concentration in tissue portion of body region Y (kilograms per liter)
$F_{W,B}$ = volume fraction of water in blood
$F_{W,YT}$ = volume fraction of water in tissue portion of body region Y
$F_{Pl,B}$ = volume fraction of plasma in blood
Q_Y = volumetric blood flow rate from body region Y (liters per minute)
t = time (minutes)
V_{YB} = blood volume in capillary bed of body region Y (liters)
V_{YT} = volume of tissue portion of body region Y (liters)
X_B = bound drug concentration (amount of bound drug per unit of effective binding macromolecules) from the blood pool (micromoles per kilogram)
X_{YB} = bound drug concentration in capillary bed of body region Y (micromoles per kilogram)
X_{YT} = bound drug concentration in tissue portion of body region Y (micromoles per kilogram)

represented physically as compartments in series or parallel. Neither the compartments nor the parameter values necessarily correspond to any anatomical structure or physiological parameter. Nevertheless it is common to label the first compartment as the blood or plasma and the others as tissue compartments. Alternatively they are termed the extracellular, intracellular and intercellular compartments. This type of model is often referred to as a compartment model. A typical example of a three compartment model is illustrated in Figure 2.3.2. Many functional models of the pharmacokinetics of suspected uraemic toxins were developed in the decade 1965 - 1975. Urea and creatinine were the principal toxins studied and most models consisted of one or two compartments. Table 2.3.1 lists the significant examples. Very few functional models of drugs associated with acute poisoning are reported in the literature. Winchester et al. (1974) developed a two compartment model of paracetamol pharmacokinetics in dogs. Smith et al. (1973) used a similar model to describe the pharmacokinetics of pentobarbitone in man.

Structural and functional models represent the upper and lower limits of abstraction in pharmacokinetic modelling. Functional models are extremely simple in concept and do not allow for many known pharmacological realities, e.g. protein binding or biotransformation and other non-linear processes. Therefore, many recent models in the pharmacokinetic literature combine one or more structural realities with a basic functional model. (van Rossum, 1977). However, few of these models are concerned with toxins applicable to this thesis. The exception is the work of Levy and co-workers on salicylate pharmacokinetics. (Levy, 1965 and Levy et al., 1972). As with the simple functional models the compartments in combined models do not necessarily correspond to any anatomical structure.

The type of model chosen to describe the pharmacokinetics of a particular toxin depends on many factors. These include the available physiological and pharmacological data on the toxin, the use to which the model is to be put and the precision required for that application. By its very nature a structural model represents an 'average' patient whereas a functional model applies to

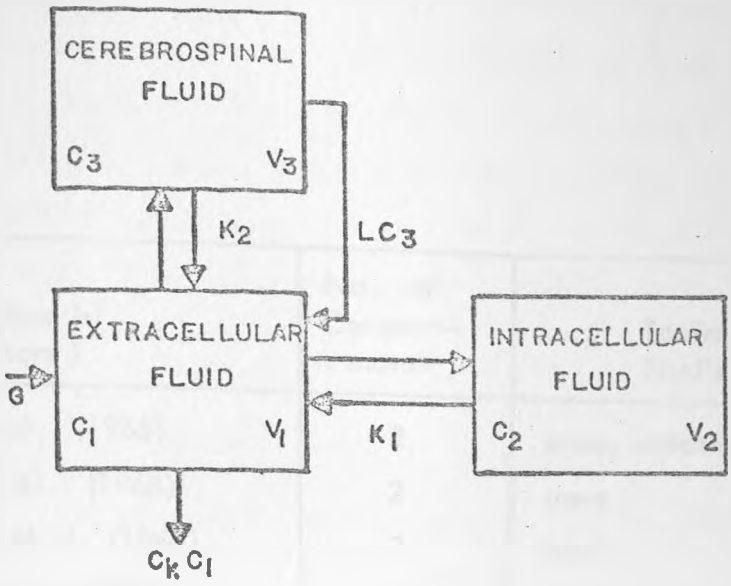

Extracellular:

$$\frac{V_1 dC_1}{dt} = G + K_1(C_2 - C_1) + K_2(C_3 - C_1) - C_k C_1 + LC_3 + IR \quad (1)$$

Intracellular:

$$\frac{V_2 dC_2}{dt} = K_1(C_1 - C_2) \quad (2)$$

Cerebrospinal fluid:

$$\frac{V_3 dC_3}{dt} = K_2(C_1 - C_3) - LC_3 \quad (3)$$

Figure 2.3.2 Typical Three Compartment, Functional Pharmacokinetic Model (after Gormley and Bell, 1970)

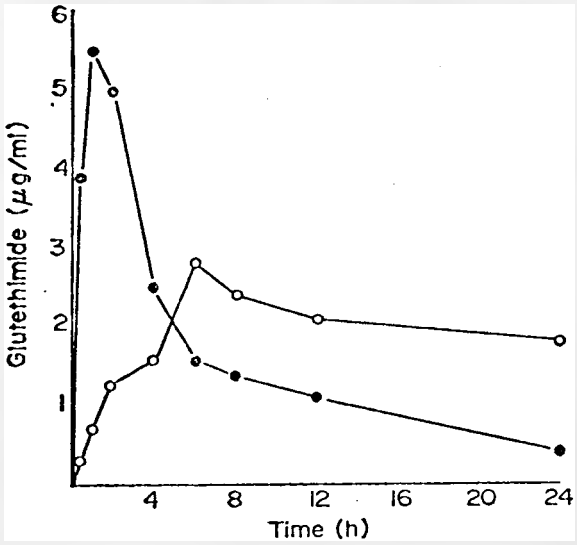

Concentrations of glutethimide in plasma of two subjects given 500 mg test doses. Each point is the mean of duplicate assays. Subject A, 56·8 kg, solid line; subject B, 67·6 kg, broken line

Figure 2.3.3 Example of the Pharmacokinetic Variations from Patient to Patient (after Curry, 1974)

Author (s) (Years)	No. of Compart-ments	Toxins Studied
Bell et al. (1965)	2	urea, creatinine
King et al. (1968)	2	urea
Rastogi et al. (1968)	2	urea
Wolf et al. (1970)	2	urea, creatinine
Abbrecht and Prodany (1971)	2 & 3	urea, creatinine, water
Babb et al. (1971) & (1972)	1	general model for any uraemic toxin
Gormley & Bell (1971)	3	urea (CSF pressure)
Rameriz et al. (1973)	3	general model for any uraemic toxin
Sausse et al. (1974)	1	urea, creatinine, uric acid, vitamin B
Wideroe et al. (1974)	1	general model for any uraemic toxin
Dombeck et al (1975)	2	creatinine
Popovich et al. (1975)	3 to 5	urea, creatinine, uric acid, vitamin B , insulin

Table 2.3.1 Summary of Compartmental Models of Uraemic Toxins (1965 - 1975)

a particular patient. A combined model also applies to a particular patient although it assumes certain 'average' parameters i.e. protein binding coefficients. Variations between patients are often very large. An example of these variations is shown in Figure 2.3.3. Therefore, although, intuitively, a structural model seems to provide a better description of the pharmacokinetics, it does not follow that a simpler, functional model will not be just as accurate in particular applications.

2.3.2 Rate limiting processes in toxin removal

With respect to removal of toxin from the body, the rate limiting pharmacokinetic process is of critical importance. In the simplest model, a single compartment, the rate limiting step is necessarily the elimination process (or processes). Elimination may involve natural excretion or biotransformation as well as extracorporeal detoxification. Winchester et al. (1974) showed that the natural excretion can be affected by an extracorporeal detoxification device and that the role of the latter in treating a patient is overestimated as a result. Nevertheless, it is true to say that if the natural excretion and biotransformation are effectively constant clearance processes, then the larger the clearance of the extracorporeal device, the more rapid will be the removal of toxin.

In multi-compartment and structural models, however, it is possible for transport between two of the compartments or body regions to be rate limiting. In these cases, increase in the device clearance above a threshold does little to improve the overall rate of toxin removal. This is in spite of the fact that the blood may be substantially cleared of toxin. Once the therapy ceases toxin 'rebounds' into the blood and the concentration rises again. (Gillette, 1973, Widdop et al., 1975 and Martin et al., 1977). Excessive rates of toxin clearance from the blood result in disequilibrium phenomena between body compartments. For example, in haemodialysis for chronic renal failure, large gradients in the concentrations of urea between the cerebrospinal fluid (CSF) and the blood result in osmotic flow of water into the CSF causing nausea. (Kennedy et al., 1964). A small creatinine disequilibrium and subsequent rebound also occurs. (Rastogi et al. 1968).

Clearly it is futile to increase the clearance of an extracorporeal detoxification device above the level where inter-compartment transport forms the rate limiting step in toxin elimination.

The work in this thesis assumes that elimination by the extracorporeal detoxification device is the rate limiting step. Under these conditions the most complex pharmacokinetic model reduces to a single compartment. This simplification provides a rational basis on which to judge the effects of a time dependent inlet concentration on the performance of a perfusion device. There is, of course, an intermediate state where neither the device nor the intercompartment transport is the rate limiting step. In such cases the complex interactions in the pharmaco--kinetic model become significant and the performance of a detoxification device must be judged by modelling the complete pharmacokinetics of each toxin under investigation. In the first instance these interactions are best studied by applying a constant clearance to plasma compartment rather than introducing the complexities of the time dependent clearance of a perfusion device.

2.4 Previous Studies of Mass Transfer in Perfusion Devices

Quantitative investigations in the literature into sorbents are principally directed at industrial applications. Work specific to theraputic medicine in general, and perfusion devices in particular, tends to be empirical. This is true of all major research groups investigating perfusion devices, including the group at the University of Strathclyde (Walker, 1974, Edwards, 1975, Maini, 1975, Townsend, 1977, Courtney et al., 1977 and Gilchrist et al., 1975.) The work in this thesis represents a major break from the empirical tradition. Those studies that have previously broken with this tradition and either quantified the mass transfer parameters or investigated the significance of these parameters on performance, are highlighted below.

2.4.1 Mass transfer in haemoperfusion columns

Dedrick et al. (1967) assumed the rate of toxin removal in a batch experiment to be the maximum rate of removal in a haemoperfusion column. Hence, batch studies could be used to predict the upper limit of clearance in the column. The correspondence between the predicted clearance and clinical data was "remarkable and probably somewhat fortuitous". Considering the assumptions in Dedrick's model and the fact that the rate parameter in the model was "arbitrarily chosen", such correspondence might not have been unexpected.

Dunlop et al. (1976) measured various hydrodynamic, sorption and mass transfer properties in four designs of haemoperfusion column. However, certain features of the experimental technique and the data analysis are dubious. This is discussed further in Sections 3.4 and 3.6. Even accepting the soundness of the experiments and the analysis, the relationship between the system parameters such as the external mass transfer coefficient, and the overall column performance is not discussed. Therefore it is not possible to perceive the real significance of the parameter values.

In the thesis by van Zutphen (1975), the mass transfer properties

of the Adsorber Film device (Section 1.3) were interpreted by comparing experimental results with constant pattern solutions from the literature. However, the existence of a constant pattern curve in the Adsorber was never proven. Therefore, the results are not reliable. In any case, since other haemoperfusion columns do not operate in the constant pattern regime (Section 6.2), such results are not generally applicable.

Holland et al. (1977) examined the performance of the haemoperfusion column, based on carbon impregnated fibres, developed at the Southern Research Institute (Section 1.3). However, the external mass transfer coefficients were calculated using an incorrect analysis. (Section 3.4). As a result the whole significance of the external mass transfer coefficient to the initial performance of a haemoperfusion column was lost. Therefore, although this is a recent publication, its net contribution to our understanding of the performance of haemoperfusion columns is less than that of Dedrick et al. (1967).

Cooney and Sheih (1972) and Chang, F.H.I., et al. (1973) examined the influence of recirculation, i.e. a single pool, patient model, on the performance of a packed bed, perfusion device. However, the results are based on a linear isotherm whereas the isotherms in most medical applications are highly non-linear. In addition, the mass transfer is assumed to be controlled by the intraparticle diffusion described by a simplified linear driving force model (Section 3.4). This too is not typical of existing haemoperfusion columns (Chapter 6). Therefore, although the results are interesting in that they predict the adsorption/desorption effect that can occur in a recirculation experiment, the details are not relevent to existing haemoperfusion columns.

A similar conclusion applies to the perfusion column model proposed by Shettigar and Deepak (1977). They assume a linear isotherm based on experimental data they obtained for activated carbon. These isotherms are quite unlike others in the literature, both in shape and magnitude. (Sparks et al., 1966 , Meier 1972). Further, the parameter values used to predict the typical performance of a haemoperfusion column are totally unrealistic.

The column has about 60 gm of activated carbon (the exact amount is not quoted) but the magnitude of the isotherm capacity results in the above mass being equivalent to about 10 gms of a typical activated carbon. The performance of this equivalent 10 gm column in treating a typical uraemic patient is simulated by combining the column model with a pharmacokinetic model taken from the literature. Not surprisingly, only a negligible mass of toxin is removed. Under these circumstances, conclusions regarding the influence of the system parameters on performance are meaningless. Because the device had so little capacity, the inlet concentration drops less than 5% - typically only 2%. Therefore the model of the patient is superfluous and the result could have been obtained for a single pass input. These shortcomings are disguised by the graphical presentation adopted by the authors.

Neither the simulations of Shettigar and Deepak nor those of Cooney and Sheih and Chang, F.H.I., and co-workers were validated. If they had been, the basic flaws in the assumptions and parameter values would have been identified.

2.4.2 Mass transfer dialysate and ultrafiltrate perfusion devices

Blaney et al. (1968) modelled the mass transfer in a cyclic dialysate regeneration cartridge. Simulations of the model gave excellent predictions of experimental results although details of the model were not given. However, the dialysate regeneration cartridges considered in this thesis are non-cyclic so these results are not applicable.

Decker et al. (1971) presented in vitro data for dialysis against an activated carbon slurry. However, since the basic mass transfer parameters were not measured, the results are not suitable for extrapolation to clinical conditions.

2.4.3 Summary

It is obvious from this review that very little effective work has been done to quantify the controlling mass transfer processes in perfusion devices.

2.5 Thesis Methodology and General Assumptions

The following methodology was undertaken to achieve the thesis aim outlined in the Introduction, i.e. to identify the controlling mass transfer processes in perfusion devices, with particular emphasis on haemoperfusion columns.

Chapter 1 revealed that the most important perfusion device is the haemoperfusion column; hence the emphasis on this type of device. In the main, haemoperfusion columns are constructed as cylindrical, packed beds of sorbent. In addition, all the dialysate and ultrafiltrate regeneration cartridges discussed in Chapter 1 are packed beds. Therefore, a mathematical model, based on this design of column, provides a suitable vehicle with which to achieve the major portion of the thesis aim. Other methods of dialysate and ultrafiltrate perfusion are also modelled, although not to the same depth as with the perfusion column model.

In all cases, the performance of the perfusion device is investigated on the basis of models validated *in vitro*. Having identified the salient mass transfer parameters and quantified their influence on the *in vitro* performance, the results are extrapolated *aprioi* to include pertinent *in vivo* parameters. This rationale allows the fundamentals to be understood in a controlled experimental regime, prior to introducing the uncertainties of *in vivo* performance.

Details of the methodology and the assumptions are outlined below.

2.5.1 Methodology

(i) Develop a simplified mathematical model of a packed bed, perfusion column (Chapter 3)

Unlike previous models of packed bed (sorption) columns, this model included all four mass transfer elements that occur in practical perfusion columns, namely both external and solid diffusion mass transfer resistances, a highly non linear isotherm

and axial dispersion. The simplification was achieved by using a quadratic driving force model for the solid diffusion.

(ii) Estimate the values of parameters in the column model from batch 'in vitro' experiments (Chapter 4)

This included the validation of the quadratic driving force model. Although this model has been used in packed bed models previously, it has not been used to estimate solid diffusivity from batch experiments.

(iii) Validate the column model (Chapter 5)

Very few models of adsorption columns in the literature have been validated - a serious omission. The column model was validated by comparing in vitro experiments on adsorption columns with simulations based on the model and the parameter values estimated in section (ii).

(iv) Use the column model to identify the controlling mass transfer processes in haemoperfusion columns (Chapter 6)

Initially the parameter sensitivity was examined for a constant inlet concentration. This allowed the controlling mass transfer processes to be easily identified. Later studies examined the sensitivity when the model was attached to a single compartment patient model. Because of the knowledge gaps in the relation--ships between the pharmacokinetics and the clinical condition of a patient it was logical to identify the rate controlling processes under these, the simplest possible clinical conditions.

(v) Introduce 'in vivo' features associated with haemoperfusion (Chapter 6)

This was an extension of the simple in vitro column model to include clinical features that occur in acute poisoning and acute hepatic failure such as protein binding and distribution in the red blood cells.

(vi) Identify the controlling mass transfer processes in dialysate and ultrafiltrate devices (Chapter 7)

In each case the performance of the overall detoxification system was considered, i.e. the dialyser or ultrafilter plus the sorbent element. Hence, mass transfer models of dialysers and ultrafilters were introduced. The contribution of the sorbent to the overall performance was identified in semi--quantitative terms by using asymptotic solutions of simplified models of each device. The details vary from device to device. Although the perfusion column model was applicable to dialysate and ultrafiltrate regeneration cartridges, the operation of these devices was such that asymptotic solutions were sufficient to examine the important mass transfer features.

2.5.2 Assumptions

An implicit assumption in this methodology is that the mass transfer in a perfusion device provides a meaningful measure of the clinical performance. Direct measurements of toxin removal (i.e. clearance) only have significance if (a) the toxin (or toxins) has been positively identified and (b) if the relation--ship between concentration of the toxin in the blood (or other tissue compartment) and the clinical symptoms is understood. Both assume the toxin (s) can be readily measured. From Chapter 1 it is clear that the identity of most toxins in acute hepatic failure and chronic renal failure is uncertain. This is not such a problem in acute poisoning, however the relationship between toxin concentration and symptoms, in these cases, is often obscure. Therefore at present it is not possible to draw up a performance specification simply in terms of blood concentrations.

Clinically the performance of blood detoxification devices is assessed largely by indirect methods, e.g. by monitoring changes in clinical condition and symptoms such as coma level in the patient. Changes in toxin concentration in the blood, where the toxin or suspected toxin can be measured, is only of secondary importance. Such data merely adds to the overall clinical

picture of the patient.

In the absence of a precise mass transfer specification, perfusion devices are designed and applied clinically by a process of intuition and empiricism. This thesis does not attempt to solve the problem of mass transfer specification, however identification of the controlling mass transfer processes in such devices will make the above process less intuitive and less empirical.

Another major assumption on which this thesis is based is that there is no competitive adsorption or ion exchange in the sorbent-based devices. From Chapter 1 it is clear that all cases of blood detoxification involve more than one possible toxin. Therefore, the possibility arises that toxins will compete for sorption sites. Where multiple sorption occurs it is assumed to be independent and therefore non-competitive, i.e. different toxins bind to different sites on the sorbent. This is discussed further in Section 3.2.

The work also assumes the extracorporeal detoxification device is the rate limiting element in the elimination of toxin. This was discussed in Section 2.3. Other minor assumptions are highlighted in the appropriate sections in subsequent chapters.

CHAPTER 3

MODELS OF SORPTION AND MASS TRANSFER IN BATCH EXPERIMENTS AND PERFUSION COLUMNS

CHAPTER 3

MODELS OF SORPTION AND MASS TRANSFER IN BATCH EXPERIMENTS AND PERFUSION COLUMNS

3.1 Introduction

The basic sorption and mass transfer processes associated with the removal of a solute from solution by a granular adsorbent or ion exchange resin are well documented in the industrial and chemical engineering literature. Mathematical models describing these processes are reviewed in this chapter. From this review suitable individual models and combinations of models are chosen to meet two of the thesis objectives:- construction of a simplified model of a perfusion column and quantification of individual mass transfer parameters from in vitro experiments.

3.2 Models of Adsorption and Ion Exchange

Although adsorption and ion exchange are very complex processes at a molecular level it is possible to characterize the net movement of molecules or ions onto the sorbent by an equilibrium isotherm. Experimentally, an equilibrium state exists between the quantity of sorbate adsorbed or exchanged and the concentration of the sorbate in the adjacent fluid. This is assumed to be an instantaneous, dynamic equilibrium, sorbate being adsorbed and desorbed at equal rates with a net (equilibrium) quantity of sorbate on the sorbent at any time. The functional relationship between the net quantity of sorbate adsorbed or exchanged and the sorbate concentration in the fluid at equilibrium is an equilibrium isotherm. (Isotherm because the equilibrium is temperature dependent and so must be measured at constant temperature.) The most convenient way to incorporate experimental isotherms into a mathematical model is to fit a continuous algebraic function to the data.

i.e. $q = F(c)$ at constant temperature

where q = quantity adsorbed or exchanged per unit weight or sorbent or solid phase concentration

and c = concentration of sorbate in the fluid in contact with the sorbent or fluid phase concentration

3.2.1. Adsorbent isotherms

Several theoretical studies have predicted the form of the function, F, for adsorption of gases. These expressions are based on either the molecular kinetics at the adsorbent/fluid interface or the thermodynamics of adsorption . The most widely used are the Langmuir and the Freundlich equations. The Freundlich equation was originally empirical although it has subsequently been derived theoretically. (Smisek and Cerny, 1970).

For adsorption from dilute solutions, however, the kinetic and thermodynamic complexities prohibit the derivation of theoretical equations for the equilibrium isotherms. In the absence of such equations any suitable algebraic function of concentration can be used to describe the adsorption

isotherm. However, because of the historical links with gaseous adsorption, the Langmuir and Freundlich equations are the principal expressions for describing equilibrium isotherms for adsorption from dilute solution. The Langmuir and Freundlich equations are given below.

$$\text{Langmuir Equation;} \quad q = \frac{A\,c}{1+Bc} \qquad \text{EQ.3.1}$$

$$\text{Freundlich Equation;} \quad q = \eta\, c^{\beta} \qquad \text{EQ.3.2}$$

These equations can be conveniently normalized with respect to the maximum fluid-phase concentration, c_o and the corresponding maximum solid-phase concentration, q_o . After rearrangement, Equations 3.1 and 3.2 become

$$Y = \frac{X}{R + (1-R)X} \qquad \text{EQ.3.3}$$

$$Y = X^{\beta} \qquad \text{EQ.3.4}$$

where $Y = q/q_o$, $X = c/c_o$ and $R = 1/(1+Bc_o)$

The ratio, R, is called the equilibrium parameter and it defines the shape of the Langmuir isotherm. Figure 3.2.1 shows the shape of the normalized Langmuir and Freundlich isotherms for varying values of R and β respectively. An isotherm that has a decreasing slope (i.e. R or $\beta<1$) is referred to as favourable while one with an increasing slope (R or $\beta>1$) is unfavourable. The intermediate case, where R and β equal one, is the linear isotherm. Linear isotherms seldom occur in practice. However, because a linear isotherm simplifies the mathematics and facilitates algebraic solutions to many problems, theoretical studies of adsorption devices often assume this type of isotherm. (Weber and Chakravorti, 1974.)

Most adsorbate/adsorbent combinations exhibit a favourable isotherm. The upper limit of the favourable isotherm, the irreversible isotherm, occurs when R or β is zero. Then the amount adsorbed is constant irrespective of the fluid-phase concentration. Therefore, if the concentration decreases, no net desorption of adsorbate occurs, i.e. the adsorption process is irreversible. The assumption of irreversible adsorption also simplifies the mathematics. Systems

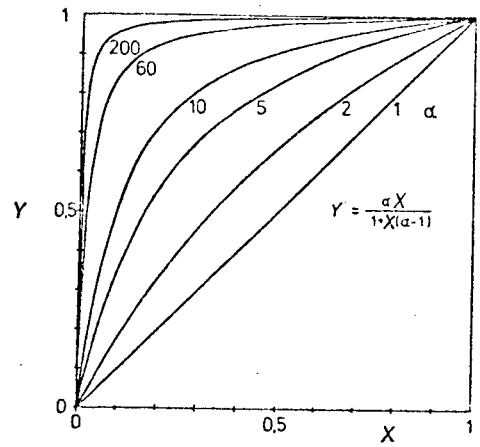

Langmuir Isotherm
(R = 1 / α)

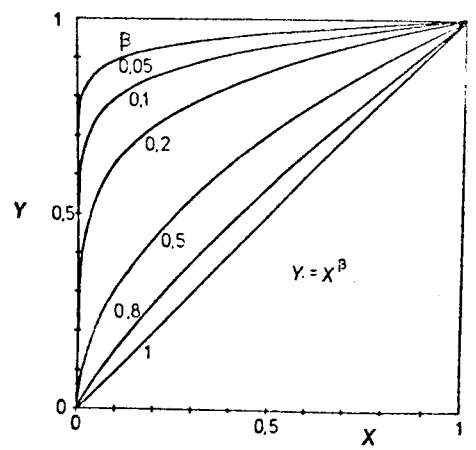

Freundlich Isotherm

Figure 3.2.1 Shapes of Normalized Isotherms
(after Neretnieks, 1976 a)

with highly non-linear isotherms have been modelled successfully by assuming irreversible adsorption. (Dedrick and Beckman, 1967; Weisz and Hicks, 1967; Weisz and Zolleringer, 1967; DiGiano and Weber, 1972; Suzuki and Kawazoe, 1974 and Spahn and Schlunder, 1975.)

Although Langmuir and Freundlich isotherms have different shapes there is often nothing to choose between the two given the usual experimental spread in isotherm data. (Meier, 1972). Nevertheless, Freundlich isotherms are more sensitive if a wide range of fluid-phase concentration (several decades) is involved. (Sparks et al., 1977). When three or more decades of fluid-phase concentration are spanned, a combination of isotherms is usually required. Weber and Morris (1964) used separate Langmuir equations to describe respectively the 'high' and 'low' concentration isotherms for a set of data. Dedrick and Beckmann (1967) and Spahn and Schlunder (1975) employed the same approach with separate Freundlich equations to cover different sections of the isotherm (about two decades to each section). Dedrick and Beckmann also fitted a combined linear/Langmuir isotherm to their data. Mathews (1975) developed an empirical, Langmuir/Freundlich, combined isotherm to fit his results.

3.2.2 Ion exchange isotherm

For the exchange of homovalent ions on a resin, i.e.

$$A^{+} (sol^{n-}) + B\ (resin) \rightleftharpoons A\ (resin) + B^{+} (sol^{n-})$$

the equilibrium can be expressed by a simple mass-action relation

$$K = \frac{q_A\ c_B}{q_B\ c_A} \qquad \text{EQ.3.5}$$

where K = equilibrium constant or selectivity coefficient.

q = molar conc. of ions on resin or solid-phase conc.

c = molar conc. of ions in solution or fluid-phase conc.

subscripts A and B refer to the two ions.

Since it is an exchange process the total number of ions on the resin and in solution are known from the initial conditions. If these are

respectively, q_o and c_o and if Equation 3.5 is normalized with respect to these, then

$$K = \frac{Y\ (1 - X)}{X\ (1 - Y)} \qquad \text{EQ.3.6}$$

where $Y = q_A / q_o$ and $X = c_A / c_o$

Equation 3.6 can be rearranged to give Y as a function of X, i.e.

$$Y = \frac{X}{R + (1-R)\ X} \qquad \text{EQ.3.7}$$

where $R = 1/K$

Therefore, the homovalent ion exchange equilibrium is equivalent to a Langmuir adsorption isotherm with the equilibrium parameter, R, equal to the inverse of the ion exchange equilibrium, K. Hence general mass transfer solutions using a Langmuir isotherm are valid for both physical adsorption and homovalent ion exchange.

Heterovalent ion exchange is more complex. Approximations based on the Langmuir isotherm are given by Vermeulen, (1958) and Hiester and Vermeulen, (1952). However, heterovalent ion exchange is outwith the scope of this thesis.

3.2.3 Multiple sorbates

Every application of sorbents in medicine involves more than one potential sorbate. Even in acute poisoning where there is only one toxin sorbate, other non-toxic metabolites or ions in the blood may be adsorbed or exchanged. These sorbates may compete for the sorption sites i.e. competitive adsorption or ion exchange. In these cases a competitive equilibrium isotherm is used. Competitive isotherms are traditionally described by an extended Langmuir equation (Perry et al., 1973), i.e.

$$q_i = \frac{A_i\ c_i}{1 + \sum B_i c_i} \qquad \text{EQ.3.8}$$

Typically only binary sorbate systems are studied. Mathews (1975) and Jain and Snoeyink (1973) investigated binary sorbate isotherms for phenolic compounds on activated carbon. Both employed modified versions of equation 3.8 with limited success.

Sparks et al. (1977) considered the limiting case of competitive sorption from blood in vitro. Single sorbate isotherms for activated carbon and ion exchange resins in buffer solutions of barbiturate were compared with the corresponding isotherms in plasma and blood. The reduction in equilibrium capacity (up to four fold) was attributed to equilibrium competition for sites by metabolites in the blood. As the effect of protein binding was not delineated it is impossible to say that the capacity reduction was due entirely to competitive sorption.

Applications of competitive isotherms to mass transfer models of sorbent devices are fairly recent. Hsieh et al. (1977) produced the first general model of a multiple adsorption column with fluid film and intraparticle diffusion resistances. Even so, the solid diffusion was only described by a linear driving force model. Previous models by Weber and Crittenden (1975) and Bradley and Sweed (1975) neglected intraparticle and external diffusion respectively. Klein et al. (1967) modelled the equilibrium condition i.e. where all mass transfer resistance is negligible. The model by Hsieh and co-workers provides a test bed on which to increase our knowledge of competitive adsorption in sorption columns. Unfortunately, it has not been validated by experimentation, so the results must be accepted cautiously. Bradley and Sweed (1975) made the critical observation that multiple solute analyses are restricted by our ability to obtain the required kinetic and adsorption data.

Before possible competitive adsorption and ion exchange can be considered in perfusion devices it is crucial that the single solute kinetics are thoroughly understood. Therefore, this thesis, in common with the majority of the work in the literature, is concerned only with single solute sorption, i.e. single solute isotherms as discussed previously. This is not such a major limitation as it may first appear. If each type of sorbate is adsorbed or

exchanged on different sites on the sorbent then the sorption processes are independent, and each of the sorbates can be considered as separate cases of single solute sorption. That is, multiple sorbates and single solute sorption are not necessarily mutually exclusive terms.

3.3 Intraparticle Diffusion

Adsorbents are either natural or synthetic materials of microporous structure with complex internal pores. The pores range from several Angstroms diameter up to 10,000A , although most of the internal volume is associated with pore diameters less than 50 A. The adsorption capacity results from the large internal surface area afforded by the pore structure (e.g. 500 to 1200m / gm). However, the pore structure also provides a tortuous route which the sorbate must negotiate in diffusing from the fluid surrounding an adsorbent particle to the internal adsorptive surface. Similar conditions apply in ion exchange resins.

The ion exchange resins employed in blood detoxification devices consist of a synthetic polymeric matrix. The exchangable ions are distributed evenly throughout the resin particle, attached to the many branches of the matrix. This matrix is either a 'gel' type resin or a macroporous resin. Gel type resins are hydrophilic and swell on immersion in aqueous solution. The sorbate ion reaches the exchange sites deep in the resin particle by diffusing through the swollen copolymer matrix. Macroporous resins have a greater degree of cross linking in the matrix. This causes a pore structure, similar to that in adsorbents, to develop. Ions diffuse through macroporous resins either along the formed pores or through the swollen matrix between the pores (as in the gel type).

3.3.1 Intraparticle diffusion mechanisms

The structure of every granule of a given sorbent is different and the path taken by an individual sorbate molecule through the granule is probably unique. Nevertheless it is possible to predict quite accurately the net movement of molecules in a granule by applying very simplistic models of intraparticle diffusion. Two types of model based on Fickian diffusion have been proposed, viz., pore diffusion and solid or surface diffusion. In both cases all the sorbent granules are assumed to be identical and homogeneous. Most models assume spherical granules although a limited number consider

cylindrical ones.

In pore diffusion the sorbate diffuses through the pores, in the fluid-phase. There is radial symmetry and at each point in the particle the fluid-phase sorbate is in equilibrium with the solid-phase sorbate on the adjacent internal surface, in accordance with the equilibrium isotherm. The rate equation at any radial point is given by

$$\varepsilon_p \frac{\partial c}{\partial t} + \rho_p \frac{\partial q}{\partial t} = D_p \varepsilon_p \left(\frac{\partial^2 c}{\partial r^2} + \frac{a}{r} \frac{\partial c}{\partial r} \right) \qquad \text{EQ.3.9}$$

where ε_p = porosity of particle

ρ_p = apparent density of particle

D_p = pore diffusivity (assumed constant)

c = fluid-phase concentration

q = solid-phase concentration

r = radius of particle

a = geometric constant

= 1, for cylinders

= 2, for spheres

The solid or surface diffusion model assumes the sorbate diffuses in the solid-phase. The equilibrium isotherm applies between the fluid-phase and solid-phase concentrations at the external surface of the particle as well as at the internal surfaces of the pores. The rate equation for solid diffusion is

$$\varepsilon_p \frac{\partial c}{\partial t} + \rho_p \frac{\partial q}{\partial t} = D_s \rho_p \left(\frac{\partial^2 q}{\partial r^2} + \frac{a}{r} \frac{\partial q}{\partial r} \right) \qquad \text{EQ.3.10}$$

where D_s = solid diffusivity (assumed constant).

The amount of sorbate accumulated in the fluid-phase within the particle is usually only a fraction of that in the solid-phase. Therefore the first term in Equations 3.9 and 3.10 is often omitted.

Pore and solid (or surface) diffusion are sometimes assumed to occur in parallel. The rate equation for this combined diffusion model is formed by adding the right hand side of Equation 3.9 to that of Equation 3.10.

$$\varepsilon_p \frac{\partial c}{\partial t} + \rho_p \frac{\partial q}{\partial t} = D_p \varepsilon_p \left(\frac{\partial^2 c}{\partial r^2} + \frac{a}{r} \frac{\partial c}{\partial r} \right) + D_s \rho_p \left(\frac{\partial^2 q}{\partial r^2} + \frac{a}{r} \frac{\partial q}{\partial r} \right) \quad \text{EQ. 3.11}$$

The solid and pore diffusivities, D_s and D_p, are calculated for a sorbate/sorbent pair on the basis of batch experiments. A quantity of sorbent is placed in a well mixed bath of sorbate solution and the fall in sorbate concentration with time is monitored. The sorbate kinetics are then simulated using one of the intraparticle diffusion models together with the isotherm and, if applicable, a model of external diffusion (Section 3.4). The diffusivity is adjusted until the simulation matches the experimental results.

The pore diffusivity is related to the diffusivity of the sorbate in the sorbent by the following equality.

$$D_p \equiv \frac{D_l}{\mu}$$

where D_l = diffusivity of sorbate in the solvent

μ = tortuosity factor

However, the majority of papers that consider pore diffusion do not include the porosity on the right hand side of Equation 3.9. Therefore, the effective value of pore diffusivity is $D_p \varepsilon_p$. Hence the above equality becomes

$$D_{pore} \equiv \frac{\varepsilon_p D_l}{\mu}$$

where D_{pore} = effective diffusivity = $\varepsilon_p D_p$

The tortuosity factor is an empirical coefficient that relates the pore and liquid diffusivities. Values of μ usually fall within the range 2 to 6. (Suzuki and Kawazoe, 1974 and Di Giano and Weber, 1972.) However, as it is not possible to estimate the tortuosity independently, the above formulae cannot be used to predict the pore diffusivity apriori. Likewise, the solid diffusivity cannot be predicted in advance.

Experimental values of pore and solid diffusivities vary greatly from sorbent to sorbent (for a given sorbate). For instance, Spahn and Schlunder (1976) measured the pore diffusivities of phenylacetic acid in eleven types of activated carbon and found the values ranged from 3.0×10^{-9} to 3.0×10^{-10} cm^2/sec, a factor of 10. Examination of the values of pore and solid diffusivity given in the literature reveals no simple correlation between the diffusivity for a given sorbate and the internal, physical properties of the sorbent. In addition, there is no general relationship between the size of a sorbate molecule and the diffusivity in a particular sorbent. Therefore, it is necessary to measure the intraparticle diffusivity directly for each sorbent and sorbate combination. In order to do this one must first choose which of the above models provides the best description of the intraparticle diffusion.

3.3.2 Comparison of intraparticle diffusion mechanisms

The choice of intraparticle diffusion mechanism is potentially a difficult one. Pore and solid diffusion are only the theoretical extremes of the molecular transport processes that may occur in a sorbent particle. Combined diffusion is an intermediate compromise. All three mechanisms involve gross simplifications of reality. At best they are only functional models of intraparticle diffusion. Despite this, reviews on mass transfer in sorbent particles relate the diffusion mechanism to the structure of the sorbent, i.e. pore diffusion in porous adsorbents and solid diffusion in gel type ion exchange resins. (Perry et al., 1975 and Vermeulen, 1958). If a sorbent particle has a porous structure it does not necessarily follow that the pore diffusion model will provide the best description of the kinetics.

Fortunately the need to choose between intraparticle diffusion mechanisms is eliminated if appropriate batch experimental conditions are employed. Hashimoto et al. (1975) compared the exact solutions for pore and solid diffusion, respectively, in a theoretical batch experiment where the external mass transfer resistance was zero. Provided a total of not more than 80% of the original sorbate in solution was adsorbed or exchanged, then there was no significant difference between the sorbate kinetics for the two mechanisms (i.e. within the usual scatter of experimental data). This was supported by a similar theoretical study by Neretnieks (1976a). In most batch experiments however, the external mass transfer resistance although quite small, is not zero. Nevertheless, it is reasonable to assume that the pore and solid diffusion kinetics retain their similarity so long as the intraparticle diffusion is the dominant mass transfer resistance (Neretnieks, 1976b).

If the batch kinetics based on pore and solid diffusion are indistinguishable, it is only necessary to use one of the models to calculate the intraparticle diffusivities. The corresponding values of D_s and D_p are simply related by the particle distribution ratio , Λ_p where

$$\Lambda_p \equiv \frac{\rho_p q_o}{c_o} \qquad \text{and} \qquad D_s \equiv \frac{D_p \varepsilon_p}{\Lambda_p}$$

Dedrick and Beckmann (1967) and Hashimoto et al. (1975) compared the two models in batch experiments with several types of activated carbon and confirmed the theoretical studies. In the cases where more than 80% of the sorbate was removed, and the simulated kinetics diverged , the experimental data was best simulated by the solid diffusion model. This trend also applied when Hashimoto et al. (1977) compared simulations of a packed bed, perfusion column based on pore and solid diffusion respectively.

These results suggest that, when the two intraparticle kinetics diverge, solid diffusion may provide a better model for activated carbon. In this thesis the intraparticle diffusion is described by a solid diffusion model.

3.3.3 Approximations to intraparticle diffusion equations

The intraparticle diffusion equations 3.9, 3.10 and 3.11 combine with the equilibrium isotherm to form complex non-linear partial differential equations, the solutions of which are often unstable, (Huang, 1975). The aim of this thesis is to identify the controlling mass transfer processes in perfusion devices and not the stability criteria of non-linear partial differential equations. Therefore, simplified models of intraparticle diffusion were employed, i.e. models that are both straightforward, stable and, above all, easy to apply.

Several simplified rate equations have been developed to approximate solid diffusion in sorbent particles. Glueckauf and Coates (1947) proposed an empirical, linear driving force (LDF) expression for the rate of accumulation of sorbate in the particle, i.e.

$$\frac{d\bar{q}}{dt} = k_l \left(\frac{D_s}{d_p^2}\right) \left(q^* - \bar{q}\right) \qquad \text{EQ.3.12}$$

where $\bar{q}$ = average solid-phase conc. in particle

q^* = solid-phase conc. at the external surface of the particle (in equilibrium with the adjacent fluid phase.)

k_l = empirical coefficient for LDF model

d_p = diameter of particle

The value of k_l is found by comparison of the exact solutions to diffusion problems with those based on the LDF approximation.

Vermeulen (1953) proposed a similar rate expression based on a quadratic driving force (QDF)., i.e.

$$\frac{d\bar{q}}{dt} = k_q \left(\frac{D_s}{d_p^2}\right) \left(\frac{q^{*2} - \bar{q}^2}{2\bar{q}}\right) \qquad \text{EQ. 3.13}$$

where k_q = empirical coefficient for QDF model

Different values have been assigned to the empirical coefficients, k_l and k_q . By comparison between the exact and approximate solutions for the shape of the constant pattern breakthrough curves for an irreversible isotherm Vermeulen (1953) suggested k_l and k_q were both equal to $4\pi^2$ Subsequently, Vermeulen (1958) developed a general expression for k_q based on the shape parameter, R, of the isotherms, and a second empirical coefficient ψ_q where

$$k_q = 60\psi_q$$

and

$$\psi_q = \frac{\pi^2}{(\pi^2 R + 15(1-R))} \qquad \text{EQ.3.14}$$

Hall et al. (1966) refined this expression and developed a similar expression for ψ_l in the linear driving force model. For a given value of R, the midpoint slopes of the constant pattern breakthrough curves based on the LDF and QDF rate equations were equated to the slopes of the exact solution by varying ψ_l and ψ_q respectively. The resulting expressions for ψ_q and ψ_l were

$$\psi_q = (R^{1.5} + 1.688\,(1-R))^{-1} \qquad \text{EQ.3.14a}$$

$$\psi_l = (R^{1.06} + 1.125\,(1-R)^{1.06})^{-1} \qquad \text{EQ.3.15}$$

Other more complex rate expressions for solid diffusion were suggested by Gluenkauf (1955)

$$\frac{d\bar{q}}{dt} = 4\pi^2 \left(\frac{D_s}{d_p^2}\right)(q^* - \bar{q}) + \left(1 - \frac{\pi^2}{15}\right)\frac{dq^*}{dt} \qquad \text{EQ.3.16}$$

$$\frac{d\bar{q}}{dt} = 4\pi^2 \left(\frac{D_s}{d_p^2}\right)(q^* - \bar{q})\left(\frac{3}{4}q^* + \frac{1}{4}\bar{q}\right)/\bar{q} \qquad \text{EQ. 3.17}$$

However, unlike the LDF and QDF rate equations, Equations 3.16 and 3.17 were not adopted by other authors.

An empirical rate equation for pore diffusion was proposed by Vermeulen and Quilici (1970). It is written in terms of the normalized, solid-phase concentration even though pore diffusion is by definition, diffusion of sorbate in the fluid-phase, i.e.

$$\frac{dY}{dt} = \psi_p \left(\frac{60\ D_p}{\Lambda_b\ d_p^2}\right) \left\{\frac{Y^* - \bar{Y}}{\sqrt{1 - (1-R)\ \bar{Y}}}\right\} \qquad \text{EQ. 3.18}$$

where $Y = q/q_o$, $Y^* = q^*/q_o$ and $\bar{Y} = \bar{q}/q_o$

Λ_b = bed distribution coefficient

$$= \frac{\rho_b q_o}{c_o}$$

ρ_b = bulk (or bed) density

ψ_p = empirical coefficient for pore diffusion

The coefficient, ψ_p , is based on the midpoint slope of the constant pattern breakthrough curve (as per Hall et al., 1966).

$$\psi_p = \left(R^{2.00} + 1.83\ (1-R)^{0.92}\right)^{-1} \qquad \text{EQ.3.19}$$

In the literature, the above rate equations have been used almost exclusively to predict breakthrough curves. One of the few exceptions is Spahn and Schlünder (1975), where solid diffusivities were estimated from batch experiments with a LDF approximation. Although the LDF approximation gives reasonable results for constant pattern breakthrough curves it is far too insensitive to accurately predict the kinetics in a batch system. Not surprisingly, therefore, the results of Spahn and Schlünder were unsatisfactory. In this thesis the more sensitive QDF approximation is used to find the solid diffusivities.

3.3.4 Validation of QDF approximation

The quadratic driving force approximation does not have to be validated rigorously since the same model is used both to estimate the solid diffusivity and to describe the intraparticle diffusion in the complete perfusion column model. However, as this approximation has not been used in the literature to estimate solid diffusivities, it is instructional to compare simulations of the

sorbate kinetics in a batch experiment produced by the exact and approximate solid diffusion models respectively.

Equation 3.13 was developed for spherical geometry. However, since one of the sorbents investigated in this thesis is in the form of a cylindrical pellet, it was necessary to validate the QDF approximation both for spherical and cylindrical geometries. For convenience, it was assumed that the form of the rate equation is the same for both cases. Hence, the value of the coefficient k_q determines the shape of the respective sorption kinetics. Exact solutions exist for solid diffusion in spheres and infinite cylinders where the external diffusion resistance is zero and the surface concentrations (fluid and solid) are constant (Section 3.5.2). These solutions are presented in the form of a infinite series by Crank (1975) and as numerical values by Berthier (1952). The assumption of constant surface concentrations is equivalent to having an irreversible isotherm. Simulations of the batch kinetics based on the QDF approximation and an irreversible isotherm were compared with these exact solutions. The results are presented in Figure 3.3.1.

By using $\log\tau$ rather than τ as the abscissa, the shapes of spherical and cylindrical particle kinetics, for the QDF approximation, become identical. Differences in the values of k_q for the two types of particle merely cause the kinetic curve to be displaced horizontally. This horizontal shift equals the log of the ratio of the k_q values. Hence, the effect of changes in k_q can be found by sliding the QDF kinetics horizontally.

For spheres, agreement between the exact and approximate solutions is excellent for fractional saturations greater than 0.5 and k_q equal to the value suggested by Hall et al. (1966) for an irreversible isotherm (i.e k_q = (60/1.688)= 35.55). Differences between the solutions for fractional saturations less than 0.5 is compensated by the fact that the kinetics in at least part of this region are controlled by fluid film resistance, and not intraparticle diffusion, in a typical batch experiment.

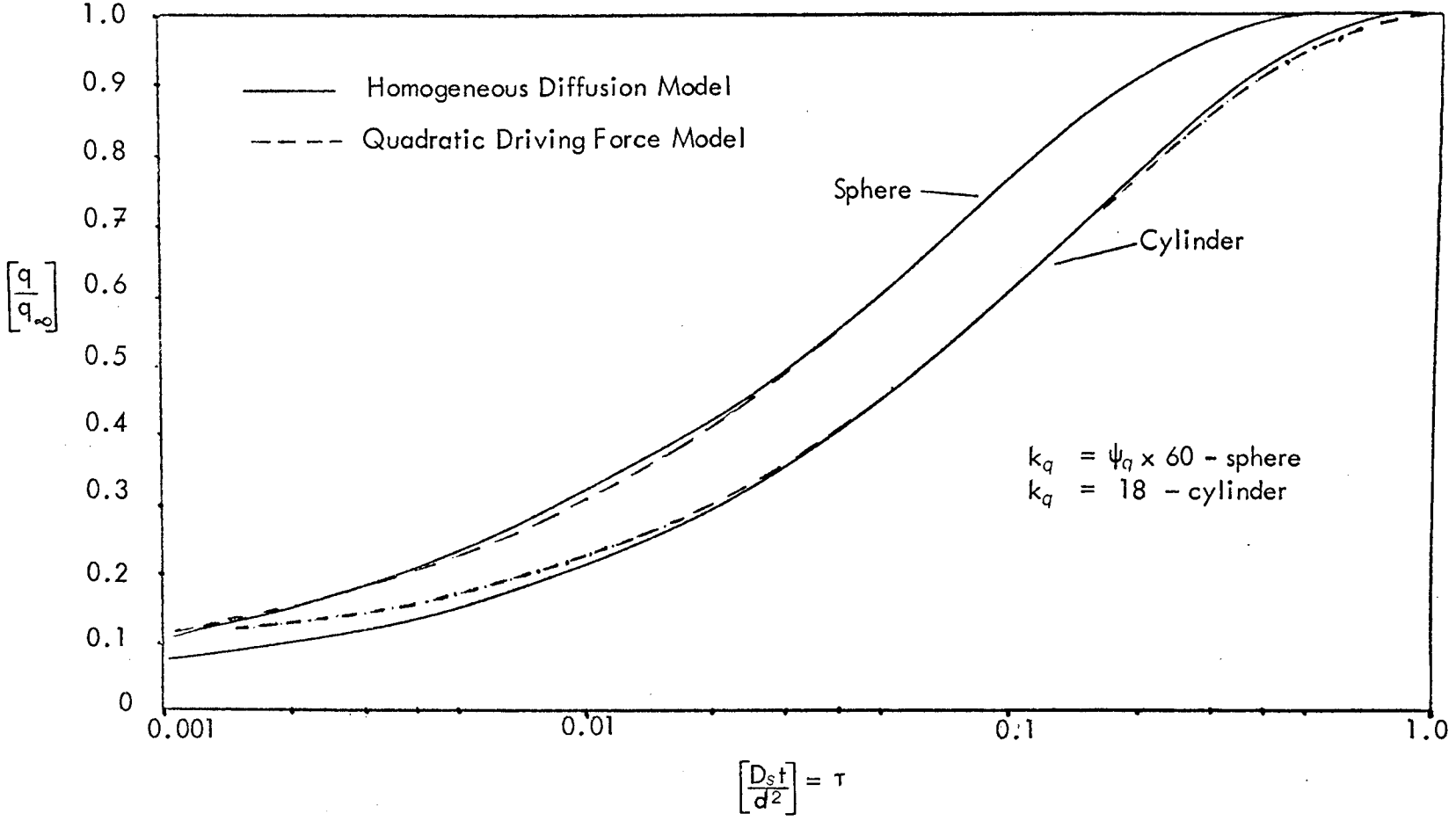

Figure 3.3.1 Comparison of Homogeneous Diffusion and QDF Driving Force Models

The agreement between the two solutions for the infinite cylinders is not nearly so good. Large errors occur at both extremes of saturation. As with the spheres the discrepancies at the low fractional saturations will be largely marked by the fluid film resistance in most experiments. However, those at large saturations will always exist. The apparent diffusivity in this region is larger than that in the central portion of the sorption kinetics. If the QDF solution is adjusted to contain the exact solution over the range of fractional saturation, 0.2 to 0.98, then k_q varies from 16 to 21. Therefore experimental results should fall within the limits of the QDF model for these values of k_q . If k_q has a value of 18 the QDF model provides a good fit over the range 0.3 to 0.7. Therefore, with infinite cylinders, ψ_q equals (18/60) = 0.3 for R equal to zero.

Hall et al. (1966) showed that the value of k_q depends upon the value of R for diffusion in spheres. Presumably a similar dependence applies to k_q for sorption in infinite cylinders. However, since the preceding analysis only considers the case of an irreversible isotherm it is not possible to predict the form of the dependence. In the absence of this data, it is assumed that k_q is constant for all R. This does not affect the results of the simulations as the same assumption applies both to the estimation of D_s in the batch experiment and to the use of that D_s in the perfusion column model. However, it does imply that the value of D_s may differ from that predicted from the solid diffusion equation.

An important observation, based on a comparison of the sorption kinetics in spheres and cylinders, is that the effective solid diffusivity in a sphere is approximately twice that in an infinite cylinder i.e. if the diffusivity in the cylinder is double that in the sphere then the two kinetics will roughly coincide. Therefore, if a particular sorbent material has an intrinsic diffusivity due to its structure, then spherical particles will produce faster sorption kinetics than cylindrical ones of the same diameter.

3.3.5 Effect of particle size distribution on intraparticle diffusion

The solid diffusion kinetics are dependent upon the inverse square

of the particle diameter. Studies in the literature use the average particle size in the range to estimate the solid diffusivity. However, since the kinetics are related to the square of the diameter, size effects are much larger than might at first be thought.

Assume the distribution of particle sizes is uniform across the range of mesh sizes. Initially, the small size particles dominate the kinetics. As equilibrium is approached the larger particles dominate. Therefore, the overall kinetics will fall between the two limits set by the solutions for maximum and minimum particle sizes respectively. Hence, it is unlikely that a single solution based on the mean particle diameter will provide a good fit to all the experimental data. It is not surprising therefore that the models in Furusawa and Smith (1974) and Hashimoto et al. (1975) did not provide an accurate simulation over the complete kinetics. Conversely, one is suspicious of models that do provide excellent simulations where a range of particle sizes is involved, i.e. Suzuki and Kawazoe (1974).

By considering the ratio (D_s / d_p^2) in the solid diffusion model it is possible to quantify the effect of d_p upon the sorption kinetics. If D_s is based on the average value of d_p then, the kinetic solutions for the maximum and minimum values of d_p, i e. d_{max} and d_{min}, have effective diffusivities equal to

$$D_{max} \equiv D_s \left(\frac{d_{av}}{d_{min}}\right)^2 \quad \text{and} \quad D_{min} \equiv D_s \left(\frac{d_{av}}{d_{max}}\right)^2$$

Table 3.3.1 shows values of D_{max} and D_{min} for various ranges of mesh sizes used in the literature. These values reveal that the apparent solid diffusivity at the extremes of the batch kinetics may be 20% larger or smaller than the actual value.

The effect of particle size on the kinetics is seen clearly in the simulations of the experimental results in Section 4.3.

Mesh Range	Particle Sizes (mm)	Average Diameter (mm)	$\frac{D_{s_{max}}}{D_s}$	$\frac{D_{s_{min}}}{D_s}$	Study
	0.210-0.246	0.228	1.185	0.862	
	0.246-0.295	0.271	1.22	0.845	Furusawa and Smith (1974)
	0.495-0.589	0.542	1.20	0.85	
	0.701-0.833	0.767	1.20	0.85	
	0.833-0.991	0.912	1.20	0.85	
30/35	0.51-0.58 [1]	0.548	1.16	0.90	Mathews (1975)
35/40	0.41-0.51 [1]	0.459	1.26	0.81	Meier (1972)
48/60	0.25-0.30 [1]	0.273	1.20	0.83	Huang (1974)

Note 1) Approximate size range.

Table 3.3.1 Effect of Particle Size on Apparent Solid Diffusivity

3.4 External Diffusion

There are two mechanisms involved in the development of the external diffusion resistance in perfusion devices : the fluid film resistance and the membrane resistance. The first is common to all devices while the second occurs only in haemoperfusion columns where the sorbent is coated with a bio--compatible membrane.

The fluid film resistance is visualized as resulting from a laminar sublayer adjacent to the sorbent particle. For turbulent bulk flow, the physical existence of a laminar sublayer has been questioned. Recent models have, in one instance, replaced the laminar sublayer by an eddying sublayer and in another, abandoned the concept of a discrete boundary layer altogether (Skelland, 1974). Nevertheless, the boundary layer analogy provides a simple and accurate model for external diffusion. The membrane resistance is measured by assuming the membrane is a homogeneous, solid phase through which the sorbate molecules can diffuse. The membrane is also assumed to be of uniform thickness, although this is known not to be the case (Meier, 1972).

The fluid film boundary layer and the membrane are assumed to form two concentric shells around the sorbent particle. As both of these shells are very thin (typically several microns), the diffusion resistance through each of them is calculated on the assumption of parallel geometry. The two resistances are in series, thus the combined external resistance is equal to the sum of the two. Therefore, since the diffusion resistance is equal to the inverse of the mass transfer coefficient, we have

$$\frac{1}{k_e} = \frac{1}{k_f} + \frac{1}{k_m} \qquad \text{EQ.3.20}$$

where k_e = external mass transfer coefficient

k_f = fluid-film mass transfer coefficient

k_m = membrane mass transfer coefficient

The membrane mass transfer coefficient is equal to the effective sorbate diffusivity in the membrane divided by the membrane thickness. In accordance with Fickian diffusion, the mass transfer rate, $\dot{m}$, at the external surface of the sorbent is given by

$$\dot{m} = k_e A_p (c_b - c_s) \qquad \text{EQ.3.21}$$

where A_p = total external surface area of particles

c_b = mixing cup conc. in bulk fluid

c_s = fluid phase conc. at the particle surface

As there is no accumulation of sorbate at the surface of the particle, the mass transfer rate at the external surface of the particle must equal that within the particle, driven by intraparticle diffusion.

The fluid film mass transfer coefficient can be measured experimentally or estimated from correlations in the literature. These two methods are discussed below for batch experiments (agitated particle suspensions) and packed beds respectively.

3.4.1 External diffusion in batch experiments

In a batch experiment the sorbate concentration in bulk fluid has a finite initial value. The corresponding liquid phase concentration at the surface of the particle is zero. Therefore $k_e A_p$ can be calculated directly from the initial mass transfer rate (i.e. the rate of sorbate removal from the bulk fluid) and the initial bulk concentration using Equation 3.21. Alternatively, this equation can be integrated at $t = o$ to give

$$k_e = \frac{V_b}{A_p} \times \frac{d}{dt} \left[\ln \frac{c_o}{c_b} \right]_{t=o} \qquad \text{EQ.3.22}$$

where V_b = volume of sorbate solution

c_o = value of c_b at $t = o$

A graph of $\ln (c_o / c_b)$ versus time is usually linear for the first few minutes, thus

the initial slope is readily calculated.

In order to calculate k_e , the external surface area of the sorbent particles, A_p , must be known, This is easily found for regular geometries such as spheres or cylinders. However, with irregular particles, A_p is more difficult to measure. Fortunately, the critical parameter pertaining to external mass transfer both in batch and packed bed systems, is the product, $k_e A_p$. Therefore an accurate estimate of A_p is not essential. Nevertheless, k_e is a more fundamental parameter so it is therefore useful to be able to estimate A_p .

The fluid film coefficient is usually correlated with the physical and hydrodynamic parameters in terms of the three controlling dimensionless numbers; the Sherwood number (Sh), the Reynolds number (Re) and the Schmidt number (Sc), i.e.,

$$\left(\frac{k_f\, d}{D_l}\right) \alpha \quad f\left\{ \left(\frac{d\, u_s \rho}{\mu}\right) \;,\; \left(\frac{\mu}{\rho D_l}\right) \right\} .$$

or $\qquad Sh \alpha \quad f\ (Re,\ Sc) \qquad\qquad$ EQ.3.23

In batch experiments , u_s is the average velocity of the bulk fluid relative to the particles; a quantity that is not easily measured. Fortunately, Kolmogoroff's Theory of isotropic local turbulence provides a method of relating, u_s , and hence the Reynolds number to the specific power dissipated by the impeller. In correlations based on the specific power dissipated, the fluid film coefficient should be independent of the dimensions of the agitated vessel. (Brian et al., 1969). However, there is conflicting experimental evidence in the literature. Letterman et al. (1974) and Furusawa and Smith (1973) were able to fit data from different size agitator vessels onto a single correlation. In contrast Levin and Glastonbury (1972) found their data was dependent upon the impeller to vessel diameter ratio , in addition to the specific power.

Some authors have correlated Sh and Sc with the speed of revolution of the impeller. (Weber and Morris, 1963, Suzuki and Kawazoe, 1975 and Spahn

and Schlunder, 1975). The agitator speed is, of course, related to the specific power input to the vessel via the torque-speed curve. The fluid film coefficient sometimes approaches an asymptotic limit as the speed is increased. This phenomenon indicated that the maximum relative velocity between the particles and the bulk fluid, for the particular agitation design, has been reached.

The experimental vessels, for which correlations have been drawn, are cylindrical with several longitudinal baffles fixed to the walls. The agitation is provided by an impeller mounted on a longitudinal shaft. If a vessel of fundamentally different design is employed and the nature of the turbulence in the bulk flow is different, then the correlations are unlikely to hold (Suzuki and Kawazoe, 1975). This applies to the batch experiments in this thesis. Therefore, the fluid film coefficients must be measured directly.

3.4.2 External diffusion in packed beds

The fluid film coefficients in packed beds are normally measured by the technique of partial dissolution of solid particles. A packed bed is constructed with particles made of a substance (usually benzoic acid) that will dissolve slowly as water is passed through the bed. The value of the coefficient is calculated from the steady state rate of dissolution into the water. The data from these experiments is presented as a correlation between the j-factor of the Chilton-Colburn analogy and the Reynolds number where,

$$j_D \equiv \frac{Sh}{Re\ Sc^{1/3}} = \frac{k_e}{u_s} Sc^{2/3} \qquad \text{EQ.3.24}$$

Figure 3.4.1 illustrates such a correlation based on the accumulated data of many authors, for both spherical and cylindrical particles. The standard deviation in the j-factor at a given Re exceeds $\pm$ 20% in some regions of the correlation. Every experimental study and review includes an empirical or theoretical correlation equation. Table 3.4.1 presents a representative list of these equations. All the equations have been arranged in a common format, i.e.

$$\frac{Sh}{Sc^{1/3}} = C_i Re^{Y} \qquad \text{EQ.3.25}$$

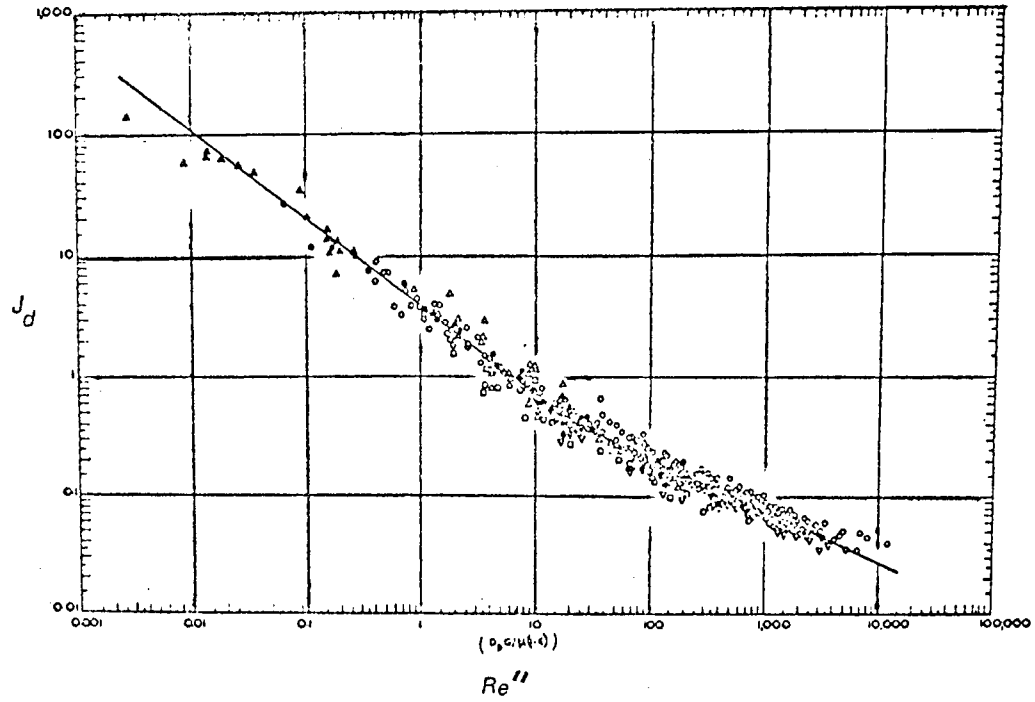

Figure 3.4.1 External Diffusion Mass Transfer Correlation Curve for Packed Beds (after Upadhyay and Tripathi, 1975)

$$Sh\ Sc^{1/3} = C_1\ Re^{\gamma}$$

Author (s)	C_1	γ	Range
Hougen and Watson (1947)	1.82	0.49	$Re < 350$
Carberry (1960)	1.89	1/2	$Re > 0.2$ ($\varepsilon_b = 0.37$)
Wilson and Geankoplis (1966)	2.7	1/3	$0.002 < Re < 55$ ($0.35 > \varepsilon_b > 0.75$)
Miyauchi (1971)	1.39	1/3	$4 \times 10^{-4} > Re > 10^{-3}$ ($\varepsilon_b = 0.4$)
Kataoka et al (1972)	3.14	1/3	$5 \times 10^{-3} > Re > 50$ ($\varepsilon_b = 0.4$)
Sherwood et al (1975)	1.17	0.585	$10 > Re > 2500$

Table 3.4.1 Comparison of Correlation Equations for External Mass Transfer in Packed Beds

Like the correlation, these equations illustrate deviation in the experimental data obtained in different investigations. It is clear that a precise and reliable value of mass transfer coefficient cannot be estimated on the basis of these correlations or equations.

There are two further problems associated with the use of fluid film mass transfer correlations for perfusion columns. Firstly, the flow in perfusion columns is controlled by a pulsatile, peristaltic pump. The effect of this upon the coefficients is not well documented, although it is clear that such effects are not negligible. (Drasuk and Smith, 1964). Secondly, in haemoperfusion columns, which form the bulk of the perfusion devices, the membrane resistance must also be considered. Meier (1972) has shown that it is impossible to predict apriori the membrane resistance on a coated sorbent, given the resistance in a flat sheet of the same membrane material.

Therefore it is necessary to measure the fluid film or the external mass transfer coefficient directly. This involves analysis of the initial response of the effluent concentration to a concentration step at the inlet of the column. In common with the dissolution experiments the flow in the column is usually assumed to be plug flow, although it is possible to allow for the effects of axial dispersion.

Since there is initially no sorbate in the column (either on the sorbent or in the void fluid) then sorbate removal during the initial pass of the concentration step through the column, is controlled by the external diffusion mass transfer. If the rate of external mass transfer is slow (i.e. either k_e or A_p is small) or if the flow rate is rapid then breakthrough occurs after one mean residence time (MRT). That is, if the characteristic time for external mass transfer exceeds the mean residence time of the column then a significant number of sorbate molecules in the input step will be able to pass through the column without being transferred to the sorbent. The value of the effluent concentration at this initial breakthrough is found by solution of the mass transfer equations for a sorbent column over the first few MRT's. Diffusion within the

particles is initially negligible. Therefore, an isotherm equation is not necessary and the solution is independent of the shape of the isotherm.

The two mass transfer equations governing a sorbent column in these circumstances are:-

Column Mass Balance

$$\varepsilon_b \frac{\partial c}{\partial t} + \rho_b \frac{\partial \bar{q}}{\partial t} + U_s \frac{\partial c}{\partial z} = \varepsilon_b D_a \left(\frac{\partial^2 c}{\partial z^2}\right)_t \qquad \text{EQ.3.26}$$

External Diffusion

$$\rho_b \frac{\partial \bar{q}}{\partial t} = k_e \, a_p \, (c - c_s) \; ; \; c_s = o \qquad \text{EQ.3.27}$$

where
- z = length co-ordinate of column
- ρ_b = bulk density of particles
- ε_b = bed porosity
- a_p = external mass transfer area/unit volume ($= A_p / V$)
- U_s = superficial velocity
- D_a = axial dispersion coefficient
  - = o for plug flow

The inclusion of the axial dispersion term on the right hand side of Equation 3.26 produces the most general representation of the problem. Equations 3.26 and 3.27 are solved in Appendix A2, for both zero and finite axial dispersion.

For zero axial dispersion (i.e. plug flow) a change of time variable is required to eliminate the discontinuity that occurs in the solution at one mean residence time. This discontinuity occurs because fluid elements in the concentration step applied to the column at $t = o$ cannot reach the end of the column before one MRT. With finite axial dispersion, however, it is theoretically possible for an infinitely small number of such elements to travel down the column at infinite speed and thereby exit at $t = o$. In other words the solution for $c = f(z,t)$ in Equation 3.26 with axial dispersion is continuous

over all z and t . It is possible to solve the equations in the axial dispersion case, with or without the modified time variable.

The solutions to Equations 3.26 and 3.27, for both plug flow and axial dispersion, are listed below. The variables are normalized using the following equalities

$$X = c/c_o \; ; \; \bar{z} = z/L \text{ and } \theta' \equiv \theta - \bar{z}$$

where θ $= t/\bar{t}$ (Section 3.6)

c_o = inlet step conc. at $t = o$

L = length of column

Typical forms of the function $X = F(\theta', \bar{z})$ for both cases are shown in Figures 3.4.2 and 3.4.3. These two figures illustrate the effect of the change in the time variable as well as depicting graphically the meaning of the initial break--through.

Initial breakthrough with plug flow

$$X_{BT} = \exp(-N_e) \qquad \text{EQ.3.28}$$

$$\text{where } N_e \equiv \frac{k_e A_p}{F}$$

Hence, N_e , the number of external mass transfer units, can be calculated direct from the normalized breakthrough, X_{BT} .

The number of external mass transfer units is the critical parameter in respect of perfusion column performance (Chapter 6). However, the more fundamental, k_e can be estimated from a knowledge of A_p and F. By conducting experiments at different flow rates it is possible to identify the respective fluid film and membrane mass transfer coefficients k_f and k_m , from the changes in k_e . The membrane coefficient is estimated by extrapolating

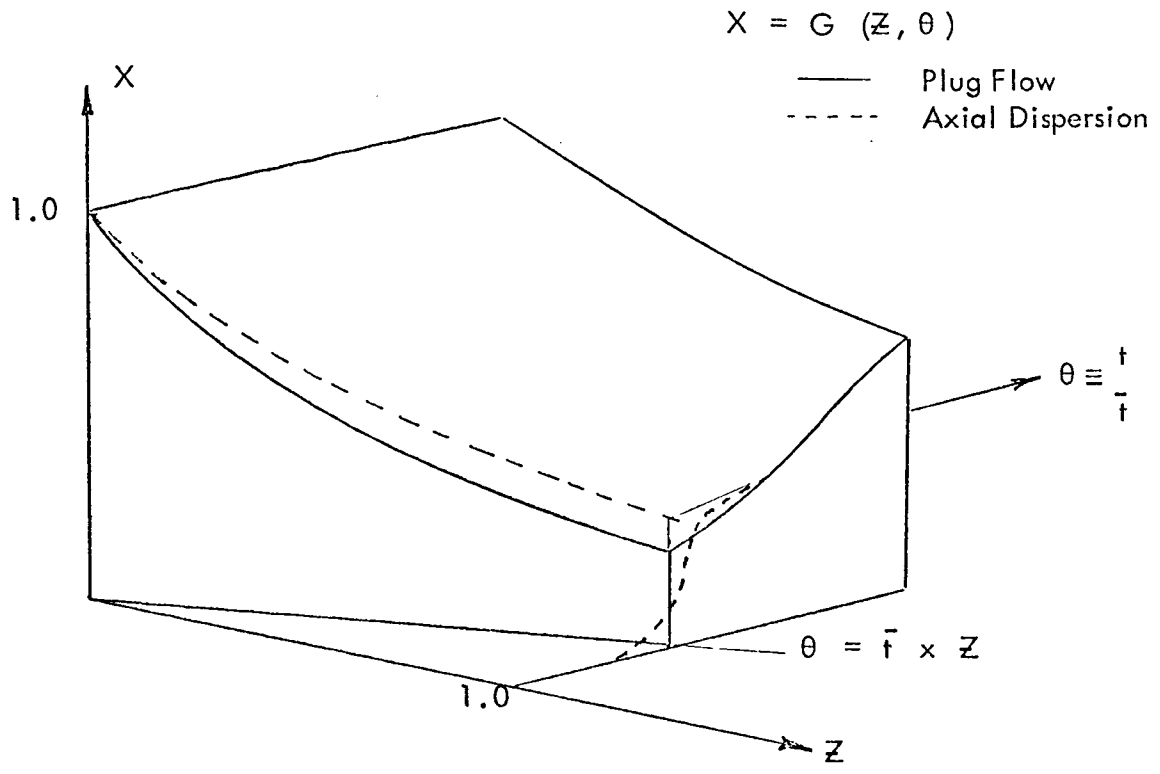

Figure 3.4.2 Initial Breakthrough - Discontinuity at $\theta = \bar{t} \times Ƶ$ $X = G(Ƶ, \theta)$

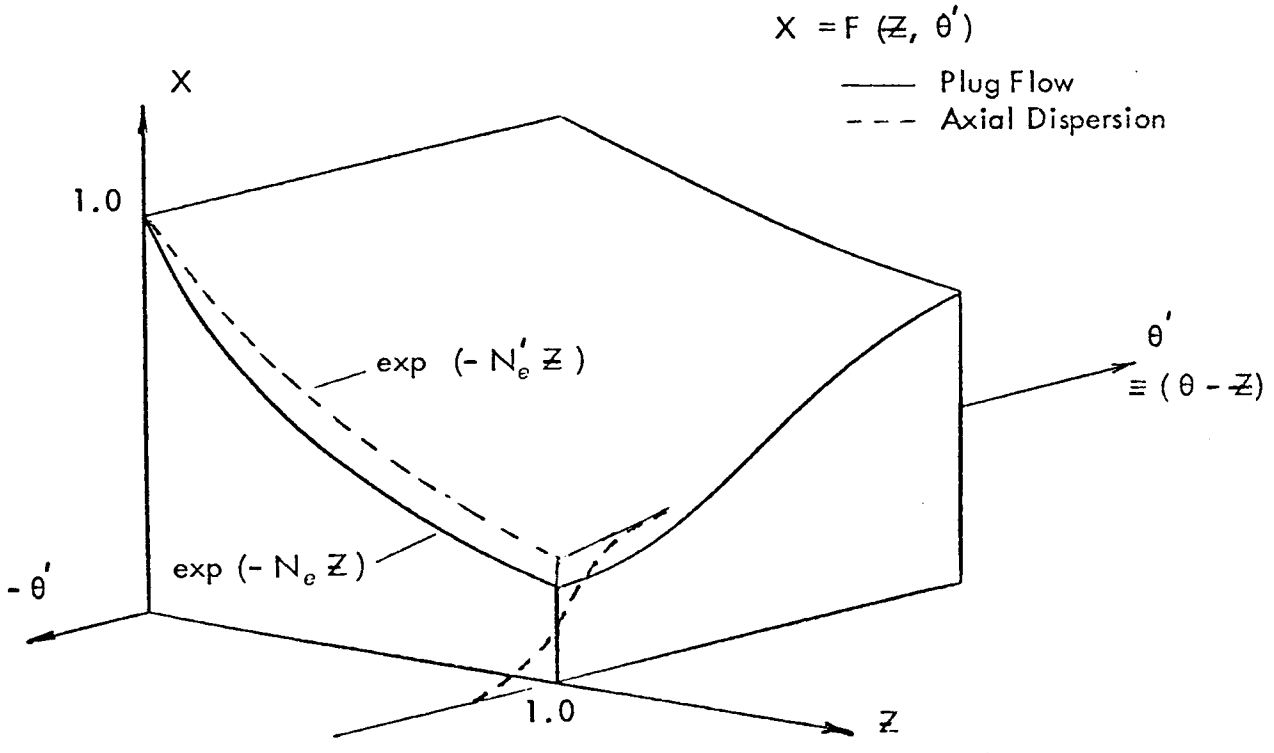

Figure 3.4.3 Initial Breakthrough - Modified Time (θ') $X = F(Z, \theta')$

k_e versus F to infinite flow rate. (At infinite flow $k_f = \infty$, so $k_e = k_m$). The value of k_f at the various flow rates is then deducted from k_e via Equation 3.20.

Initial breakthrough with axial dispersion

$$X_{BT} \doteq \exp\ (-N_e') \qquad \text{EQ.3.29}$$

where $$N_e' \equiv \frac{Pe_L}{2}\left\{\left(1 + \frac{4\,N_e}{Pe_L}\right)^{1/2} - 1\right\}$$

and $$Pe_L \equiv \frac{U_i\,L}{D_a} = \text{longitudinal peclet no.}$$

$$U_i = \text{interstitial velocity} = (U_s\ /\varepsilon_b)$$

From Figures 2.4.2 and 2.4.3 it is clear that initial breakthrough with axial dispersion requires a more subtle interpretation than that with plug flow. In the solution of Equation 3.26 in Appendix A2 it was assumed that the slope of the breakthrough curve, with time, just beyond the sigmoid portion of the curve, is very small. This assumption can be tested in each experimental case investigated. Now, if the slope is small, then the projection of the curve back to one MRT represents the apparent, initial breakthrough. It is the value of this projection that is given by Equation 3.29. As expected, the value X_{BT} in Equation 3.29 reduces to that in 3.28 if D_a goes to zero (i.e. $Pe_L \rightarrow \infty$). As with the plug flow case, values of k_e, k_f and k_m can be estimated from experimental values of N_e.

Rosen (1952) developed Equation 3.28 by taking the asymptotic limit of the general solution for the effluent concentration in a sorbent column, with a linear isotherm. As Rosen's solution, unlike the one developed here, assumes a linear isotherm it was not necessarily applicable to non-linear isotherms. In fact, no subsequent work in the literature has shown Equation 3.28 to be applicable for all isotherms. For this reason perhaps, very few authors have attempted to measure the external diffusion coefficient directly in sorbent columns.

Westermark (1975) employed Equation 3.28 (from Rosen's work) to measure the fluid film coefficients for a column with a sorbent with an approximately linear isotherm. The coefficients were in reasonable agreement with two correlations in the literature.

Dunlop et al. (1976) developed Equation 3.28 from an asymptotic analysis of steady state mass transfer in the classic cocurrent, mass or heat transfer case. At steady state, the mass transfer rate in such a device is given either by a mass balance across the inlet and outlet ports of the exchanger or by the overall mass transfer coefficient times the area for mass transfer and the log-mean concentration difference, i.e.

$$\dot{m} = F\,(c_{in} - c_{out}) = k_e\, A_p\, \Delta c \qquad \text{EQ.3.30}$$

where Δc = log mean conc^{n} difference.

If the inlet and outlet concentrations in the fluid to which the solute is transferred (the secondary fluid) are zero then this expression reduces to Equation 3.28. The carbon is assumed to be analogous to this secondary fluid. Although this approach gives the correct relationship for the external mass transfer coefficient, the steady state assumption associated with Equation (3.29) does not hold and it is necessary to justify the applicability of the equation. This was not done explicitly by Dunlop and co-workers. In addition, the effluent concentration values used to calculate k_e were described as those values "when steady state had been reached.....after at least four void volumes". As no 'steady state' exists for the effluent concentration in a perfusion column it is difficult to interpret their results. The paper is poorly written, so it is often impossible to understand the rationale behind sections of the work. Nevertheless, it appears that the concept of the initial breakthrough was not thoroughly grasped by Dunlop et al (1976).

Holland et al. (1977) completely misinterpreted the performance of sorbent columns. The fluid phase in the column was assumed to form a single,

well-mixed pool. Although the particular adsorber reported in the paper may, in the limit have approached this condition, the flow pattern was quite unlike that in all existing commercial haemoperfusion columns. Even accepting the well mixed pool assumption, the equation used to calculate the fluid film resistance was based on a batch system and not on flow through, a single pool reactor. A consequence of their analysis was that the concept of the initial breakthrough was completely overlooked.

3.5 Batch Experiments

3.5.1 Introduction

Batch experiments are employed to estimate equilibrium isotherms and intraparticle diffusivities. Generally separate experiments are involved for each of these objectives. For equilibrium isotherms, small volumes of sorbate solution and sorbent are contacted until equilibrium is reached. Depending upon the size of the sorbent particles and the sorbate kinetics this can take anything from several minutes (Meier, 1972) to several months, (Dedrick and Beckmann, 1967), to occur. Provided equilibrium is known to have been reached then by a simple mass balance one point on the isotherm is calculated for each experiment. Experiments designed to estimate intraparticle diffusivities are obviously concerned with the sorbate kinetics prior to reaching equilibrium. Analysis of these kinetics involves the intraparticle diffusivity, the isotherm, the mass balance in the vessel and possibly the fluid film coefficient. This process is simplified if certain asymptotic limits apply.

3.5.2 Asymptotic solutions

Infinite bath experiments. If the quantity of sorbate in solution is very large compared to the capacity of the sorbent in the experiment, then the sorbate concentration will only fall a negligible amount in saturating the sorbent. If, in addition, the fluid film resistance is negligible then the fluid phase concentration and the solid phase concentration at the surface of the particles are approximately constant throughout the experiment. Therefore, for a solid diffusion model the problem reduces to the classical non-steady state diffusion in a homogeneous particle, solutions for which have been given by Crank (1975) for spherical and cylindrical geometries. Infinite bath experiments are best suited to gaseous adsorption (Testin and Stuart, 1967), however Dedrick and Beckmann (1967) employed it successfully for liquid phase adsorption. In such experiments the difficulty arises that the kinetics must be monitored by direct measurement of the sorption onto the particle whereas for finite bath experiments the decline in sorbate concentration in the bulk fluid is measured. Di Giano and Weber (1973) developed a complex apparatus to satisfy the infinite bath

assumption in cases where a significant quantity of sorbate is removed from solution. An infusion pump operated by a feedback control system maintained a constant concentration in the bulk fluid. However, as the fluid film resistance was finite the above solution was not applicable and the kinetic equations had to be solved directly.

Linear isotherms. In the unlikely event that the equilibrium isotherm is linear, then the classical solutions for diffusion in homogeneous particles for both finite and infinite baths apply (Crank, 1975). In addition, with a linear isotherm pore diffusion is merely a special case of solid diffusion, so all these solutions are applicable to pore, solid or combined diffusion models.

Irreversible isotherms. The irreversible isotherm provides a good approximation to many experimental isotherms. When combined with a pore diffusion model, an unique solution, based on the concept of a moving sorption front travelling into the particle is obtained for either finite or infinite baths. Unlike the other asymptotic solutions, fluid film resistance can be included in the model. Weisz (1967) gives the solution for an infinite bath and no fluid film resistance. DiGiano and Weber (1972), Suzuki and Kawazoe (1974) and Spahn and Schlunder (1975) separately developed solutions for finite baths and fluid film resistance. Although the three solutions are naturally identical, it requires considerable algebraic manipulation to reduce them to a common form. The discrepancy between the solution for the irreversible isotherm and that for pore diffusion with the exact non-linear isotherm depends upon the relative size of the bath. (Neretnieks, 1976 (a) and (b)). Solid diffusion with an irreversible isotherm and a finite bath is equivalent to diffusion in a homogeneous particle with a constant surface concentration. The solution to this problem is in Crank (1975). This is the same as for solid diffusion from an infinite bath.

3.5.3 Kinetic equations employed in thesis

None of the asymptotic solutions apply to the experiments in this thesis so the sorbate kinetics were simulated directly. The intraparticle diffusion was described by a solid diffusion model based on the quadratic driving force

Intraparticle Diffusion

$$\frac{d\bar{q}}{dt} = \psi_q \cdot \frac{60\, D_s}{d_p^2} \cdot \frac{q^{*2} - \bar{q}^2}{2\bar{q}} \qquad \text{EQ. 3.13}$$

Isotherm

$$q^* = \frac{A\, c^*}{1 + B\, c^*} \qquad \text{EQ. 3.1}$$

Mass Balance in Bath

$$V_b \frac{d c_b}{dt} = M \frac{d\bar{q}}{dt} \qquad \text{EQ. 3.31}$$

External Diffusion

$$V_b \frac{d c_b}{dt} = k_e A_p \, (c_b - c_b^*) \qquad \text{EQ. 3.32}$$

where

$\bar{q}$	=	average solid phase conc. in sorbent (mg/gm)
c^*	=	fluid phase conc. at surface of particle (mg/ml)
q^*	=	equilibrium solid phase conc. corresponding to c^* (mg/gm)
c_b	=	bulk fluid phase conc. (mg/ml)
V_b	=	vol. of sorbate solution (ml)
M	=	mass of sorbent (gm)
A and B	=	Langmuir equation constants
k_e	=	external mass transfer coefficient (cm/sec)
A_p	=	external surface area of particles (m^2)
D_s	=	solid diffusivity (cm^2/sec)
d_p	=	particle diameter (cm)

Figure 3.5.1 Equation of Batch Sorption Kinetics

(QDF) approximation. The equations describing sorption in a batch experiment are summarized in Figure 3.5.1.

3.5.4 Neretniek's Normograms

A recent paper by Neretnieks (1976,b) provides a new method for estimating the pore and solid diffusivity, when asymptotic solutions do not apply, without conducting a complete simulation. Two normograms summarize the respective pore and solid diffusion kinetics in a batch system with a finite external diffusion resistance and a Freundlich isotherm ($\beta = 0.2$). The external mass transfer coefficient, the kinetic half time (i.e. the time at which 50% saturation is reached), the isotherm and the mass to volume ratio, are used in conjunction with the normograms to extimate D_s or D_p . The normogram for solid diffusion is presented in Figure 3.5.2. Values of F and $\mathcal{D}_s\ Sh_s\ t_{1/2}$ or $\mathcal{D}_p\ Sh_p\ t_{1/2}$ are calculated from the above data and the corresponding value of $\mathcal{D}_s\ t_{1/2}$ or $\mathcal{D}_p\ t_{1/2}$ found on the normogram. The diffusivity (D_s or D_p) is calculated from this. Apart from the obvious shortcoming that this technique is restricted to $\beta = 0.2$ there are other problems. Solutions only exist for a limited range of values of F (the normalized mass to volume ratio) and no account is made for the particle size effects discussed in Section 3.3. Nevertheless these normograms do provide a first estimate for the diffusivity. In Chapter 4 the values of D_s from direct simulation of the batch kinetics are compared to those from the solid diffusion normogram.

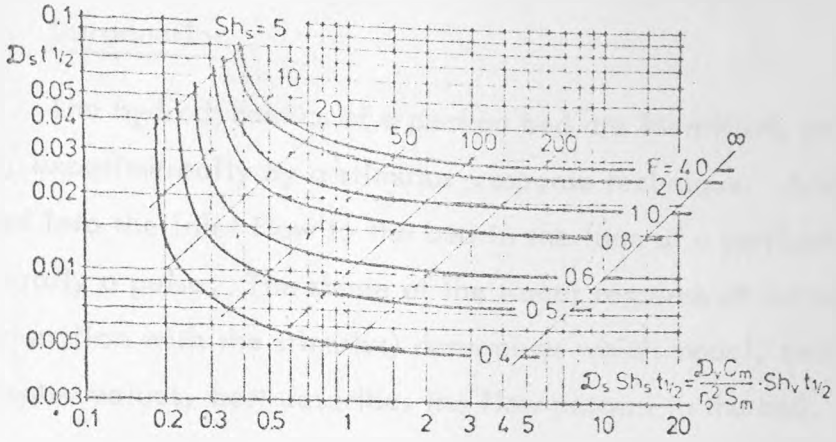

Halftime for finite bath as function of film transfer coefficient with flow ratio as parameter. Freundlich isotherm $\beta = 0.2$, surface diffusion.

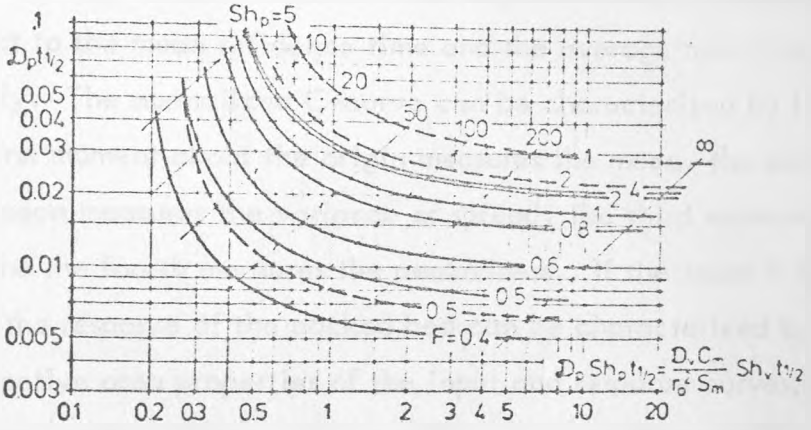

Halftime for finite bath as function of film transfer coefficient with flow ratio as parameter. Freundlich isotherm $\beta = 0.2$, pore diffusion. – – – –, saturation isotherm.

$$\mathcal{D}_s \equiv \frac{D_s}{r_p^2} \qquad \mathcal{D}_p \equiv \frac{D_p \varepsilon_p c_o}{r_p^2 \rho_p q_o} \qquad F \equiv \frac{V_b c_o}{M q_o}$$

$$Sh_s \equiv \frac{k_e d_p}{D_s} \frac{c_o}{\rho_p q_o} \qquad Sh_p \equiv \frac{k_e d_p}{D_p \varepsilon_p}$$

Figure 3.5.2 Normograms for Estimating Solid and Pore Diffusivities (after Neretnieks, 1976 b)

3.6 Hydrodynamics of Packed Beds

3.6.1 Introduction

The hydrodynamics of a packed bed are identified, or at least interpreted, experimentally by a stimulus-response technique. A tracer material is introduced into the inlet flow to the bed in the form of a particular input or stimulus, usually a pulse. The shape of the tracer response at the outlet of the bed (in conjunction with the stimulus) determines which model, and corresponding set of parameter values, best describes the flow pattern in the bed.

If the tracer input is an ideal pulse (delta function) the response curve is called a C-curve. A typical C-curve is shown in Figure 3.6.1. The time and the tracer concentrations in the response curve are usually normalized with respect to the mean residence time and the average tracer concentration respectively. The normalized C-curve can be characterized by its area properties e.g. the first moment about the origin measures the mean, the second moment about the mean measures the variance or spread, the third moment measures the skewness and the fourth measures the peakedness. If the input is a non-ideal pulse then the response of the packed bed can be characterized by the difference in the respective area properties of the input and response curves, provided the hydrodynamic model is linear. (Figure 3.6.1). The rationale for using area properties is outlined in Section 3.6.2.

3.6.2 Axial dispersed plug flow

For reasons of simplicity most models of the mass transfer in packed beds, such as haemoperfusion columns, assume plug flow i.e. a flat velocity profile across the bed. (The C-curve for plug flow is an ideal pulse displaced one mean residence time; see Figure 3.6.1.) In reality, however, mixing between the voids causes local fluctuations in the flat velocity profile. These fluctuations cause the fluid molecules in a thin element entering the bed to be dispersed axially as that element passes along the bed. The result is the typical C-curve in Figure 3.6.1. This dispersion process can be described by an axial dispersed plug flow model. The equation of continuity for axial dispersed plug

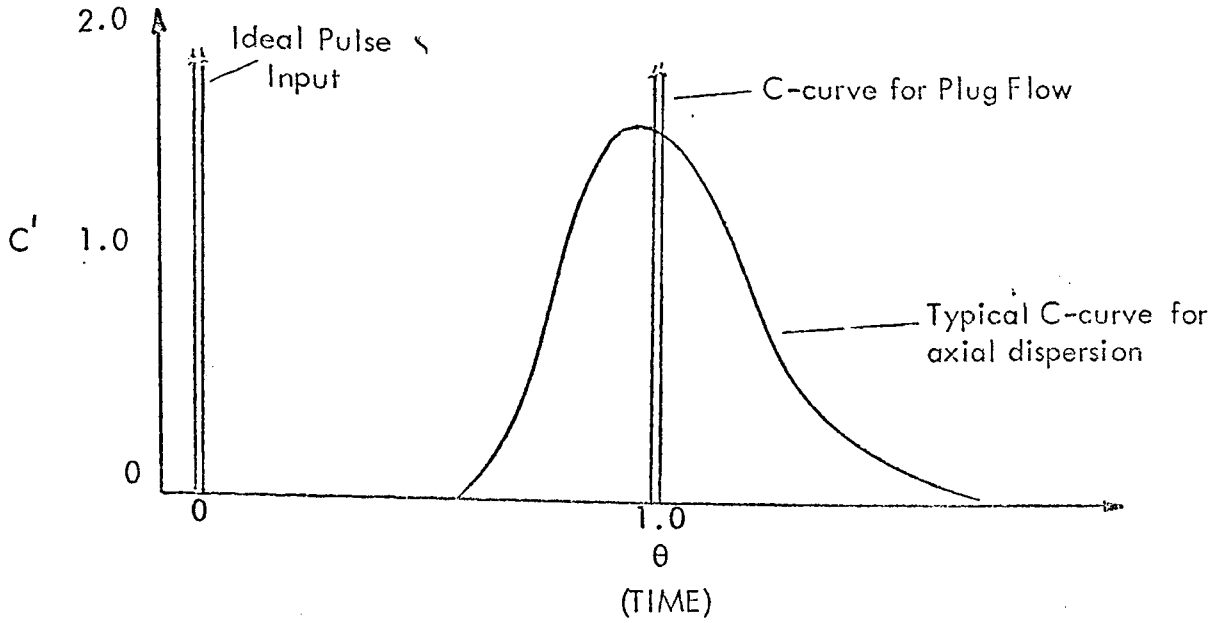

Terms

Mean Residence Time (MRT) $= \bar{t} \equiv$ volume of vessel available to flow / volumetric flow rate through vessel

Average Tracer Concentration $= \bar{c} \equiv$ quantity of tracer / volume of vessel

Normalized Time $= \theta \equiv \left(\frac{t}{\bar{t}}\right)$

Normalized Concentration $= c' \equiv \left(\frac{c}{\bar{c}}\right)$

Mean of Normalized c-curve $= \mu \equiv \dfrac{\int_0^\infty \theta\, c'\, do}{\int_0^\infty c'\, do} = \int_0^\infty \theta\, c'\, do$

Variance of Normalized c-curve $\sigma^2 \equiv \dfrac{\int_0^\infty \theta^2 c'\, do}{\int_0^\infty c'\, do} = \int_0^\infty \theta^2 c'\, do$

For a non-ideal pulse input

$$\Delta\mu = \mu_{response} - \mu_{input}$$

and $$\Delta\sigma^2 = \sigma^2_{response} - \sigma^2_{input}$$

($\Delta\mu_{in} = \Delta\sigma^2_{in} = 0$ for an ideal pulse)

Figure 3.6.1 Normalized Tracer-Response Curves and Associated Terminology

flow in a packed bed is

$$\frac{\partial c}{\partial t} + U_i \frac{\partial c}{\partial z} = D_a \frac{\partial^2 c}{\partial z^2} \qquad \text{EQ.3.33}$$

where z = longitudinal co-ordinate
t = time
U_i = interstitial velocity ($\equiv U_s / \varepsilon_b$)
D_a = axial dispersion coefficient

The dispersion is characterized by the axial dispersion coefficient, D_a . The corresponding dimensionless group is the axial Peclet number, which can be defined with respect to either the particle diameter or the bed length, i.e.

$$Pe_L \equiv \frac{U_i L}{D_a} \quad \text{and} \quad Pe_d \equiv \frac{U_i d_p}{D_a}$$

where L = length of bed
d_p = diameter of particle

When the axial dispersion coefficient is negligible then plug flow exists in the bed.

Although Equation 3.33 is quite straightforward, difficulties arise in solving it for realistic boundary conditions, i.e. those likely to be encountered experimentally. There are two distinctly different types of experiment; (a) those investigating fundamental dispersion phenomena in ideal vessels and (b) those investigating dispersion in practical chemical reactors. For type (a), the experimental details can be adjusted to comply with boundary conditions for which a simple solution of Equation 3.33 exists. For type (b) such adjustment is not always possible. In addition, type (b) experiments often involve modelling the hydrodynamics in the inlet and outlet zones of the packed bed. When there is finite dispersion in the inlet and outlet, Equation 3.33 must be complemented by two analogous continuity equations describing the dispersion in these zones.

Solutions of the dispersion equation (or equations) are calculated in the Laplace domain by a technique devised by Aris (1958). For all but the simplest boundary conditions the inverse transformation of the solution, into the time domain, is impossible. Fortunately, however, the area properties of the solution in the time domain are simply related to the derivatives of the Laplace domain solution with respect to the Laplace operator. The first and second moments, the mean and variance respectively, are readily calculated in this manner. Therefore the solutions in the literature, such as those in Levenspiel and Bischoff (1963), are presented in terms of the mean and variance of the C-curve for ideal input pulses and the difference in the respective means and variances ($\Delta\mu$ and $\Delta\sigma^2$) for non-ideal pulses rather than in terms of equation of the response curve.

In the general case, $\Delta\mu$ and $\Delta\sigma^2$ are functions of the Peclet number in the packed bed plus the Peclet number in the inlet and outlet sections and the normalized position(s) of the measurement point(s) in the experimental scheme. If the Peclet numbers in the inlet and outlet zones are estimated apriori then the only unknown variable is the Peclet number in the packed bed. The value of the Peclet number is obtained by equating the normalized experimental mean or variance difference with the expressions from the model. This procedure assumes implicitly that the model provides a valid description of the experiment. The model should be validated explicitly. Unfortunately some authors apply the expressions for Peclet numbers without validating the model. The paper by Dunlop et al. (1976), investigating the hydrodynamics of haemoperfusion columns, is a case in point.

The experimental scheme employed in this thesis to measure the axial dispersion coefficients in haemoperfusion columns is discussed in detail in Chapter 4. Briefly, a pulse was injected into the inlet tube to the column and the response was measured in the outlet tube. Physical constraints in the experimental apparatus forces the injection and measurement points to be situated at distances of up to half the column length from the ends of the column. The flow in the inlet and outlet tubes was turbulent so the axial dispersion in these sections was assumed to be zero. The solution for axially dispersed plug

Response to Ideal Input Pulse with Zero Axial Dispersion in Inlet or Outlet Sections

$$c' = \exp\,(Pe_L/Z) \sum_{n=1} \frac{(-1)\quad 8}{4a_n^2 + 4\,Pe_L + Pe_L^2} \exp\,(-a_n\,t) \qquad \text{EQ.3.34}$$

where $a_n = \dfrac{Pe_L^2 + 4a^2}{4\,Pe_L}$ and $\tan a_n = \dfrac{4\,Pe_L a_n}{4a_n^2 - Pe_L^2}$

$$\mu = 1 \quad \text{and} \quad \sigma^2 = \frac{2}{Pe_L} - \frac{2}{Pe_L^2}\left(1 - \exp\,(-Pe_L)\right) \qquad \text{EQ. 3.35}$$

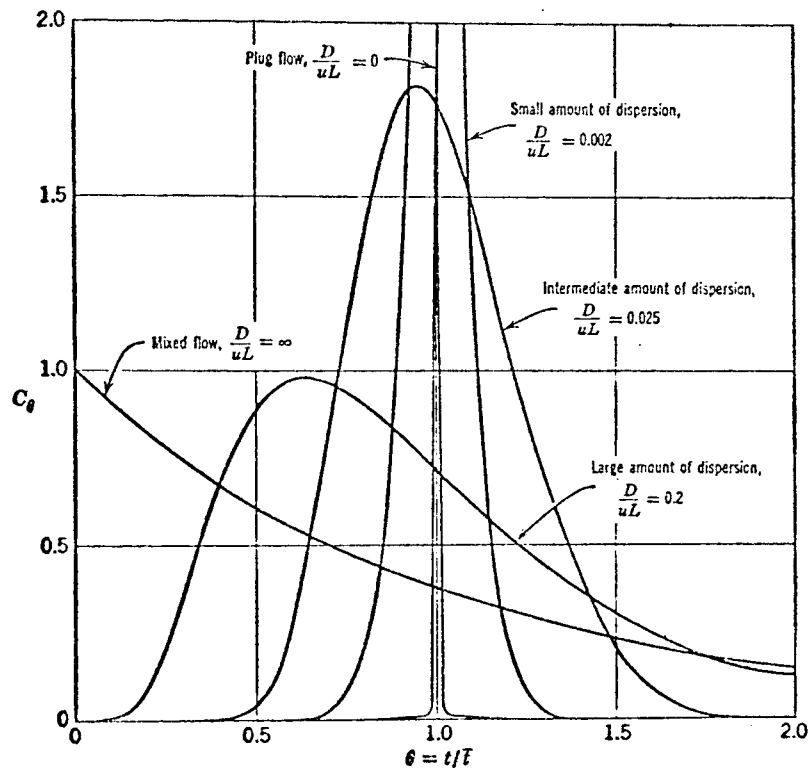

Figure 3.6.2 Axial Dispersed Plug Flow in Packed Beds (after Levenspiel, 1972)

flow under these conditions is given by Himmelblau (1970). The solution is based on an ideal input pulse so the experimental pulse was assumed to be ideal, although it was known to have a significant tail. Details of the solution are presented in Figure 3.6.2. Because there is no dispersion in the inlet or outlet tubes, there is no mixing across the column boundaries and the mean of the response curve is unity. Vessels exhibiting this condition are termed closed vessels.

3.6.3 Mixing cell models of axial dispersion

A quite different approach to describing dispersion phenomena in packed beds is provided by the mixing cell or tanks-in-series models. The packed bed is conceived as a finite number of ideal stirred tanks connected in series. This type of model is not directly related to the axial dispersed plug flow models, although the two can be compared through their area properties, especially the variance. Intuitively the mixing cell model provides a more realistic representation of the flow in a packed bed with the voids in the successive sections of the bed forming a series of well-mixed cells. This model is especially applicable for blood detoxification devices, where the flow is maintained by a pulsatile (peristaltic) blood pump.

Levenspiel and Bischoff (1963) have reviewed mixing cell models. The basic model consist of n identical cells, each containining one nth of the bed volume. Plug flow is assumed in the inlet and outlet tubes, i.e. the bed is a closed vessel. The response of the model to a general input function is developed in the Laplace domain. Inversion of the solution into the time domain is restricted to the case of an ideal pulse input. For a non-ideal pulse the solution is expressed in terms of $\Delta\mu$ and $\Delta\sigma^2$. Figure 3.6.3 summarizes the results. Comparison of the variances of the axial dispersed plug flow model and the mixing cell model (for an ideal pulse) shows that for large values of Peclet number the number of cells, n , is approximately equal to half the Peclet number.

However, neither the axial dispersed plug flow nor basic mixing

(a) Response to Ideal Input Pulse

$$c' = \frac{n^n}{(n-1)!}\,\theta^{n-1}\exp(-n\theta) \qquad \text{EQ.3.36}$$

$$\mu = 1 \quad \text{and} \quad \sigma^2 = \frac{1}{n} \qquad \text{EQ.3.37}$$

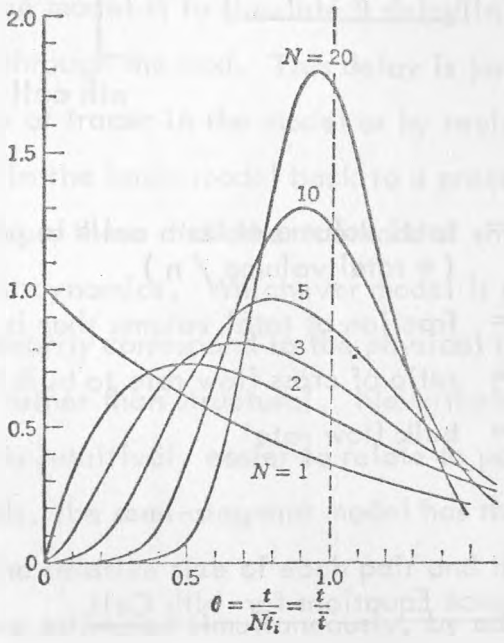

(b) Response to Non-Ideal Pulse

$$\Delta\mu = 1$$
$$\Delta\sigma^2 = \frac{1}{n} \qquad \text{EQ.3.38}$$

Figure 3.6.3 Simple Mixing Cell Model of Axial Dispersion

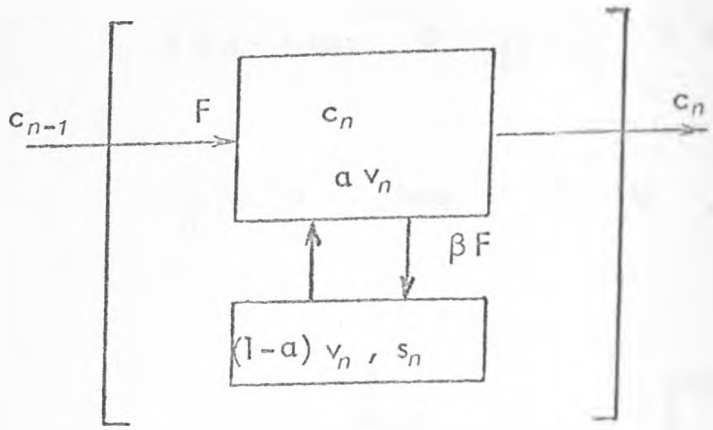

where
- v_n = total volume of both cells in pair (= total volume / n)
- a = fraction of total volume that is 'dynamic'
- β = ratio of cross flow rate to bulk flow rate
- F = bulk flow rate

Mass Balance Equations for Nth Cell

$$a v_n \frac{d c_n}{d t} = F (c_{n-1} - c_n) - \beta F (c_n - s_n) \qquad \text{EQ.3.39}$$

$$(1 - a) v_n \frac{d s_n}{d t} = \beta F (c_n - s_n) \qquad \text{EQ.3.40}$$

Figure 3.6.4. Multiparameter Mixing Cell Model

cell models can simulate all the deviations from plug flow that occur in practical haemoperfusion columns. Channelling, recirculation, eddying in 'blind' corners etc., all contribute to non-ideal, axial dispersion in such devices. A simple method of accounting for these features is to assume that part of each cell in the basic mixing cell model is semi-stagnant. Each of the cells in the previous model is replaced by a pair of cells with a limited cross flow between the two. (See Figure 3.6.4). This model is termed a multi parameter, mixing cell model.

For convenience, the pairs of cells are assumed to be identical i.e. the nth pair of cells are identical to the first pair, the second pair and so on. The net effect of the model is to simulate a delay in the passage of some of the tracer as it passes through the bed. This delay is just as easily created by specifically delaying a fraction of tracer in the model or by recirculating a fraction of the output of one cell in the basic model back to a preceding cell. Levenspiel and Bischoff (1963) discuss these and other methods of simulating non-ideal features in packed bed hydrodynamics. Whichever model is chosen the features in the model do not necessarily correspond to the physical reality in the bed. The models are all functional rather than structural. Nevertheless the semi-stagnant model used in this thesis is intuitively easier to relate to possible reality. Unlike the previous two models, the semi-stagnant model has three parameter values, the number of cells, the relative size of each pair and the magnitude of the cross flow. All three are estimated simultaneously, by adjusting their values until the model response adequately simulates the experimental response curve for a given input pulse. Fortunately this process is not as difficult as it may appear if the cross flow is quite small compared to the bulk flow through the bed. (Levenspiel, 1972).

3.6.4 Correlations of axial dispersion in packed beds

Correlations of axial dispersion in the literature generally refer to Pe_d or its inverse, the intensity of dispersion, while most of the models give results in terms of Pe_L or its inverse. Pe_d is the more fundamental of the two since the basic dispersion process is related to the diameter of the particles rather than the length of the bed. However, Pe_L is more suited to the models

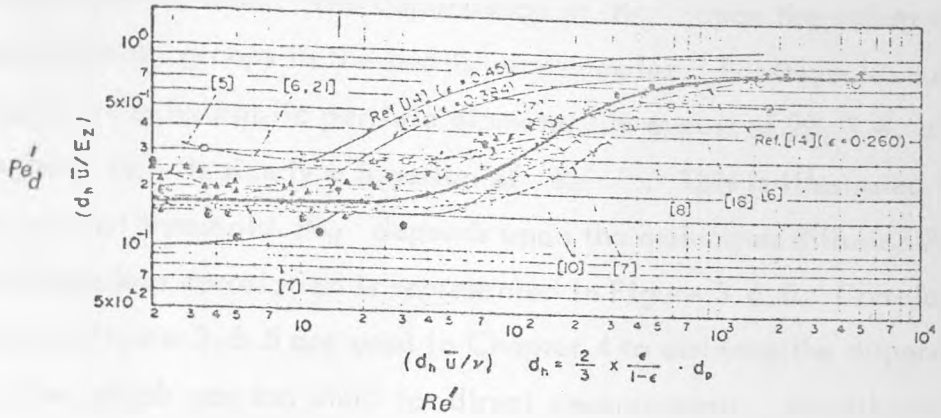

Re'	<20	40	70	100	150	200	300	500	1000	>3000
Pe'_d	0·170	0·190	0·233	0·290	0·385	0·49	0·60	0·70	0·79	0·83

Numerical values from mean correlation curve

Figure 3.6.5 Correlation of Axial Dispersion Data in Packed Beds for $Re' > 20$ (after Miyauchi and Kikuchi, 1975)

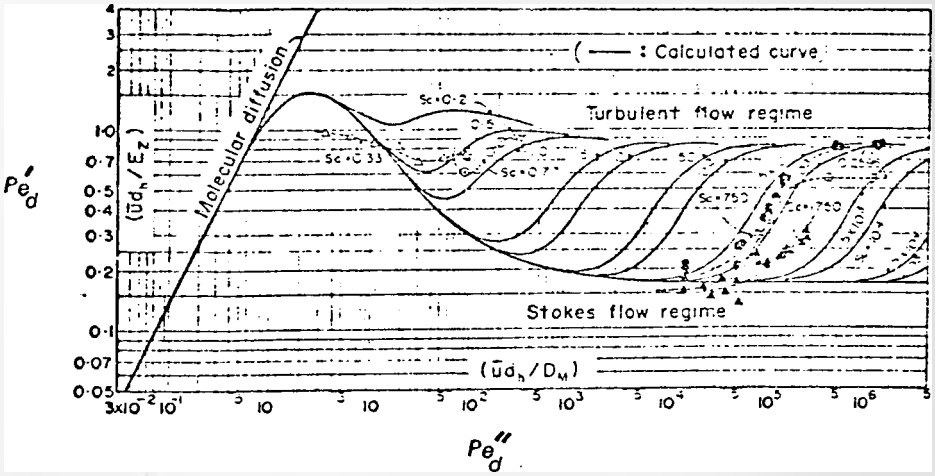

Figure 3.6.6 General Correlation Curves for Axial Dispersion in Packed Beds (after Miyauchi and Kikuchi, 1975)

as it relates the degree of dispersion that develops experimentally e.g. the longer a particular type of packed bed the smaller the relative dispersion. Miyauchi and Kikuchi (1975) reviewed and summarized the accumulated dispersion data in packed beds. The dependence of Pe_d upon the values of the other dimensionless groups in the bed is very complex. For Reynolds number (Re') based on the hydraulic particle diameter, in excess of 20, i.e. above the Stokes regime, Pe_d is simply a function of Re' . This is illustrated in Figure 3.6.5. Below that threshold Pe_d depends upon the molecular diffusion Peclet number. The complete correlation is represented in Figure 3.6.6. Correlations of the type in Figure 3.6.5 are used in Chapter 4 to estimate the dispersion in a column which was too small for direct measurements. As with the mass transfer correlations discussed in Section 3.4, wide variations occur between the different investigations. Fortunately the effect of dispersion on column performance is almost negligible (Chapter 6). Therefore, the values obtained from the correlations are acceptable.

3.7 Models of Packed Bed Perfusion Columns

The sorption, mass transfer and hydrodynamic models discussed in the preceding sections are combined here to form the general model of a packed bed, perfusion column. As with the combined model for batch experiments, certain asymptotic solutions exist. Outside the domain of these solutions the general model equations must be solved directly to simulate the perfusion column.

3.7.1 Asymptotic solutions

All asymptotic solutions for sorption in packed beds make two assumptions (i) plug flow, i.e. no axial dispersion and (ii) a constant inlet concentration.

The most important asymptotic solutions are those based on the constant pattern breakthrough assumption. (Section 2.3). Constant pattern behaviour only occurs for favourable isotherms (Section 3.2). Solutions exist for a variety of combinations of isotherm shapes and controlling mass transfer mechanisms. Vermeulen (1958) summarized the solutions for irreversible isotherms with solid diffusion, pore diffusion, external diffusion and a combination of external and solid diffusion controlling the mass transfer. The more general case of a Langmuir isotherm with external and solid diffusion (described by the linear and quadratic driving force approximations) were also discussed. Hall et al. (1966) employed the intraparticle diffusion equation to develop constant pattern solutions for the solid and pore diffusion mechanisms, for both Langmuir and Freundlich isotherms. Fleck et al. (1973) extended this analysis to include combined mass transfer control, i.e. pore plus external diffusion, solid plus external diffusion, solid plus pore diffusion and pore plus solid plus external diffusion. The only application of these results to perfusion devices is in the design of dialysate and ultrafiltration perfusion systems. This is discussed further in Chapter 7. Constant pattern solutions are of no use in the design of haemo--perfusion columns, since these devices operate well outside the constant pattern regime.

Asymptotic solutions also exist where the intraparticle diffusion is controlled by pore diffusion and the isotherm is irreversible. External diffusion can also be included. These solutions are not reliant upon the constant pattern assumption. Bischoff (1969) developed the general solution for fixed bed reactors and Cooper and Libermann (1970) independently produced the solution to the particular case of packed bed, sorption devices. Brauch and Schlunder (1975) applied the solution, with reasonable success, to data on the adsorption of organic solutes onto activated carbon in a packed bed. However, these solutions have limited applicability to perfusion devices as they do not take into account the falling inlet concentration that occurs with such devices clinically.

3.7.2 Lumped parameter model of a perfusion column

One of the objectives of this thesis is that the models be simple and easy to use, and hence the wider their application and acceptance. The conventional method of modelling a packed bed, sorption column with axial dispersion involves a first and a second order partial differential equation with three independent variables together with a non-linear isotherm equation. The solution of the equations in this distributed model is not only complex but also potentially unstable. By introducing the quadratic driving force approximation for the intraparticle diffusion and the mixing cell model for the axial dispersion the column model reduces to a series of ordinary differential equations, i.e. a lumped parameter model, whose solution is both stable and straightforward. The only disadvantage is that for very small values of axial dispersion the number of cells in the model becomes large, and the number of differential equations rises in proportion. Therefore, it is only realistic to use the lumped parameter model for moderate to large values of axial dispersion.

The lumped parameter model is constructed from the elemental sorption and mass transfer processes discussed in the preceding sections. For simplicity the axial dispersion is restricted to the basic mixing cell model, i.e.

the effects of semi-stagnant regions are ignored. The model consists of a number of identical cells linked in series. Each of the cells contain a fluid phase and a sorbent phase. All elements of each phase in a given cell are in equilibrium, i.e. the fluid and sorbent phases are well mixed. The bulk flow cascades from cell to cell as in the basic mixing cell dispersion model. A typical cell and the controlling kinetic equations are shown in Figure 3.7.1. For convenience, these equations are normalized as shown in Figure 3.7.2.

Other authors have modelled the kinetics in packed bed , sorbent devices using distributed models. Weber and Chakravorti (1974) reviewed many of the papers. A novel feature of the model developed here is the inclusion of axial dispersion and in particular the lumped parameter description of this phenomenon. The only work investigating the effect of axial dispersion is that by Colwell and Dranoff (1969) and (1971). They used the distributed description. However, the results are limited to near linear isotherms and are therefore not applicable to the work in this thesis. Weber and Crittenden (1975) included axial dispersion; however, mass transfer in their model was controlled solely by external diffusion. They also tested a lumped parameter model similar to the one developed here. However, they incorrectly assumed that there was no dispersion in this model - dispersion is implicit in the lumped parameter model. In addition, their model only incorporated an external diffusion, mass transfer resistance.

With respect to perfusion devices in general, and haemoperfusion columns in particular, the model developed here is the first to have included all the mass transfer features that occur in practice, i.e. a non-linear isotherm, external and internal diffusion resistance and axial dispersion. Other models of perfusion devices (Section 2.2) have failed to include one or more of these features.

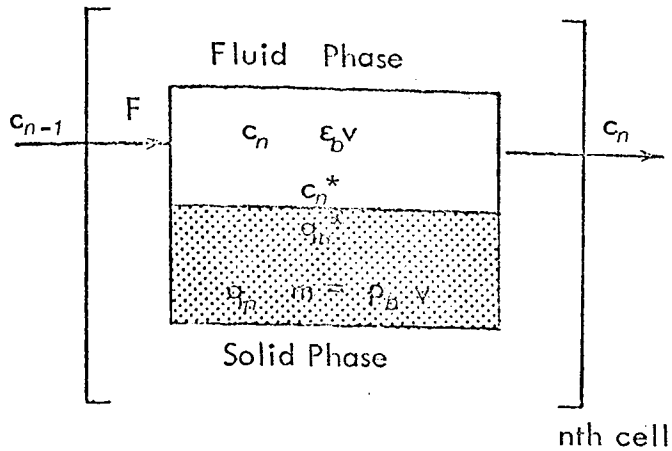

c_n = bulk fluid phase conc. (mg/ml)

q_n = average solid phase conc. (mg/gm)

v = total volume of nth cell (ml)

m = $\rho_b v$ = sorbent mass (gm)

c_n^* = fluid conc. at surface (mg/ml)

q_n^* = solid conc. at surface (mg/gm)

F = volumetric flow rate (ml/sec)

a_p = surface area of sorbents (cm /ml) (per unit vol. of sorbent)

ε_b = porosity of bed (-)

Mass Balance in Fluid Phase

(Rate of Accumulation = Net Convection into Cell -Flux into Sorbent)

$$\text{i.e.} \quad v\varepsilon_b \frac{d c_n}{d t} = F (c_{n-1} - c_n) - k_e a_p (1 - \varepsilon_b) v (c_n - c_n^*) \qquad \text{EQ. 3.41}$$

Equilibrium Isotherm at Fluid/Solid Interface

$$\text{i.e.} \quad q_n^* = \frac{A c_n^*}{1 + A c_n^*} \quad \text{or} \quad c_n^* = \frac{q_n^*}{(A - B q_n^*)} \qquad \text{EQ. 3.42}$$

Mass Balance in Solid Phase

(Rate of Accumulation = Intraparticle Flux = Flux into Sorbent)

$$\text{i.e.} \quad \rho_b v \frac{d q_n}{d t} = \rho_b v \psi_q \frac{60 D_s}{d_p^2} \left(\frac{q_n^{2*} - q_n^2}{2 q_n} \right) = k_e a_p (1 - \varepsilon) v (c_n - c_n^*) \qquad \text{EQ. 3.43}$$

Integration of Concentrations

$$q_n = \int_0^t q_n \, d t + q_{n_o} \qquad \text{EQ. 3.44}$$

$$c_n = \int_0^t c_n \, d t + c_{n_o} \qquad \text{EQ. 3.45}$$

Figure 3.7.1 Equations Describing the Nth Cell in Perfusion Column Model

Normalized Variables

$$\Lambda \equiv \frac{\rho_b q_o}{c_o} \qquad X_n \equiv \frac{c_n}{c_o}$$

$$N_e \equiv \frac{k_e a_p (1-\varepsilon_b)\, n\, v}{F} \qquad Y_n \equiv \frac{q_n}{q_o}$$

$$N_s \equiv \frac{60\, D_s}{d_p^2} \cdot \frac{\Lambda n v}{F} \qquad c_o = \text{normalizing fluid phase concentration}$$

$$T \equiv \frac{F}{n v \Lambda}\, t \qquad q_o = \frac{A c_o}{1 + B c_o}$$

n = no. of cells

Normalized Equations of Nth Cell

$$\frac{d X_n}{d T} = \frac{\Lambda}{\varepsilon_p}\left[n (X_{n-1} - X_n) - N_e (X_{n-1} - X_n^*)\right] \qquad \text{EQ. 3.46}$$

$$Y_n^* = \frac{X_n^*}{R + (1-R) X_n^*} \quad \text{or} \quad X_n^* = \frac{R Y_n^*}{(1 - (1-R) Y_n^*)} \qquad \text{EQ. 3.47}$$

$$\frac{d Y_n}{d T} = N_s \psi_q \frac{Y_n^{2*} - Y_n^2}{2 Y_n} = N_e (X_n - X_n^*) \qquad \text{EQ. 3.48}$$

$$Y_n = \int_0^T \dot{Y}_n\, d T + Y_{n_o} \qquad \text{EQ. 3.49}$$

$$X_n = \int_0^T \dot{X}_n\, d T + X_{n_o} \qquad \text{EQ. 3.50}$$

Figure 3.7.2 Normalized Equations Describing the Nth Cell in Perfusion Column Model

3.8 Computer Implementation

The ordinary differential equations in the lumped parameter column models, plus those for the batch experiments, are readily solved using a modelling or simulation computer package. One of the most widely used packages is the Continuous Systems Modelling Program or CSMP (Speckhart and Green, 1976).

3.8.1 CSMP

CSMP is based on FORTRAN and it was developed for the IBM System 360. The following brief description of CSMP is based on that by McArthur (1972) in "A Users Guide to CSMP".

CSMP is designed to simulate the behaviour of continuous dynamic systems. It is not tailored for any specific discipline. The input language enables the user to prepare statements describing a physical system for either a block diagram or a differential equation representation of that system.

The core of a continuous system simulation program is integration. CSMP provides the user with a choice of seven integration routines varying in complexity from a fixed step, rectangular method to a double precision Milne, fifth-order, predictor-corrector method which automatically adjusts the integration interval to meet user-specified error criteria. User supplied routines may be employed if none of the above seven methods is suitable.

Compared with general purpose high level languages such as Fortran, CSMP language statements are simple to construct and relatively few are required to describe highly complex systems. The program does accept standard Fortran statements, allowing the user to augment the analogue-type block statements of CSMP with the logical branching and conditional capabilities of Fortran. Standard fixed format output is provided for printing and print-plotting variables at user-selected increments of the independent variable. Also available are simple facilities for performing a sequence of runs of the same model structure with different parameters, integration interval, etc.

3.8.2 Algebraic or implicit loops

As CSMP is based on integration, algebraic loops cause problems. An algebraic loop is formed when a particular variable at a given time cannot be expressed as an explicit function of the other variables. In other words the variable is a function of itself at any time step. In terms of a block diagram of the model, an algebraic loop is a loop in where there is no integration or other memory function (i.e. a delay).

By equating the fluid film and the intraparticle diffusion fluxes at the surface of the sorbent particles, one generates an algebraic loop. Therefore, both the batch and perfusion column models (Sections 3.5 and 3.7) involve algebraic loops. (See Figure 3.8.1).

CSMP deals with algebraic loops by use of the IMPLICIT FUNCTION. At each integration time step, the IMPLICIT FUNCTION solves the algebraic loop for the implicit variable by an iterative procedure. The user provides an initial estimate of the value and an error limit for the calculated value. If an acceptable value is not calculated in 100 iterations the program is terminated. This avoids excess computer time. The form of the IMPLICIT FUNCTION statements is illustrated in the computer listing in Appendix 3.

An indirect consequence of the IMPLICIT FUNCTION is that the CSMP array (or specification) format cannot be used. This format allows identical groups of equations to be expressed in terms of an array of integrations and corresponding dynamic equations, thereby providing a shorthand description of the model equation. This is illustrated in the axial dispersion, mixing cell models in Appendix 3. Since the column model includes the IMPLICIT FUNCTION it must be written longhand.

3.8.3 Modifications to QDF formula

The quadratic driving force expression, Equation 3.43 and 3.48, includes division by solid phase concentration. As this is initially zero in all

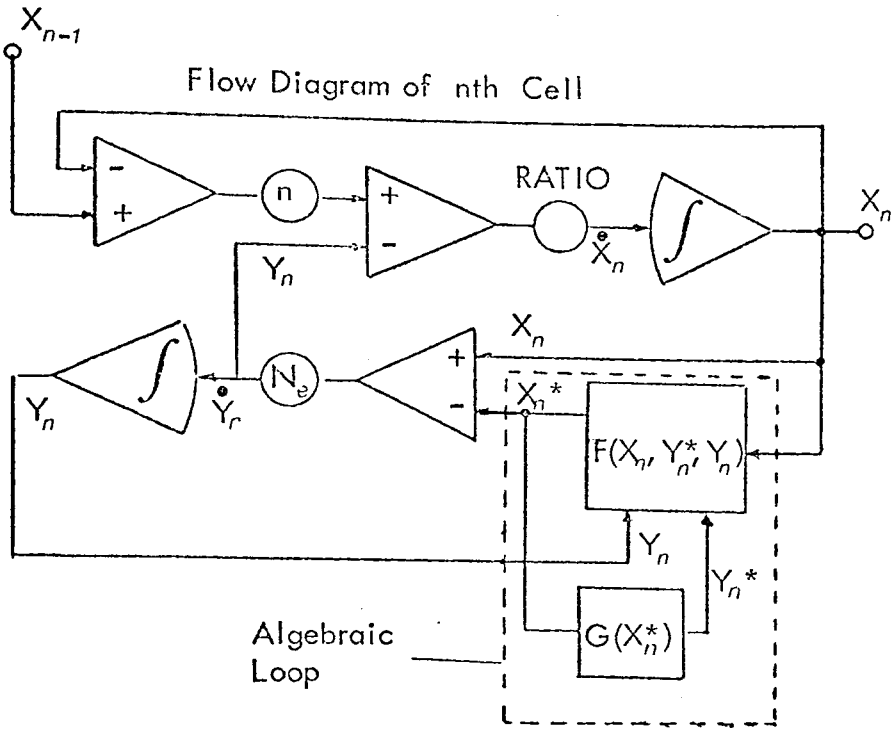

Equations

$$\dot{X}_n = \text{RATIO} \cdot (n \cdot (X_{n-1} - X_n) - \dot{Y}_n)$$

$$X_n = \int_0 \dot{X}_n \, dt + X_{n_0}$$

$$\dot{Y}_n = N_e (X_n - X_n^*)$$

$$Y_n = \int_0 \dot{Y}_n \, dt + Y_{n_0}$$

Algebraic Loop

$$X_n^* = X_n - \frac{N_s \psi_a}{N_e} \left(\frac{Y_n^{2*} - Y_n^2}{2 Y_n} \right) = F(X_n, Y_n^*, Y_n)$$

$$Y_n = X_n^* / (R + (1-R) X_n^*) = G(X_n^*)$$

Figure 3.8.1 Algebraic Loop in Cell Model

instances, division by zero is implied. This difficulty was overcome by adding a constant to the denominator, i.e.

$$\frac{d\,Y_n}{d\,T} = \psi_q \; N_s \left(\frac{Y\,n^{*2} - Y\,n^2}{2\,Y_n + Y_{00}} \right) \qquad \text{EQ. 3.51}$$

where $Y_{00} = 10^{-4}$, say. The effect of Y_{00} on the solution is discussed in Chapter 6.

3.8.4 Computer listings of models

Computer listings of the models for batch experiments, axial dispersion in a column and sorption in a packed bed column are presented in Appendix 3.

CHAPTER 4

ESTIMATION OF THE SORPTION, MASS TRANSFER, AND HYDRODYNAMIC PARAMETER VALUES IN PERFUSION COLUMNS

CHAPTER 4

ESTIMATION OF THE SORPTION, MASS TRANSFER AND HYDRODYNAMIC PARAMETER VALUES IN PERFUSION COLUMNS

4.1 Introduction

This chapter summarizes the results of in vitro experiments to determine the basic sorption, mass transfer and hydrodynamic parameter values in several perfusion columns, i.e. it fulfils part (ii) of the methodology (Section 2.5). The parameter values were calculated by the techniques outlined in Sections 3.2 to 3.6 of Chapter 3. Some of these parameter values were inserted into the perfusion column model (Section 3.7) for validation of that model in Chapter 5. Others were used in Chapter 6 to investigate the influence of parameter values upon perfusion column performance.

Data was collected for two commercial haemoperfusion columns, the Haemocol and the Adsorba 300C (Table 1.2.2), and for two non-commercial perfusion columns, the Detoxyl-S and a small Wrights chromatography column. The Detoxyl-S is a non-commercial variation of the Detoxyl 1 (Table 1.2.2). Detailed descriptions of these columns are presented in Section 4.5

Although this thesis is concerned with sorbents in general, the experiments discussed here are restricted to adsorption on the activated carbons used in the perfusion columns listed above. Table 4.1.1 presents the pertinent physical properties of each of these carbons. The Norit RBX-1 is used in the Adsorba 300C and in the Detoxyl-S. The BDH carbon was used in the Wrights chromatography column and the SS610 is from the Haemocol. Although in both applications, the RBX-1 pellets are coated with semipermeable membranes, the samples used in the adsorption and mass transfer experiments discussed in this chapter, were uncoated as was the BDH carbon. The effect of coated versus uncoated RBX-1 is investigated in Chapter 6. On the other hand, the SS610 granules discussed here were coated as in the Haemocol perfusion column.

Properties	Activated Carbon		
	NORIT RBX-1	BDH	SS 610 (coated)*
Supplier	Norit Clydesdale	British Drug Houses	Smith & Nephew Limited
Particle Shape	Cylindrical Pellets	Spherical Beads	Irregular Granules
Particle Size	1.0 mm ϕ x 2.5 mm long	0.3 - 1.0 mm diameter	1.65 mm - 3.33 mm
Bulk Density, ρ_b (gm/ml)	0.51[1] 0.465[2]	0.565[1] 0.586[2]	0.38[2]
Particle Density, ρ_p (gm/ml)	0.88[3] 0.80[3]	0.90[1]	0.635[3]
Bed Porosity, ε_b (ml/ml)	0.42[2]	0.37[3]	0.40[2]
Internal Area[2] (BET area) m^2/gm	930	-	-
Pore Vol[2] (ml/gm) (>30A)	0.445	0.195	0.290

Notes

1 Measured by author

2 Quoted by manufacturer

3 Calculated from formula - $\rho_p = \rho_b / (1 - \varepsilon_b)$

* Properties calculated for SS610 coated with 2% w/w Hydrogel as in Haemocol perfusion column

Table 4.1.1 Physical Properties of Activated Carbons Investigated

The four sorbates chosen for study with the above perfusion columns and activated carbons were creatinine (MW = 113), sodium salicylate (MW = 160), sodium phenobarbitone (MW = 254) and paracetamol (MW = 151), i.e. one suspected uraemic toxin and three drugs associated with acute poisoning. Analytical techniques for these sorbates are listed in Appendix 4.

Unless otherwise stated, all experiments were conducted at 37° C in phosphate buffer solution, pH 7.4.

4.2 Adsorption Isotherm Experiments

4.2.1 Experimental apparatus

The equilibrium isotherm experiments were conducted in stoppered, 500 ml conical flasks. The flasks containing carbon particles and sorbate solution were agitated on an incubator/orbital shaker (Gallankamp Co. Ltd., Model INR -200).

4.2.2 Experimental method

Samples of carbon were weighed out and added to 100 ml of buffer solution in a flask. The carbon was equilibrated with the buffer and the air in the internal pores of the carbon was expelled (degassing) by shaking the carbon/buffer mixture for 24 hours at 37° C. In the case of the coated SS610 the mixture was steam sterilized at 116°C for 30 minutes, i.e. the same conditions as in preparing the Haemocol. (The above pre-treatments were employed in all the experiments discussed in this chapter.) The sorbate was added to the flask in a second 100 ml of buffer solution. Preliminary experiments established suitable weight to volume ratios for carbon and sorbate to achieve equilibria that were easy to measure and also the approximate time taken to reach those equilibria. In all the subsequent experiments the existence of an equilibrium was confirmed by taking daily measurements for at least three days beyond the estimated equilibrium time. The salicylate experiments were conducted over four days while those with the phenobarbitone and paracetamol took six days. Details of the creatinine experiments are given in Section 4.2.4.

Several desorption experiments were also conducted. Following an adsorption experiment, the sorbate solution was decanted off and 100 ml of fresh buffer solution placed in the flask. The flask was then returned to the shaker and measurements taken after the desorption equilibria had been reached.

4.2.3 Isotherms

The isothermal points were calculated from a simple mass balance

in the equilibrated flasks. In all cases, allowance was made for the loss of sorbate due to sampling prior to reaching equilibrium. The adsorption isotherms for sodium salicylate and sodium phenobarbitone with each of the three activated carbons are presented in Figures 4.2.1 to 4.2.6.

The error bars in the values of q represent the expected, accumulated uncertainty due to measurement errors. The formula used to estimate this value is given in Appendix 5, together with the individual measurement errors.

The constants for the Langmuir equations were calculated using a Scatchard plot. From Equation 3.1

$$\frac{c}{q} = \frac{1}{A} + \frac{B}{A} c \qquad \text{EQ.4.1}$$

Therefore, if (c/q) is plotted against c a straight line results and the Langmuir constants A and B are calculated from the intercept and the slope.

If it could be assumed that there were negligible errors in the values of c and that the distribution of the errors in the values of (c/q) were normal and all had the same variance, then a linear regression could be performed to find A and B. This would also provide estimates of the possible errors in A and B resulting from measurement errors in the values of (c/q) for each c. However, there are finite measurement errors associated with c and the expected variance in the errors in (c/q) vary markedly with c. Therefore, a linear regression has no meaning if applied to this data. The values of A and B were measured by drawing a 'best fit' line by eye on each of the Scatchard plots. The points with a small value of c were weighted most heavily.

Temperature dependence. By definition, adsorption isotherms are temperature dependent. The critical question is the degree of temperature dependence. Figure 4.2.7 illustrates the difference in the BDH/Salicylate

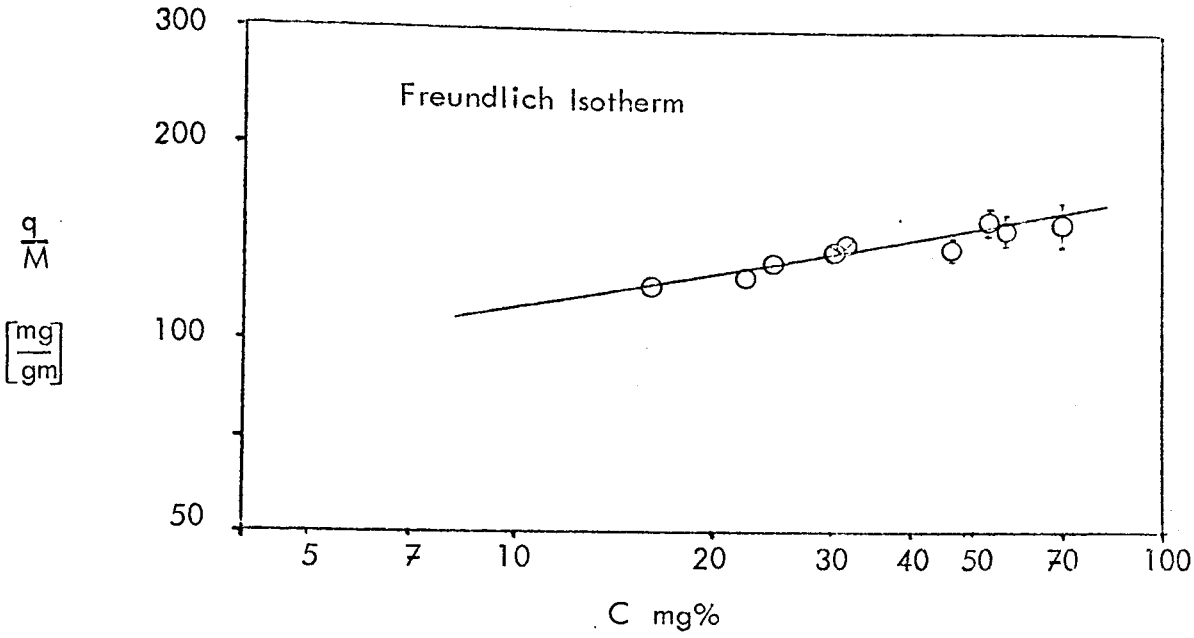

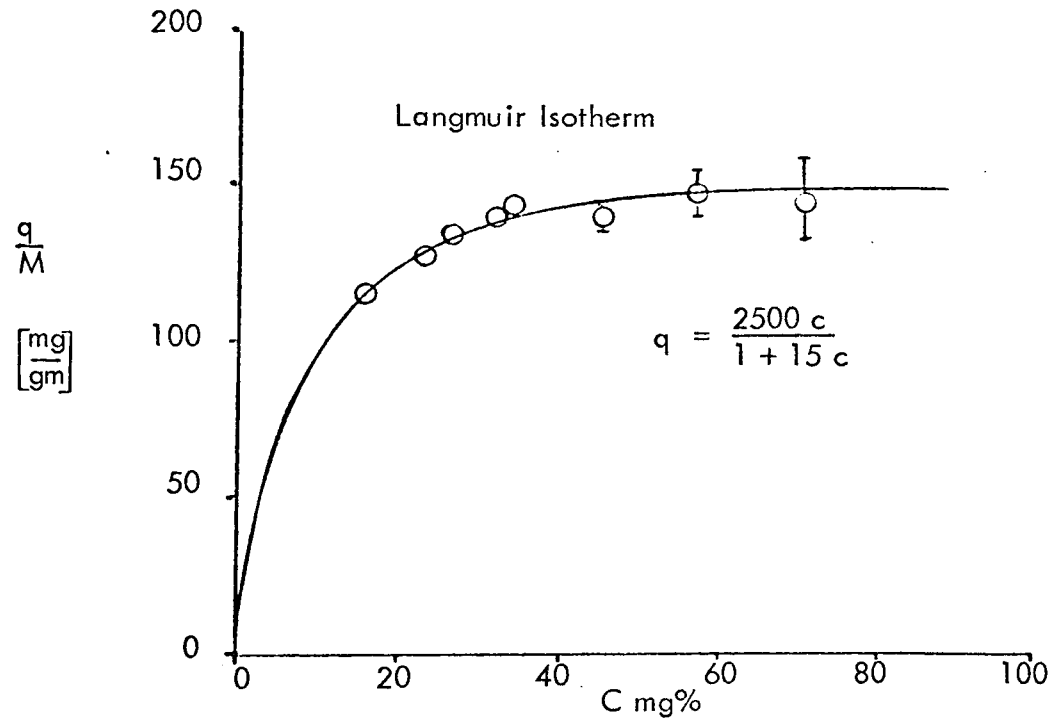

Figure 4.2.1 Isotherms for Sodium Salicylate on BDH Spherical Activated Carbon

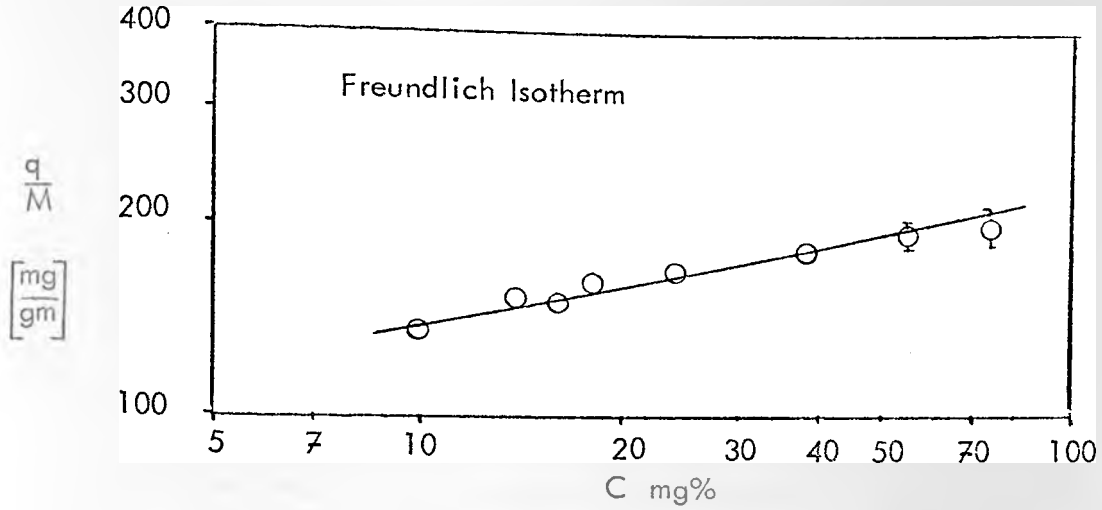

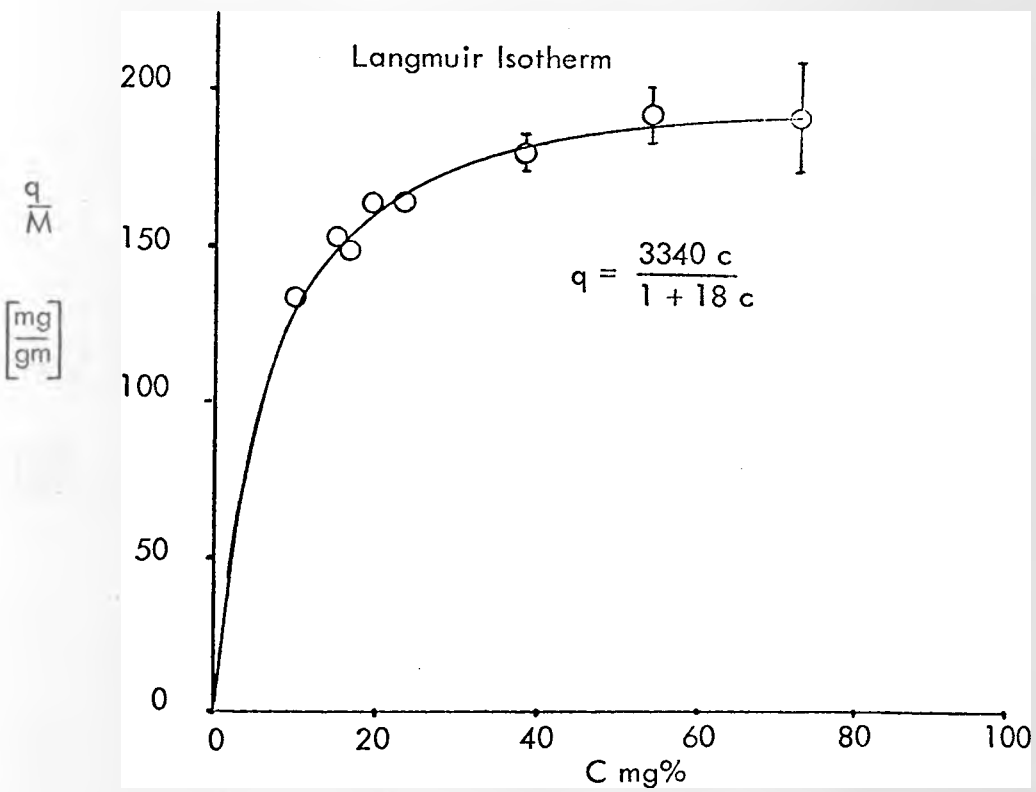

Figure 4.2.2 Isotherms for Sodium Salicylate on Norit RBX-1 Granular Activated Carbon

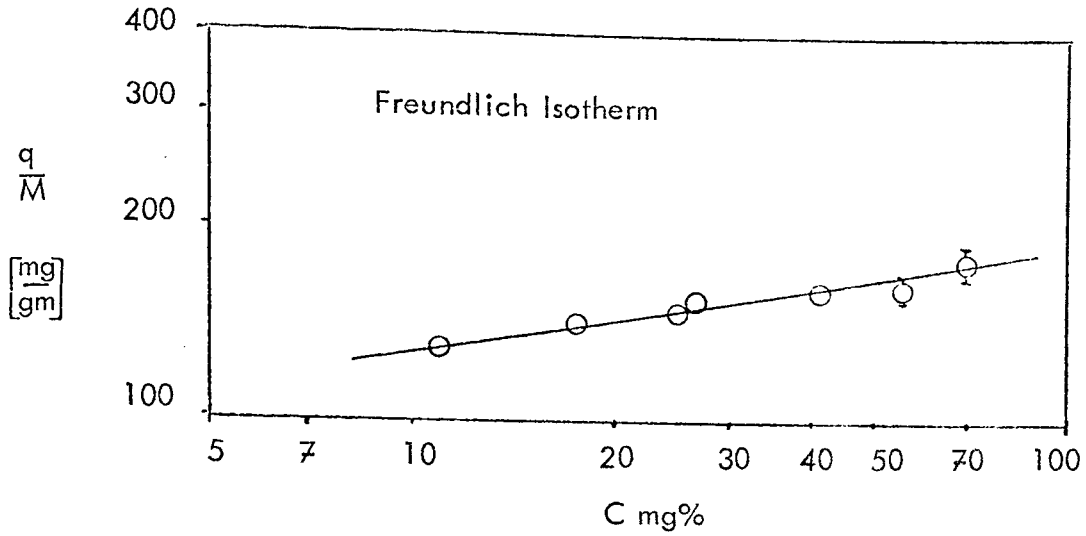

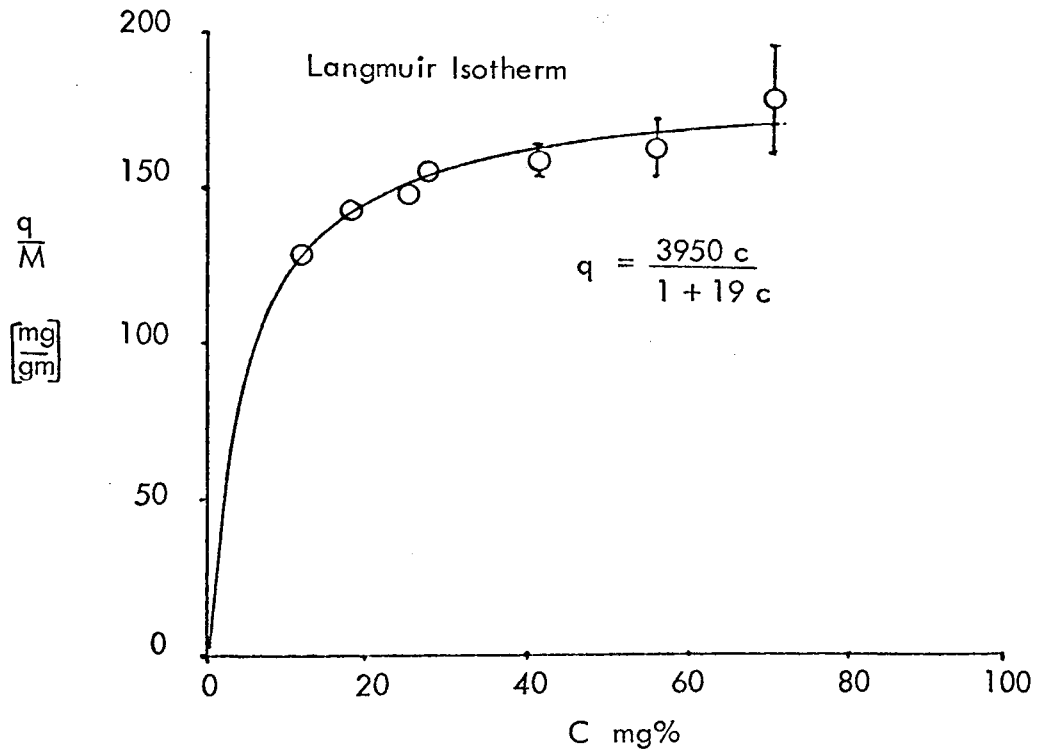

Figure 4.2.3 Isotherms for Sodium Salicylate on SS 610 (Coated) Activated Carbon

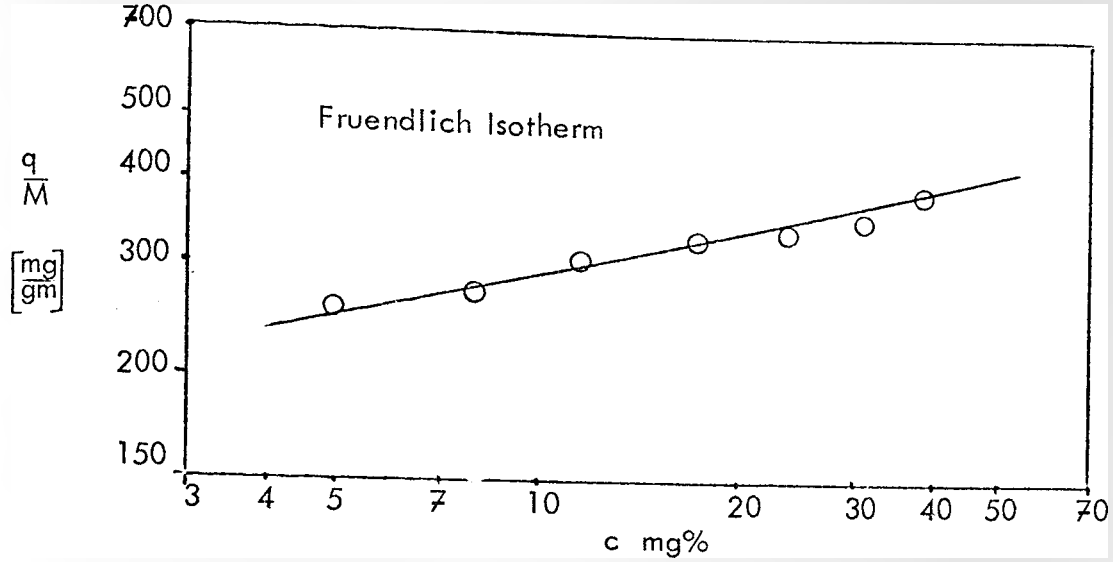

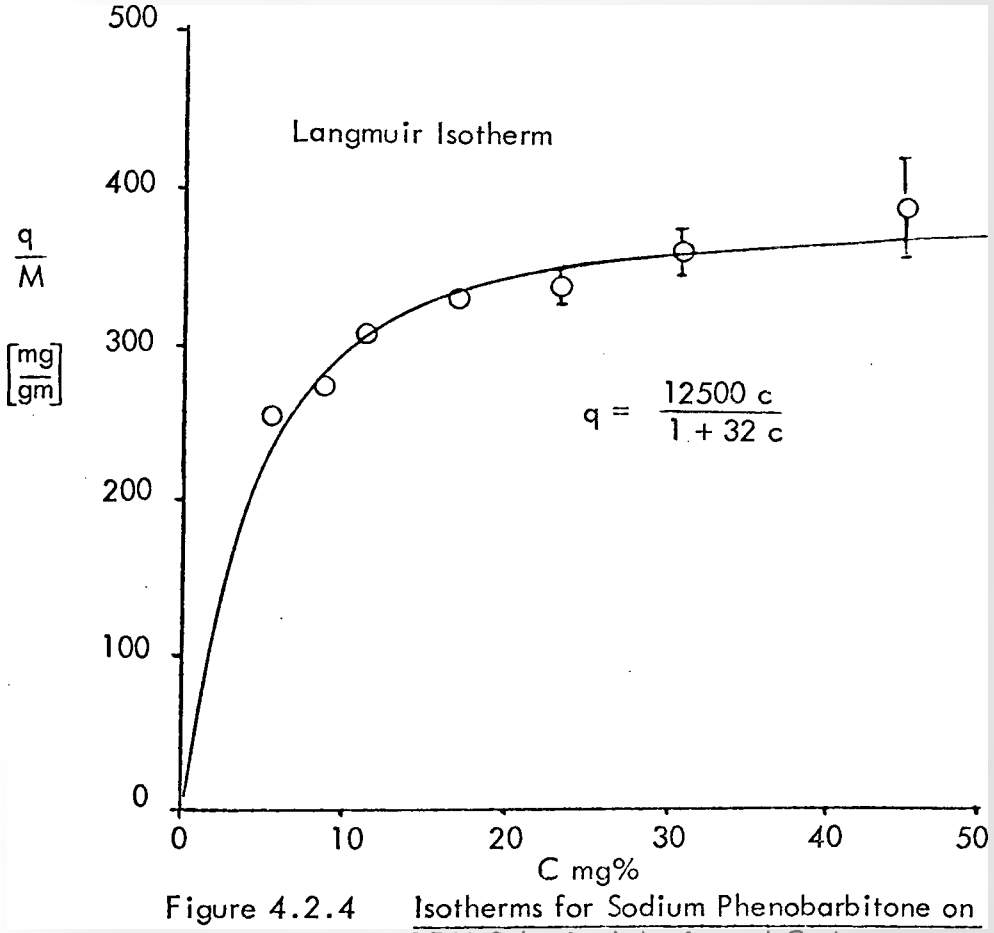

Figure 4.2.4 Isotherms for Sodium Phenobarbitone on BDH Spherical Activated Carbon

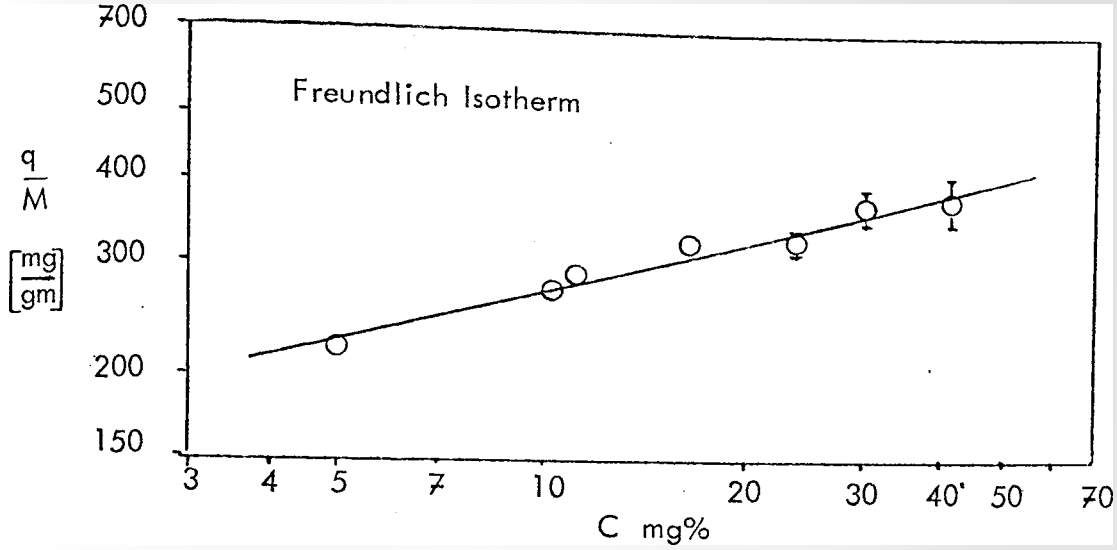

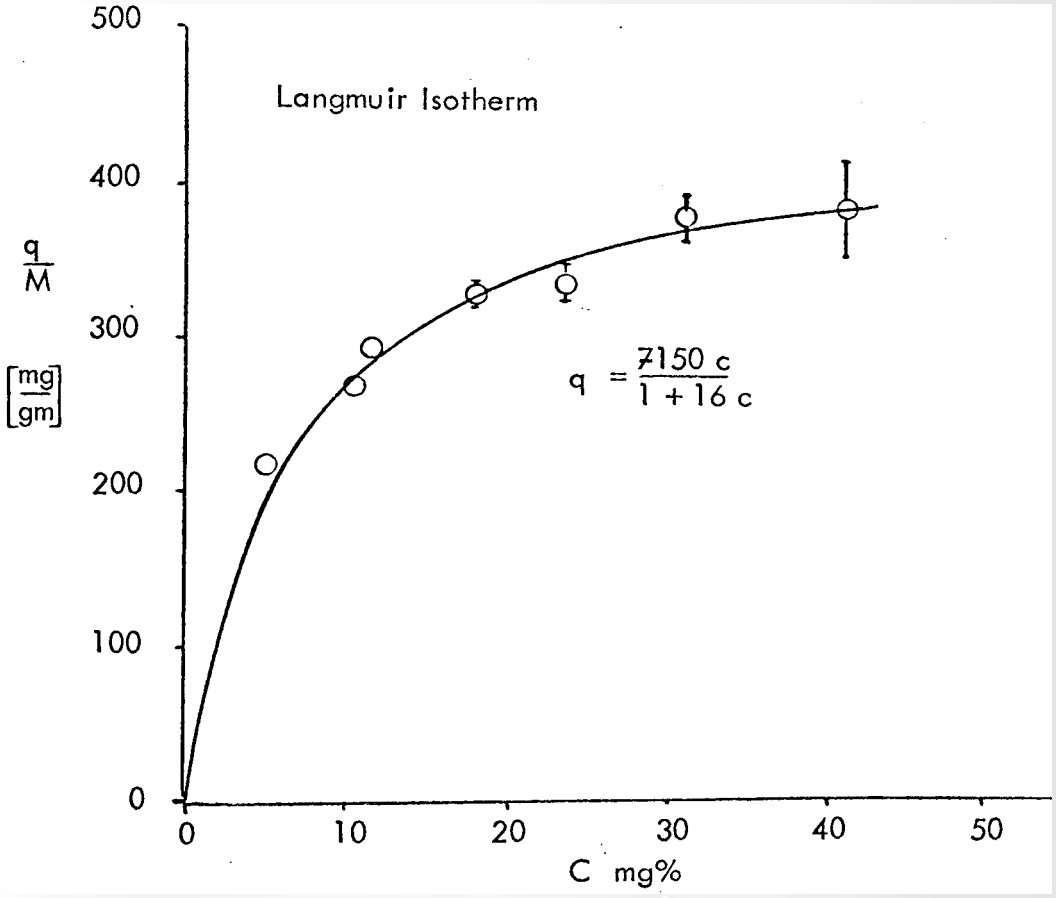

Figure 4.2.5 Isotherms for Sodium Phenobarbitone on Norit RBX-1 Granular Activated Carbon

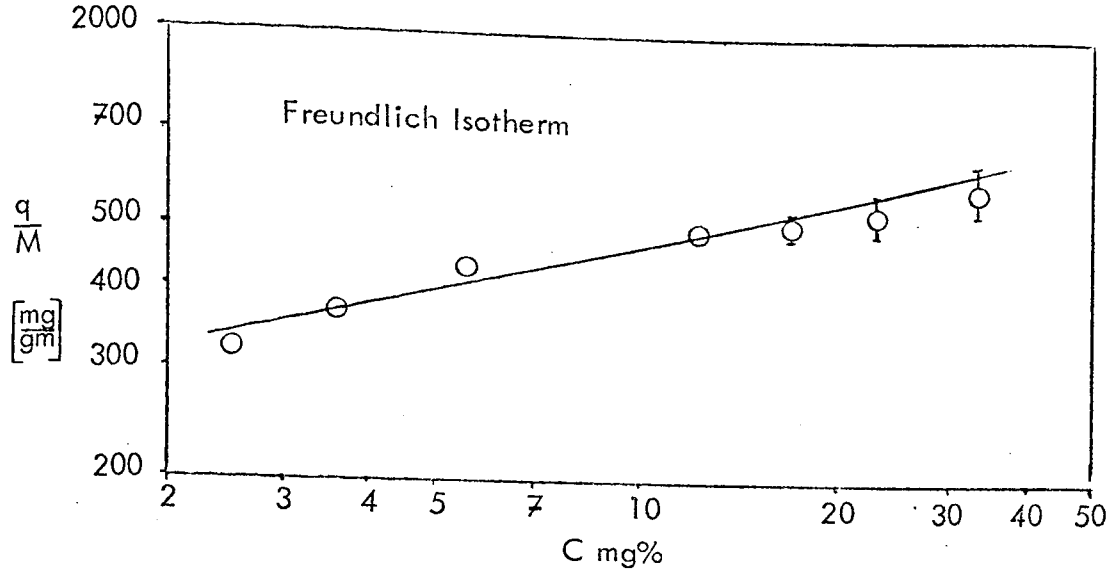

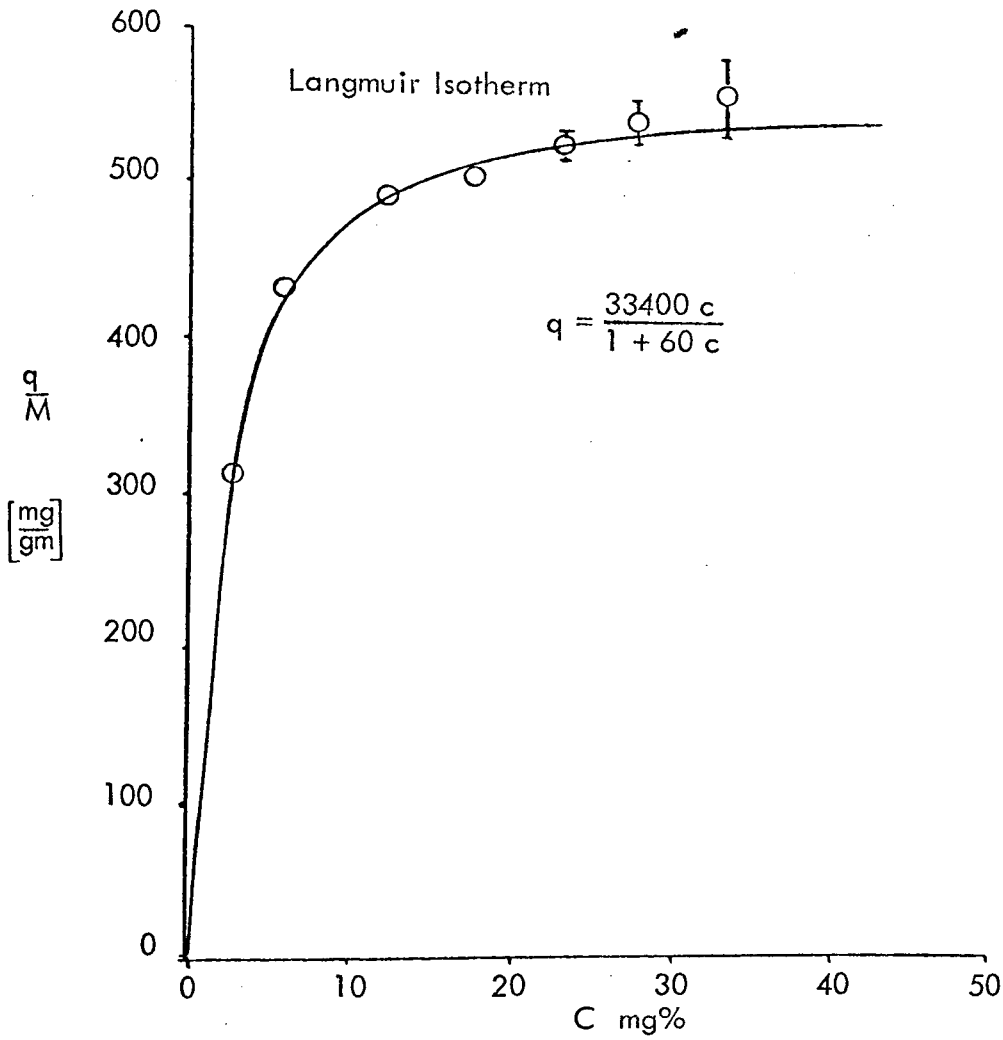

Figure 4.2.6 Isotherms for Sodium Phenobarbitone on SS 610 (Coated) Activated Carbon

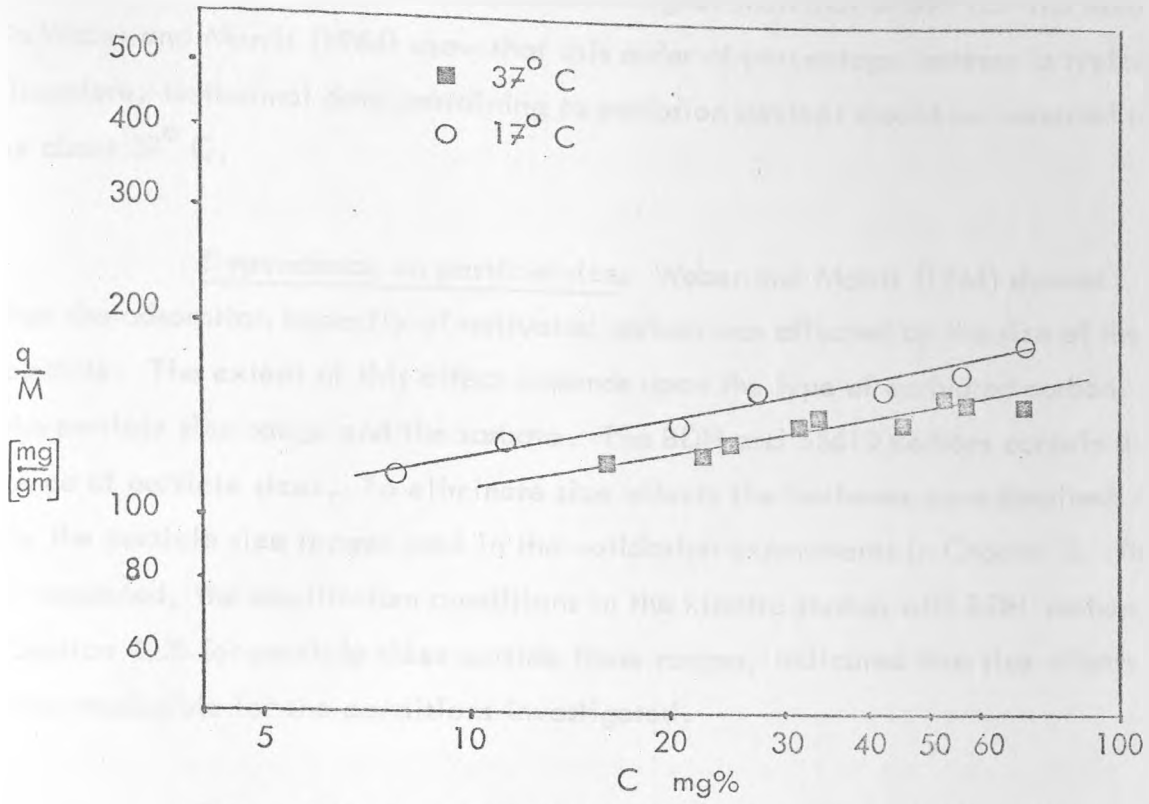

Figure 4.2.7 Effect of Temperature on Isotherm for Sodium Salicylate and BDH Activated Carbon

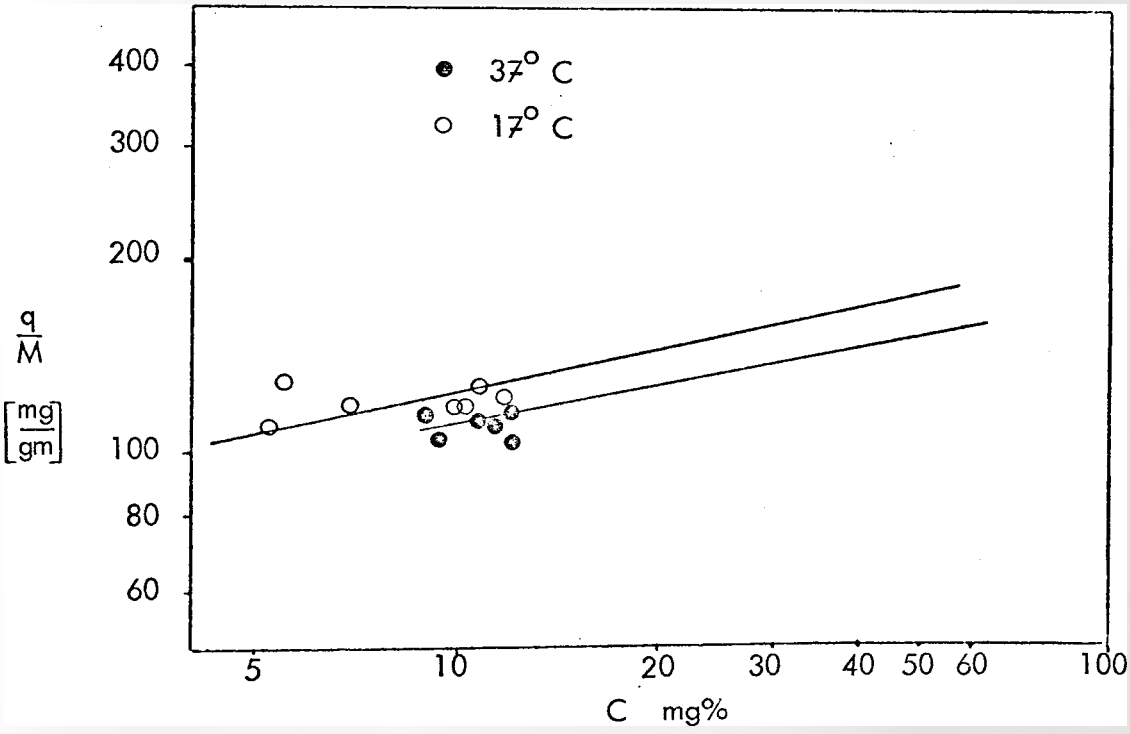

Figure 4.2.8 Desorption Isothermal Data for Sodium Salicylate on BDH Activated Carbon

isotherms for body temperature (37° C) and room temperature (17° C). The capacity at room temperature is up to 20% higher than that at 37° C. The data in Weber and Morris (1964) show that this order of percentage increase is typical. Therefore, isothermal data pertaining to perfusion devices should be measured at or about 37° C.

Dependence on particle size. Weber and Morris (1964) showed that the adsorption capacity of activated carbon was affected by the size of the particle. The extent of this effect depends upon the type of activated carbon, the particle size range and the sorbate. The BDH and SS610 carbons contain a range of particle sizes. To eliminate size effects the isotherms were obtained for the particle size ranges used in the validation experiments in Chapter 5. As it happened, the equilibrium conditions in the kinetic studies with BDH carbon, (Section 4.3) for particle sizes outside these ranges, indicated that size effects were negligible for the conditions investigated.

Desorption. It is implicitly assumed that adsorption equilibrium are reversible. The assumption was tested for the adsorption/desorption of sodium salicylate on BDH carbon. The combined adsorption/desorption data is shown on Figure 4.2.8. The experimental technique caused the desorption data to be grouped together and to have a relatively large experimental error. Nevertheless, the desorption data does fit the adsorption isotherm, as assumed.

4.2.4 Catalytic breakdown in adsorption experiments

Although the isotherm experiments with salicylate and phenobarbitone reached apparent equilibria in several days (as expected) those with creatinine and paracetamol did not. In the case of the creatinine, the concentration in solution in the flask continued to fall over a period of weeks such that the amount of creatinine removed from solution per gram of carbon was far in excess of the adsorption capacity that was expected apriori. It was assumed that the creatinine was being broken down chemically and that the carbon was catalysing the reaction. A similar conclusion was reached for the paracetamol.

The action of activated carbon as a catalyst was not completely unexpected. Carbon has long been known to be a catalyst, expecially of oxidation reactions. (Garten and Weiss, 1957 and Coughlin, 1969). Nevertheless, only one reference to catalysis in the presence of activated carbon in theraputic applications existed at the time the above isotherm experiments were conducted. Sparks et al. (1969) reported that the concentration of creatinine in an adsorption experiment decreased to a minimum and then began to rise slowly with time, when measured by a radio labelling technique. However, if measured chemically, it decreased monotonically. Catalysis was suspected. More recently the chemical conversion of creatinine has been reported by Tijssen et al. (1977). The results of this paper are broadly similar to those of the author and others at the Bioengineering Unit, University of Strathclyde. Smith et al. (1978) and McClure (1977) have quantified certain aspects of the chemical breakdown in aqueous and buffer solutions including a preliminary investigation of the reaction products. However, no data exists on the extent of the catalysis in vivo or even in blood or plasma in vitro. Sparks et al (1969) found that the breakdown that occurred in buffer solution could not be detected in gut fluid. Therefore, although catalysis is a major factor in aqueous and buffer solutions, it may be far less important clinically. Nevertheless, it severely hampers the interpretation of in vitro experiments designed to estimate the adsorption and mass transfer parameters.

The simplest approach to the problem is to assume that the breakdown has an intrinsic rate that is relatively independent of both the concentration of the sorbate and the reaction products. Under these conditions, the concentration in a batch experiment falls at a constant rate, once the adsorption capacity is exhausted. The equilibrium capacity of the carbon is found by extrapolating the concentration kinetic back to the origin and performing the usual mass balance. The rate of breakdown is proportional to the slope of concentration kinetic. In practice, not all batch experiments exhibited a constant rate of breakdown. However, provided the fall in concentration over the course of the experiment was relatively small, the rate was roughly constant. As the mass of carbon was increased, in comparison to the amount of sorbate in solution, the fall in concentration was larger and the slope of the kinetics became progressively smaller

Activated Carbon	Toxin	Temp. (°C)	Conc. Range (mg %)	$\dot{Q}$ (mg/gm/hr)
Norit RBX 1 Granules	Creatinine	17	2 - 100	2.5 ± 0.3
Coated SP610		37	10 - 100	4
Norit RBX 1 Granules	Paracetamol	37	10 - 50	0.55 ± 0.1
Coated SP610		37	10 - 50	0.4 ± 0.05
BDH spheres (0.71 -0.85)		37	10 - 50	0.2 ± 0.05

Table 4.2.1 Apparent Rates of Breakdown of of Creatinine and Paracetamol in the Presence of Activated Carbon

with time. This indicates a decline in the breakdown rate with declining concentration. Breakdown rates measured in experiments conducted in different concentration ranges showed a slight tendency to fall off with concentration although with the scatter in the data it was impossible to detect a significant trend. (Table 4.2.1). If the size of the particles is reduced, adsorption is more rapid and it is easier to distinguish between kinetics relating to adsorption and those relating to the breakdown. Hence the experiments need only last hours rather than days. However, a reduction in the particle size may also increase the adsorptive capacity of the carbon. Nevertheless, it was found that by crushing the Norit RBX-1 granules and selecting fragments in the size range 0.51 mm to 0.71 mm, the isotherm data was consistant with that obtained for the granules.

The accumulated isotherm data for creatinine and Norit RBX-1 is presented in Figure 4.2.9. The corresponding rates of creatinine breakdown are listed in Table 4.2.1. The rate of creatinine breakdown on coated SS610 carbon is also listed. However, there was insufficient data with this carbon to warrant an isotherm. In all cases the loss of creatinine due to sampling has been accounted for.

McClure (1977) estimated the dependence of this rate in Norit RBX-1 pellets on the presence of oxygen in the solution. If oxygen was bubbled into the solution then the rate was 20.8 mg/gm/hr whereas it was only 2.9 mg/gm/hr when the solution was saturated with nitrogen. The value obtained without bubbling gas through the solution was 3.9 mg/gm/hr. This is larger than that obtained by the author. This discrepancy may be due to the different pretreatment of the carbon employed by McClure, or simply difference in the batch of carbon. McClure also investigated the effect of temperature on the rate of breakdown. As expected, the rate decreased with decreasing temperature. The breakdown rate in powdered Norit RBX-1 is much larger than that in the granular form, i.e. 50 mg/gm/hr compared to 2.5 mg/gm/hr. (Smith et al. 1978). This suggests that the reaction may be limited in the granules by the diffusion of either creatinine into or reaction products out of the particle. Alternatively, the crushing of the

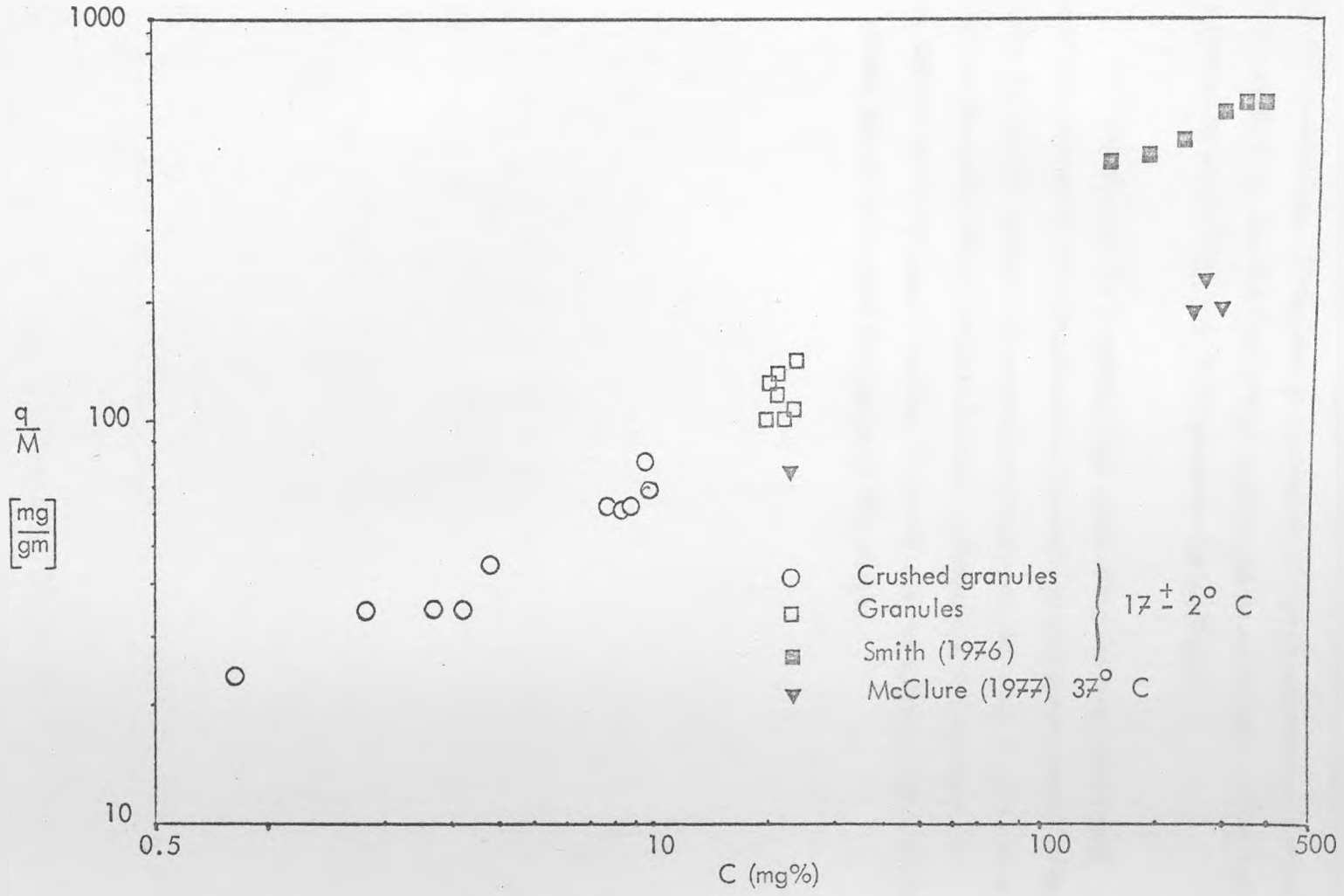

Figure 4.2.9 Accumulated Isotherm Data for Creatinine on Norit RBX-1

granules may expose more sites for the catalysis. Without further data it is impossible to state what the contribution either of these mechanism is to the rate in the granules.

With paracetamol the apparent rate of breakdown is much smaller than that for creatinine. Therefore it was easier to design experiments from which the rate of breakdown and the isothermal data could be extracted. Table 4.2.1 lists the rate data while Figure 4.2.10 presents the isotherms.

Considering the uncertainties surrounding the true nature and kinetics of the adsorption and breakdown of creatinine and paracetamol in the presence of activated carbon, all subsequent experimental work involves only sodium salicylate and sodium phenobarbitone. Although it is important that these phenomena be investigated further, in particular the clinical implications, such an investigation is beyond the scope of this thesis.

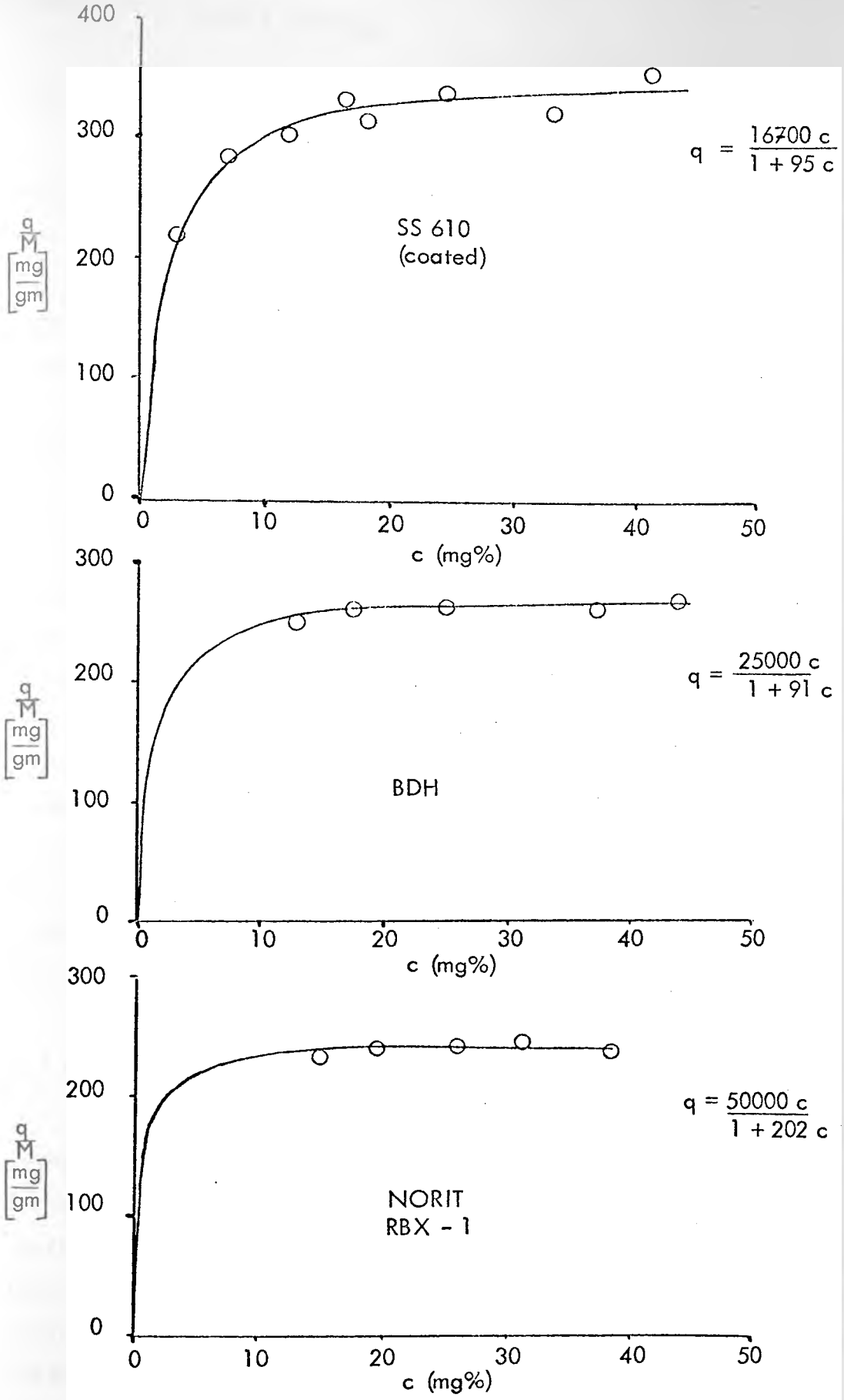

Figure 4.2.10 Paracetamol Isotherms

4.3 Batch Experiments

4.3.1 Experimental apparatus

The batch experiments were conducted in a Quickfit three necked, round bottom flask. The flask was partially submerged in a temperature controlled water bath. The contents of the flask were stirred by a single blade impeller driven by a 1/30 H.P. Multispeed Stirrer (Anderman & Co. Ltd.,London). The stirring speed was monitored by a rev-counter attached to the gear box on the stirrer. The temperature in the solution in the flask was maintained at 37°C.

4.3.2 Experimental method

After pre-treatment (Section 4.2.2) the carbon/buffer mixture was placed in the three necked flask and the impeller set at around 100 RPM. The sorbate and the remainder of the buffer solution were then added via one of the side necks and the stirring speed increased to the experimental value of 400 RPM. This transfer took less than twenty seconds and zero time was assumed to be half way through this transfer. Samples (2 ml) were withdrawn from the flask at appropriate time intervals using a syringe with a length of small bore tubing attached. During sampling the stirrer was stopped and the temperature measured via the other side neck. The sampling procedure took less than fifteen seconds. The samples were diluted 1:10 for measurement on the spectrophotometer. The speed was checked regularly between samples by the rev-counter and minor adjustments made to the motor settings.

4.3.3 External mass transfer coefficients

The external mass transfer coefficients were calculated from the initial slopes in the kinetic data from the batch experiments and Equation 3.22. For the BDH and RBX carbons the external mass transfer is composed entirely of the fluid film resistance whereas for the SS610 it consists of the membrane plus fluid film resistances. The values of specific area, a_p, for calculation of the external mass transfer coefficient, k_e , are based on the geometry of the particles. The RBX pellets are finite length cylinders and for a mean length of 2.5 mm,

the specific area is given by $(4.8/d_p)$ as opposed to $(6.0/d_p)$ for the BDH spheres. The SS610 granules pose a problem in that they do not have a regular, geometric shape. For convenience, they are represented as spheres of diameter equal to their largest dimension. This assumption does not affect the results from the batch studies as the critical parameter in the model is $k_e a_p$. (Section 3.4) The values of k_e based on the estimated, a_p , are given in Table 4.3.1 at the end of this section, together with the experimental conditions and the estimated solid diffusivities.

Effect of stirrer speed. The effect of stirrer speed on the external mass transfer coefficient was investigated for adsorption of sodium salicylate on BDH carbon. There was a steady increase of about 15% over the range 200 RPM to 500 RPM. Therefore the upper limit of relative velocity between the particles and the solution had not been reached. However, the geometry of the flask caused marked cavitation at the higher speeds resulting in minor attrition and fines generation. Therefore 400 RPM was chosen as a compromise, between increasing the mass transfer and decreasing the fines generation.

4.3.4 Solid diffusivities

Having obtained the external diffusion coefficients it is possible to simulate the batch experiments using the model in Figure 3.5.1 and thereby estimate D_s . The various experimental batch kinetics and simulations are depicted in Figures 4.3.1 to 4.3.11. The results are summarized in Table 4.3.1.

In all cases, the simulations take account of the loss of solvent (and sorbate) due to sampling. At each time of sampling the volume of solvent in the model is reduced by 2 ml. This modification to the basic batch model is illustrated in Appendix 3.

The model kinetics in the BDH (spherical) carbon take into account the range of particle diameters by depicting the solutions for the upper and lower limits of diameter in each experiment.

Activated Carbon		Sorbate	M (gm)	V_b (ml)	c_o (mg/ml)	$t_{1/2}$ (min)	k_e (cm/sec) $\times 10^{+3}$	D_s (cm^2/sec)	
Type	Av. Size (cm)							Model	Neretniek's Normogram
BDH Spheres	0.046	Sodium Salicylate	2.0	400	0.9	7.5	2.7	3.3×10^{-8}	3.3×10^{-8}
	0.067		2.0	400	0.9	13	2.4	3.6×10^{-8}	3.5×10^{-8}
	0.093		2.0	400	0.9	27	2.3	3.3×10^{-8}	3.0×10^{-8}
	0.046	Sodium Phenobarbitone	0.5	400	0.5	128	2.1	1.6×10^{-9}	1.45×10^{-9}
	0.093		2.0	400	0.5	48	1.75	1.5×10^{-9}	-
NORIT RBX - 1 Cylindrical Pellets	0.1 ϕ x 0.25 long	Sodium Salicylate	2.4	400	0.9	26	2.3	6.6×10^{-8}	6.3×10^{-8}
			1.6	400	0.9	30	2.7	6.6×10^{-8}	6.2×10^{-8}
			1.0	400	0.5	120	1.7	5.0×10^{-9}	4.5×10^{-9}
		Sodium Phenobarbitone	0.5	400	0.5	400	1.9	5.0×10^{-9}	5.4×10^{-9}
			2.5	400	0.5	26	1.8	5.0×10^{-9}	-
SS 610 (coated) Granules	0.18	Sodium Salicylate	2.0	400	0.9	60	1.00	5.6×10^{-8}	5.4×10^{-8}

Table 4.3.1 Summary of Experimental Conditions and Estimated Values of Intraparticle Diffusivity in Batch Experiments

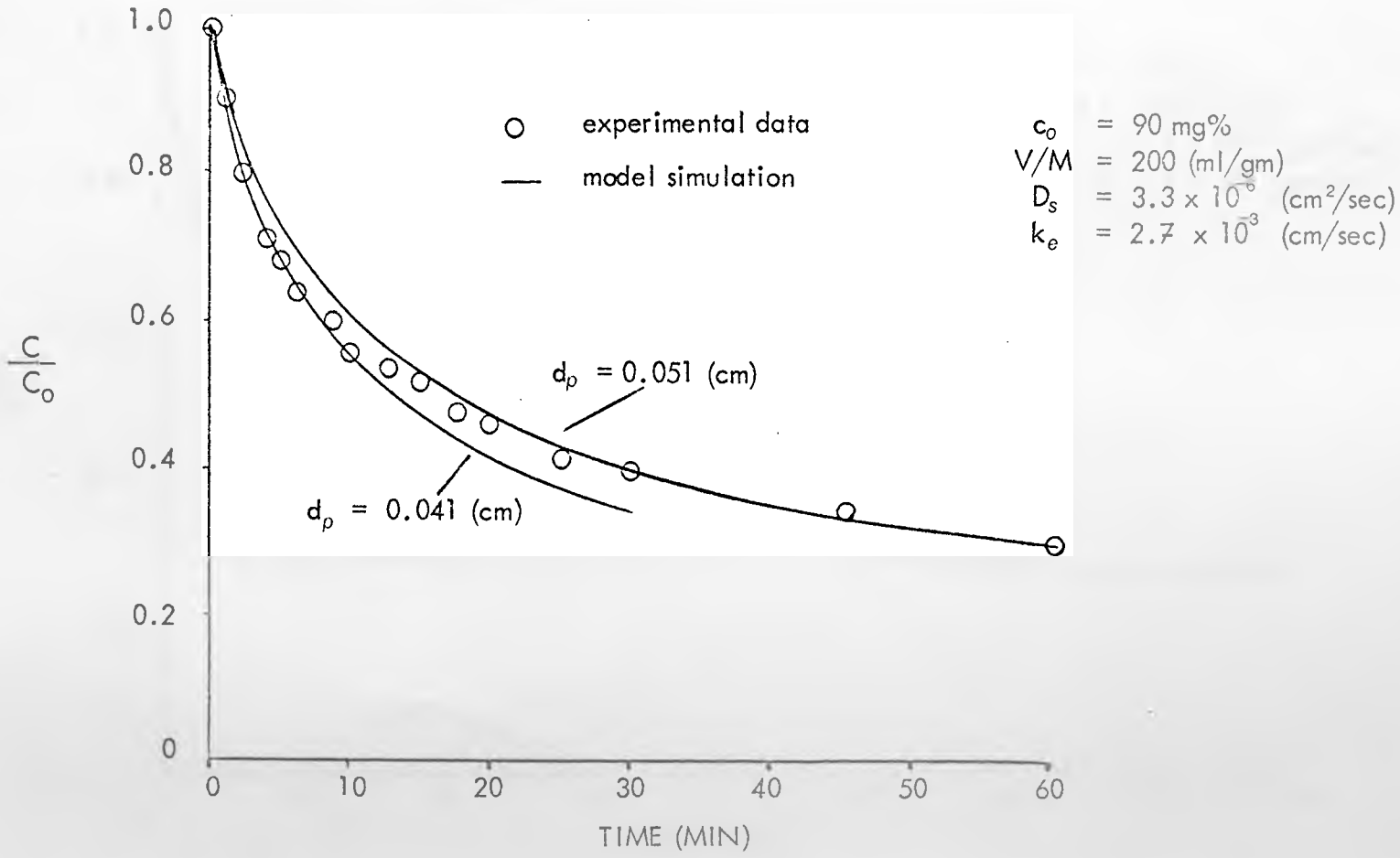

Figure 4.3.1 Batch Adsorption of Sodium Salicylate by BDH Activated Carbon

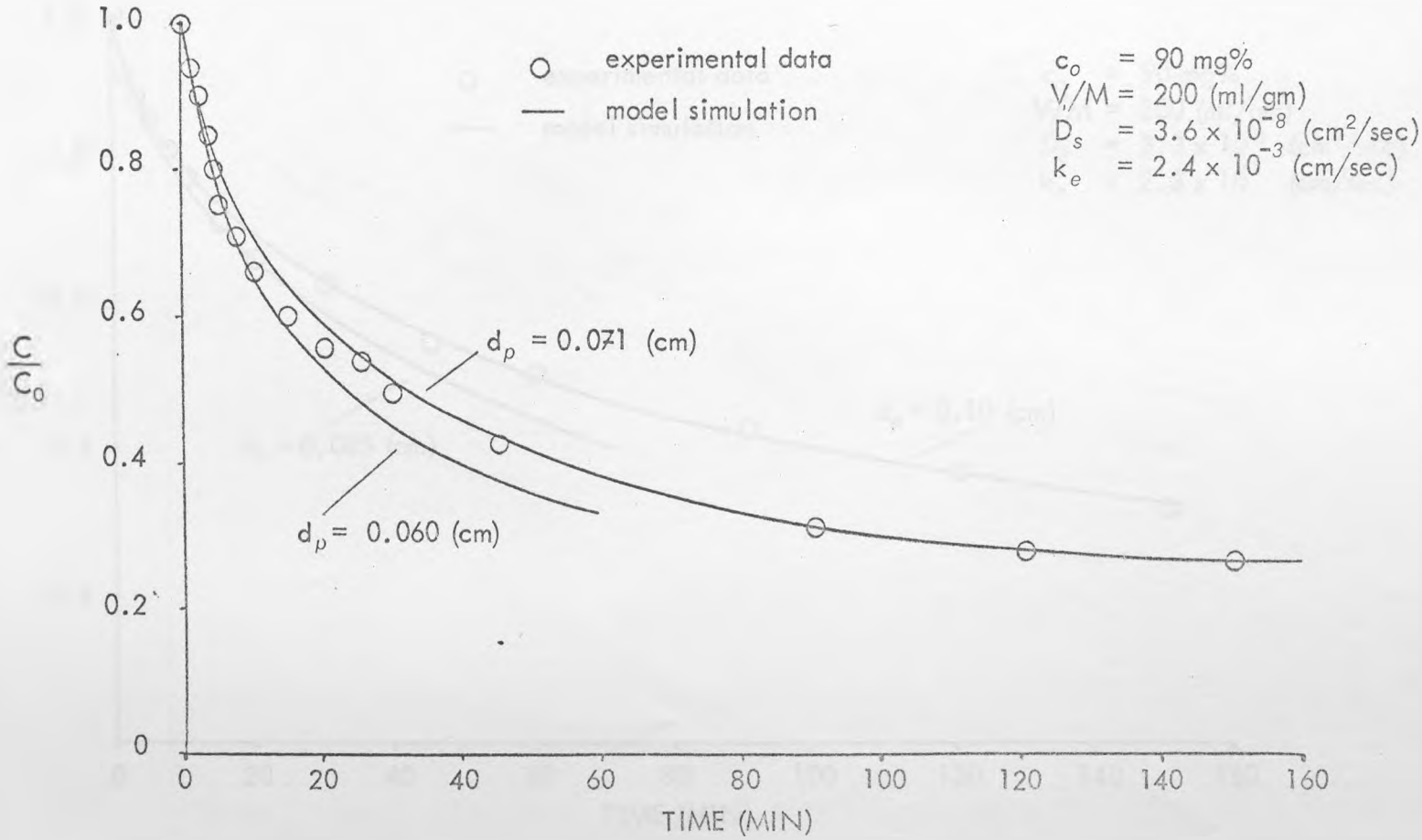

Figure 4.3.2 Batch Adsorption of Sodium Salicylate by BDH Activated Carbon

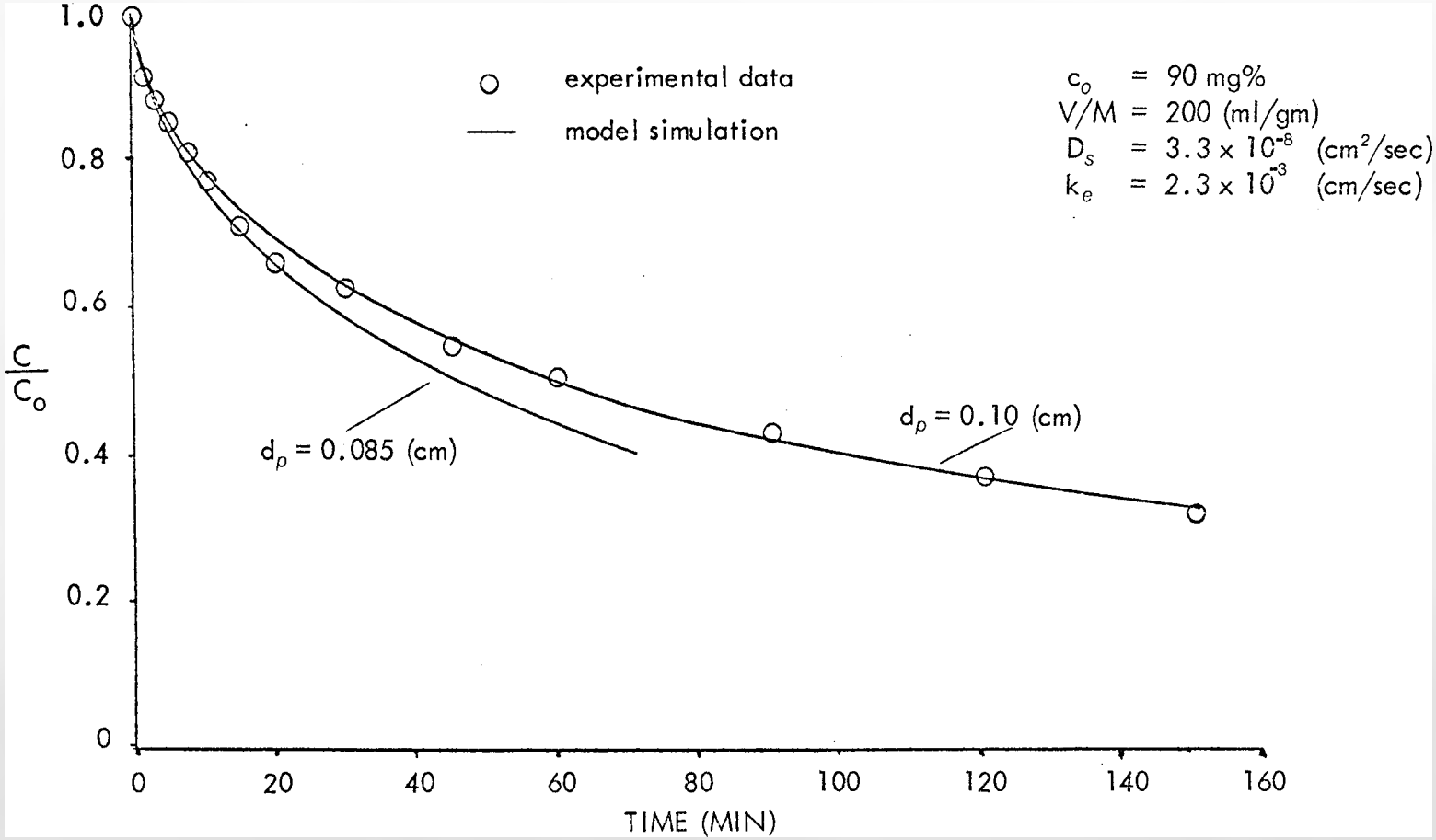

Figure 4.3.3 Batch Adsorption of Sodium Salicylate by BDH Activated Carbon

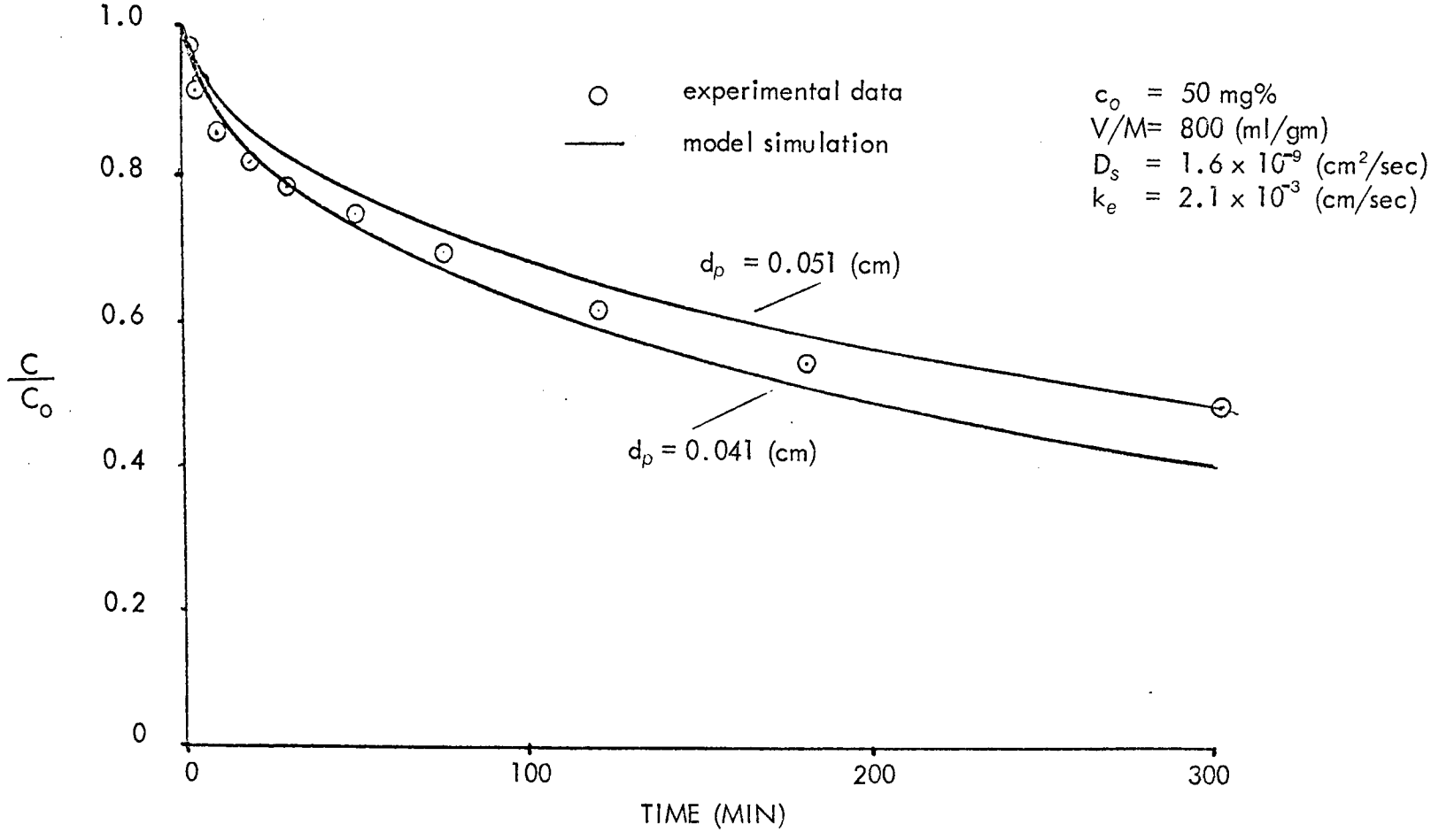

Figure 4.3.4 Batch Adsorption of Sodium Phenobarbitone by BDH Activated Carbon

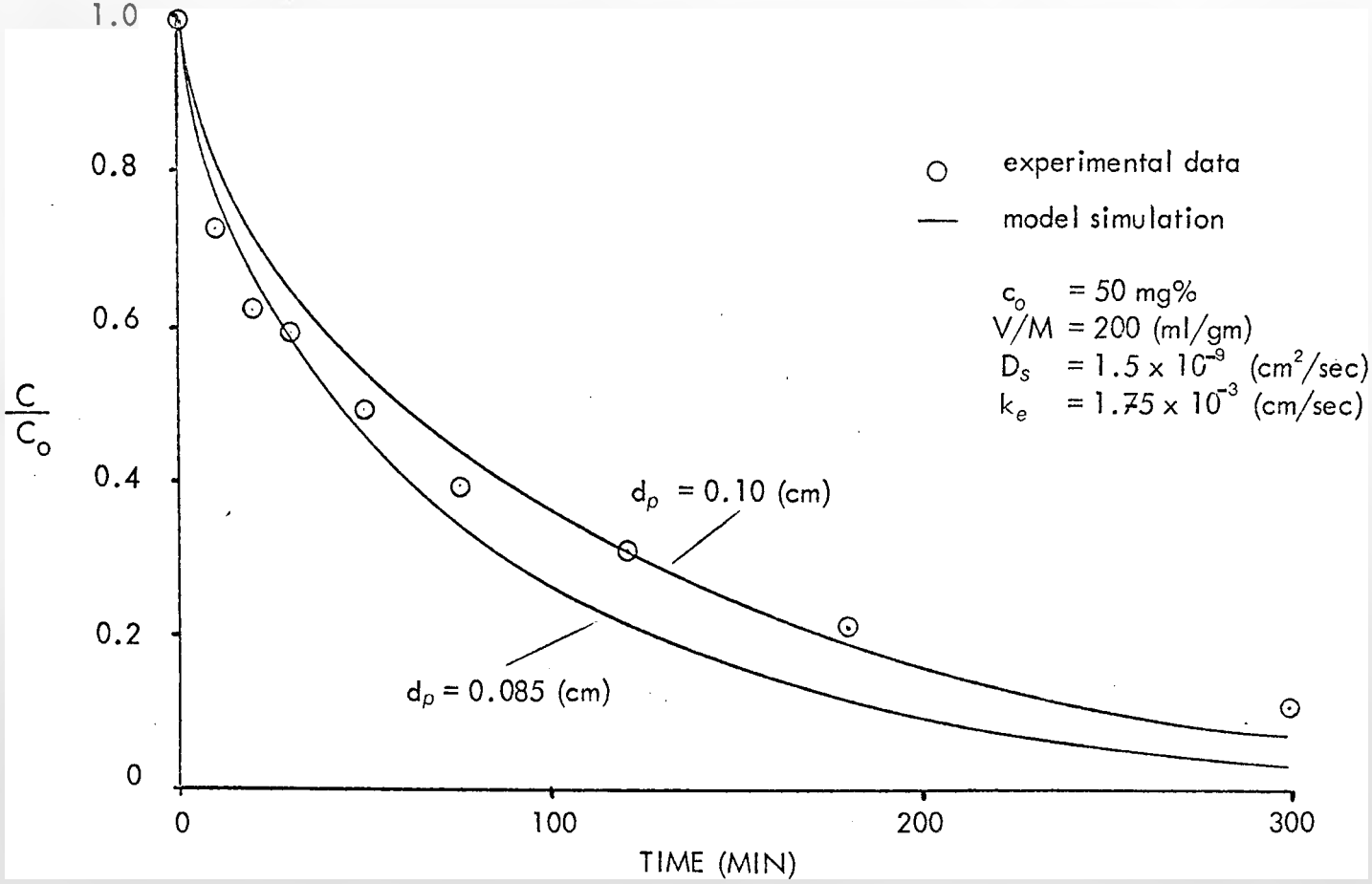

Figure 4.3.5 Batch Adsorption of Sodium Phenobarbitone by BDH Activated Carbon

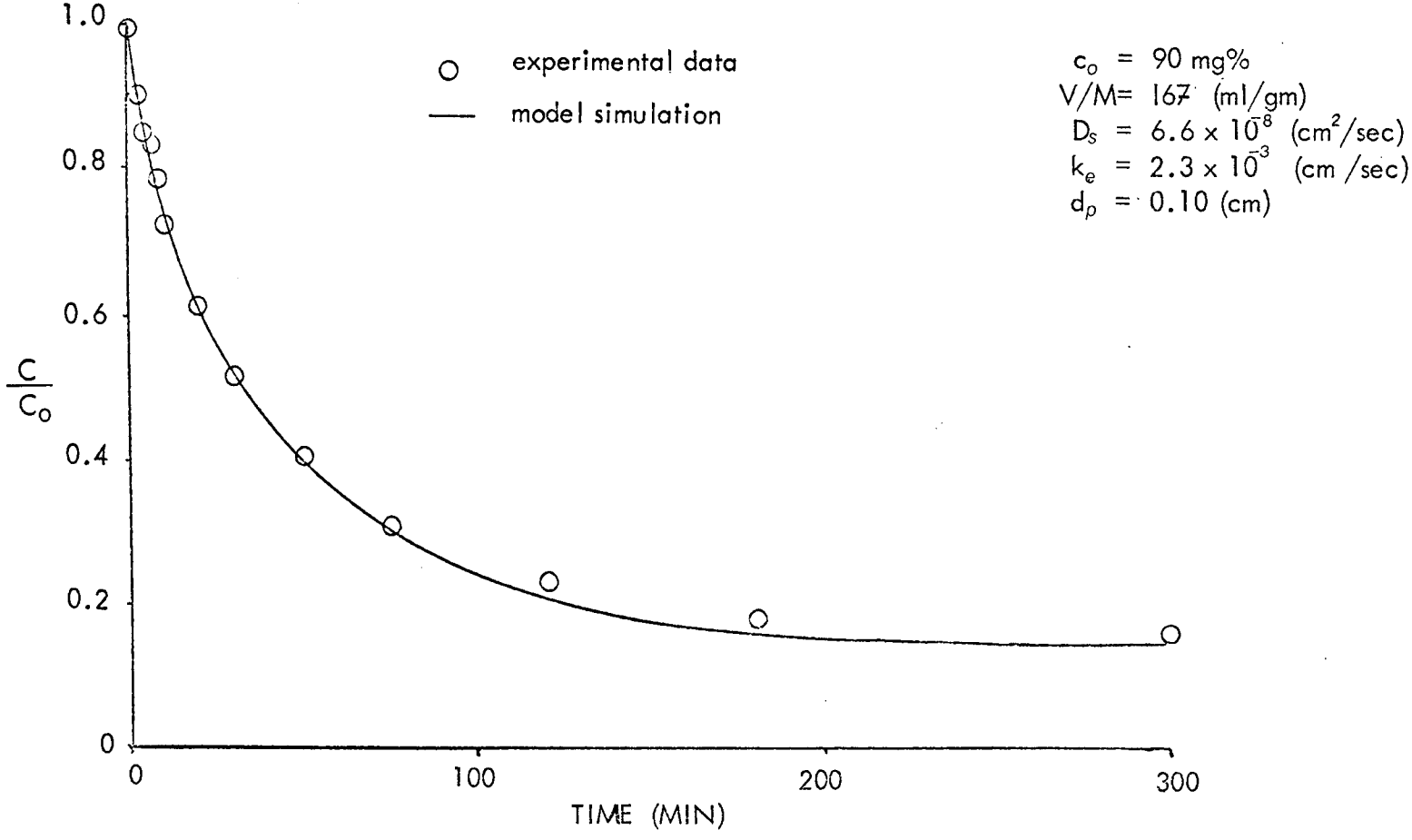

Figure 4.3.6 Batch Adsorption of Sodium Salicylate by Norit RBX-1 Activated Carbon

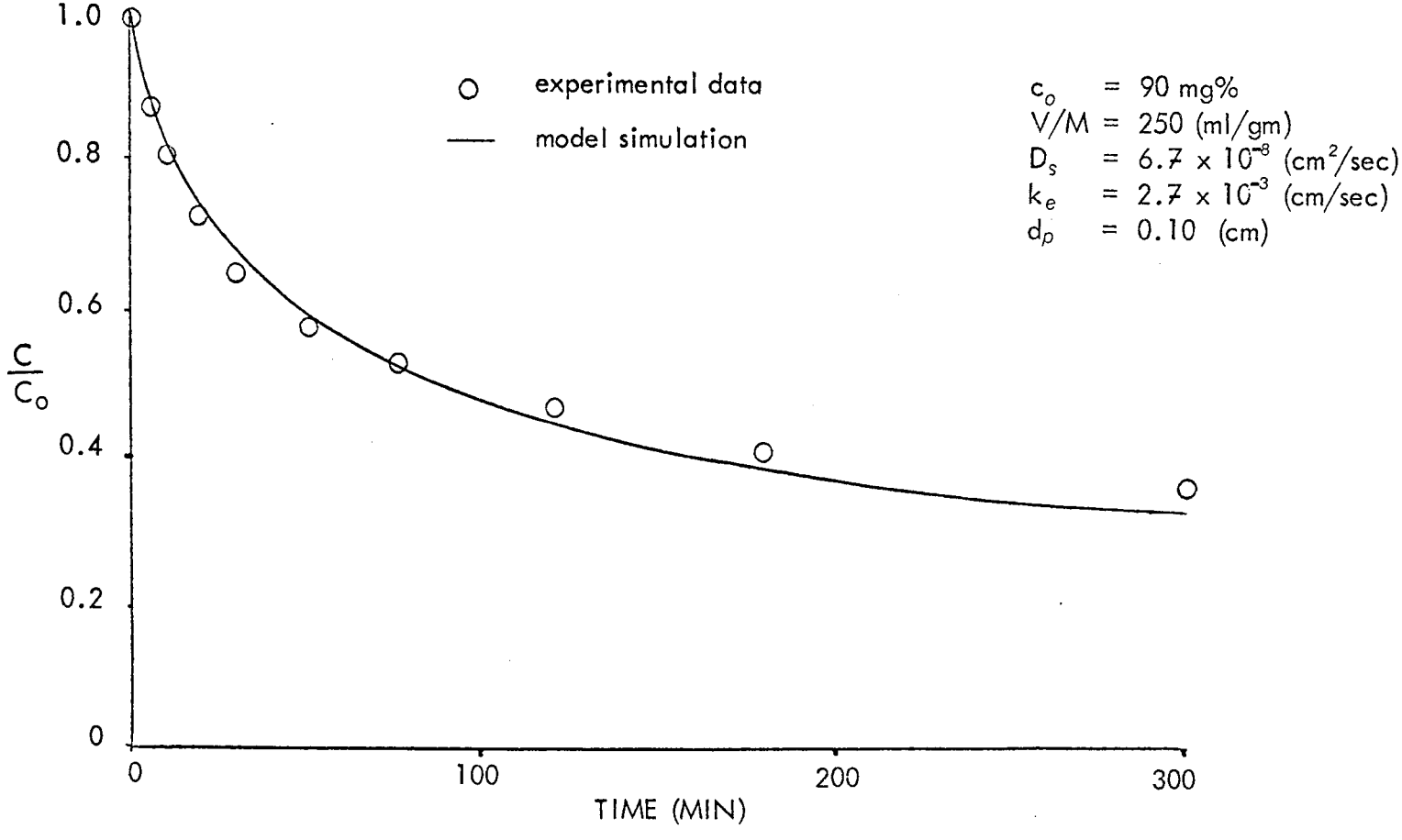

Figure 4.3.7 Batch Adsorption of Sodium Salicylate by Norit RBX-1 Activated Carbon

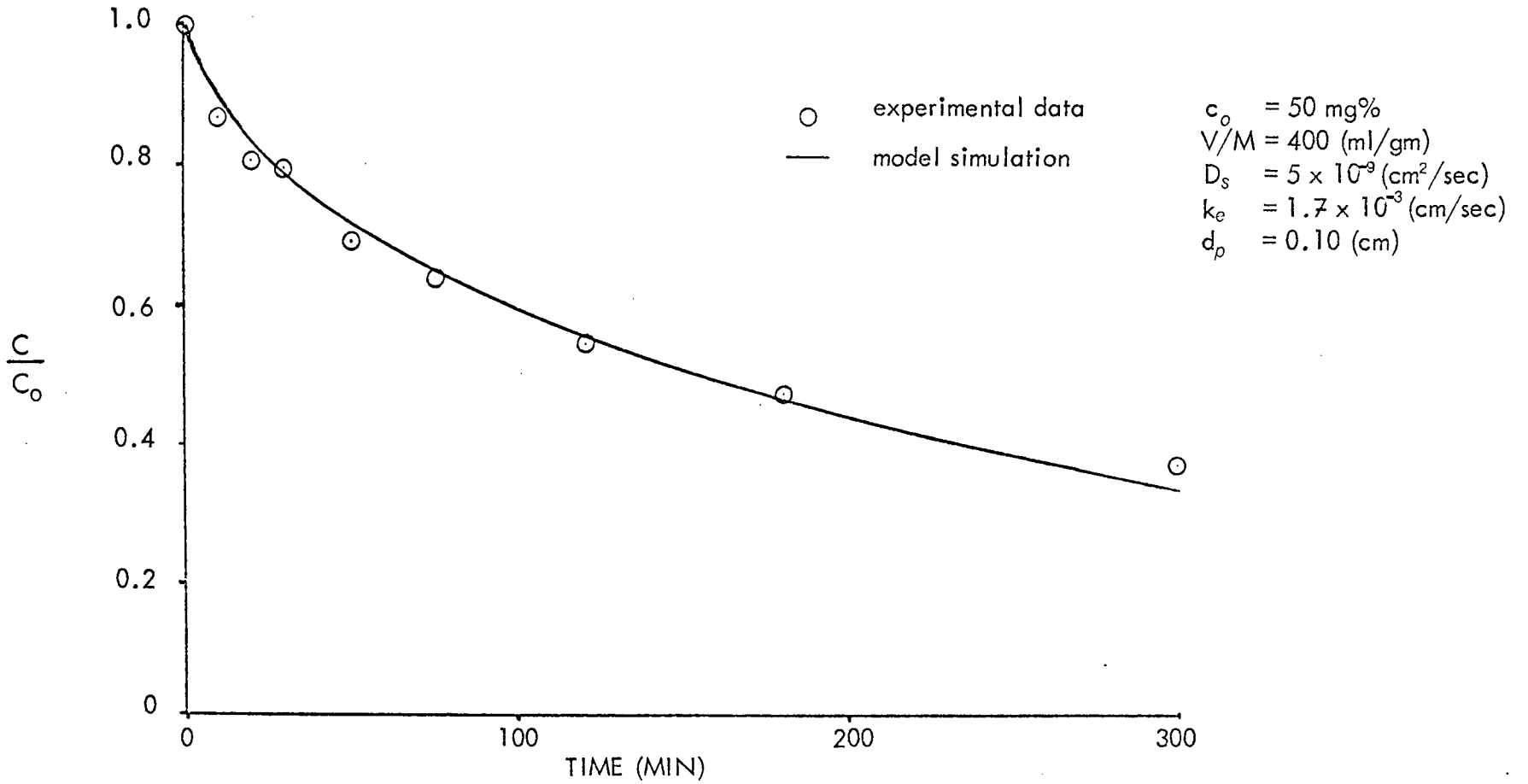

Figure 4.3.8 Batch Adsorption of Sodium Phenobarbitone by Norit RBX-1 Activated Carbon

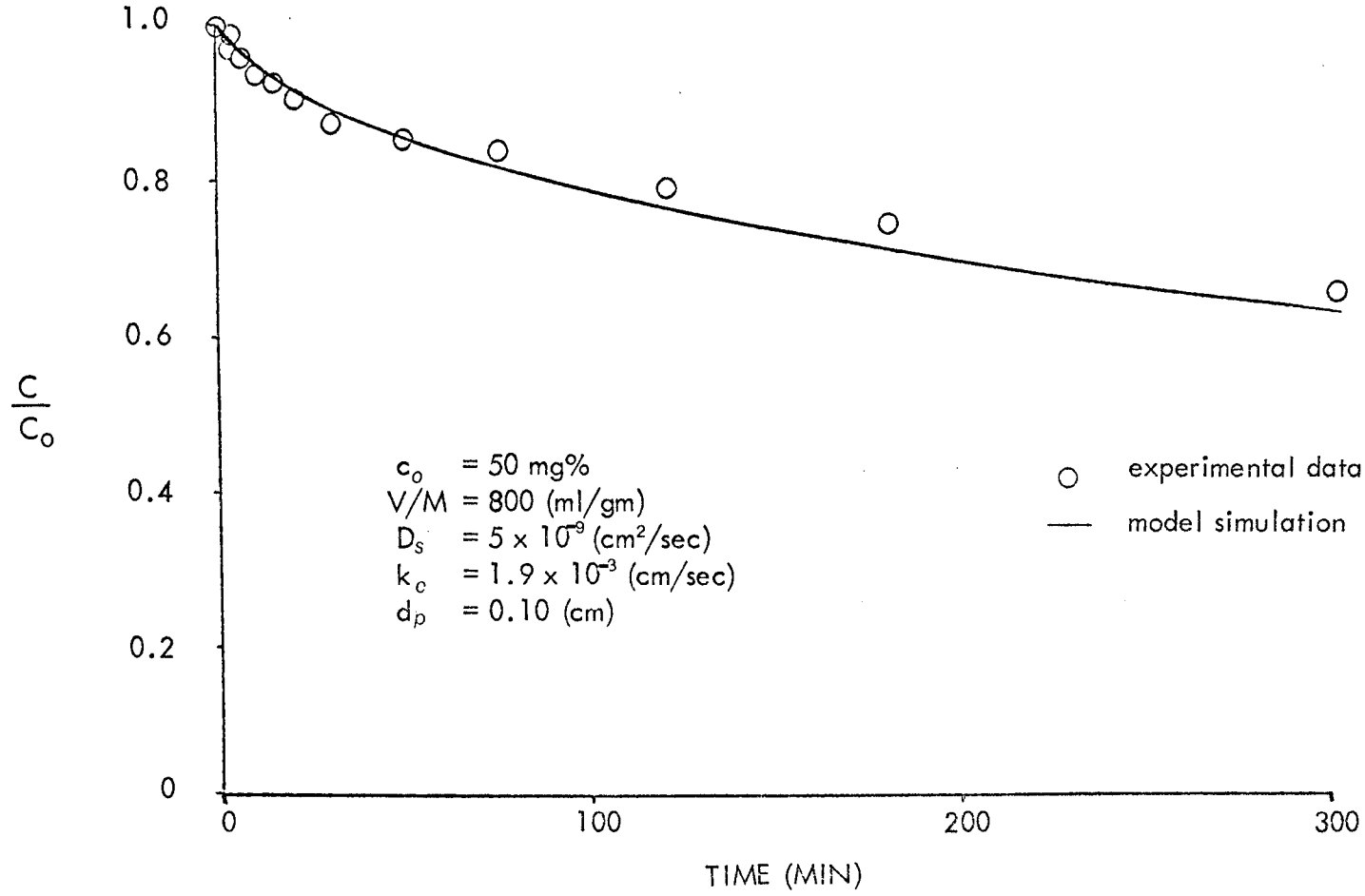

Figure 4.3.9 Batch Adsorption of Sodium Phenobarbitone by Norit RBX-1 Activated Carbon

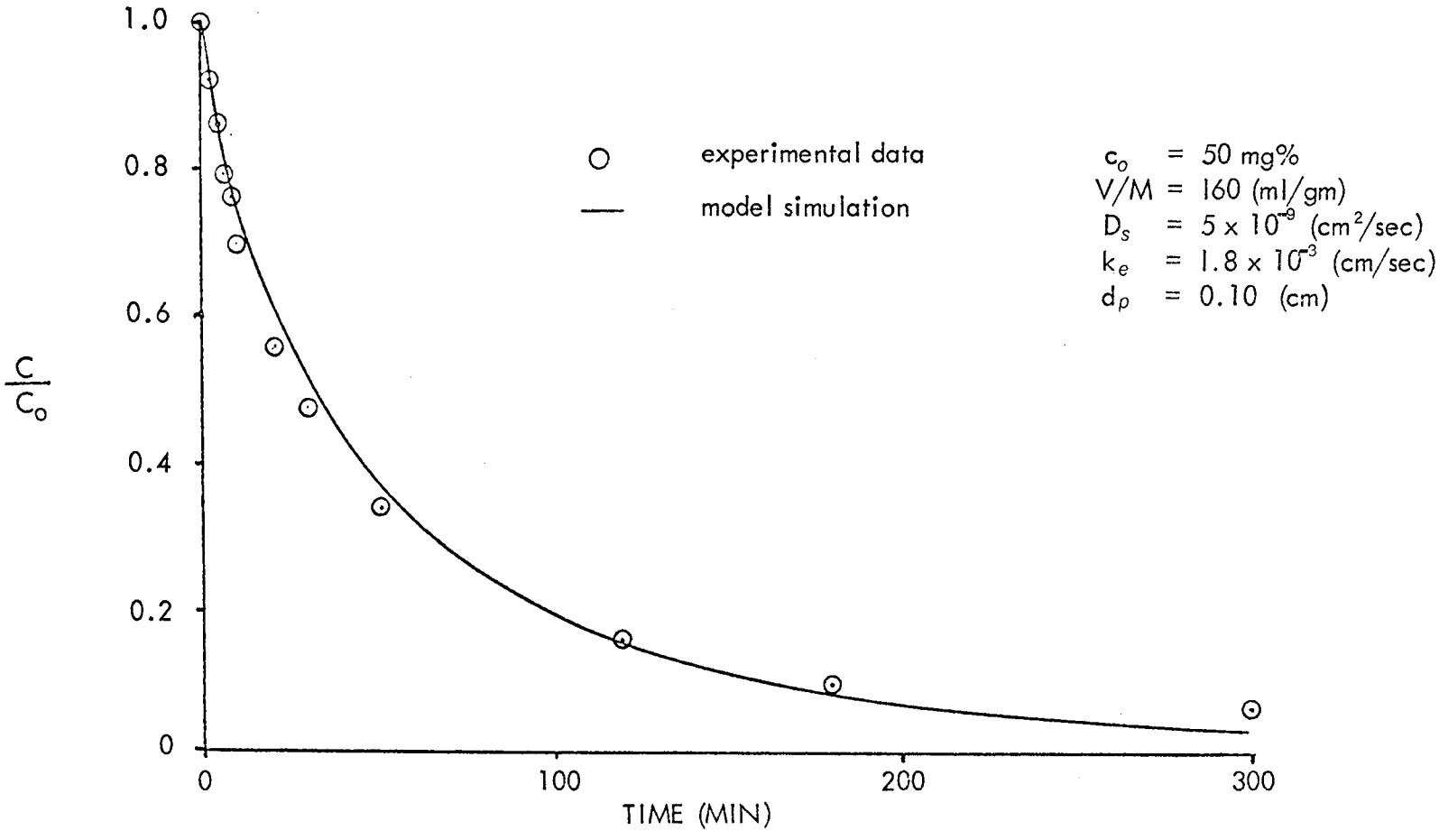

Figure 4.3.10 Batch Adsorption of Sodium Phenobarbitone by Norit RBX-1 Activated Carbon

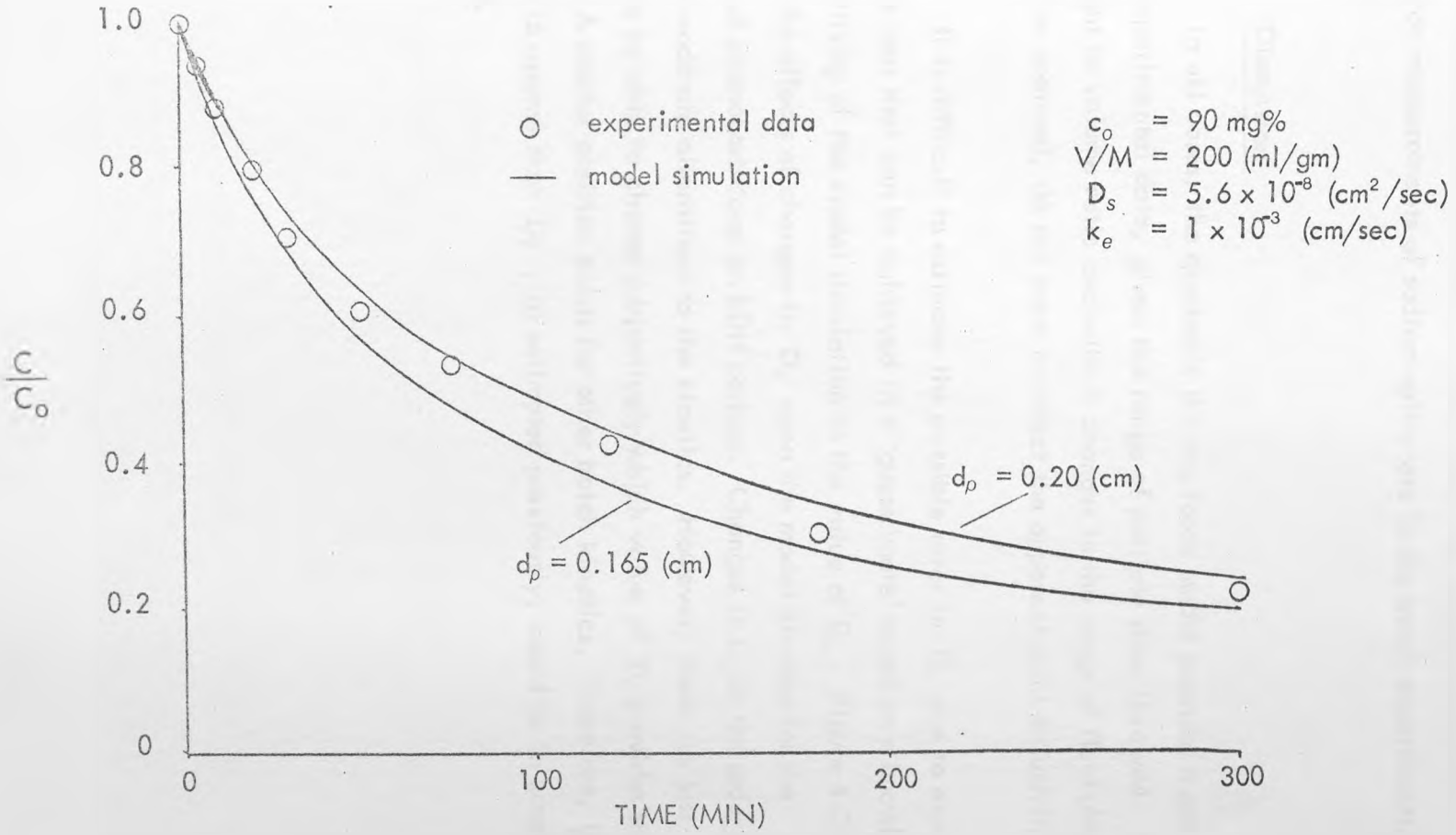

Figure 4.3.11 Batch Adsorption of Sodium Salicylate by Coated SS 610 Activated Carbon

4.3.5 Reproducibility

The reproducibility of the batch experimental technique was tested for the adsorption of sodium salicylate on BDH spheres. (V_b /M = 250 ml/gm). The spread of data over five experiments did not exceed $\pm$ 1.5 mg % at any sampling time and in most instances it was within the expected error for concentration measurements of sodium salicylate in the batch experiments, i.e. $\pm$ 1 mg %.

4.3.6 Discussion

In all cases, the quadratic driving force model provides a good fit to the experimental data, given the range of particle sizes involved. Changes in the weight to volume ratio and with it changes in the range of fluid phase concentration spanned, do not seem to affect the apparent solid diffusivity.

It is difficult to estimate the possible error in D_s due to experimental errors. The best that can be achieved in a 'guesstimate' based on a knowledge of the sensitivity of the model simulation to the value of D_s . Figure 4.3.12 illustrates the effects of changes in D_s upon the model kinetics for the adsorption of phenobarbitone on BDH carbon. Changes in D_s in the order of 10% make moderate alterations to the kinetics. However, these are just sufficient to be able to choose subjectively which value of D_s provides the 'best fit'. A similar position exists for other batch kinetics. Therefore, it is reasonable to assume that D_s , as estimated previously, could be in error of about 10%.

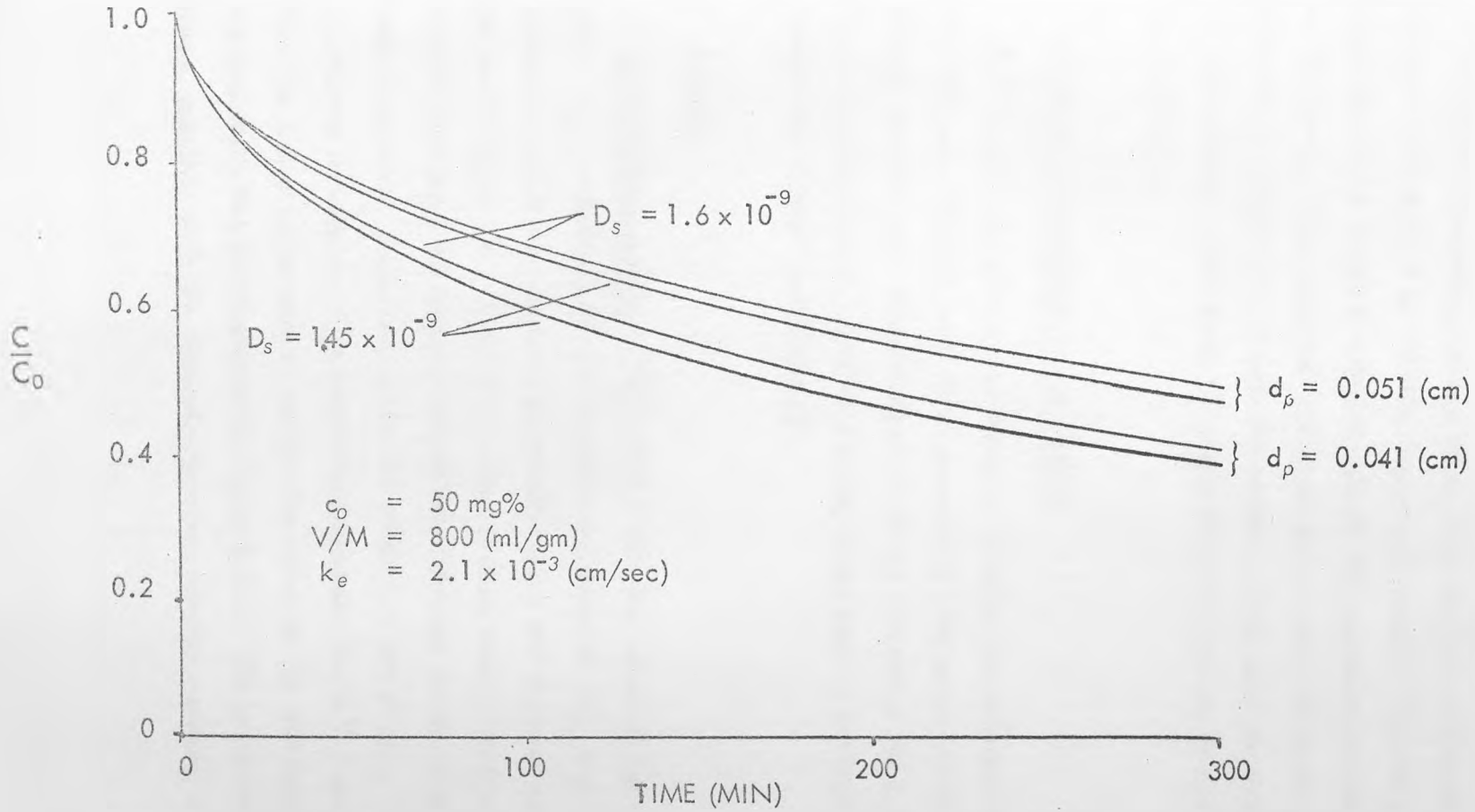

Figure 4.3.12 Sensitivity of Batch Kinetic Model to Changes in D_S

4.4 External Mass Transfer Coefficients in Perfusion Columns

The external mass transfer coefficient, k_e, in the columns studied was estimated from the initial breakthrough (Section 3.4).

The initial breakthrough was taken from the same column performance data that is used in Chapter 5 to validate the column model. Therefore, necessarily, the initial portion of the model simulation will fit the experimental data in the validation. However, since only the initial portion is used, the latter section of the data remains independent of both the model and the other parameter values estimated in this chapter. Therefore, it is still legitimate to use this section of data for the validation.

4.4.1 Experimental apparatus and method

Full details are given in Chapter 5. Briefly, the columns were set up in a single pass, flow circuit, (i.e. a constant inlet concentration). Several effluent samples were taken over the first few minutes of the column operation and the breakthrough curve was extrapolated back to one mean residence time to estimate the 'initial' breakthrough.

4.4.2 Results

BDH/Wrights column. Table 4.4.1 lists the values of the initial breakthrough, X_{BT}, together with the resultant estimates of N_e' and N_e, i.e. the apparent number of external mass transfer units and the true value allowing for axial dispersion. Since the number of mass transfer units was so large in runs W5 and W6, the value of initial breakthrough could not be detected experimentally. However, given the other five sets of data, it was possible to estimate this value. The correlation between $(Sh/Sc^{1/3})$ and Re for the other five was extrapolated to predict the value of Sh and hence N_e for runs W5 and W6. This is illustrated in Figure 4.4.1. The predicted value of N_e is given, together with the dimensionless mass transfer numbers, in Table 4.4.1.

Run Nos.	Sorbate and Particle Size	Flow Rate (ml/min)	Inlet Conc. (mg/ml)	X_{BT} (-)	N'_e (-)	N_e (-)	k_e [2] (cm/sec) $\times 10^{+3}$	Sh (-)	Re	$\frac{Sh}{Sc^{1/3}}$
W1		200	0.9	0.11	2.21	2.30	8.89	70.1	22.3	8.37
W 2/4	Sodium	40	0.9	0.025	3.70	3.96	3.02	23.8	4.46	2.73
W 5/6	Salicylate (0.85 - 1.00 mm)	10	0.9	-	-	5.7	1.11	8.7	1.12	1.04
W 7		200	0.5	0.12	2.12	2.20	8.46	66.8	22.3	8.00
W 8	Sodium	200	0.5	0.10	2.30	2.39	7.75	70.3	18.7	7.53
W 9	Phenobarbitone (0.71 - 0.85 mm)	100	0.5	0.055	2.90	3.02	4.90	4.44	9.35	4.76

Notes

1) Calculated from Figure 4.4.1

2) $a_p = 6/d_p$ with mean diameter value

Table 4.4.1 External Mass Transfer Coefficients in Wrights Perfusion Column

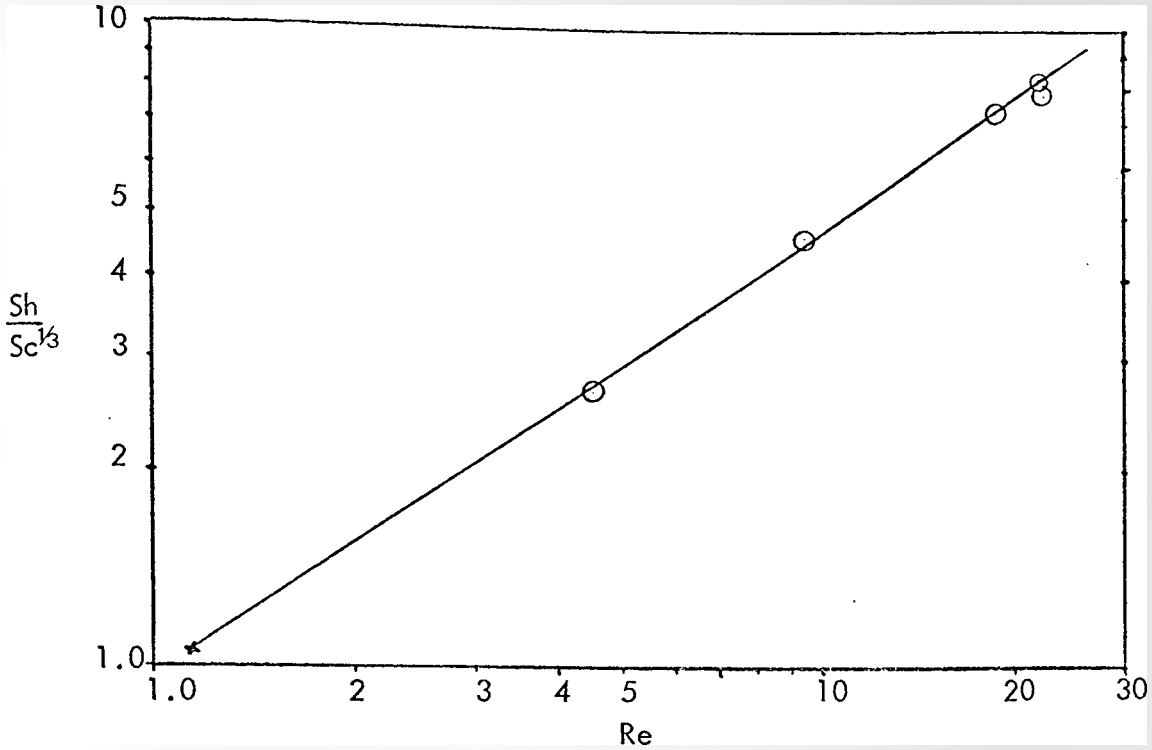

Figure 4.4.1 . Correlation to Estimate N_e in Runs W 5 and W 6

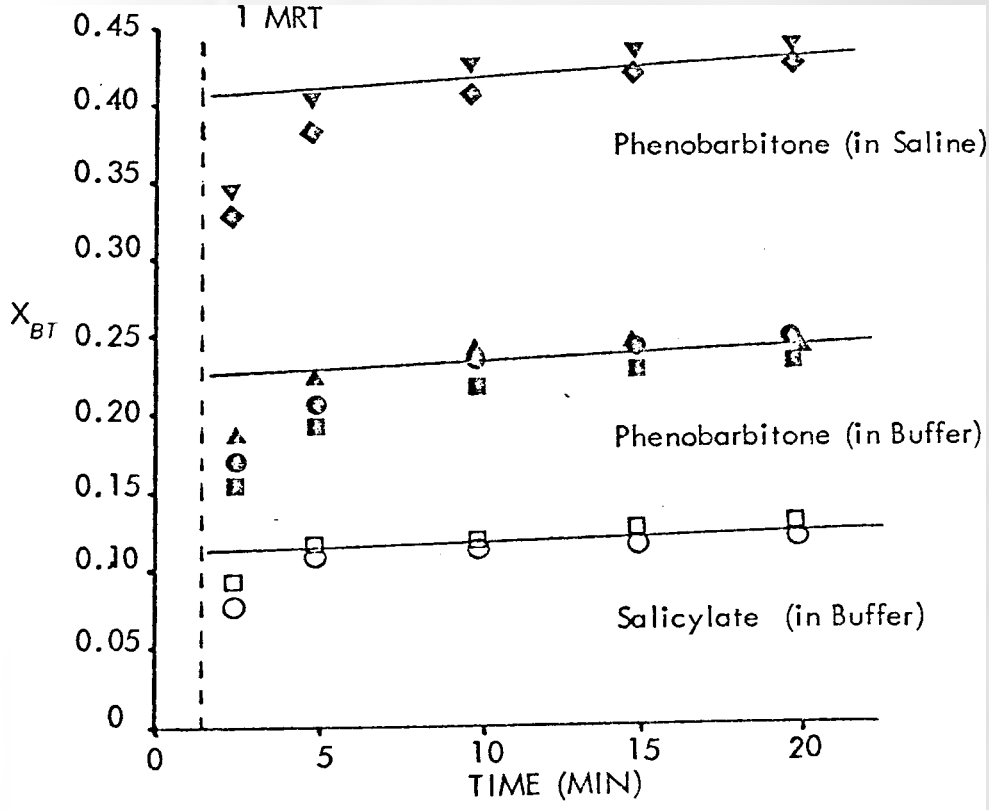

Figure 4.4.2 Estimation of X_{BT} for Haemocol

Two features of the technique used to predict N_e for runs W5 and W6 deserve comment. Firstly, the extrapolation of the data back to a value of Re much smaller than those of data is perhaps questionable. However, given the uncertainty and variability in the published external mass transfer data (Section 3.4), the above technique provides the best method of estimating the unknown N_e. Secondly, the slopes of the breakthrough curves in runs W1 and W8 are significantly greater than zero. This contravenes one of the basic assumptions on which the axial dispersion correction is based. However, from the discussion in Chapter 6 it will be seen that the probable error in the values of N_e is about 5%. This is of the same order as the possible error in all N_e values due to uncertainty in estimating X_{BT}, and it does not significantly alter the estimate of N_e for runs W5 and W6.

Haemocol. The initial breakthrough for both salicylate and phenobarbitone are shown in Figure 4.4.2. The initial breakthrough for phenobarbitone is dependent upon the solvent used, i.e. buffer solution or saline solution. In addition, the initial transients in all three cases are longer than expected on the basis of axial dispersion. That is, the transient exceeds two mean residence times. The only possible explanation for these two phenomena is that the sorbate and the solvent both effect the membrane permeability. (In the Wrights column the first effluent sample was taken at five mean residence times, hence the initial transients were not detected.) The values of N_e', N_e and k_e, based on the estimates of the initial breakthrough are listed in Table 4.4.2

Adsorba 300C. The initial breakthrough for salicylate and phenobarbitone were estimated from the clearance performance quoted by Thysell et al. (1976). The scale of the clearance curve made it difficult to estimate effects such as the long transients that occurred in the Haemocol. The values of X_{BT}, N_e', N_e and k_e for the Adsorba 300C are listed in Table 4.4.2.

Perfusion Column	Sorbate	Inlet Conc. (mg/ml)	X_{BT} (-)	N_e' (-)	N_e^1 (-)	k_e^2 (cm/sec) x 10^3
Haemocol	Sodium Salicylate	0.50	0.115	2.16	2.29	0.51
	Sodium Phenobarbitone	0.20	0.225	1.49	1.55	0.34
	Sodium Phenobarbitone (in distilled H_2O)	0.20	0.410	0.89	0.91	0.20
Adsorba 300 C	Sodium Salicylate	0.50	0.200	1.61	1.70	0.32
	Sodium Phenobarbitone	0.20	0.180	1.71	1.81	0.34

Notes:- All at 37° C and 200 ml/min flow rate in buffer solution at pH.7.4 unless otherwise stated.

n = 18 for Haemocol, n = 14 for Adsorba
A ; Haemocol - 1.5 m^2; Adsorba = 1.8 m^2

Table 4.4.2 External Mass Transfer Coefficients in Commercial Haemoperfusion Columns

4.5 Perfusion Column Hydrodynamics

The hydrodynamics were investigated by tracer experiments, with labelled human serum albumin (HSA) as the tracer. The experiments were conducted at the Scottish Universities Research Reactor Centre, National Engineering Laboratory, East Kilbride.

4.5.1 Experimental apparatus and materials

The flow circuit is shown in Figure 4.5.1. The 'capacitor' consisted of a glass wash bottle (Quickfit). The tubing was 0.5 cm (I.D.) except for sections into and out of the column which were 0.15 cm (I.D.). The section of tubing across the top of the detector was glass (0.5 cm, I.D.). This ensured that the flow geometry in the path of the detector remained constant. Although the internal diameter of the lead casing, around the detector, was 8 cm only a 2 cm length of the glass tubing was exposed to the detector. The remainder was shielded by lead blocks.

The injection apparatus was developed by How (1977). It consisted of a 0.2 ml syringe with the plunger activated by an electromagnet. The physical constraints posed by the detector and the injection apparatus plus the need to operate the column vertically, caused the injection point and the axis of the detector to be separated from the respective ends of the column by 10cm of tubing. However, since narrow gauge tubing was employed in these sections, the Reynolds number was high ($Re \simeq 6000$) and the flow turbulent. The changes in section between the outlet tube and the glass tube over the detector and at the ends of the column also contribute to the turbulence. The time delay in the inlet tube (and changes of section) was 0.3 seconds at a flow rate of 200 ml/min, while that in the outlet plus the glass tubing was 0.65 seconds. It was assumed that there was negligible axial dispersion in these sections.

The HSA was labelled with I^{131} with a specific capacity of 0.5 mCi/ml. The gamma radiation from the I^{131} was measured by a 2 inch diameter, sodium iodide scintillation counter, Type NS 59 F (No S148) from

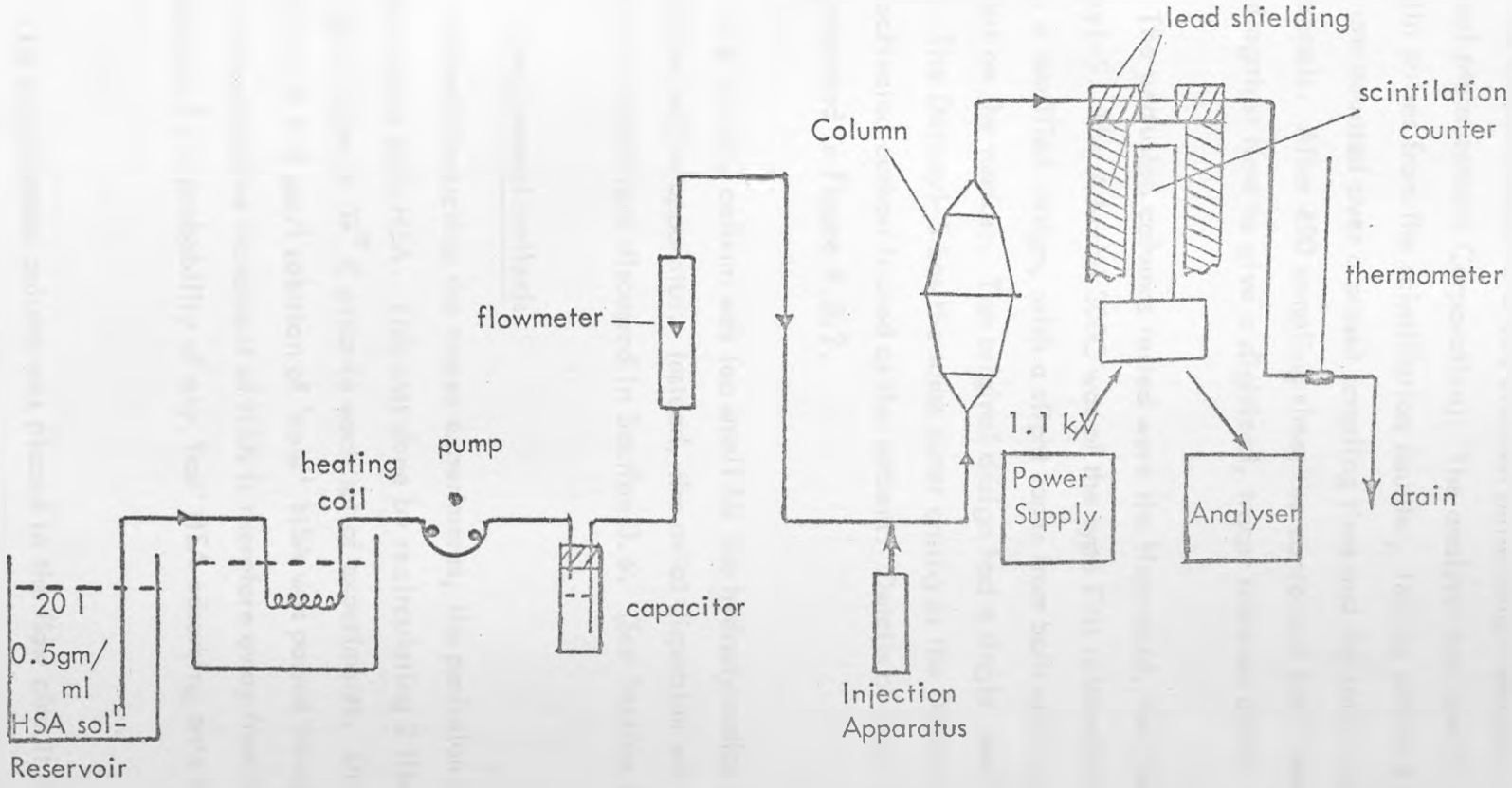

Figure 4.5.1 Flow Circuit for Hydrodynamic Experiments Conducted on Haemoperfusion Columns

ECKO Electronic Limited. The counter was powered by a high tension (1.1 KV) power supply M 2.5 K1 Supply, VG Electronics Limited. It was shielded from stray radiation, i.e. from the injection bolus, by a lead cylinder (14.4 cm OD x 8 cm ID). The output passed to a 400 channel pulse height analyser, Model 404C (Technical Measurement Corporation). The analyser was used in multiscalar mode, wherein pulses from the scintillation counter, falling within a preselected energy band, are counted over a preset sampling time and the total stored in one of the 400 channels. After 400 sampling times the contentsof each channel is then displayed against time to give a digitized, tracer response curve.

The perfusion columns tested were the Haemocol, the Adsorba 300C and the Detoxyl-S. The Adsorba 300C was of the type first released by ab Gambro. Subsequently, a modified design, with a slight taper from both ends towards the middle, was put on the market. The original design had a single taper along its entire length. The Detoxyl-S has the same outer casing as the Detoxyl-1, however Norit RBX-1 activated carbon is used as the sorbent. Details of these three columns are presented in Figure 4.5.2.

The Wrights column was too small for the hydrodynamics to be measured using the above apparatus. Instead, the axial dispersion was estimated from the standard correlations discussed in Section 3.6. (See Section 4.5.4.)

4.5.2 Experimental methods

Before conducting the tracer experiments, the perfusion columns were pre-equilibrated with HSA. This was done by recirculating 2 litres of 5 gm/l HSA for 2 hours at 37° C prior to each set of experiments. During the tracer experiments a 0.5 gm/l solution of 'cold' HSA was passed through the column. The net adsorptive movement of HSA is therefore away from the coated activated carbon and the probability of any 'hot' HSA adsorbing onto the carbon is minimized.

The equilibrated column was placed in the flow circuit and the flow adjusted to the desired value. Flow was measured at the outlet to drain

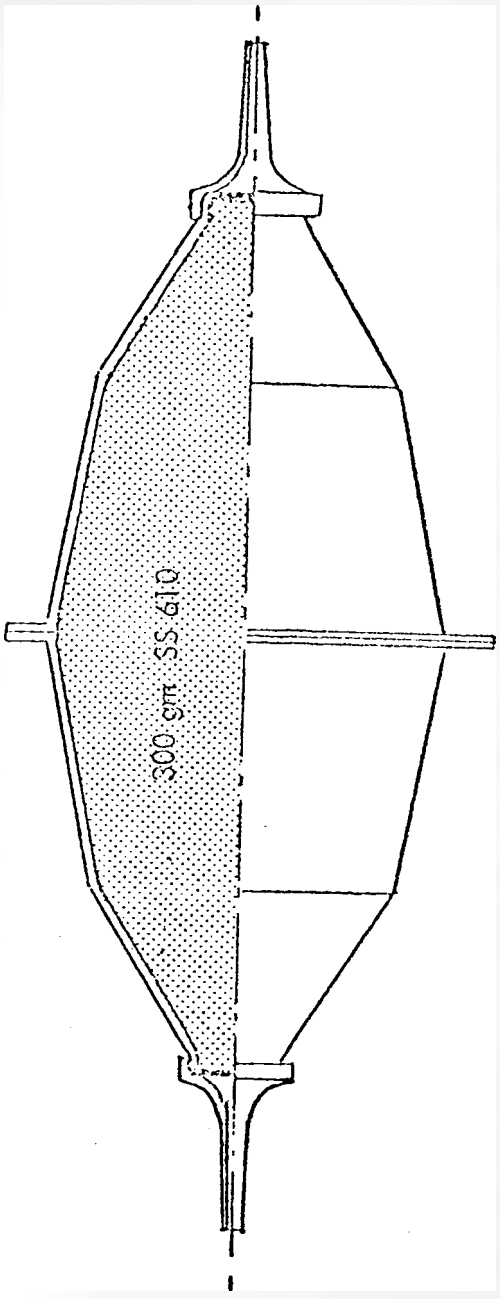

Haemocol

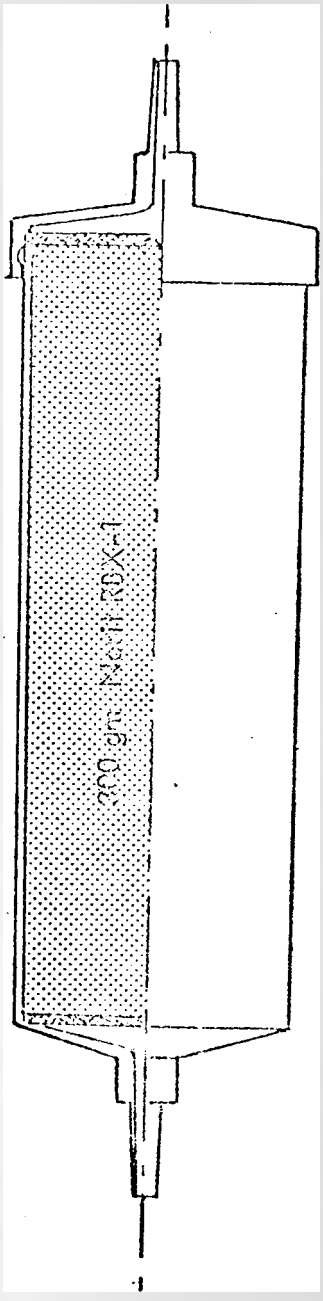

Adsorba 300 C

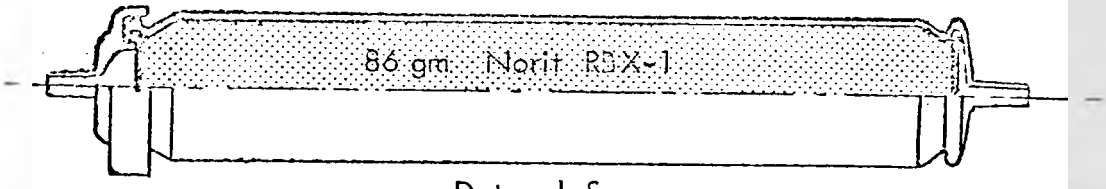

Detoxyl-S

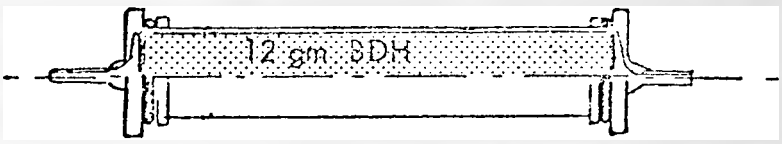

Wrights Chromatography Column

Figure 4.5.2 Perfusion Columns used in Hydrodynamic and Mass Transfer Experiments (approximately half scale)

using a volumetric cylinder and a stop watch. The flow meter in the circuit served as a check on the consistency of the flow. Measurement errors in the flow rate were less than 1%. The temperature at the outlet point was maintained at $36 \pm 1^{\circ}$ C by adjusting the temperature in the heating bath. This value takes into account the drop in temperature across the column and the outlet tubing. When the flow and temperature equilibrium had been attained, the inlet pulse was injected.

This pulse consisted of 0.2 ml (= 0.10 m Ci) of 20 gm/l HSA. Although the concentration of the bolus exceeds the 0.5 gm/l in the solution flowing through the circuit, in fact the maximum possible concentration due to this bolus in the column is less than 0.4 gm/ml. This is estimated on the basis of the peak pulse height in the first cell of the simple mixing cell model of the column. Therefore, the net desorption of HSA from the column (discussed above) is not altered by the bolus. In all cases, the injection and the multi-channel analyser were initiated simultaneously. After each run the flow rate was checked. The maximum deviation during the course of the experiment was 1% (within the experimental error).

The experimental conditions for each run are listed in Table 4.5.1. Where possible, three sequential runs were conducted on each column. Runs 1-6 were preliminary experiments to establish optimal conditions and runs 8 - 15 were used to measure the injection pulse characteristics. The static (priming) volume of each column was measured after the tracer experiments by displacing the aqueous solution in the column with a fluorocarbon of specific gravity 2.2 (FC 43, 3M Company).

Several experiments were conducted to identify the shape of the inlet pulse. For these experiments the inlet section to the column was connected directly to the glass tube over the detector. The time delay in the tubing was a total of 0.65 seconds. The multichannel analyser was started five seconds prior to the injection, to provide a better estimate of the background radiation ahead of the pulse. A typical pulse is illustrated in Figure 4.5.3. The second peak

Run No	Column Type and Number	Volume (ml) ± 1	Flow (ml/min) ± 1%	MRT = $\bar{t}$ (sec)
7	Haemocol (211677)	313	212	88.6
16			200	93.3
17			202	92.4
18			200	93.3
19	Haemocol (211768)	311	295	63.3
20			293	63.7
21			293	63.7
22			102	182.9
23			103	181.2
24			203	84.8
25	Adsorba 300C	287	202	85.2
26			202	85.2
27	Detoxyl-S (Norit filled)	70	200	21.0
28			200	21.0
31	Haemocol (211769)	319	200	95.7
32			197	97.2
33			197	97.2

Table 4.5.1. Experimental Conditions in Flow Studies

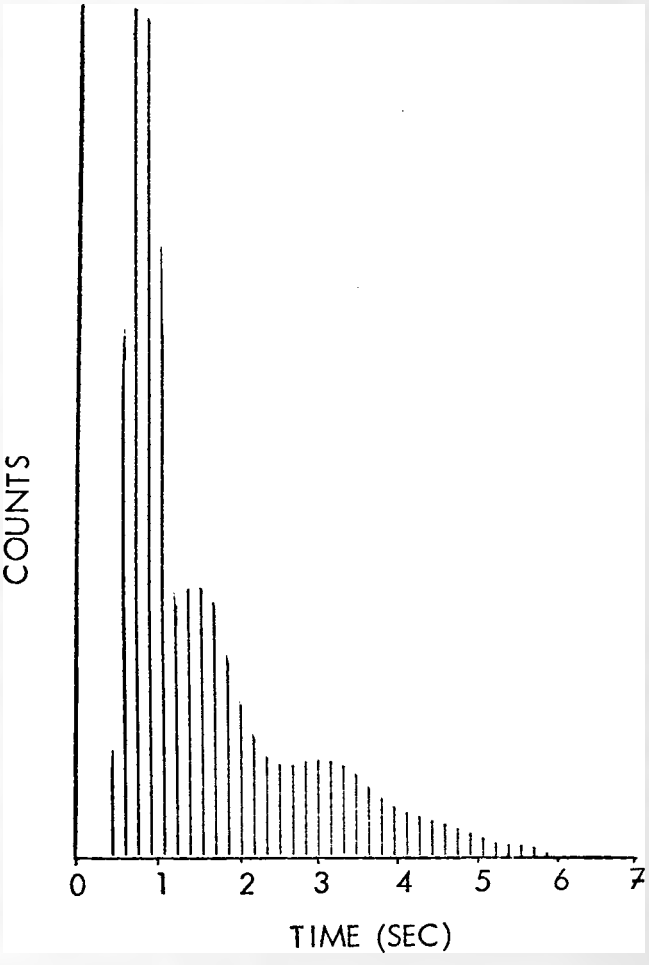

Figure 4.5.3 Typical Input Pulse used in Hydrodynamics Experiments

is probably due to part of the bolus being initially propelled upstream and then being forced back by the bulk flow. Although the pulse appears extremely 'non-ideal', in fact the contribution of the second moment of the pulse to the differential variance ($\Delta \sigma^2$) is negligible.

4.5.3 Results

A typical response curve is illustrated in Figure 4.5.4. The response curve data was analysed using the axial dispersion plug flow model (Section 3.6.2), the simple mixing cell model and the multiparameter mixing cell model (Section 3.6.3).

Axial dispersed plug flow model. The first and the second moments of the response curves were calculated, taking into account the delays in the inlet and outlet sections. The Peclet number was calculated from $\Delta\sigma^2$. Table 4.5.2 lists the results together with the formulae used.

Simple mixing cell model. The number of cells in this model were estimated, and rounded to the nearest whole number, from the moments of the response curves and Equation 3.3.8. The results are listed in Table 4.5.2.

The validity of the simple mixing cell model was tested by simulating its response to the experimental input pulse (using the values of n in Table 4.5.2) and comparing this response to the experimental data. The data from the Haemocol in Run 7 is compared with the response curve from the corresponding simulation in Figure 4.5.5. Similar results were obtained for the other experiments. Since the simulations are based on the value of n in Table 4.5.2, the response curves necessarily have the same $\Delta\mu$ and $\Delta\sigma^2$ as those of the data. However, the shape of the simulated and experimental response curves is very different. Therefore the simple mixing cell model does not provide a totally adequate description of the hydrodynamics. Response curves based on the axial dispersed plug flow model were not compared to the experimental data. However, there is a close similarity between the shapes of response curves of this model and the simple mixing cell model. Therefore it can also be assumed that the axial dispersed plug flow model does not totally describe the hydrodynamics in the haemoperfusion columns studied.

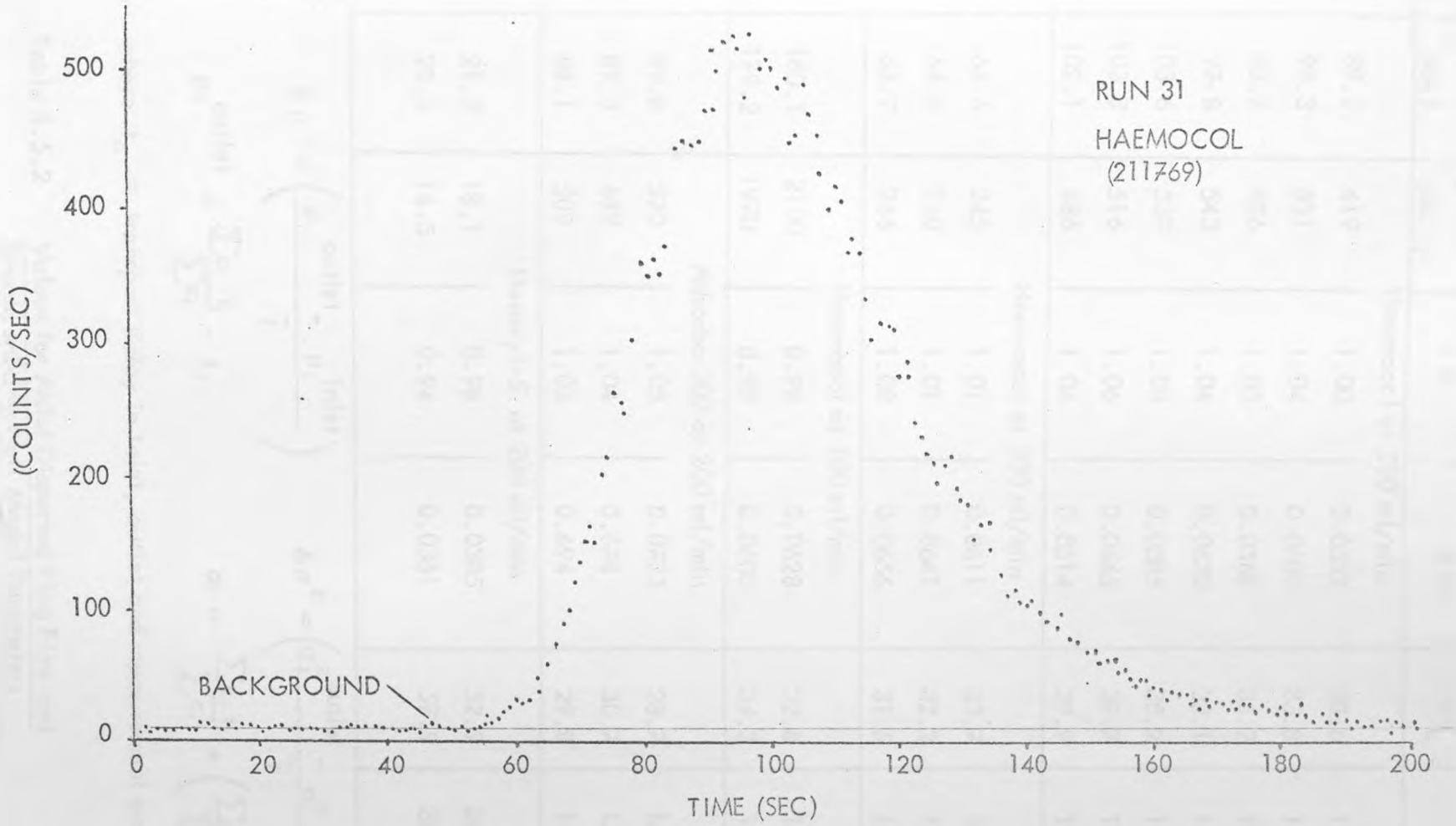

Figure 4.5.4 Typical Experimental C-Curve

Run No.	μ_t outlet (sec)	σ_t outlet (sec)	$\Delta\mu$	$\Delta\sigma^2$	Pe_L	n
			Haemocol at 200 ml/min			
7	89.2	419	1.00	0.0532	38.6	19
16	97.3	531	1.04	0.0609	33.8	16
17	98.2	486	1.05	0.0568	36.2	18
18	97.8	543	1.04	0.0623	33.1	16
31	103.6	537	1.08	0.0585	35.2	17
32	103.3	516	1.06	0.0545	37.7	18
33	102.1	486	1.04	0.0514	39.9	19
			Haemocol at 300 ml/min			
19	64.6	245	1.01	0.0611	33.7	16
20	64.6	260	1.01	0.0641	32.2	16
21	63.9	266	1.00	0.0656	31.5	15
			Haemocol at 100 ml/min			
22	180.1	2100	0.98	0.0628	32.8	16
23	179.2	1970	0.99	0.0600	34.3	17
			Adsorba 300 at 200 ml/min			
24	89.8	520	1.05	0.0723	28.7	14
25	89.3	489	1.04	0.674	30.7	15
26	88.1	509	1.03	0.694	29.8	14
			Detoxyl-S at 200 ml/min			
27	21.3	18.1	0.98	0.0385	52.9	26
28	20.5	16.5	0.94	0.0351	57.9	28

Notes

$$\Delta\mu = \left(\frac{\mu_t^{\text{outlet}} - \mu_t^{\text{inlet}}}{\bar{t}}\right) \qquad \Delta\sigma^2 = \left(\frac{\sigma_t^{2\,\text{outlet}} - \sigma_t^{2\,\text{inlet}}}{\bar{t}}\right)$$

$$\mu_t^{\text{outlet}} = \frac{\sum c_i\, t_i}{\sum c_i} - t_d \qquad \sigma_t = \frac{\sum c_i\, t_i}{\sum c_i} - \left(\frac{\sum c_i\, t_i}{\sum c_i}\right)^2$$

where t_d = transport delay in inlet, outlet and measurement sections

Table 4.5.2 Values for Axial Dispersed Plug Flow and Simple Mixing Cell Model Parameters

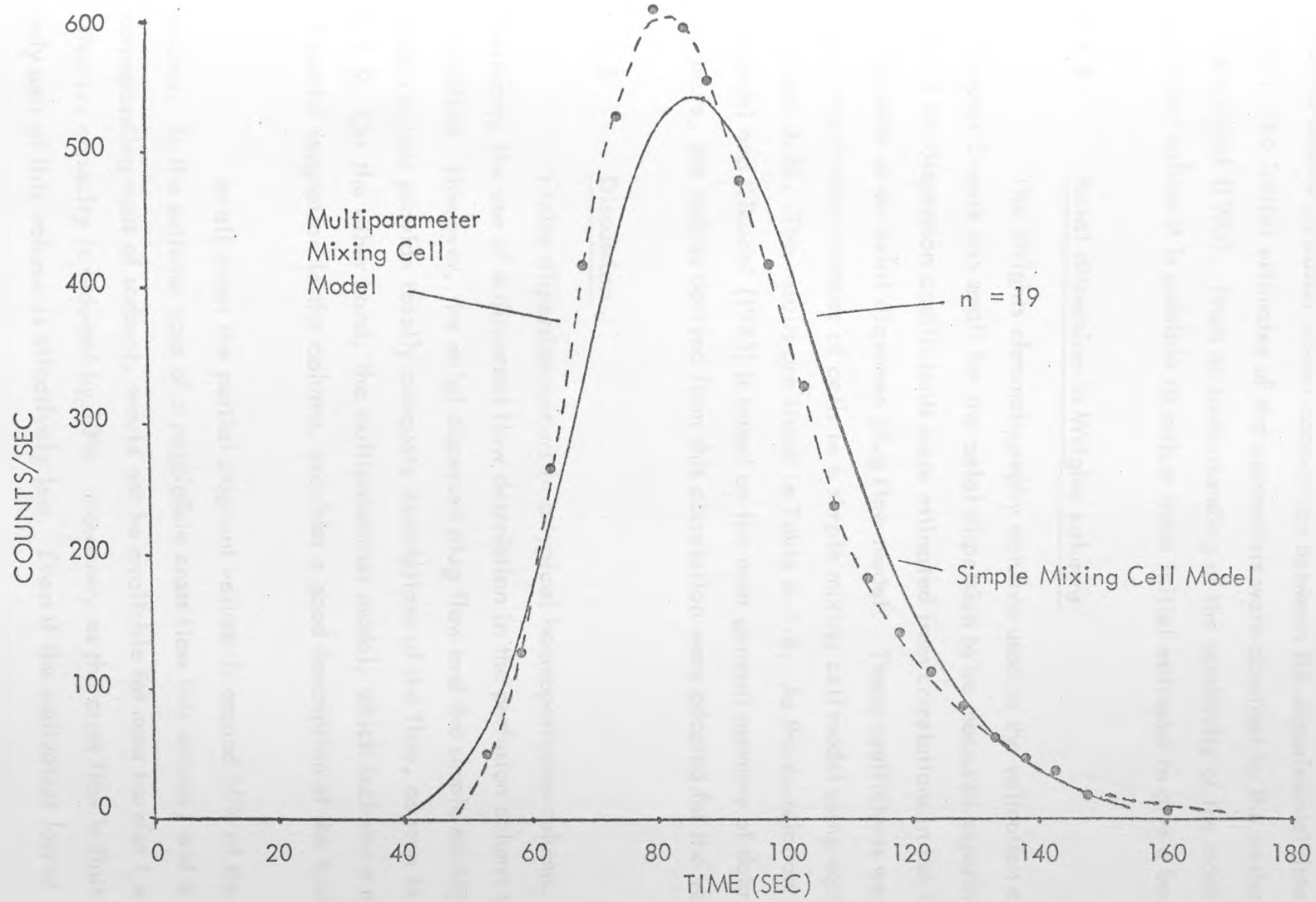

Figure 4.5.5 Comparison of Simple Mixing Cell Model and Multiparameter Mixing Cell Model for Run 07
(Parameters for Multiparameter Model in Figure 4.5.6)

Multiparameter, mixing cell model. The simulations based on this model are shown in Figures 4.5.6 to 4.5.12 and the parameter values are listed in Table 4.5.3. The experimental data is represented by the average values at five second intervals for each run. This removes the random scatter in the original data and allows an easier visual comparison between the experimental data and the model. The initial estimates of the parameters were obtained by the method outlined in Levenspiel (1972). From an understanding of the sensitivity of the model to the parameter values it is possible to adjust these initial estimates to give a best fit.

4.5.4 Axial dispersion in Wrights columns

The Wrights chromatography columns used in the validation experiments in Chapter 5 were too small for the axial dispersion to be measured experimentally. Instead the dispersion coefficients were estimated from correlations in the literature, on the basis of an axial dispersed plug flow model. These coefficients were converted into an equivalent number of cells in a simple mixing cell model using equations 3.34 and 3.36. The results are listed in Table 4.5.4. As the correlation in Mujauchi and Kikuchi (1975) is based on the most general summary of data in the literature, the values derived from this correlation were adopted for the validation.

4.5.5 Discussion

Finite dispersion occurs in a typical haemoperfusion column. Therefore, the use of a dispersed flow description in the perfusion column model is justified. However, the axial dispersed plug flow and the simple mixing cell models do not provide totally adequate descriptions of the flow, as seen in Figure 4.5.5. On the other hand, the multiparameter model, which includes a degree of partial stagnation in the column, provides a good description of the hydrodynamics.

In all cases the partial stagnant volume is around 10% of the total volume. In the extreme case of a negligible cross flow this volume, and a corresponding mass of sorbent, would not be available for mass transfer i.e. the effective capacity is reduced by 10%. However, as the cross flow is finite only part of this volume is effectively lost. Even if the equivalent loss of

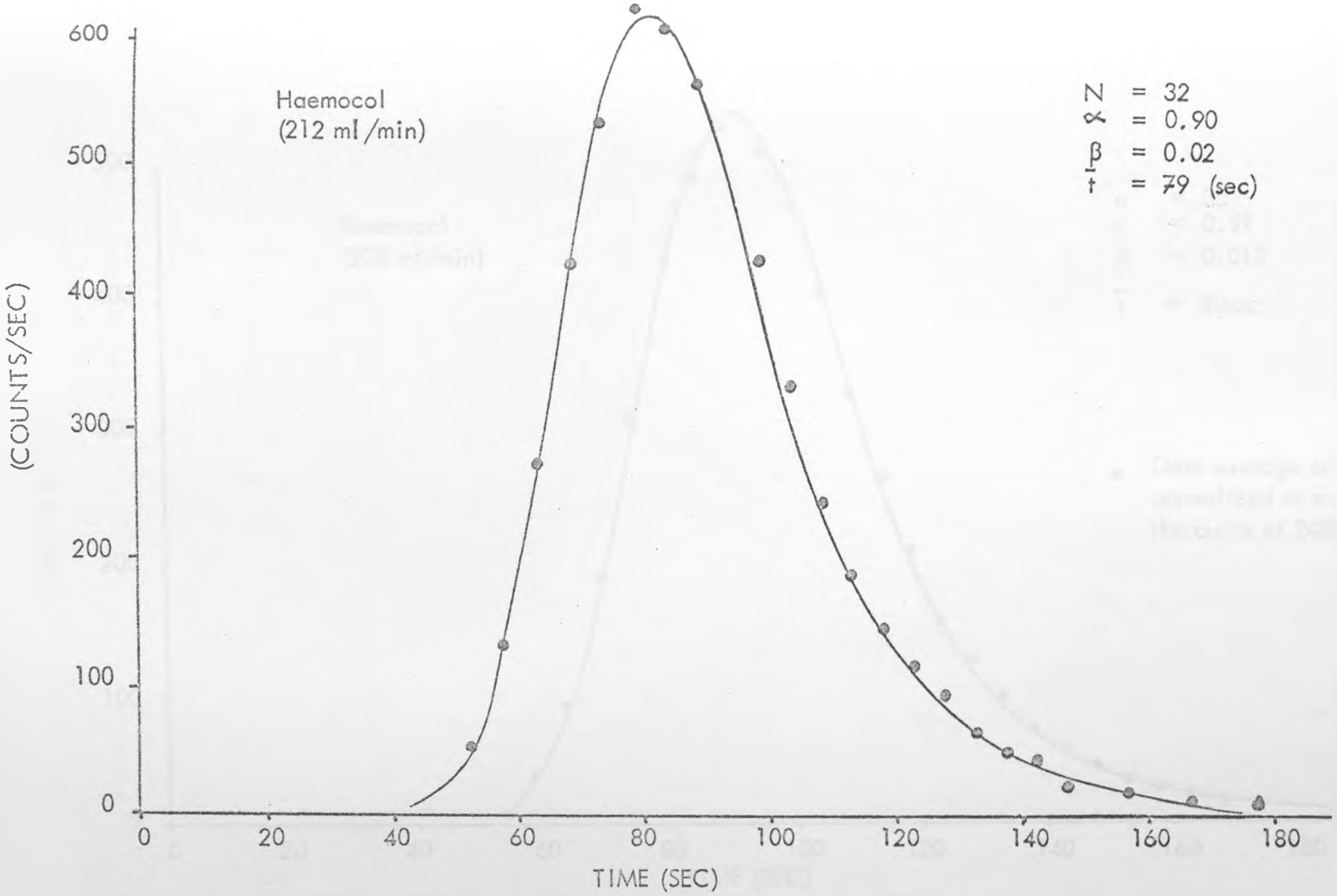

Figure 4.5.6 Comparison of Multiparameter Mixing Cell Model and Experimental Data for Run 07

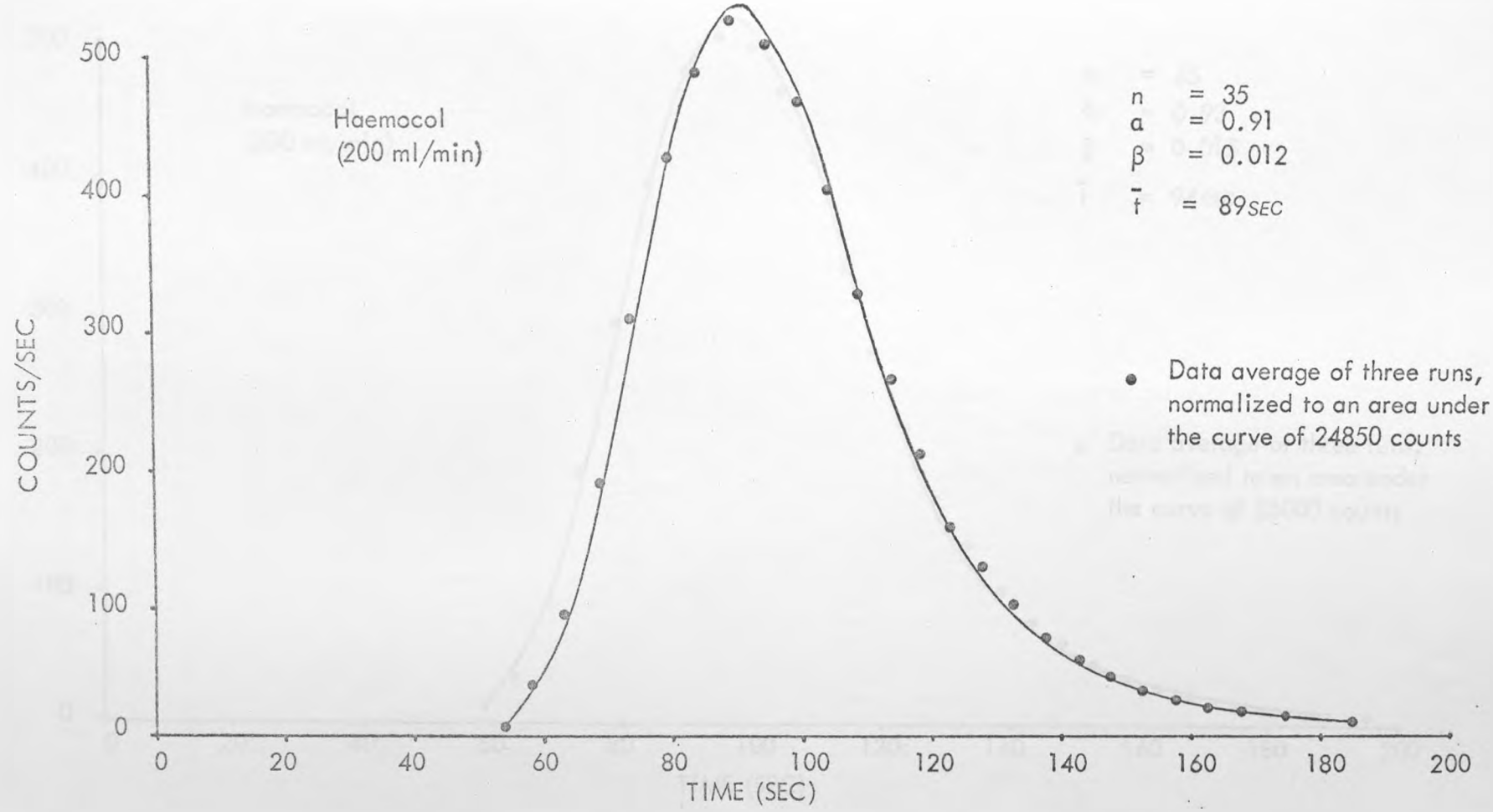

Figure 4.5.7 Multiparameter Mixing Cell Simulation of Axial Dispersion in Haemocol (Runs 16 to 18)

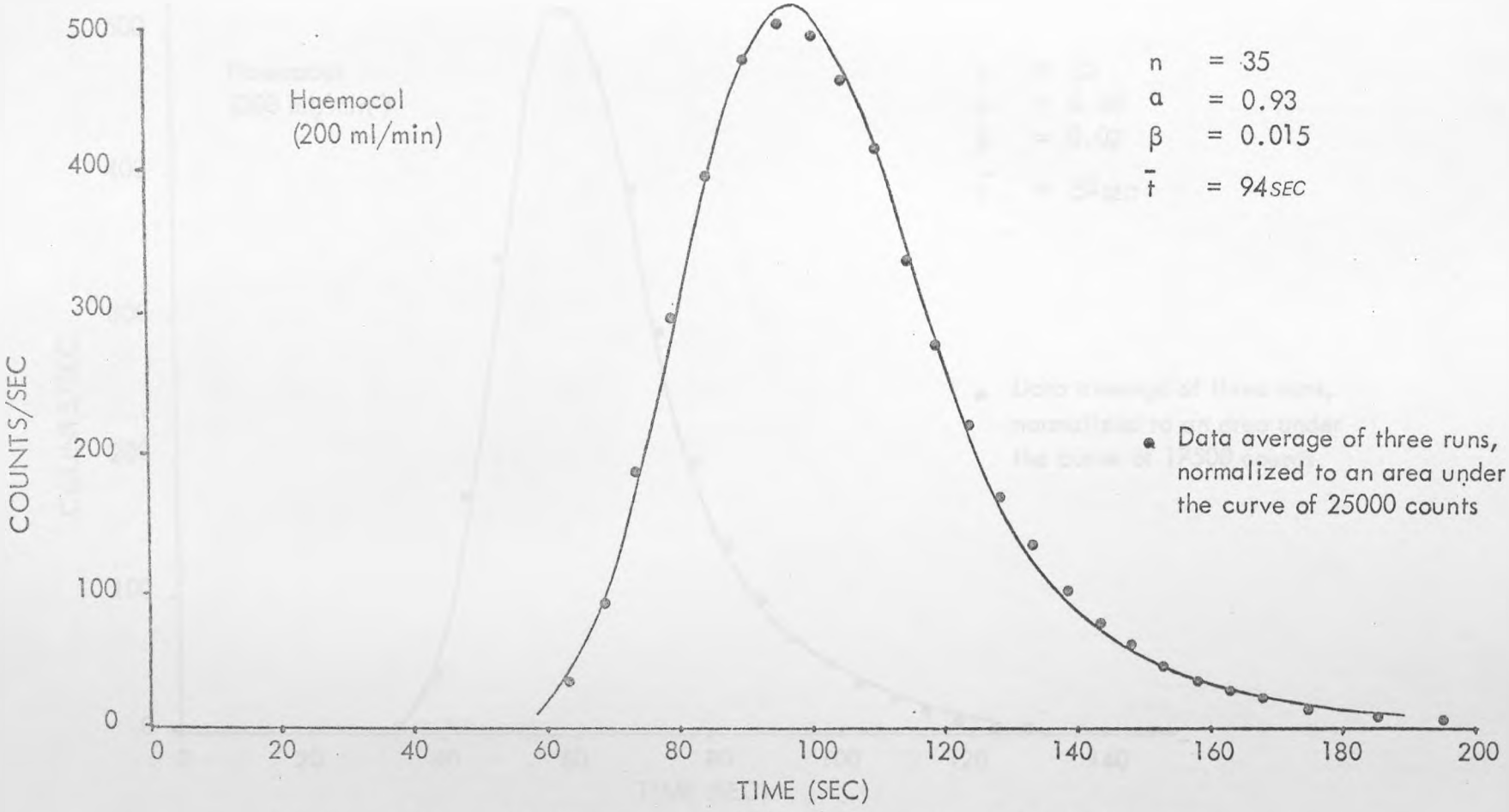

Figure 4.5.8 Multiparameter Mixing Cell Simulation of Axial Dispersion in Haemocol (Runs 31 to 33)

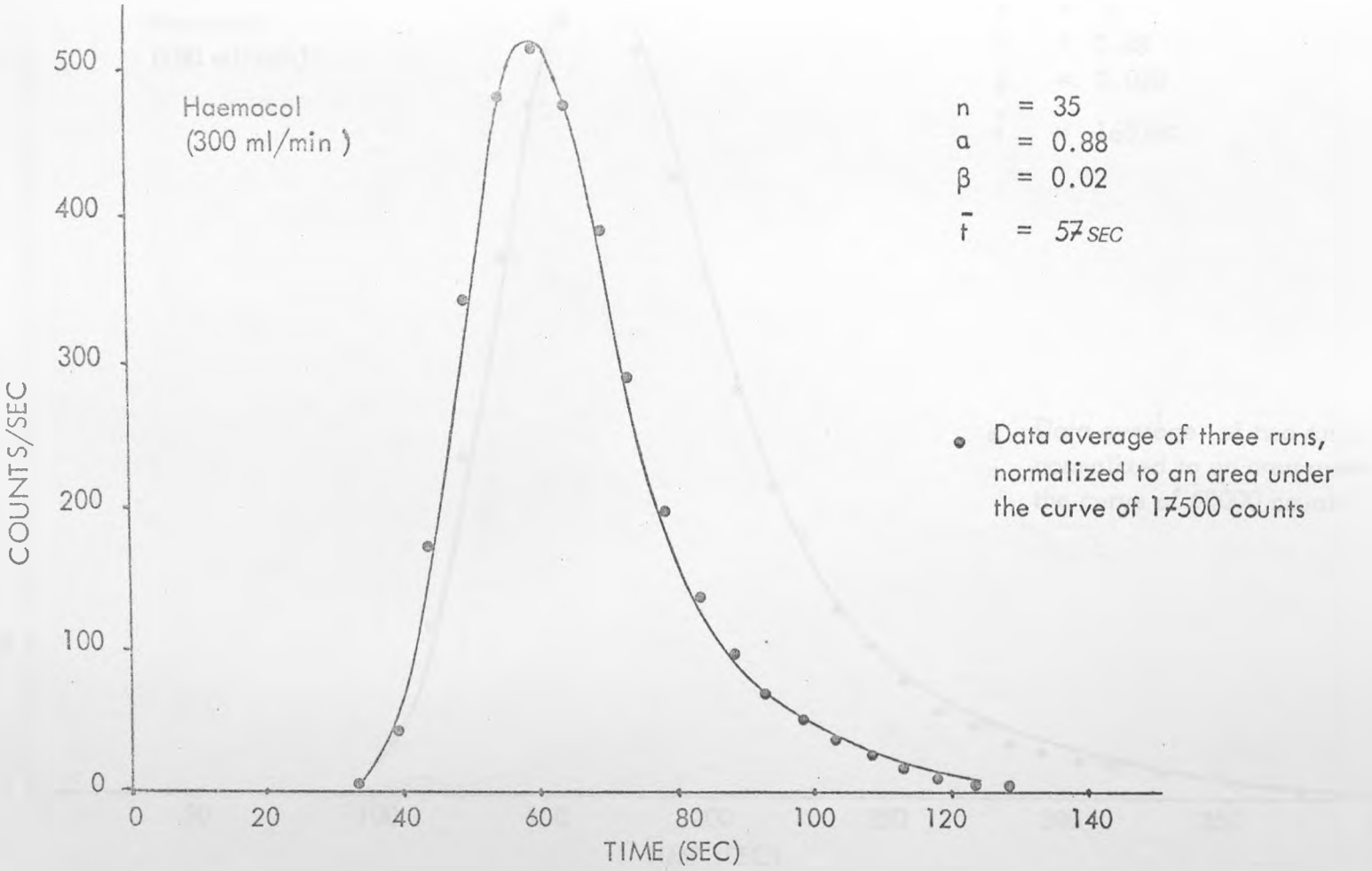

Figure 4.5.9 Multiparameter Mixing Cell Simulation of Axial Dispersion in Haemocol (Runs 19 to 21)

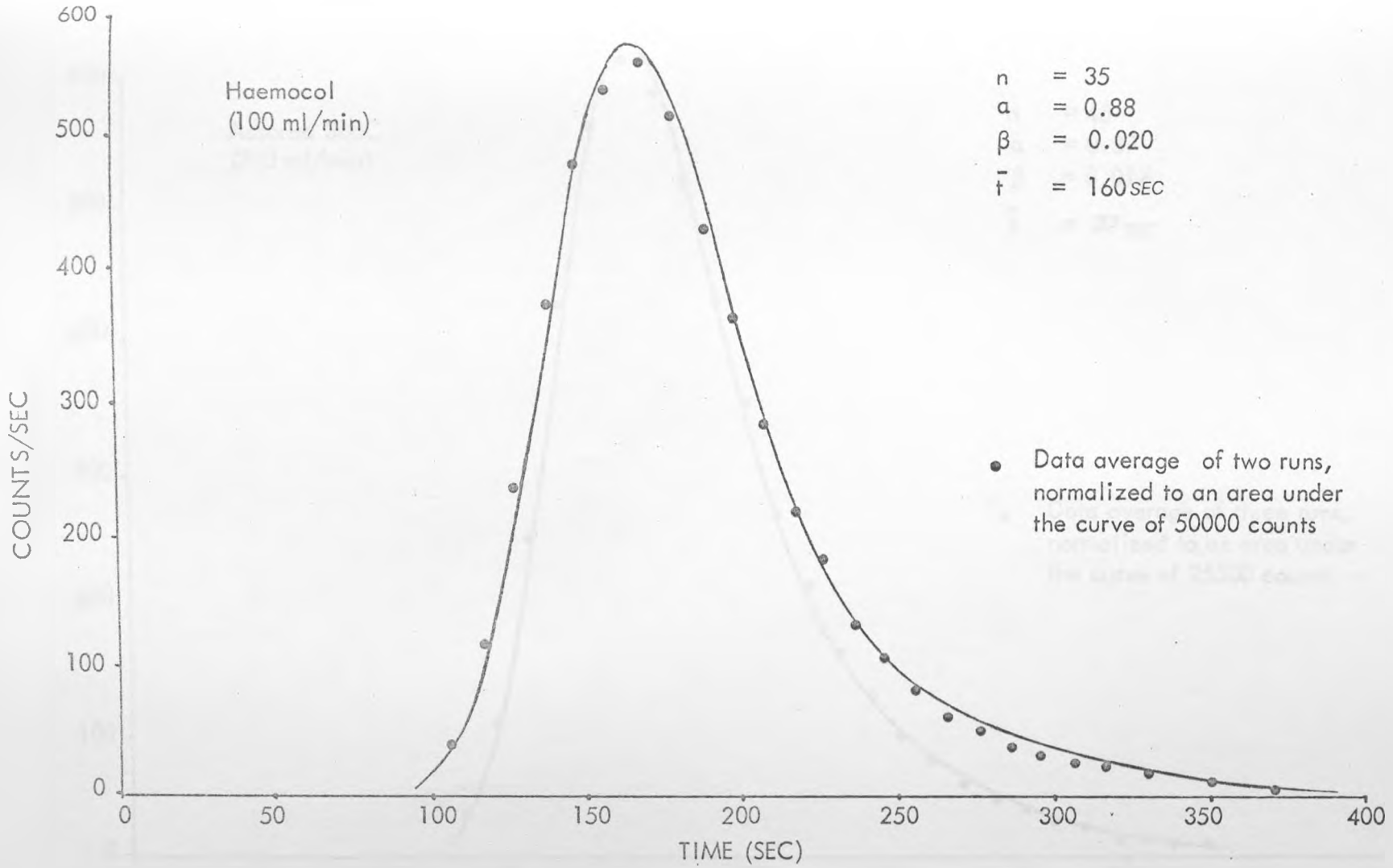

Figure 4.5.10 Multiparameter, Mixing Cell Simulation of Axial Dispersion in Haemocol (Runs 22 and 23)

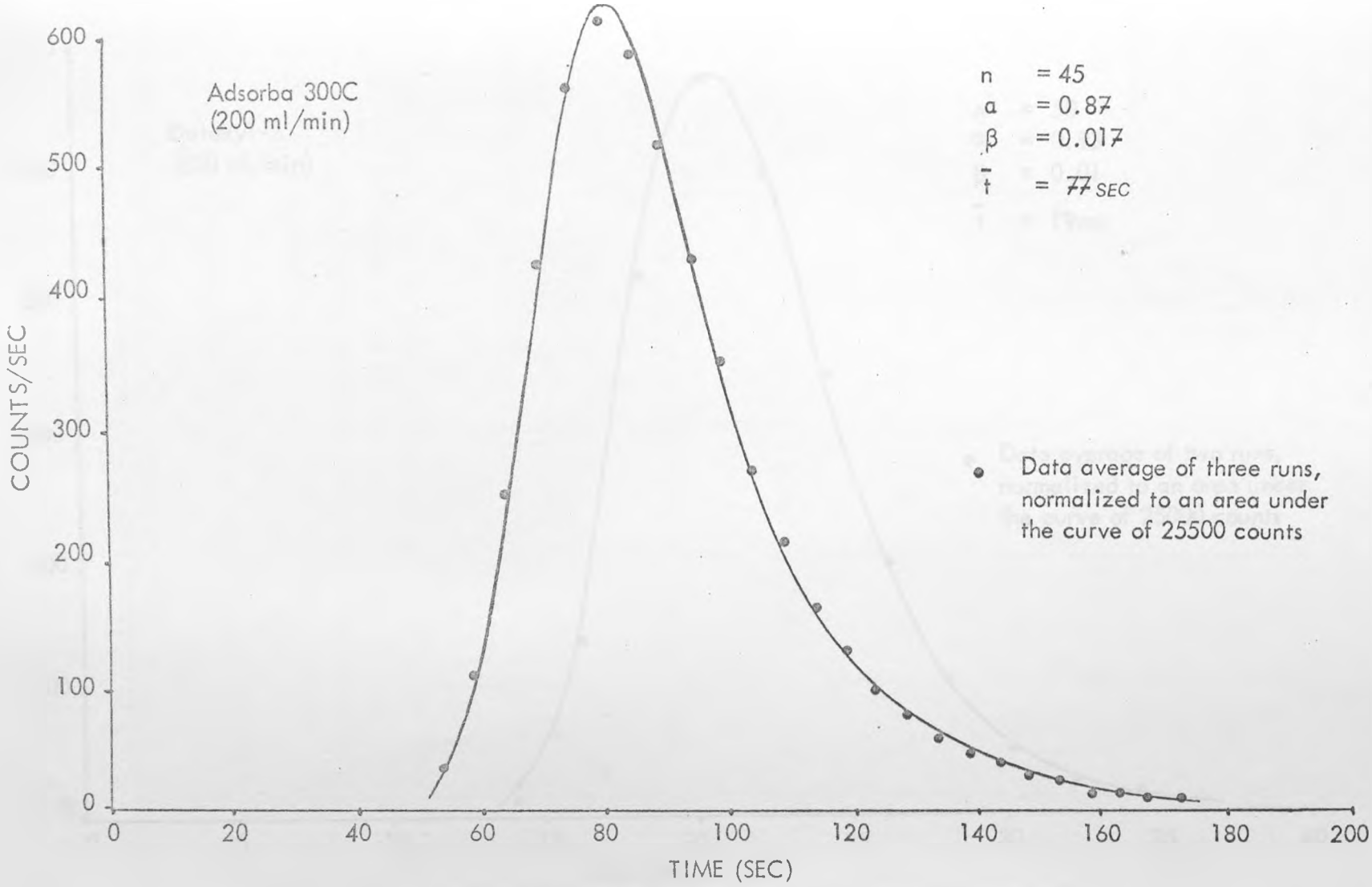

Figure 4.5.11 Multiparameter Mixing Cell Simulation of Axial Dispersion in Adsorba 300 C (Runs 24 to 26)

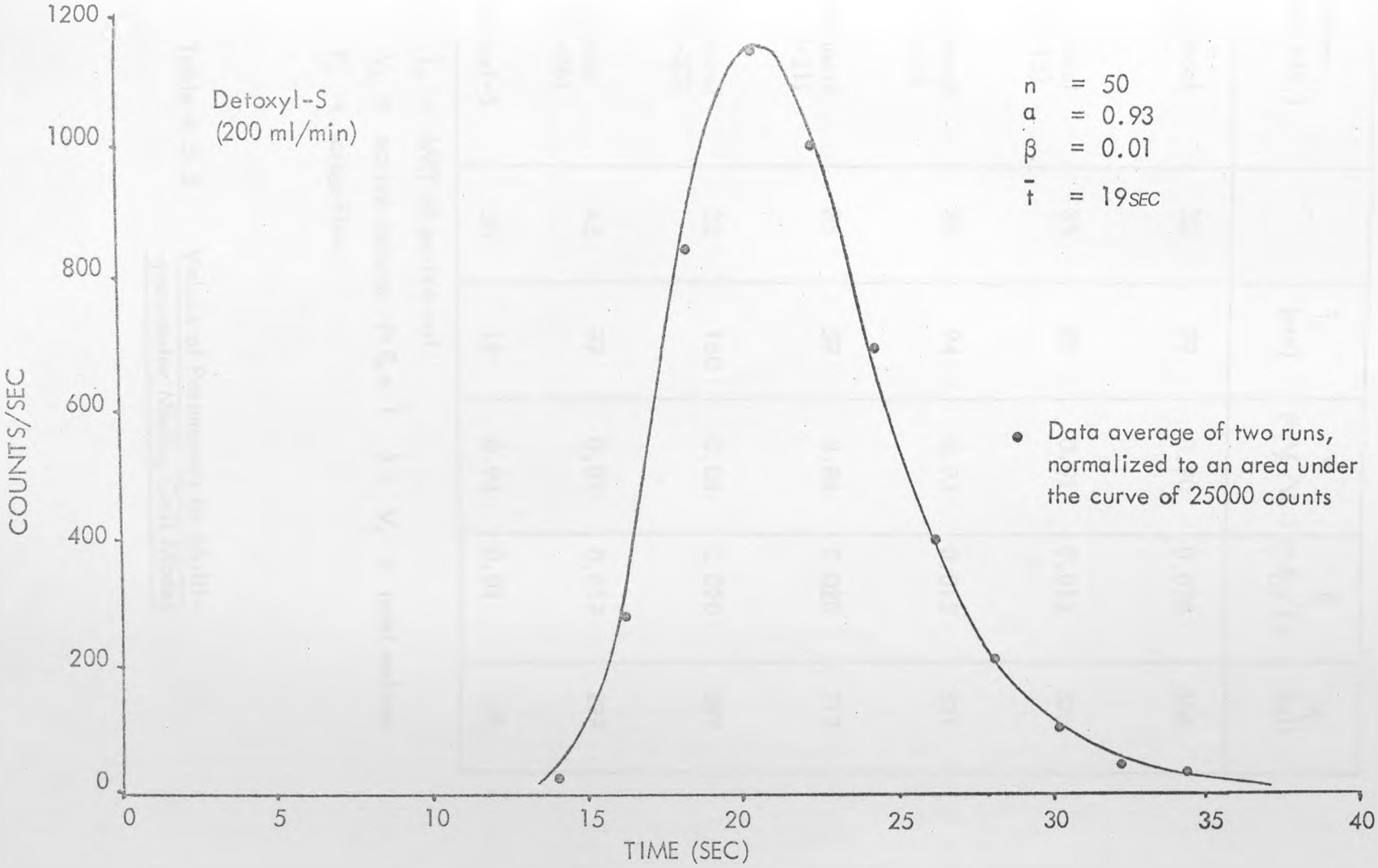

Figure 4.5.12 Multiparameter Mixing Cell Simulation of Axial Dispersion in Detoxyl-S (Runs 27 and 28)

Column (Run No.)	n	$\bar{t}_A$ (sec)	α (= V_A/V_T)	β (= F_C/F)	V_T (ml)
Haemocol (7)	32	79	0.90	0.020	308
Haemocol (16-18)	35	89	0.91	0.012	326
Haemocol (31-33)	35	94	0.93	0.015	331
Haemocol (19-21)	35	57	0.88	0.020	317
Haemocol (22-23)	35	160	0.88	0.020	309
Adsorba (24-26)	45	77	0.87	0.017	297
Detoxyl-S	50	19	0.93	0.01	69

Notes $\bar{t}_A$ = MRT of active vol.

V_A = active volume (= $F_A \times \bar{t}$) : V_T = total volume

F_C = cross-flow

Table 4.5.3 Values of Parameters in Multi--parameter Mixing Cell Model

Run	Solute	Re	Mujauchi et al (1975)		Bischoff and Levenspiel (1964)		Wilhelim (1972)	
			Pe_L	n	Pe_L	n	Pe_L	n
W 1 & 7		22.3	53	26	62	31	60	30
W 2/4	Sodium	4.46	51.5	26	59.5	30	44	22
W 5/6	Salicylate	1.12	51.5	26	58	29	44	22
W 8	Sodium	18.7	61	31	73.5	37	72	36
W 9	Phenobarbitone	9.35	61	31 *	74	37	62	31

* Values adopted for simulations

Table 4.5.4 Axial Dispersion Coefficients and No. of Cells for Wrights Columns

capacity were 5%, the resultant fall in performance of a practical haemoperfusion column would probably not exceed the scatter in performance data between devices. Therefore, considering the added complexity, computation time and cost involved, the multiparameter dispersion model was not incorporated into the complete perfusion column model. Instead, it was assumed that to a first approximation the simple mixing cell model was sufficient to describe the hydrodynamics. That is, the column model as proposed in Section 3.6 was adopted.

The hydrodynamics are also critical in defining the washout characteristics of a haemoperfusion column. At the end of a perfusion the blood that is in the column is flushed back into the patient using saline. In uraemia it is critical that a minimum of blood is lost, as the patients are anaemic. In acute poisoning, this is not a problem. As haemoperfusion is mainly used for the latter application, washout characteristics are not very important. Nevertheless, in all the columns studied, the contents of the column are washed out in under two mean residence times.

It should not be forgotten that all the mixing cell models are functional descriptions of hydrodynamics and that the parameter values do not necessarily have any physical significance with respect to the column. This is especially true of the multiparameter model. After all this model assumes an equal proportion of the semistagnant volume is associated with each cell. Apriori one would expect the semistagnant regions to be concentrated at the ends of the Adsorba 300C and the Detoxyl-S and in the middle of the Haemocol. Likewise, with the assumption that all the active cells are of equal volume. Nevertheless, both the mixing cell models provide reasonable descriptions of the hydrodynamics in a perfusion column.

CHAPTER 5

VALIDATION OF PERFUSION COLUMN MODEL

CHAPTER 5

VALIDATION OF PERFUSION COLUMN MODEL

5.1 Introduction

This chaper presents the results of the validation experiments and simulations for the perfusion column model. Based on the sorption and mass transfer data in Chapter 4, a number of simulations of the performance of the small Wrights column and the Haemocol were made using the perfusion column model developed in Chapter 3. A variety of combinations of column parameters were considered. *In vitro* perfusions were then performed on the two types of column under the corresponding experimental conditions. The ability of the model to predict these experimental results was taken as a measure of the validity of the model.

As stated in Chapter 4, the initial breakthrough of the experimental clearance curve was used to estimate the external mass transfer coefficient and N_e. Therefore, the validation does not apply to the breakthrough.

5.2 Experimental Apparatus and Method

The flow circuit used in the single pass, validation experiments for the perfusion column model is illustrated in Figure 5.2.1.

Two toxins were investigated, sodium salicylate and sodium phenobarbitone, with 0.1 M phosphate buffer solution (pH 7.4) as a blood substitute. Prior to each perfusion the column was heated by recirculating buffer solution at 37°C through the circuit. The reservoir of toxin/buffer solution was then connected and the tubing upstream of the column was flushed of toxin free buffer by diverting the flow to drain via the two-way tap. The fluid in the effluent lines were simultaneously drained. This eliminated errors in measuring the effluent volume during the perfusion. (Especially in the case of the Wrights column.) The pump speed was adjusted to that value, established during the preheating stage, giving the desired flow rate through the column and rotameter. Perfusion was initiated by switching the flow from the drain to the column. The flow rate was checked regularly with a measuring cylinder and stop watch ($\pm$ 2%); the rotameter merely provided a check on the consistency of flow.

With the Wrights column the effluent samples were taken at regular increments of volume throughput while for the Haemocol samples were obtained at set time intervals. As the Wrights columns are small a complete perfusion was quite rapid. It was more convenient therefore, to time the passage of say, 100 ml to determine the flow rate and to sample at the end of that volume for concentration measurements. For the Haemocol, however, two litres may pass between convenient sample times. Therefore, it was expedient to sample at set times and check the flow rate only over 100 or 200 ml volumes once or twice between samples. During the perfusion experiments, the temperature at the column outlet was maintained at 36°C for the Haemocol and 37°C for the Wrights. The former condition allows for the temperature drop across the column.

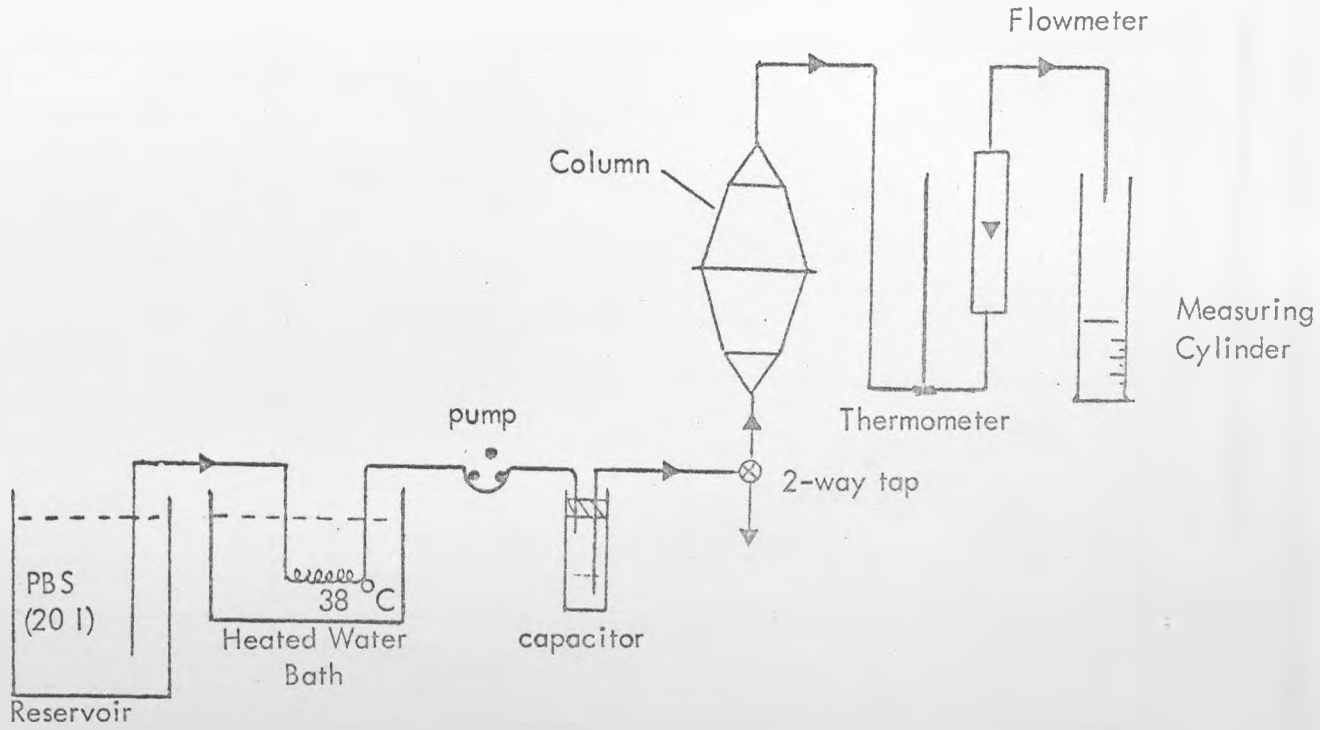

Figure 5.2.1 Flow Circuit for Mass Transfer Experiments Conducted on Perfusion Columns

5.3 Simulations

The perfusion column model is written in terms of the normalized sorption and mass transfer parameters. The appropriate parameters were calculated for the ten validation simulations, on the basis of the data in Chapter 4. The basic physical data associated with each simulation are listed, together with the normalized parameters in Table 5.3.1. In each instance, account was taken of the range of particle sizes involved. Examination of the table reveals the wide range of parameter values investigated for the validation.

Run	Perfusion Column	Sorbate	Flow Rate (ml/min)	Inlet Conc (mg/ml)	N (-)	d (cm)	N (-)	RATIO (-)	R (-)
W 1	Wright's Chromato-graphy Column (12 gm BDH Activated Carbon)	Sodium Salicylate	200	0.9	2.30	0.085 to 0.100	0.127 to 0.175	263	0.069
W 2 W 3 W 4			40	0.9	3.95		0.632 to 0.875	263	0.069
W 5 W 6			10	0.9	5.7		2.53 to 3.50	263	0.069
W 7			200	0.5	2.20		2.16 to 2.99	450	0.118
W 8		Sodium Phenobarbitone	200	0.5	2.39	0.071 to 0.085	0.034 to 0.049	1125	0.059
W 9			100	0.5	3.02		0.064 to 0.098	1125	0.059
H 1 H 2	Haemocol	Sodium Salicylate	200	0.5	2.22	0.165 to 0.333	1.01 to 4.1	357	0.095

Table 5.3.1 Experimental and Simulation Parameters Relating to the Validation Experiments for the Perfusion Column Model

5.4 Results and Discussion

The simulation results are presented in Figure 5.4.1 to 5.4.7, together with the corresponding experimental data. The axes of the graphs are presented both in normalized and actual (real time) co-ordinates. The possible error in the fractional clearance values, due to measurement errors in the concentrations, are indicated by the heights of the data points. The absolute clearance values were calculated using the nominal volumetric flow rate.

In the duplicate experiments, Runs 2 to 4 and 5 and 6, the variation between the clearance values for the different experiments was within the errors due to concentration measurement. Therefore, the techniques both of conducting the experiments, and for the Wrights columns, in preparing and assembling the columns, are reproducible.

In all instances, the model provides a good prediction of the experimental data. As expected, the kinetics are influenced by the particle size distribution. The initial portion follows the upper limit established by the smallest particles while at later times the larger particles dominate. In the case of the Haemocol experiments, the data corresponds to the simulation for the lower particle size. This is in accordance with the Wrights column studies in which the data for similar values of T was predicted by N_s for the lower d_p limit.

In conclusion therefore, the perfusion column model provides a valid description of the mass transfer in a packed, sorbent bed. As such it may be employed to test the influence of the various sorption and mass transfer parameters on the performance of perfusion columns, in particular haemoperfusion columns.

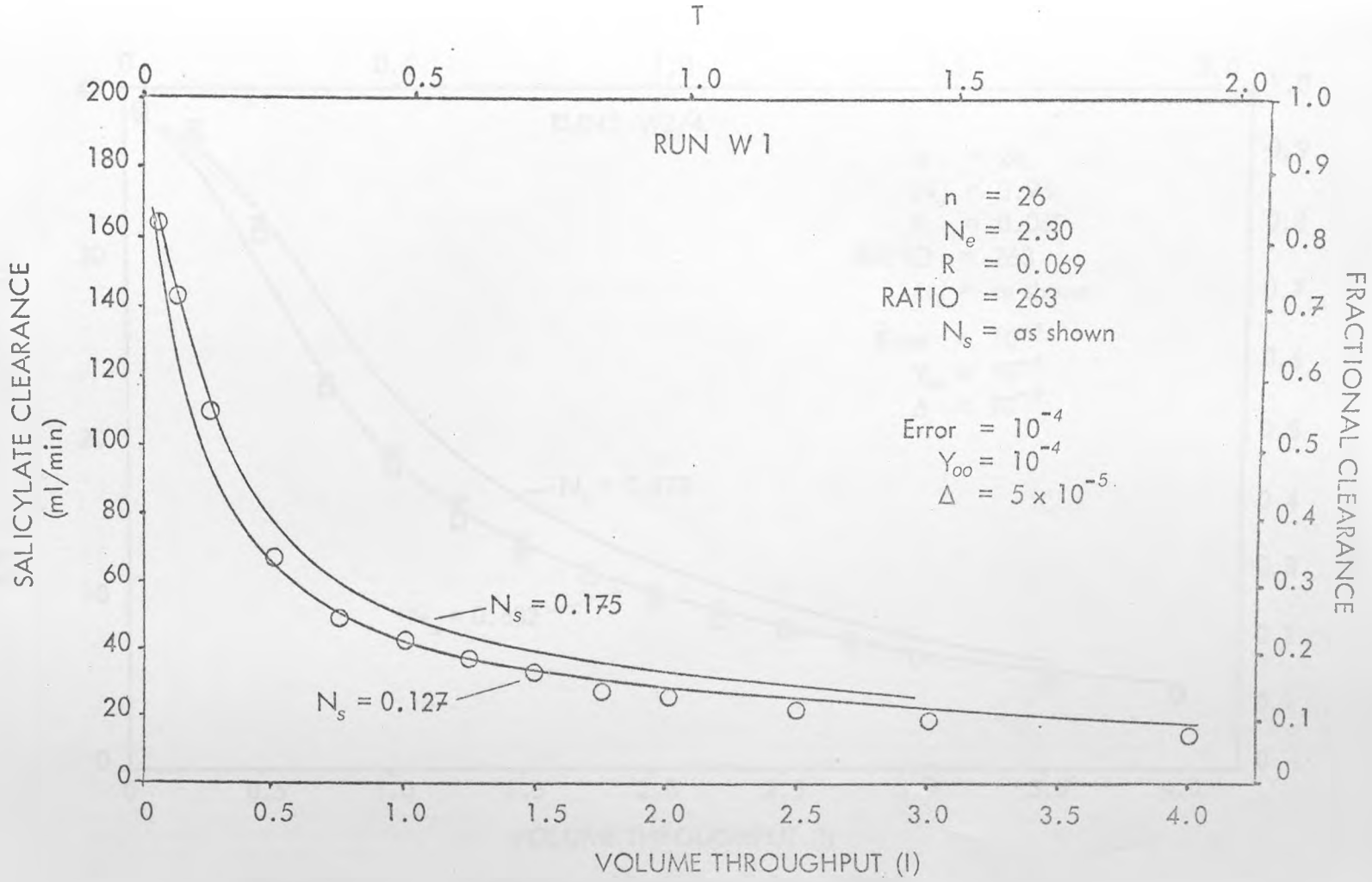

Figure 5.4.1 Validation of Perfusion Column Model Comparison of Model Simulation and Experimental Data in Run W 1

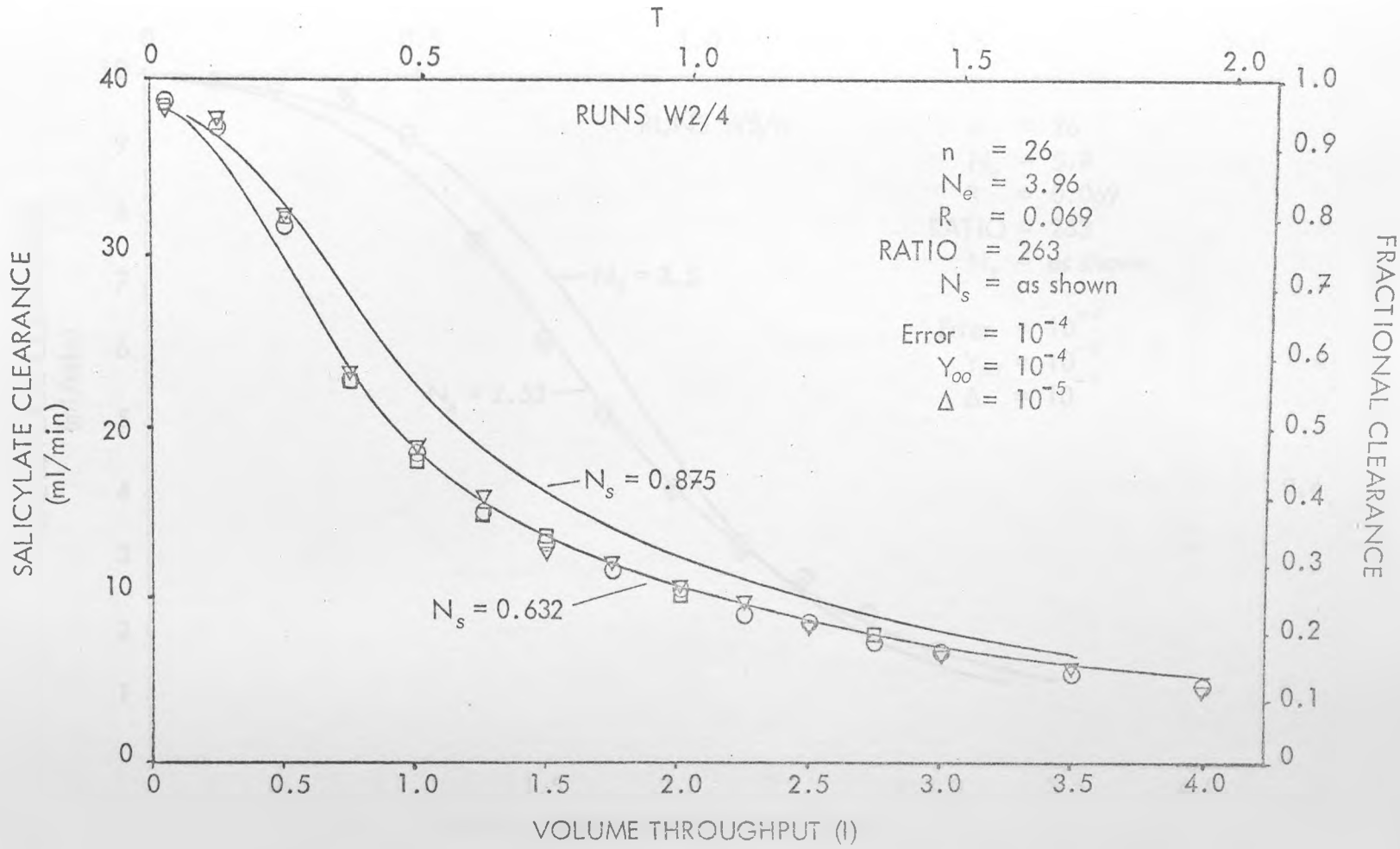

Figure 5.4.2 Validation of Perfusion Column Model Comparison of Model Simulation and Experimental Data in Runs W2 to W4

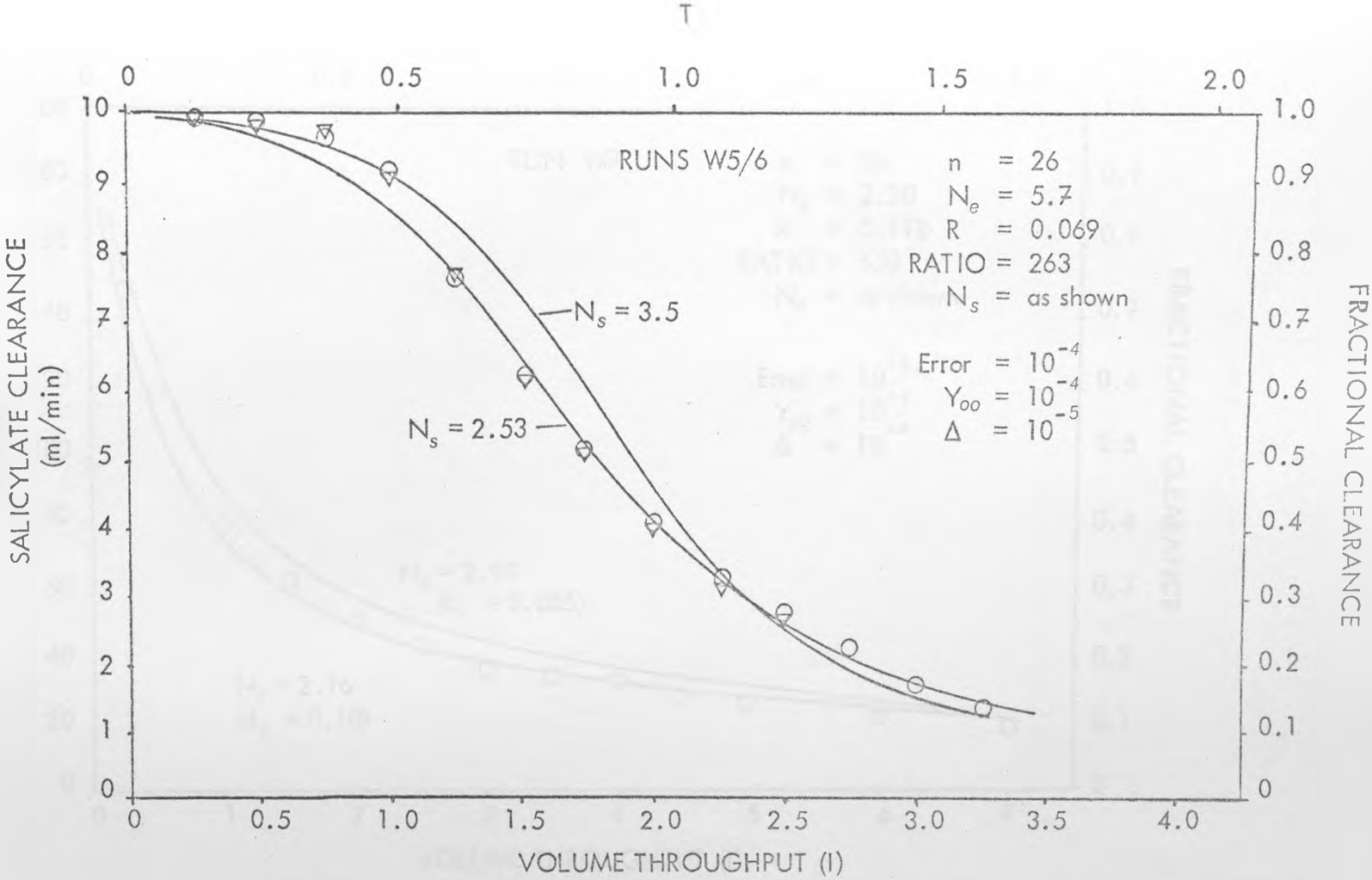

Figure 5.4.3 Validation of Perfusion Column Model Comparison of Model Simulation and Experimental Data in Runs W5 and W6

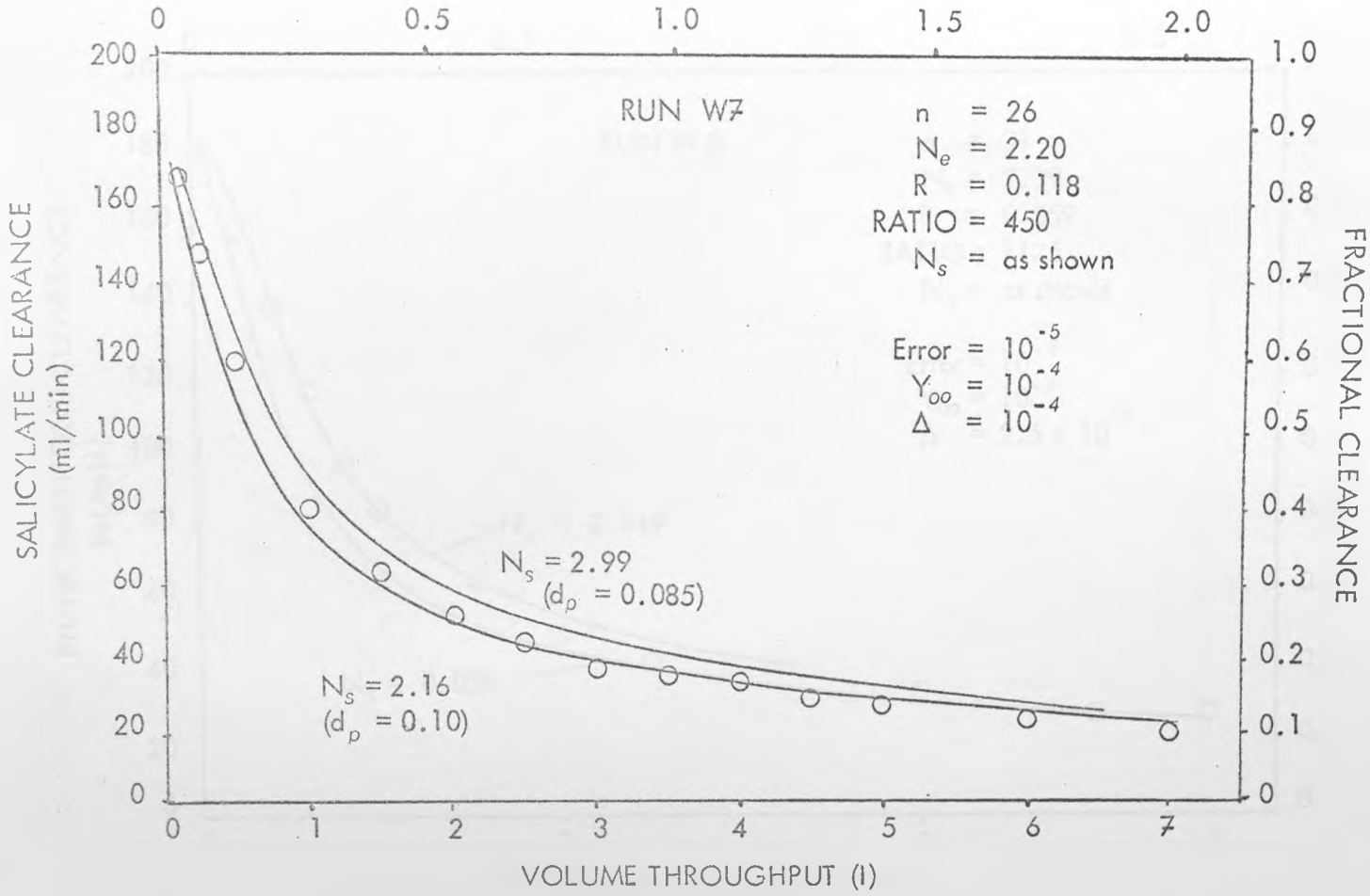

Figure 5.4.4 Validation of Perfusion Column Model Comparison of Model Simulation and Experimental Data in Run W 7

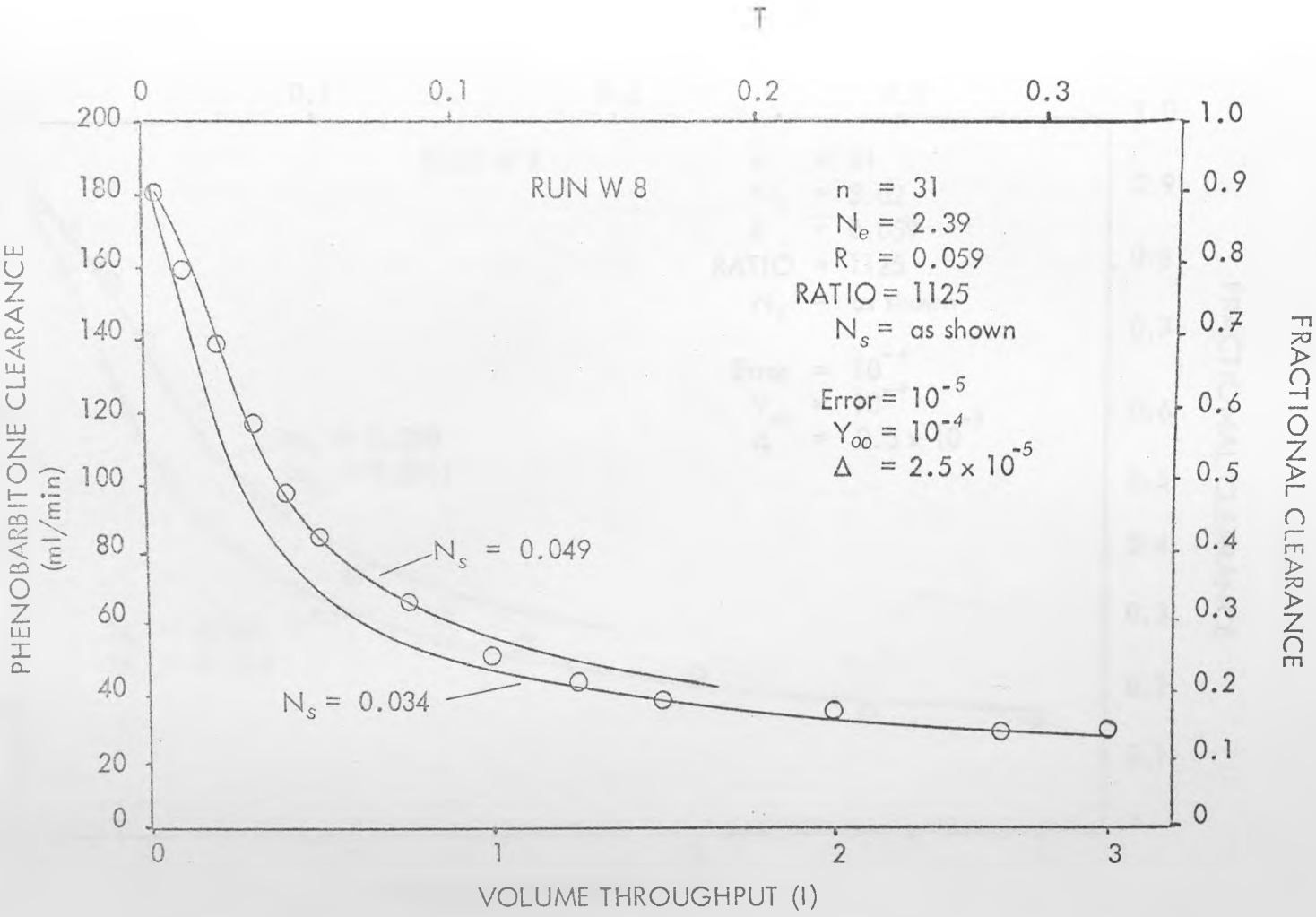

Figure 5.4.5 Validation of Perfusion Column Model Comparison of Model Simulation and Experimental Data in Run W 8

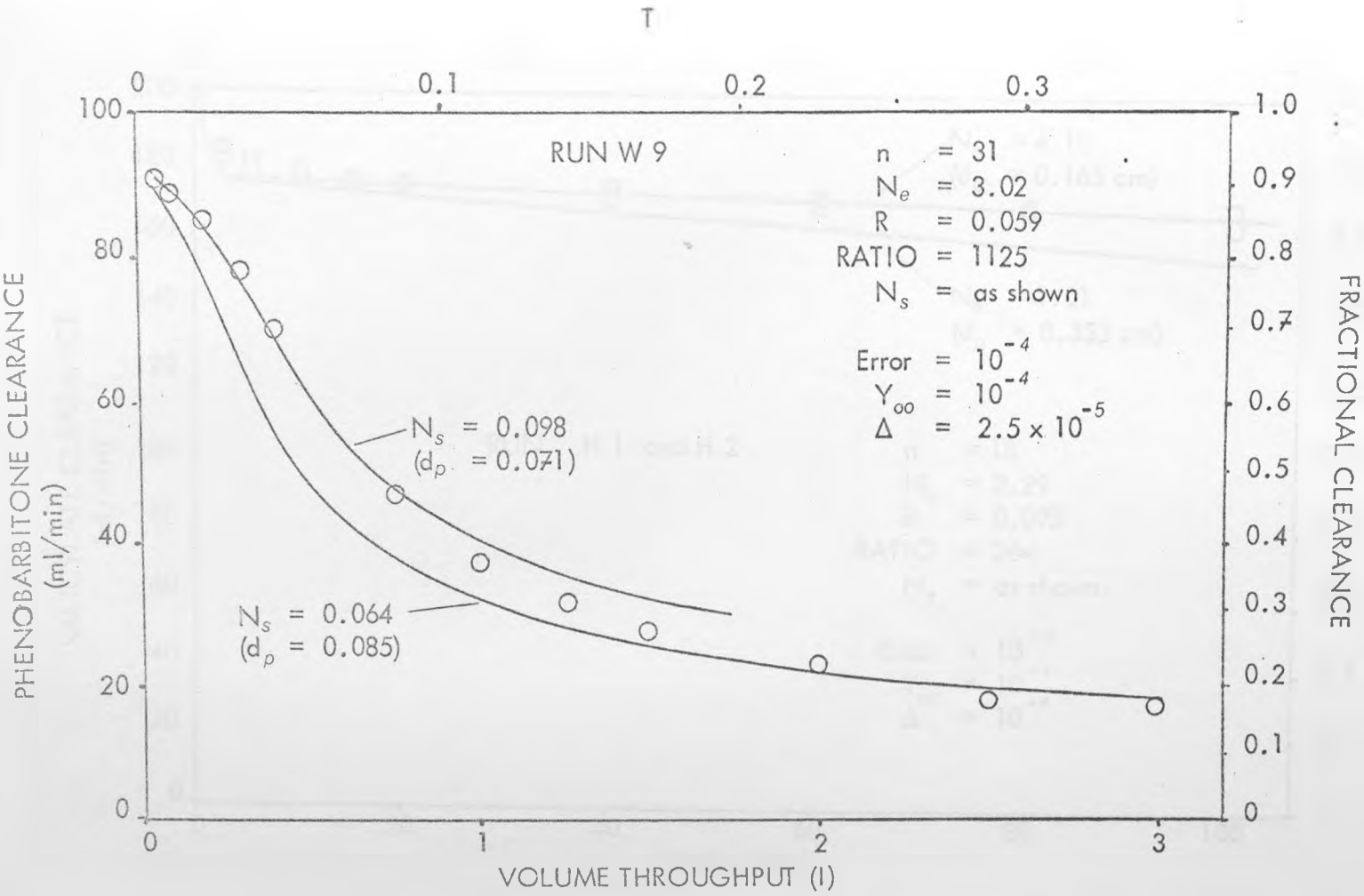

Figure 5.4.6 Validation of Perfusion Column Model Comparison of Model Simulation and Experimental Data in Run W 9

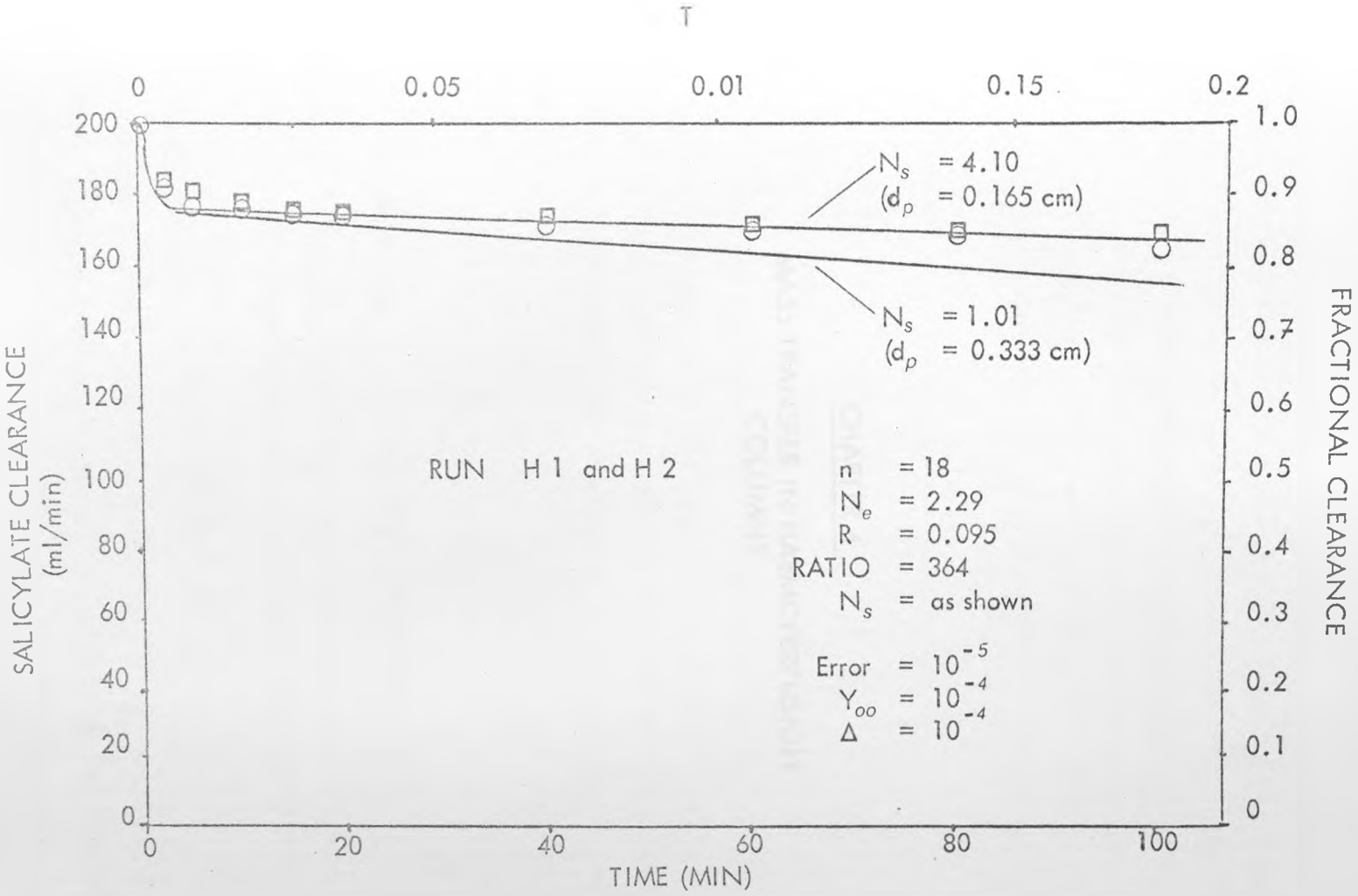

Figure 5.4.7 Validation of Perfusion Column Model Comparison of Model Simulation and Experimental Data in Runs H 1 and H 2

CHAPTER 6

MASS TRANSFER IN HAEMOPERFUSION COLUMNS

CHAPTER 6

MASS TRANSFER IN HAEMOPERFUSION COLUMNS

6.1 Introduction

Validation of the perfusion column model permits its use to study the effect of the column parameters on the haemoperfusion column performance. The normalized form of the model was used in order to reduce the number of parameters to five, i.e. N_e, N_s, RATIO, R and n. A standard set of parameter values was chosen on the basis of typical values in commercial devices. A series of simulations were conducted with four of the parameters held constant at their standard values and the fifth varied in order to identify its influence on column performance. The standard set of parameter values was

N_e	N_s	RATIO	R	n
2.0	0.5	1000	0.1	20

For each simulation the results are presented both in normalized and in 'real time' co-ordinates. The latter is calculated from the former on the assumption that the column contains approximately 300 gm of sorbent and that the flow rate is 200 ml/min. The definition of T in Figure 3.7.2 can be rearranged to give

$$T \equiv \left(\frac{F}{V_p \ RATIO}\right) t$$

where V_p = priming volume of column

Therefore t can be calculated from T if the flow rate, RATIO and the priming volume are known. The priming volume is related to the mass of sorbent thus

$$V_p = \left(\frac{\varepsilon_b}{\rho_b}\right) M$$

In many devices ε_b is approximately equal to ρ_b, i.e. the priming volume is numerically equal to the mass of sorbent. The conversion for t in subsequent figures assumes a priming volume of 300 ml and therefore approximately 300 gm

of sorbent. It should be noted that on the basis of the above parameters that each hour of perfusion corresponds to only 0.04 T. Therefore, a three hour perfusion corresponds to only 12% of the throughput capacity. Where possible the simulations are supplemented by in vitro experiments, conducted with the same protocol as the validation experiments in Chapter 5.

6.2 Effects of Normalized Parameters on Perfusion Column Performance

6.2.1 Effect of external diffusion (N_e)

The number of external diffusion mass transfer units, N_e, determines the basic performance of a haemoperfusion column. It is this parameter that establishes the maximum clearance of the device. The other normalized parameters merely control the rate of decline from this initial maximum.

In order to study the role of N_e, a variation of the perfusion column model outlined in Fig 3.7.2 was developed, i.e. an external diffusion limited model. In this model the QDF equation for the intraparticle diffusion was omitted. (i.e. $N_s = \infty$). Instantaneous equilibrium is assumed to exist between the pore fluid concentration and the solid concentration throughout the particle. As this eliminates the algebraic loop of the general model, the array format can be used to describe the external diffusion limited model. A listing of this model is presented in Appendix 3. Figure 6.2.1 illustrates the influence of N_e on performance up to one throughput capacity. Each clearance curve represents the maximum obtainable performance for any perfusion column with the particular value of N_e.

A haemoperfusion column is essentially a haemodialyser with a finite dialysate volume. The rate of mass transfer is controlled by the total diffusion resistance which comprises the external blood film resistance around the particles in series with the membrane coating resistance. The clearance is initially a maximum but accumulation of toxin in the sorbent lowers the concentration gradient between the bulk blood and the fluid in the particle pores. The rate of increase in the concentration in the pores is restricted by the highly non-linear isotherm which applies between the sorbent and the pore fluid. In the dialyser, with aqueous dialysate, however, the dialysate concentration (which is equivalent to the pore fluid concentration in the column) rises rapidly and the clearance declines exponentially. This also holds if a sorbent is placed in the dialysate, although the rate of the exponential decline

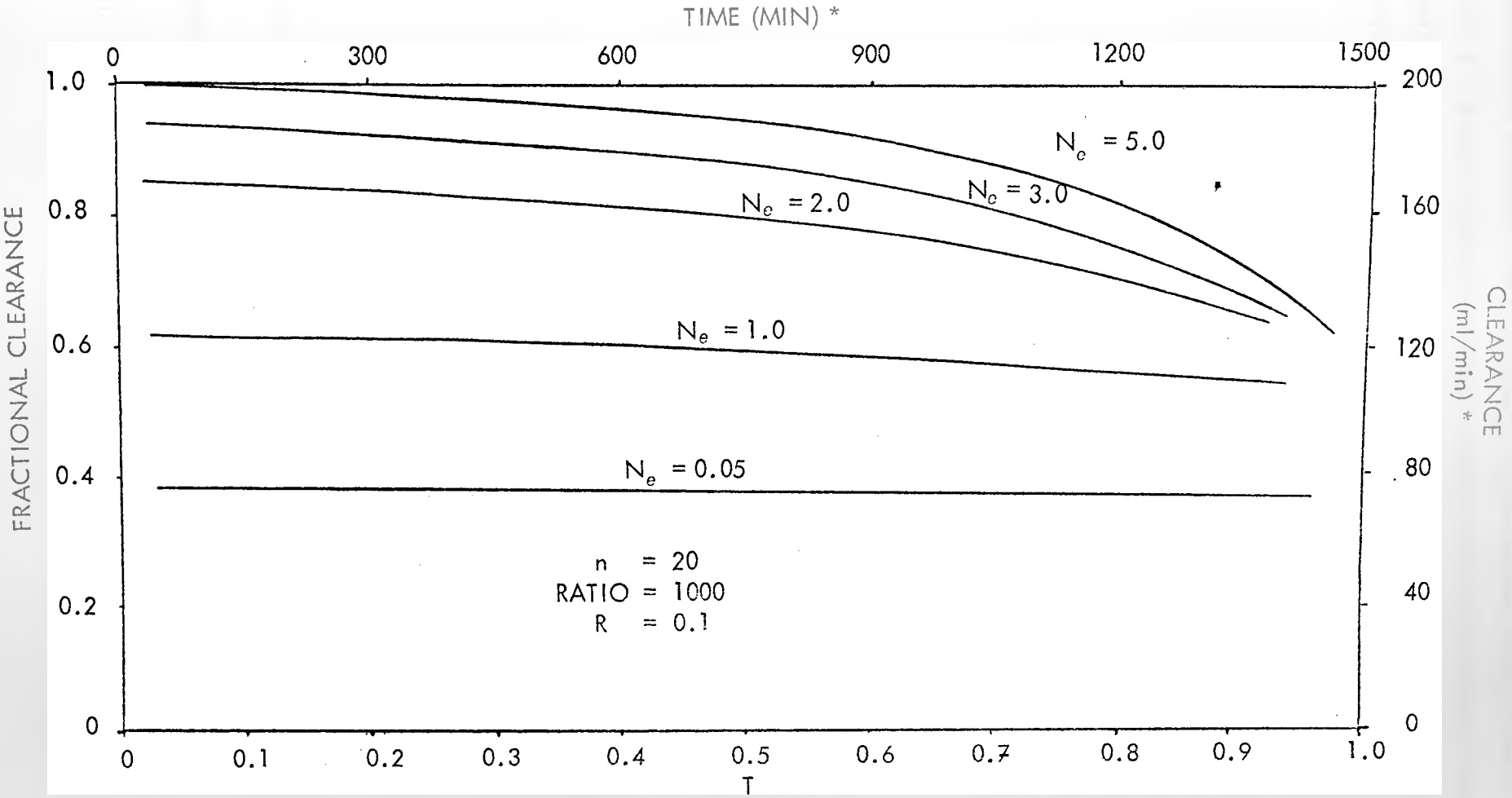

Figure 6.2.1 Effect of N_e on External Diffusion Limited Model of a Perfusion Column (Single Pass)

is moderated by the degree of non-linearity in the sorbent/toxin isotherm. In fact, there is a major similarity between an external diffusion limited haemo--perfusion column and a haemodialyser with a finite dialysate supply augmented with sorbent.

It is therefore convenient to introduce the concept of the equivalent haemodialyser, i.e a haemodialyser with the same number of external mass transfer units, N_e , as the perfusion column under investigation. In the case of dialysers N_e is usually termed N_o and it includes not only blood film and membrane mass transfer resistances but also a dialysate side film resistance. Formula for the dialysance for various haemodialyser geometries were listed in Figure 2.2.1. These were extended to include a sorbent with a linear isotherm in the dialysate. Figure 7.2.1 summarizes the modified formulae. Using these and a piecewise linear representation of a Langmuir isotherm it is possible to predict the clearance in a haemodialyser with a non-linear sorbent in the dialysate. Details are in Appendix 6. The clearance curve and the piecewise isotherm are illustrated in Figure 6.2.2. The clearance curve has two sections, with a discontinuity between the two caused by the piecewise isotherm. An approximate clearance curve based on a continuous isotherm has been drawn in by hand. The equation for the first section is

$$Cl \triangleq Q_b \left[1 - e^{-N_o}\right] e^{-\left[1 - e^{-N_o}\right]RT} \qquad \text{EQ.6.1}$$

where N_o = total number of mass transfer units

R = Langmuir isotherm, shape factor

T = throughput capacity

$$\equiv \left(\frac{Q_b \; c_b}{V_d c_{d_\infty}}\right) t$$

This equation describes the clearance for at least one throughput capacity (i.e. $T = 1$) To within 0.5% for $T < 1$ and $R = 1$, Equation 6.1 can be approximated by

$$Cl \triangleq Q_b \left[1 - e^{-N_o}\right]\left\{1 - (1 - e^{-N_o}) \; R \; T\right\} \qquad \text{EQ. 6.2}$$

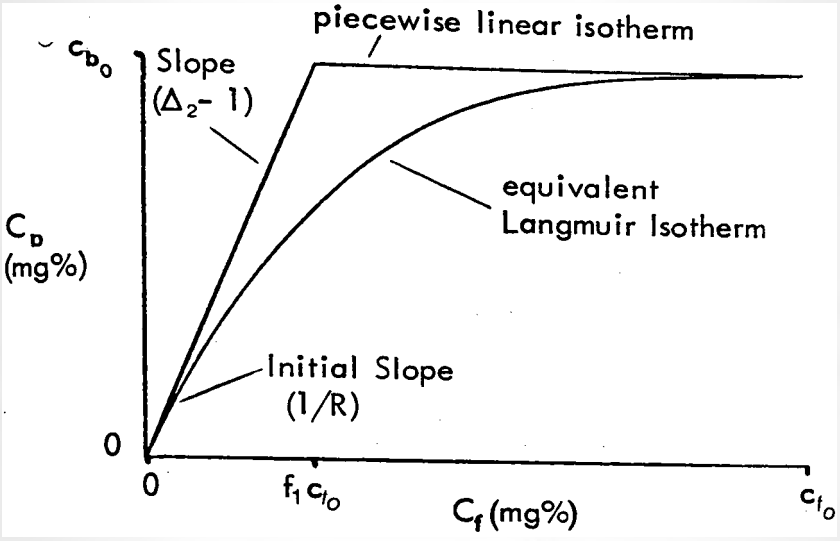

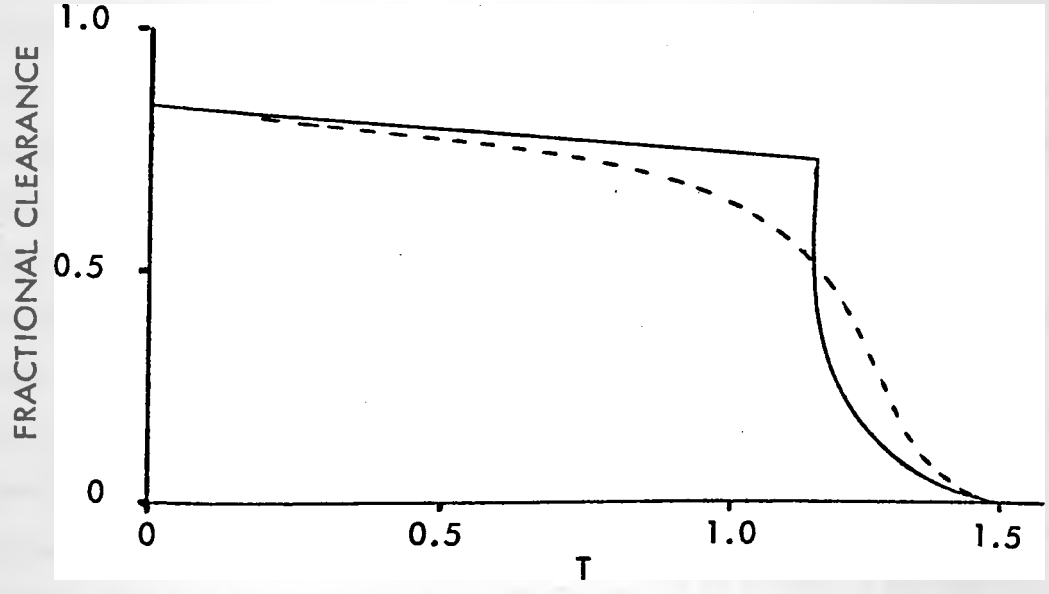

Figure 6.2.2 Piecewise Linear Isotherm and Typical Clearance in Equivalent Haemodialyser Based on that Isotherm

This equation can then be used conveniently for comparison purposes.

The correspondence between this perfusion column model and the equivalent haemodialyser is seen by considering the initial clearance in the perfusion column. From Equation 3.28 (Chapter 3), for negligible axial dispersion, the initial breakthrough is given by

$$X_o = e^{-N_e} \qquad \text{EQ.3.28}$$

Therefore, the initial clearance is

$$C\,I = Q_b\,(1 - e^{-N_e}) \qquad \text{EQ. 6.3}$$

That is the same initial value as the equivalent dialyser. The full extent of the correspondence between the two models is realized if the complete clearance curves are compared.

Figure 6.2.3 compares clearance in the equivalent haemodialyser and the external diffusion limited perfusion column models. Considering that the equivalent dialyser curves 'roll off' with time due to the smooth nature of the true sorbent isotherm, the correspondence between the two models is excellent.

The principal difference between the equivalent haemodialyser and a typical haemodialyser is that N_e is much larger than N_o. This difference is the reason for the higher initial clearance (for any given molecule) reported for haemoperfusion columns as opposed to haemodialysers. For the same blood flow rate, Q_b, larger values of N_e in the perfusion column (or equivalent dialyser) is due either to an increase in the external area for mass transfer, A_p, or a decrease in the external resistance, k_e. The difficulties in measuring A_p, especially for irregular particle shapes were outlined in Chapter 3. These apply to estimating the surface area in the major commercial haemoperfusion column, the Haemocol. On the assumption that the sorbent particles are spherical, the extremes of A_p are 0.65 m^2 and 1.3m^2. However, it is probable that the actual area is in the range 1.5 to 2.0m^2. For the Adsorba 300 the total area is 1.8m^2 (assuming an average particle length of

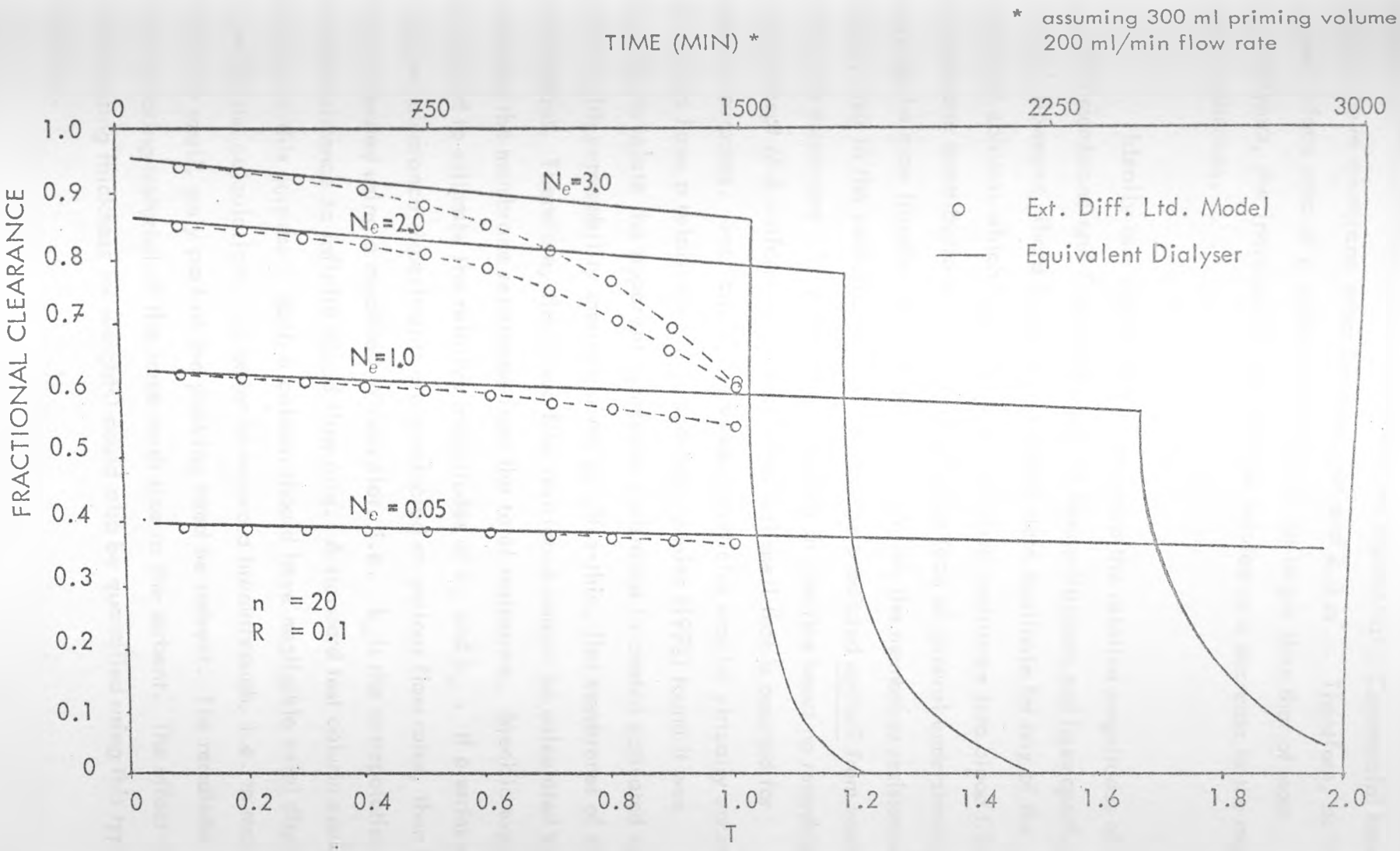

Figure 6.2.3 Comparison of Single Pass Clearance in External Diffusion Limited Model and the Equivalent Haemodialyser Model

2.5 mm). Both these estimates neglect the loss of effective area due to contact between adjacent particles, and these may be substantial. Commercial haemo--dialysers have membrane areas between 1 m^2 and 2.5 m^2 . Therefore, as the external surface area of a perfusion column is no larger than that of most haemodialysers, the increase in N_e must be related to a decrease in the mass transfer resistance.

Ideally one would like to compare the relative magnitudes of the respective membrane and film resistances in haemodialysers and haemoperfusion columns. However, there is no experimental data available for any of the commercial columns which breakdown the external resistance into blood film and membrane contributions. This is due to the lack of general understanding regarding the mass transfer in such devices. Unlike the membrane resistance in the dialyser, that in the perfusion column cannot be predicted apriori from basic data on the membrane. The membrane coating in practice bears no resemblance to the concept of a uniform thickness, spherical shell that is assumed for modelling purposes. Sections of the sorbent particles may be virtually uncoated, while others have a relatively thick coating. Meier (1972) found it was impossible to relate the apparent membrane resistance in coated activated carbon particles with permeability measurements on ultra-thin, flat membranes of the same material. Therefore, the blood film resistance cannot be calculated by subtracting the membrane resistance from the total resistance. Specific experiments are required to estimate the relative magnitudes of k_b and k_m . If a series of single pass clearance experiments are conducted at various flow rates, then k_m can be estimated using a modified Wilson plot, i.e. k_m is the extrapolation of the total resistance to infinite blood flow rate. A standard test column could be set up for this purpose. Such a column should have negligible axial dispersion, to simplify the calculations. In order to ensure a breakthrough, i.e. to make N_e sufficiently small, only part of the packing need be sorbent. The remainder would be inert packing material of the same mesh size as the sorbent. The effect of various coating thickness (or weights) could also be quantified using this type of experiment.

6.2.2 Effect of intraparticle diffusion (N_s)

The number of internal mass transfer units, N_s is the principal factor controlling the decline in clearance in a perfusion column from the upper limit established by N_e and external diffusion limited perfusion column model (or the equivalent dialyser). Figure 6.2.4 illustrates this effect. Clearly the larger N_s the smallerthe deviation from the external diffusion limited model ($N_s = \infty$).

The sensitivity of the rate of decline from the initial breakthrough is related to N_s by a sigmoid type relationship. This is illustrated in Figure 6.2.5 where the fractional clearance is plotted against N_s for various fixed values of T. For large values of N_s the fractional clearance at any given T is relatively independent of N_s. For example, at $T = 0.1$ the fractional clearance increases only 2% for an increase in N_s from 2.0 ($= N_e$) up to infinity. Therefore, even large changes of N_s in this range have a negligible effect on the column performance. The same applies for extremely small values of N_s (i.e. where N_s dominates). However at such values the clearance is so small, this extreme is not of practical interest. Between these extremes, the fractional clearance is very sensitive to the value of N_s. The range of N_s values over which this sensitivity occurs depends upon the value of T under consideration, i.e. for $T = 0.05$ the clearance declines rapidly for $N_s < 0.5$ whereas at $T = 0.5$ the decline commences in the region of $N_s = 5.0$. Therefore, the sensitivity of a perfusion column to N_s depends upon the range of throughput, T, of interest as well as the relative magnitude of N_s.

The throughput has an additional effect when the performance is considered in real time. The value of N_s is dependent upon two groups of fundamental parameters, i.e.

$$N_s \equiv \left(\frac{60\ D_s}{d_p^2}\right)\left(\frac{M\ q_o}{F\ c_o}\right) = \left(\frac{60\ D_s}{d_p^2}\right)\left(\frac{F}{V_p\ \text{RATIO}}\right)$$

$$\text{In addition}\quad T \equiv \left(\frac{F\ c_o}{M\ q_o}\right) t = \left(\frac{F}{V_p\ \text{RATIO}}\right) t$$

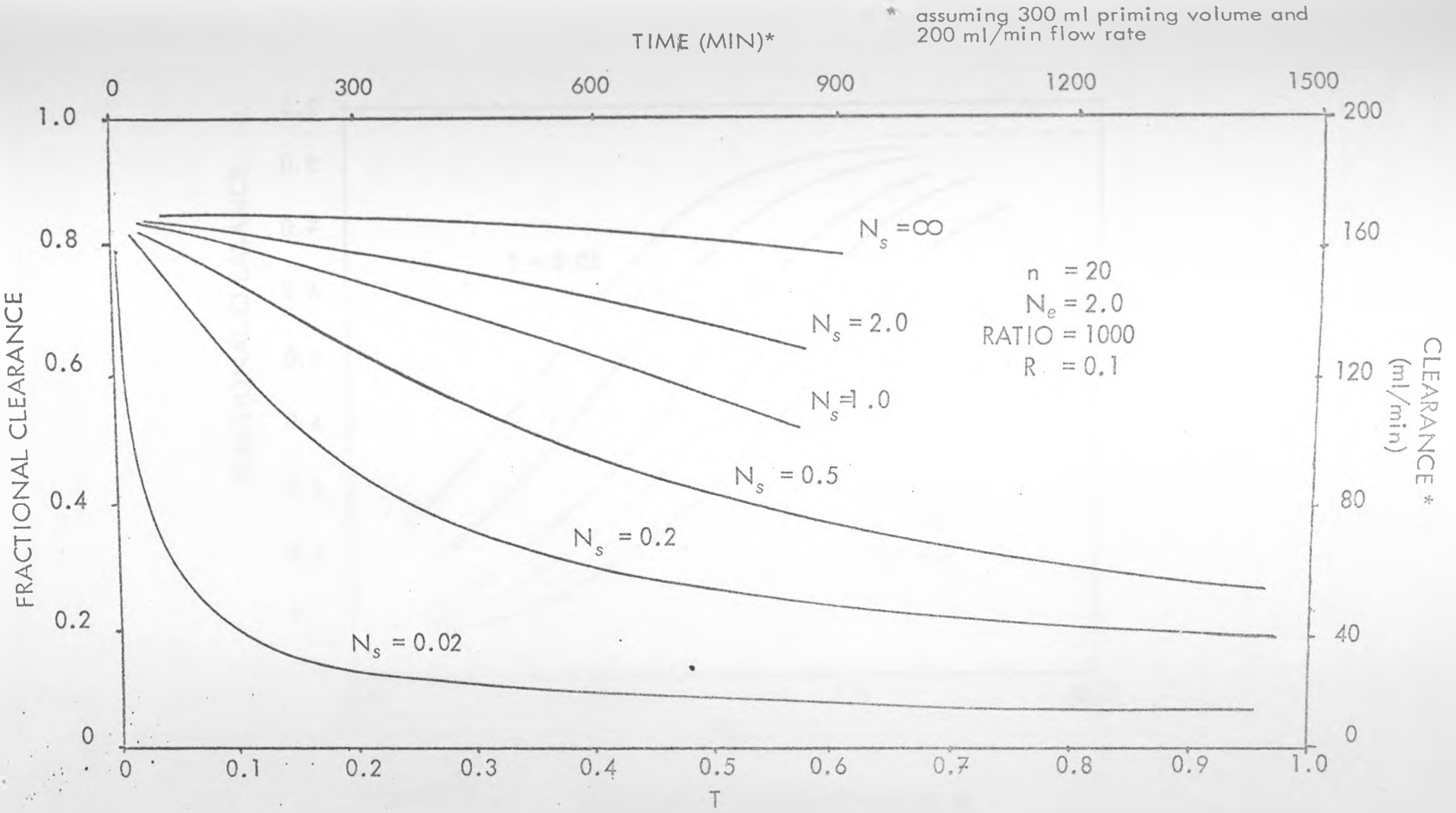

Figure 6.2.4 Effect of N_s Upon Single Pass Clearance in a Perfusion Column

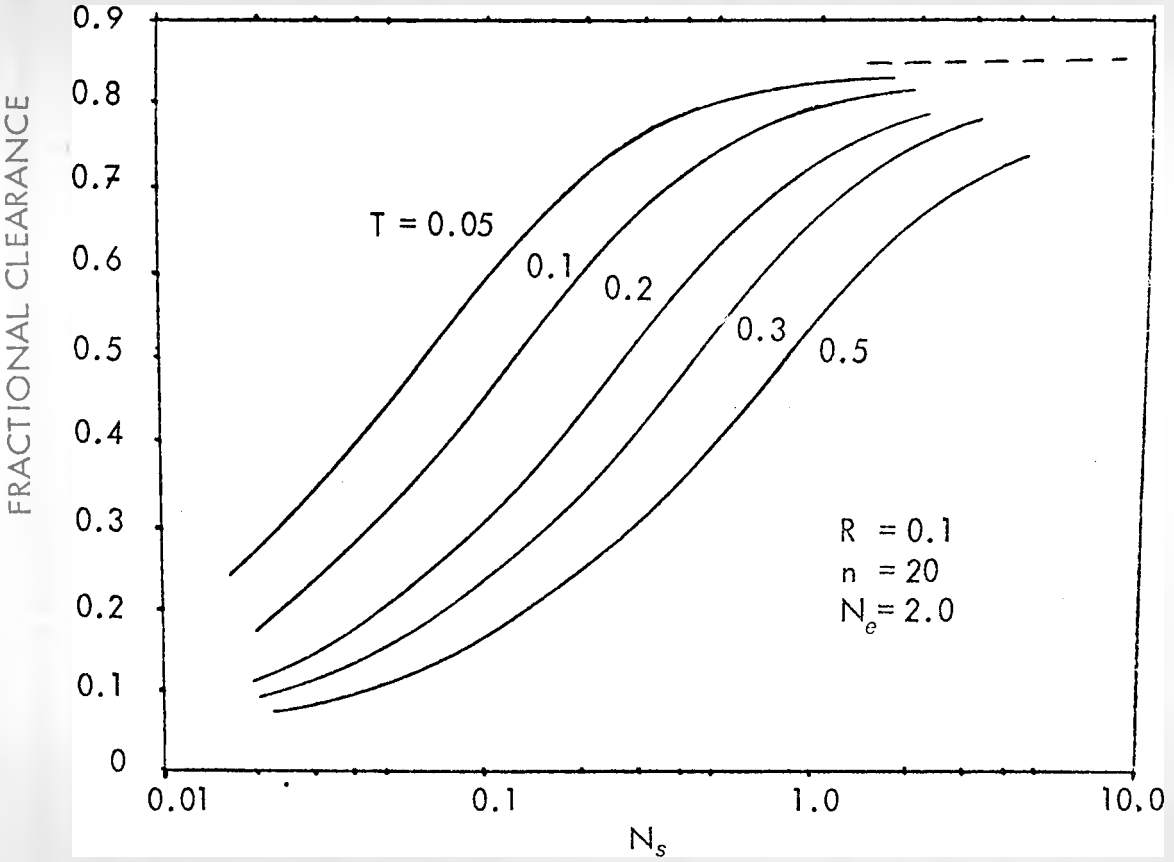

Figure 6.2.5 Sensitivity of Fractional Clearance to N_s at Fixed Values of T.

If $(M q_o / F c_o)$ is increased, N_s increases and for a constant value of T, t also increases. Hence, the decline in clearance from the initial breakthrough is reduced due to the increase in N_s. In addition, the clearance curve becomes even flatter due to the expansion in the real time axis (t). Increases in $(M q_o / F c_o)$ brought about by changes in F or the volume of sorbent (M/ρ_b) will also increase the value of N_s and therefore the initial breakthrough also increases. The second group of parameters on which N_s depends is $(60\ D_s/d_p^2)$. Clearly over the sensitive range of N_s values, relatively small changes in d_p have a marked effect on the clearance. Such effects are involved if a range of particle sizes is employed in a perfusion column (as is usually the case). This was illustrated in the validation experiments in Chapter 5. In addition, N_s is inversely proportional to d_p. Therefore, decreases in d_p cause both the initial clearance to increase and the rate of decline of clearance to decrease, i.e. a dual improvement in performance. The intraparticle diffusivity, D_s decreases rapidly with the molecular weight of the toxin. This is illustrated in Figure 6.2.6. In Chapter 3 it was shown that the diffusivity in a range of activated carbons (for a given solute) could vary by up to a decade. Therefore, the choice of sorbent structure can also be quite critical to the performance.

6.2.3 Effect of polymer coating

Although superficially the presence of the polymer coating is related to the external diffusion resistance (discussed in 6.2.1), in fact its influence extends to the intraparticle diffusivity. Therefore, it is appropriate to include a separate section discussing the effects of polymer coatings.

The only quantitative studies of the kinetics of adsorption in sorbents coated with polymers, are those of Huang (1974) and Meier (1972). Both found that the intraparticle diffusivity calculated from uncoated particles did not provide a good description of the kinetics for coated particles. Huang found that the apparent diffusivity decreased by a factor of between 4 and 7 (with a 5% coating). Although the coated and uncoated kinetics were not compared in batch experiments in this thesis, differences between the expected and the actual values of N_s in various column experiments indicate a decrease in D_s

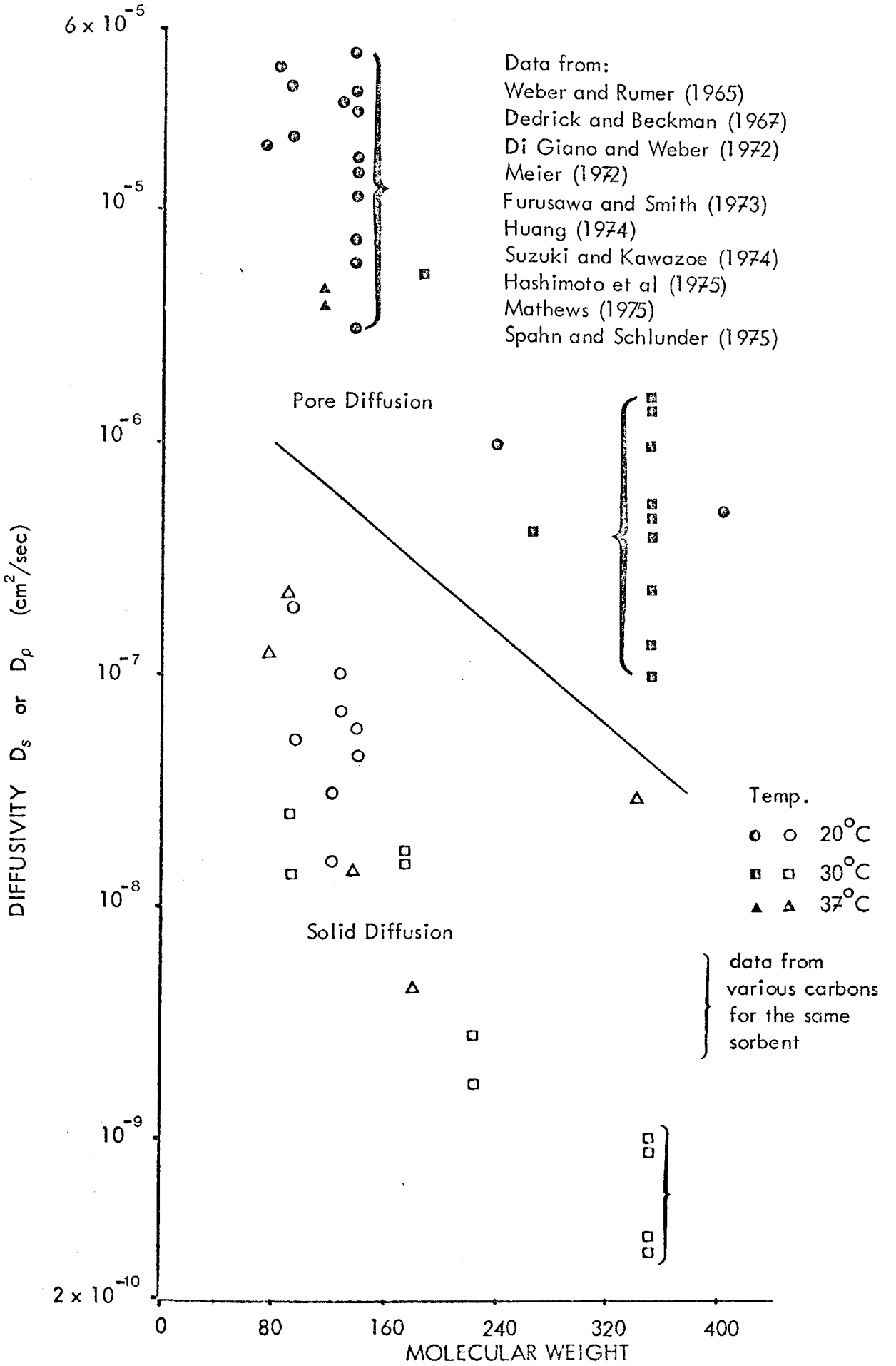

Figure 6.2.6 Variation in Intraparticle Diffusivities with Type of Carbon and Molecular Weight

due to coating.

All the results relate to coated forms of Norit RBX-1 pellets, i.e. those used in the Adsorba 300C and various prototype perfusion columns constructed at the University of Strathclyde. Simulations of the performance of the Adsorba 300C for single pass clearance of sodium salicylate and sodium phenobarbitone were performed, using the data from Chapter 4. These were compared to the quoted performance in Thysell et al (1975) and in the brochure by ab Gambro. It should be noted that these two sources do not agree precisely as to the performance of the Adsorba 300C. The simulations and the quoted data are shown in Figure 6.2.7. The predicted values of N_s , based on uncoated particles were respectively 25.6 and 4.6 for salicylate and phenobarbitone. The actual values, found by adjusting N_s until the simulation fitted the data, were 0.67and 0.25 . That is a ratio in D_s values of 38.5 and 18.5. Part of this discrepancy could be attributed to a loss of capacity of the carbon due to the coating. (The simulation assumes the capacity is unchanged.) No estimates for a possible decrease in capacity are available. However, even for large decreases (i.e. 20%) the ratio of actual and predicted D_s values only decrease to about 10 and 6 respectively.

The Adsorba 300C is coated by a cellulosic membrane. By way of comparison, the effects on D_s of the copolymer membrane developed by Courtney et al. (1977) were briefly investigated. The only available data using toxins other than creatinine is that in the thesis of Walker (1974) and Edwards (1975). For adsorption of sodium salicylate the respective values of the predicted and the actual values of N_s were 3.8 and 1.17; i.e. a D_s ratio of 3.3. Although this is for a much smaller coating weight (1%) it is comparable to the results of Huang. As with the Adsorba 300C results, the effects of loss of capacity have not been accounted for. However, data in Walker (1974) suggests that such effects are minimal for such small coating weights. Figure 6.3.4 (in Section 6.3) shows the simulation and the data for the above example.

From the preceding it is clear that the polymer coating effects

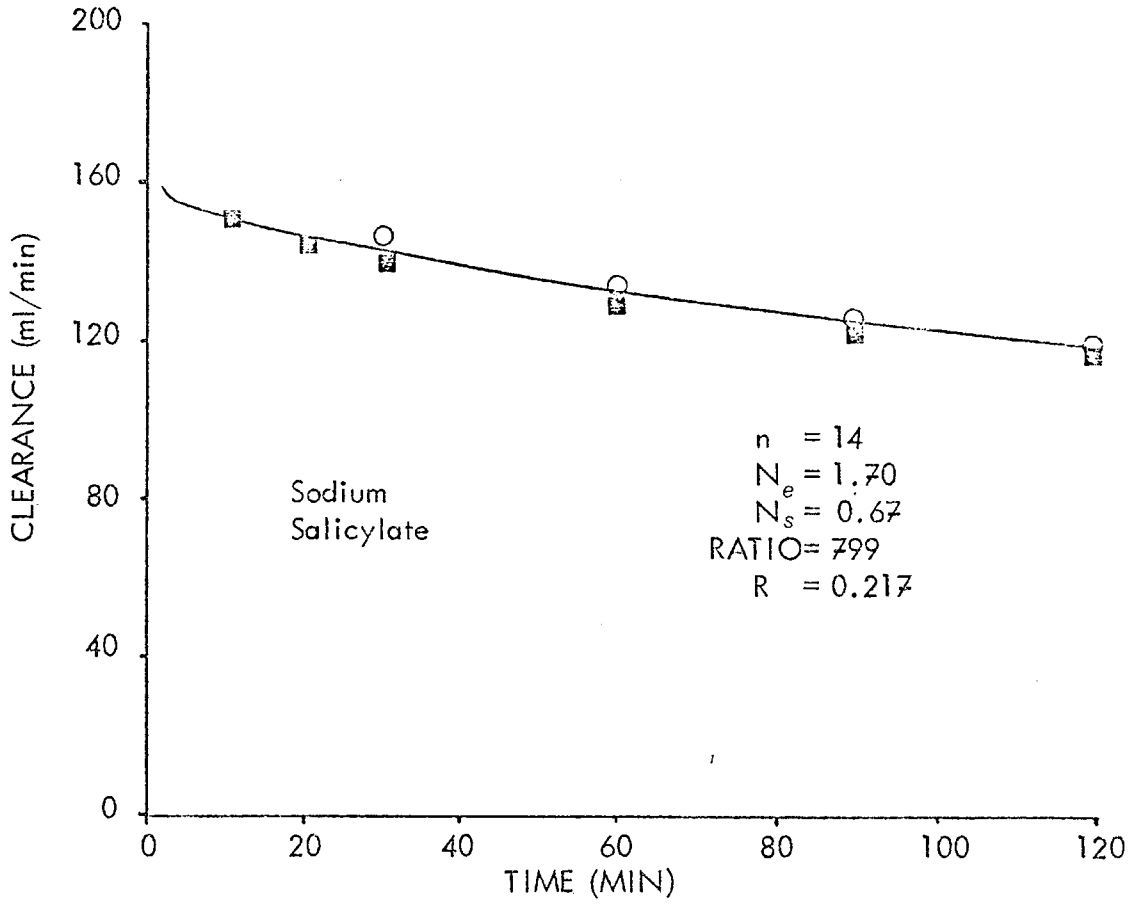

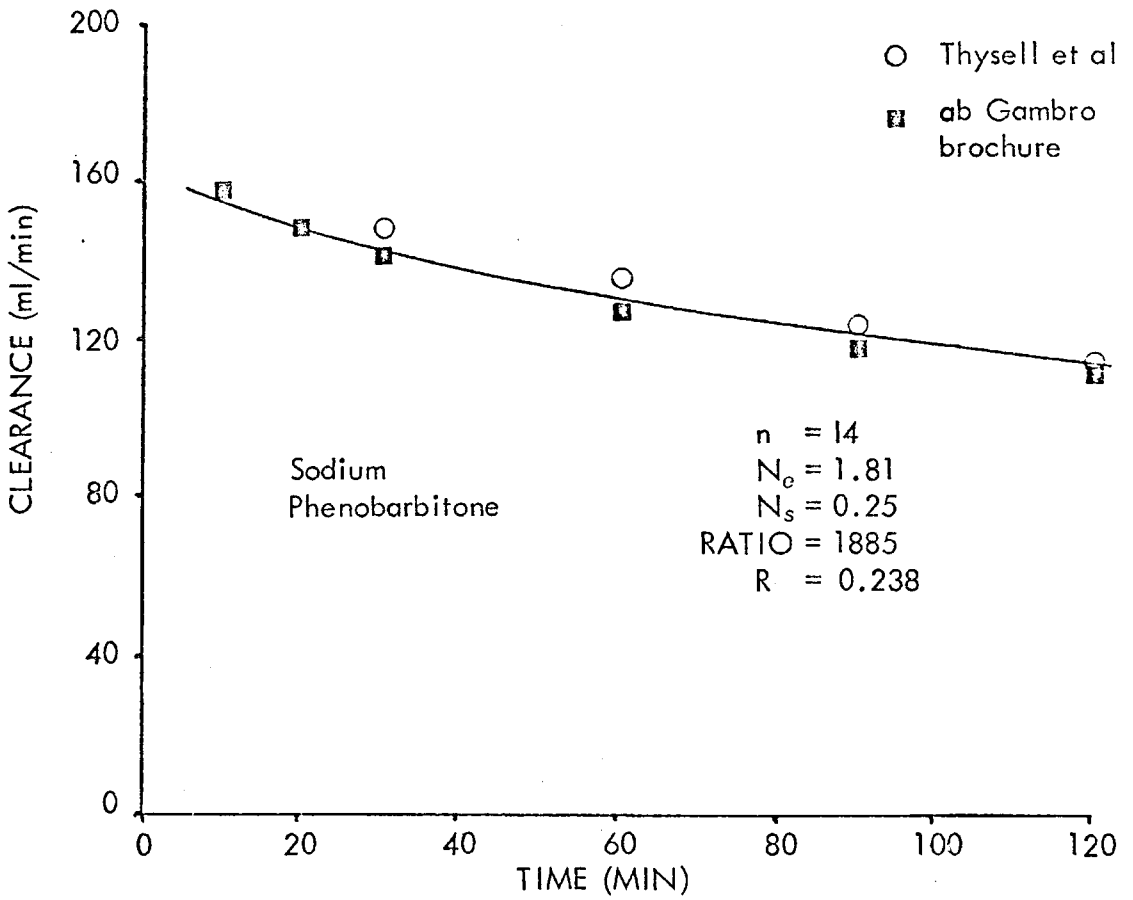

Figure 6.2.7 Single Pass Performance of Adsorba 300C
(Comparison of Data and Simulation)

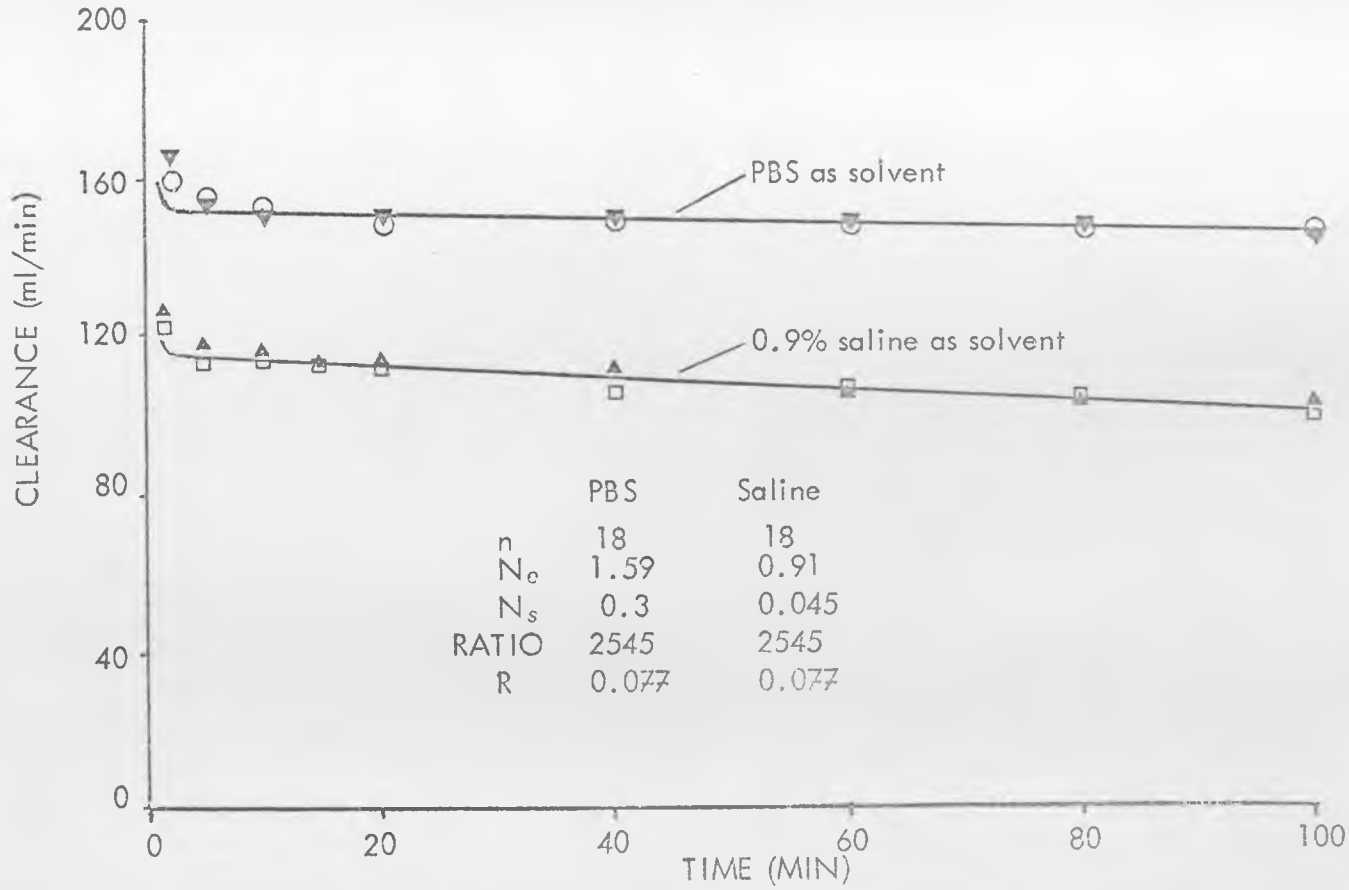

Figure 6.2.8 Effect of Solvent on Initial Breakthrough in Haemocol

the intraparticle diffusivity, presumably by partially filling pores in the particle. Therefore, from the mass transfer viewpoint, not only it the choice of the structure of the sorbent important, but so to is its interaction with the polymer coating. In this regard the possible loss of capacity should also be examined for given carbon/coating combinations.

Another effect relating to the polymer coating occurs in the Haemocol. Single pass clearance experiments were conducted for sodium phenobarbitone using phosphate buffer and isotonic saline as the respective solvents. The experimental details were the same as in Chapter 5. The different solvents caused changes both in the initial breakthrough and in the later kinetics. This implies changes in N_e and N_s . Figure 6.2.8 illustrates this phenomenon. A possible explanation is that the two solvents influenced the degree of swelling of the hydrophilic, Hydrogel membrane used in the Haemocol. This effects not only the membrane resistance but also the intraparticle diffusivity, as per the discussion above.

6.2.4 Effect of isotherm shape (R)

Compared to N_e and N_s the isotherm shape factor, R, has a relatively minor influence on the shape of the clearance curve. Figure 6.2.9 illustrates the extent of the effect of R, over the range of values likely to be encountered in practice. The largest differences occur up to $T = 0.5$ i.e. over the throughput range of importance to all practical perfusion columns. The smaller the value of R, that is the more non-linear the isotherm, the nearer the clearance in a column with a finite intraparticle diffusion resistance approaches the upper limit established by the equivalent haemodialyser. In essence, the more non-linear the isotherm, the longer the initially large concentration differences between the bulk fluid and the surface of the sorbent can be maintained. That is, the influence of the intraparticle diffusivity is effectively delayed.

6.2.5 Effect of sorbent capacity (RATIO)

The capacity effects the clearance in two ways. In terms of the normalized response, RATIO ($= \rho_b q_b / c_o$), defines the ratio between the sorbent

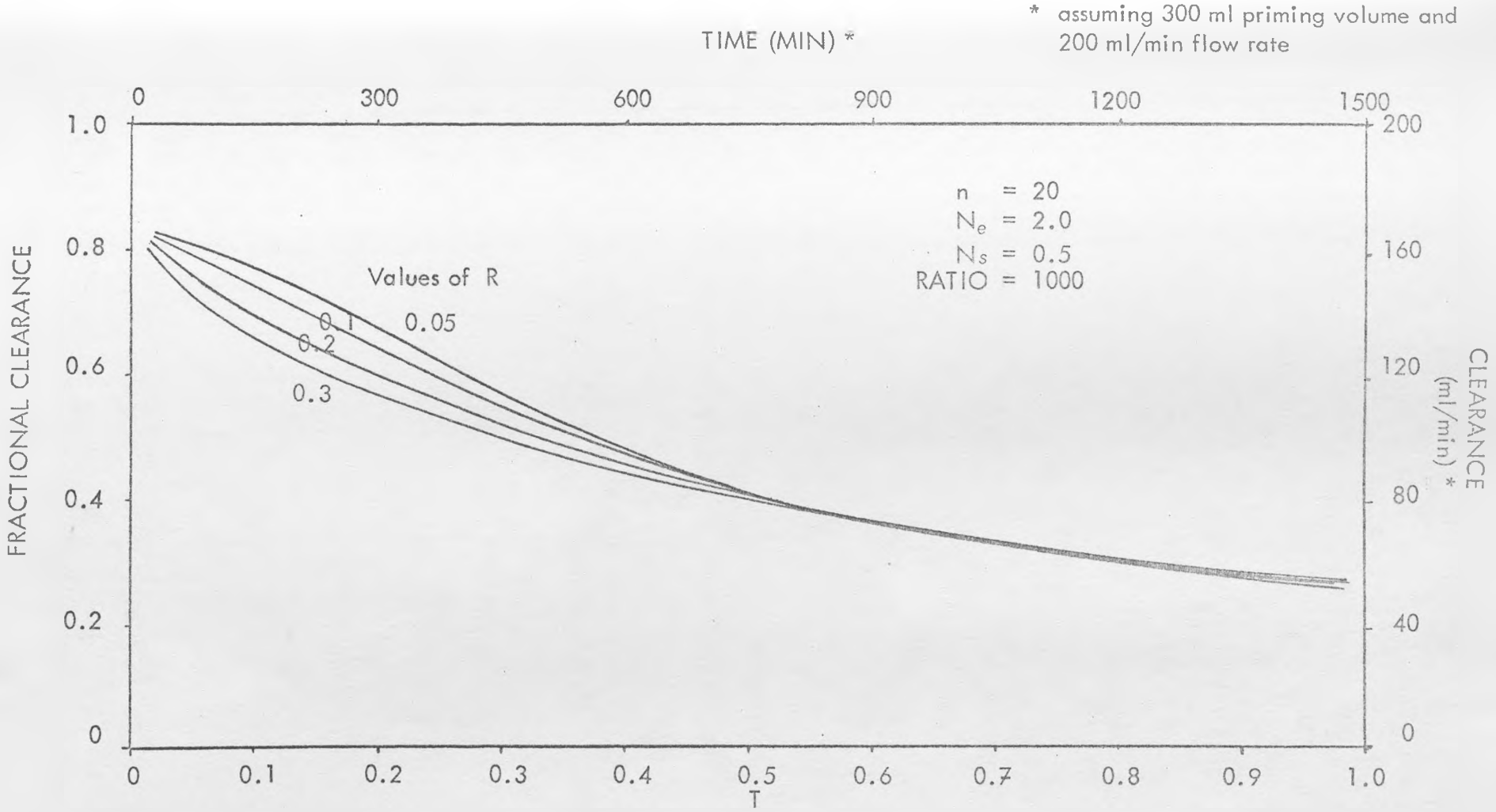

Figure 6.2.9 Effect of R on Single Pass Clearance of a Perfusion Column

capacity of a column and the mean residence time (MRT). It therefore determines at what value of throughput the 'hydrodynamic breakthrough' occurs. This is illustrated in Figure 6.2.10. In practical devices, one MRT is a small fraction of a throughput, i.e. for RATIO = 1000, 1 MRT = 10^{-3} T.

RATIO also converts the throughput capacity into real time. For a given value of T, the larger the value of RATIO, the larger is the corresponding value real time, t. This effect, together with the corresponding influence of RATIO on N_s , was discussed in 6.2.2

6.2.6 Effect of axial dispersion

The axial dispersion coefficient, or in the lumped parameter model, the number of cells, n, effects the shape of the hydrodynamic breakthrough. In particular it changes the apparent breakthrough concentration. This phenomenon was discussed in Chapter 3. The extent of these changes is illustrated in Figure 6.2.11. Here the apparent number of external diffusion mass transfer units, N_e' based on simulations by the external diffusion limited model are compared to the values of N_e predicted by Equation 3.29 in Chapter 3. As expected, the two are in perfect agreement for moderate to large values of n, i.e. a small degree of axial dispersion. However, for small values of n, (i.e. n = 10) the two solutions diverge. This presumably occurs because of differences between the mixing cell model of axial dispersion and the continuous PDE model at large values of axial dispersion. (Levenspiel, 1962).

The extent of the effect of axial dispersion on the initial breakthrough is modified by the presence of intraparticle diffusion resistance. As N_s decreases from a value of infinity in the external diffusion limited model, it causes the slope of the effluent concentration curve immediately after breakthrough to increase. This contravenes an assumption in the analysis which led to Equation 3.29. Therefore, the corrections based on this Equation no longer apply. An estimate of the correction due to axial dispersion in conjunction with intraparticle diffusion was made by measuring the apparent breakthrough concentration and

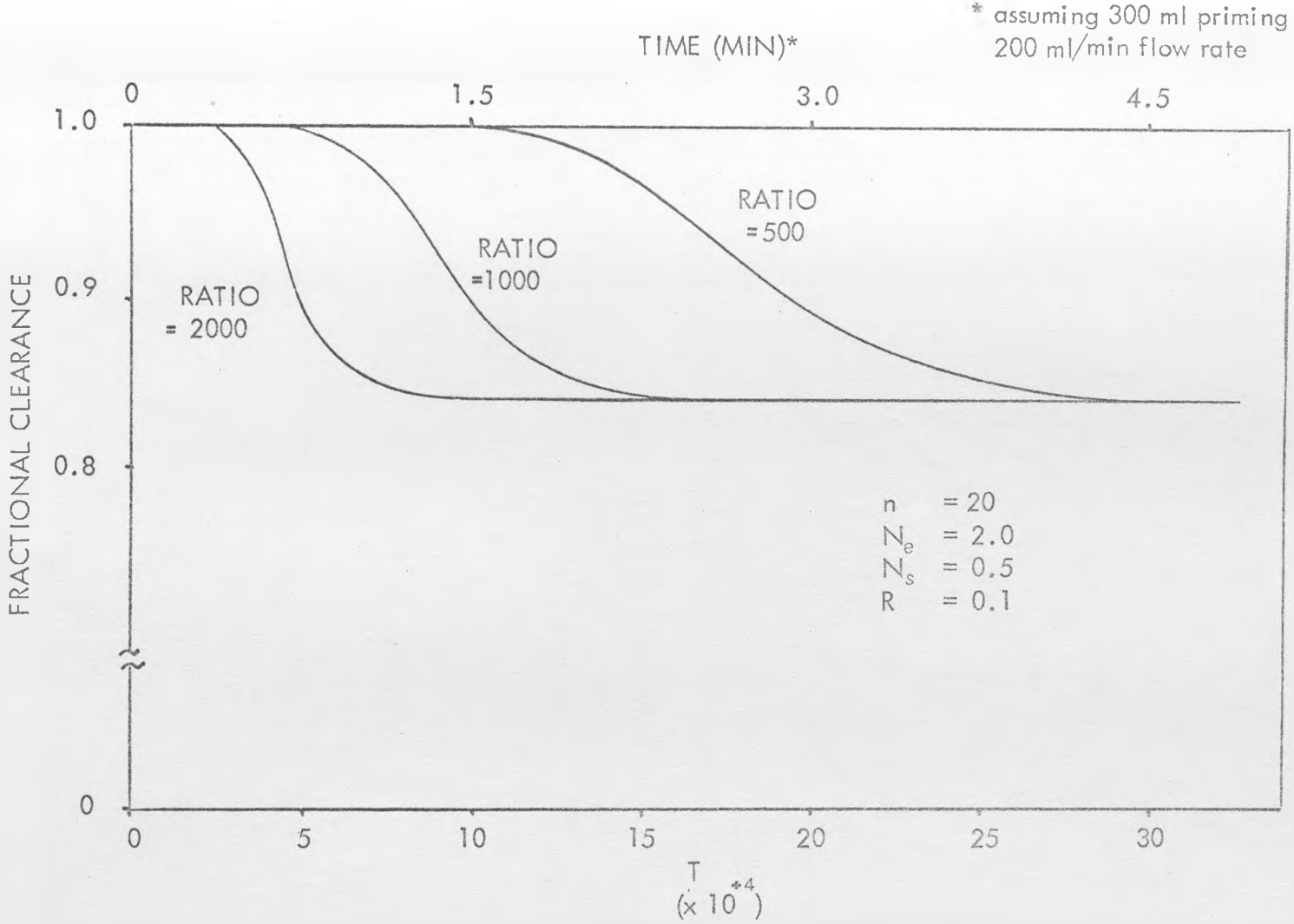

Figure 6.2.10 Effect of RATIO on Hydrodynamic Breakthrough in a Perfusion Column Model

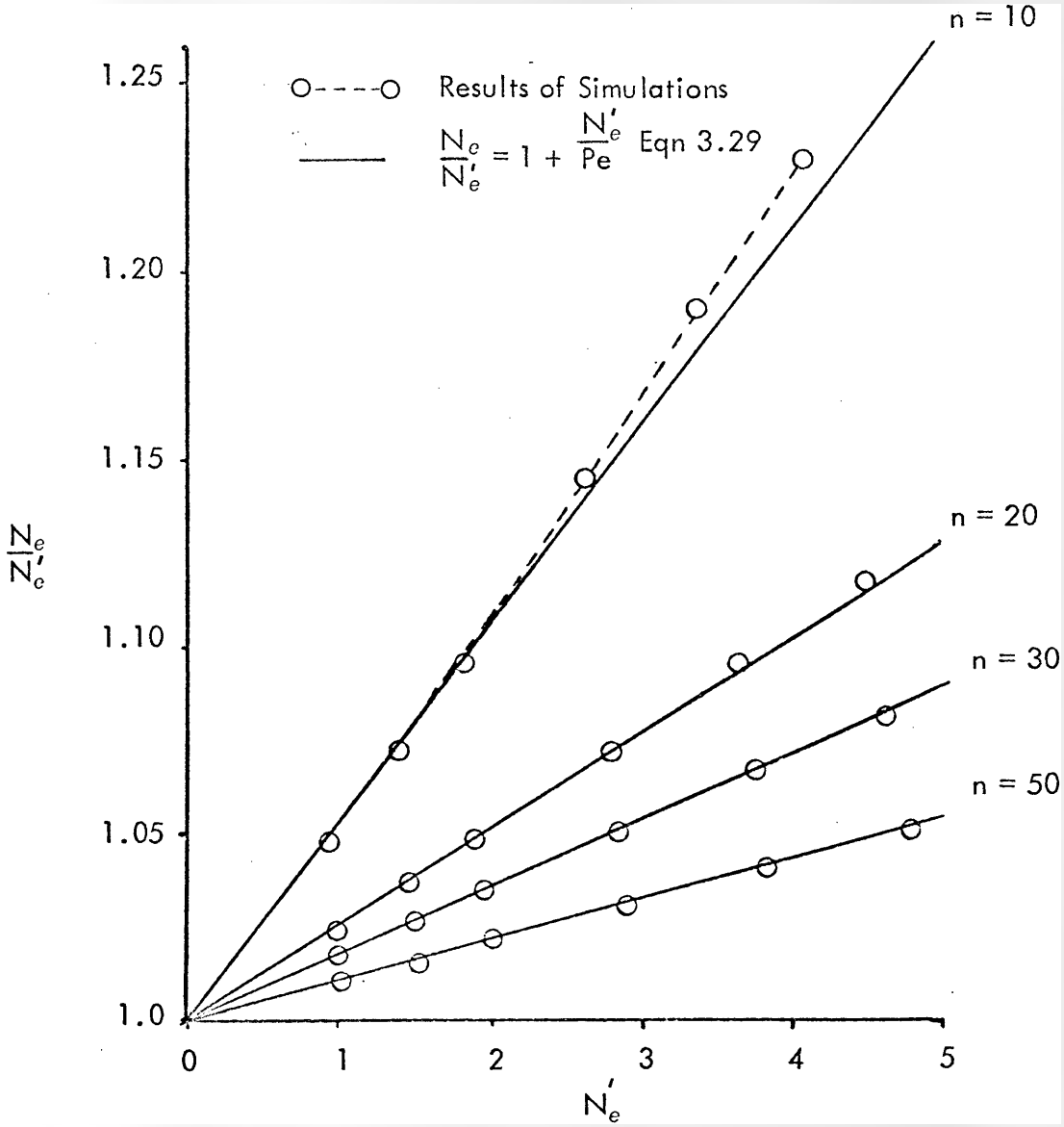

Figure 6.2.11 Influence of Axial Dispersion of Initial Breakthrough - Comparison between External Diffusion Limited Model and Equation 3.29

hence N_e' for various combinations of N_e and N_s . These are illustrated in Figure 6.2.12. Clearly as N_s begins to dominate the mass transfer kinetics, so the influence of N_s on the apparent breakthrough increases.

In practice the changes in N_e' and hence in the initial breakthrough do not affect the overall clearance kinetics. For small N_s , relatively large changes in N_e have little effect on the kinetics. Only the kinetics over the first 5 or 10 mean residence times are influenced by N_e for small N_s . After that time the kinetics for the various values of N_e are virtually identical. The error in X_o and hence the initial section of the kinetics caused by not using the correct value of N_e is less than 5%. Therefore, corrections due to axial dispersion alone (as defined by Equation 3.29) are probably sufficient in most practical instances. However, corrections for N_s must be considered when interpreting experiments of the type outlined in 6.2.1, depending upon the precision required for k_e .

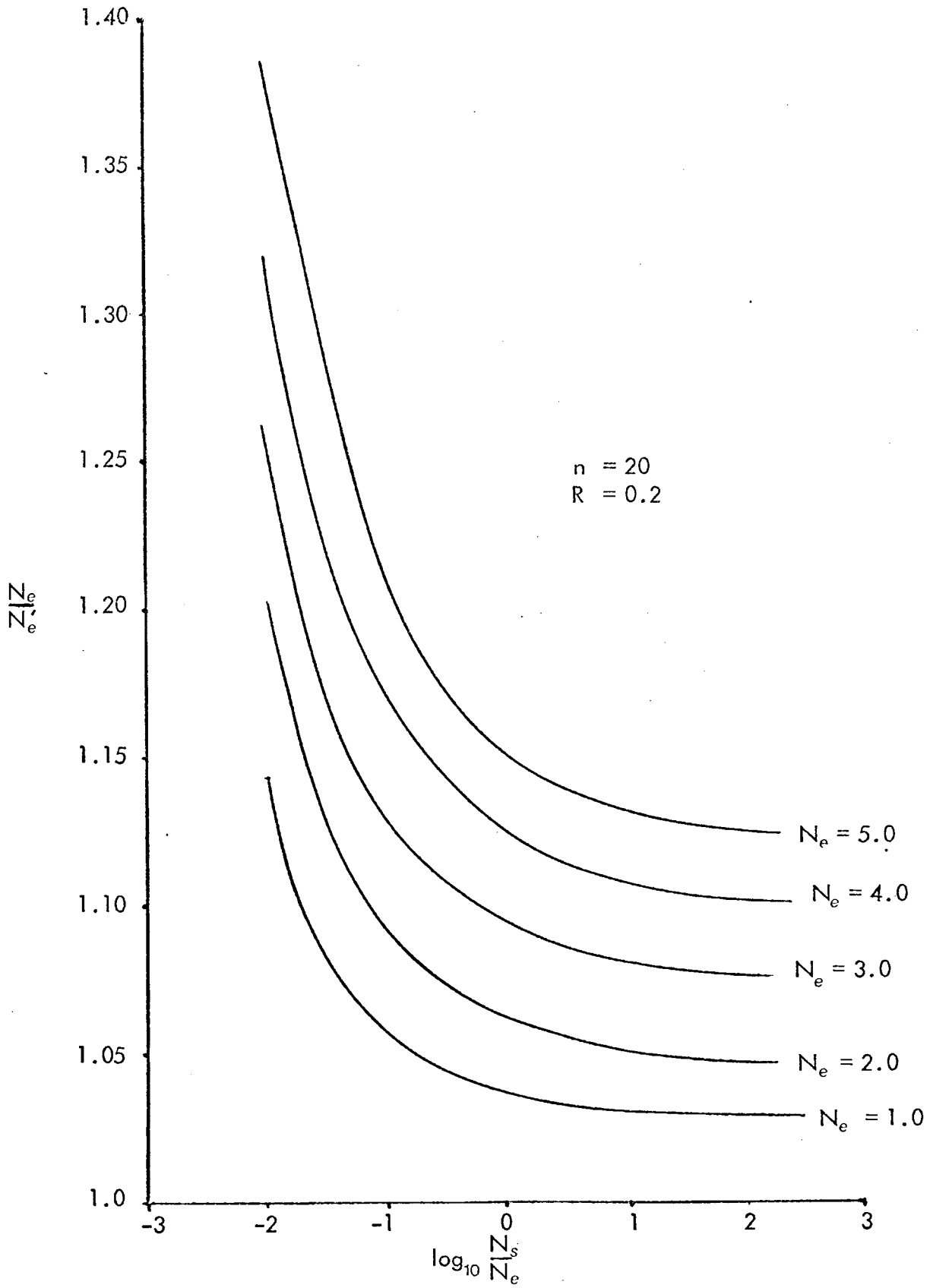

Figure 6.2.12 Influence of Axial Dispersion in Conjunction with N_s on the Apparent Number of External Mass Transfer Units, N

6.3 Recirculation Clearance Characteristics

Although single pass experiments provide a convenient method of observing the effect of the various parameters on column performance, they do not allow for the practical reality that the inlet concentration falls during a clinical perfusion. One way to investigate the effect of a steadily declining inlet concentration is to perform recirculation experiments, i.e. *in vitro* experiments where a well mixed bath of toxin solution simulates a single pool, patient. Such an experiment may not adequately simulate the clinical pharmacokinetics. However, it only introduces one further parameter, the volume of the bath, and it therefore provides a simple method with which to study the above.

From the knowledge gained in Section 6.2, it is possible to predict *apriori*, the effect of a declining inlet concentration. Firstly, the external diffusion, mass transfer and hence the initial breakthrough, is independent of the inlet concentration. Therefore, this feature of the clearance curve is identical to that in the single pass case. However, the number of intraparticle diffusion, mass transfer units (N_s) is proportional to RATIO. As the inlet concentration decreases, the effective value of RATIO increases monotonically to an asymptotic upper limit equal to the initial slope of the isotherm. This increase in RATIO and hence in N_s, causes the clearance curve to become progressively flatter, i.e. to move toward the ideal upper limit established by the external diffusion limited model. This tendency is restrained by the loss of toxin from the recirculation bath. Clearly a steady state equilibrium is reached between the column and the bath. As the bath concentration falls and this equilibrium is approached, the concentration driving force in the particles decreases with a corresponding decrease in the clearance.

Both the initial increase in clearance over the single pass experiments and the later decline as equilibrium is approached, are observed in *in vitro* experiments and in simulations. For the purpose of simulations the equations governing the mass balance in the recirculation bath must be added to the basic model. (Figure 3.7.2), i.e.

$$V_b \frac{d c_o}{d t} = F (c_{out} - c_o) \qquad \text{EQ.6.4}$$

where V_b = volume of bath

c_o = concentration in bath

c_{out} = outlet conc.^{n} from column.

Equation 6.4 is normalized in the usual manner to give

$$\frac{d X_o}{d T} = CAP. (X_{out} - X_o) \qquad \text{EQ.6.5}$$

with $CAP = \frac{M q_o}{V c_o} = \frac{\text{capacity of column at } c_o}{\text{quantity of toxin in recirculation bath}}$

(i.e. c_o at $t = 0$)

In practice, this additional Equation was included in the model used to simulate the single pass experiments with CAP set to zero.

Figure 6.3.1 illustrates the effect of recirculation on the clearance using the perfusion column model. The corresponding single pass clearance (CAP = 0) is included for comparison. The relatively early decline in clearance for larger values of CAP is misleading. For example, although the clearance for CAP=30 declines rapidly for $T > 0.15$, in fact 99% of the equilibrium concentration in the bath is reached before this decline occurs.

Figures6.3.2 and 6.3.4 present the results of three in vitro recirculation experiments. The first two depict the performance of the Haemocol with a 5 litre recirculation bath, with respectively sodium salicylate and sodium phenobarbitone as the toxin. In both cases the value of CAP is quite large, and the clearance does not exceed that of the single pass experiments. Within 50 minutes the bath concentrations are less than 20% of the original values and the clearance is beginning to fall off slowly. It is worth noting the relatively large measurement errors in the clearance values.(See Appendix 4). The correspondence

* assuming 300 ml priming volume and 200 ml/min flow rate

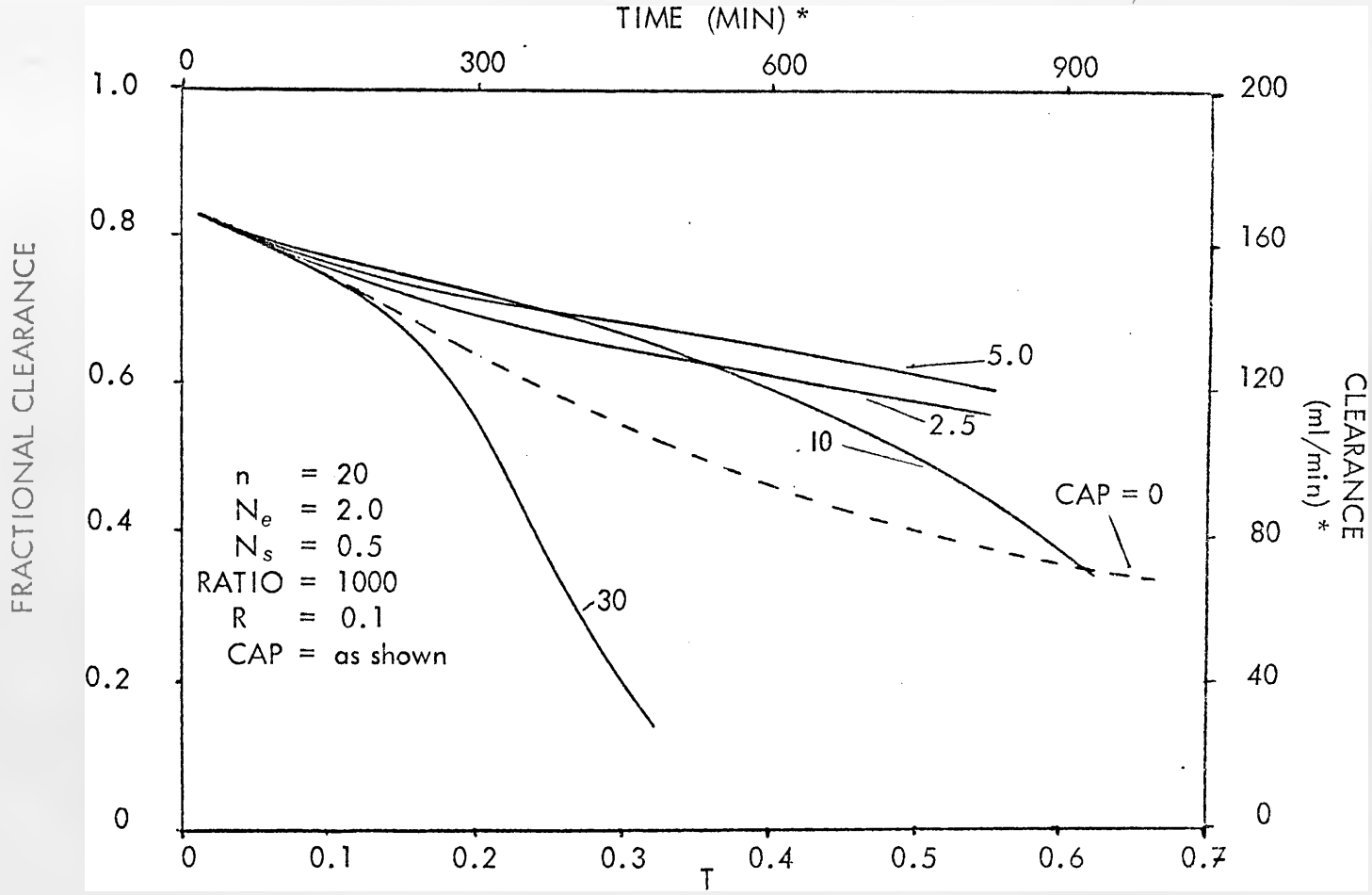

Figure 6.3.1 Effect of Recirculation (CAP) on Clearance in Perfusion Column

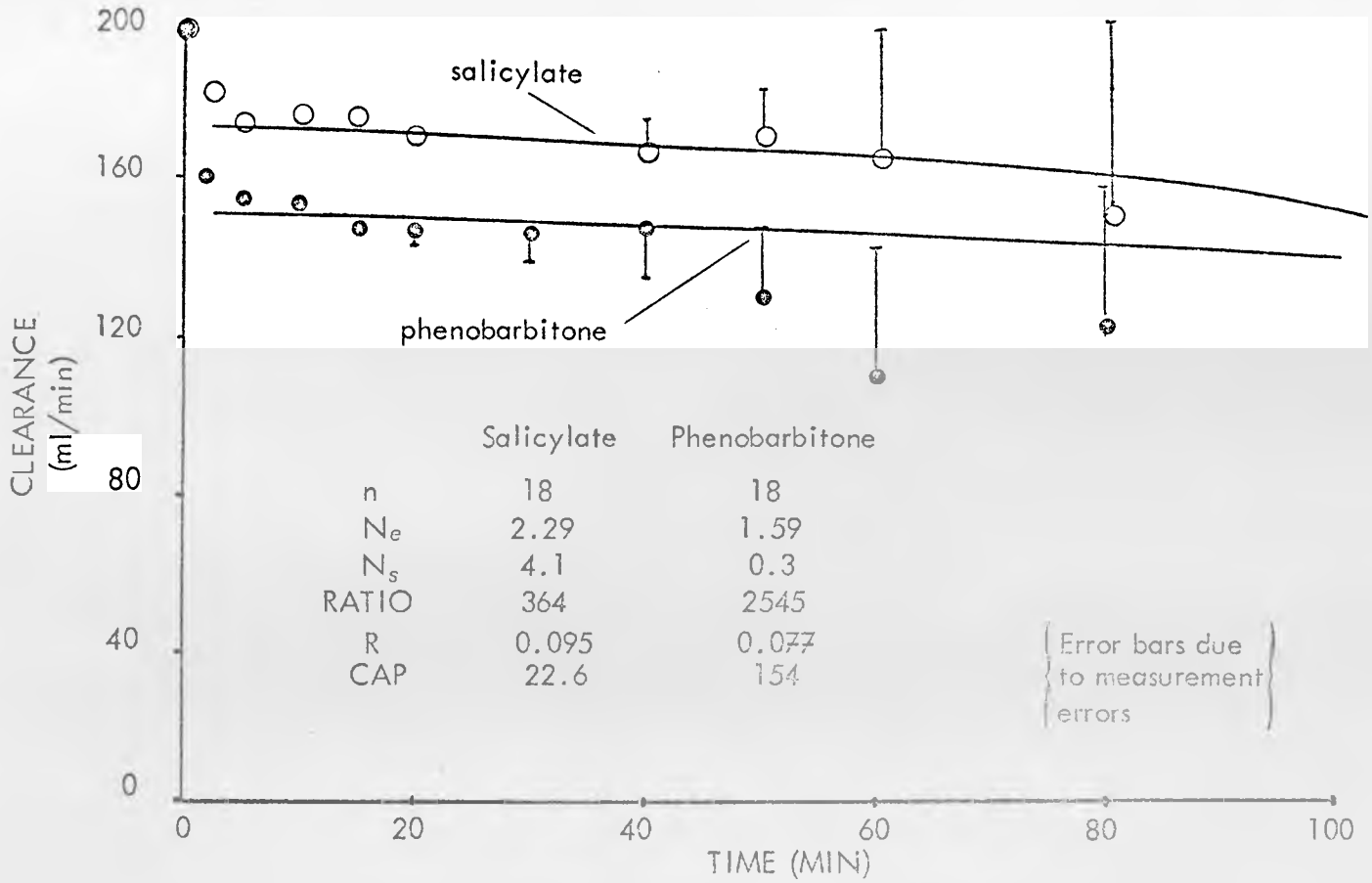

Figure 6.3.2 Recirculation Experiments with Haemocol
Comparison of Clearance Data and Simulations

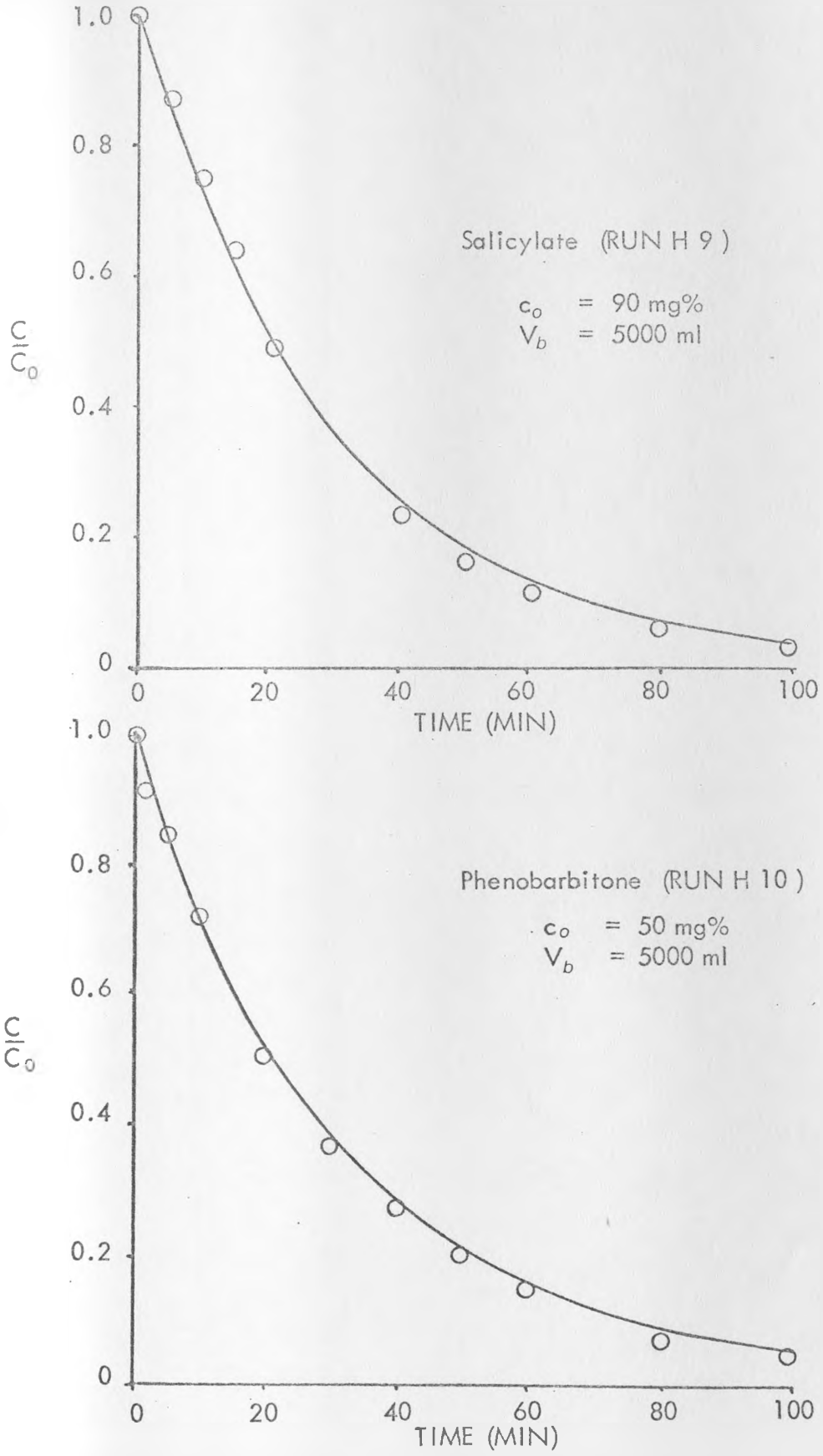

Figure 6.3.3 Fall in Reservoir Concentration in Recirculation Experiments with Haemocol (Comparison of Data and Simulations)

between the simulation and the experimental data for the Haemocols is better illustrated by comparing the concentration kinetics in the bath alone. (Figure 6.3.3). This does not suffer to the same degree from the compound effects of error.

Figure 6.3.4 is based on data from Walker (1974) and Edwards (1975) for a 100 gm column of Norit RBX-1 pellets with a 1% coating of an acrylonitrile copolymer. The values of N_e and N_s were found from the single pass clearance data (Section 6.2). The recirculation experiment was then simulated using these values and the calculated value of CAP. The difference between the clearance curves for the two types of experiment is quite marked. However, it should be remembered that as the inlet concentration is steadily falling in the recirculation experiment, the rates of toxin removal are actually smaller. In a single pass experiment the clearance is proportional to the rate of mass transfer, $\dot{m}$. Therefore, if $\dot{m}$ is calculated throughout the recirculation experiment, this is proportional to an equivalent single pass clearance. The equivalent single pass clearance for the above recirculation data is shown in Figure 6.3.4. As expected, it has the same initial clearance, thereafter the clearance (that is $\dot{m}$) declines much more rapidly than in the single pass experiment. The trend illustrated here applies to all simple recirculation experiments, i.e. the rate of mass transfer $\dot{m}$ is always less than that in a single pass experiment, despite increases in the clearance.

From the clinical viewpoint, however, clearance is the important performance parameter. Therefore, the fact that the clearance is higher (overall) in the recirculation experiment, as compared to the single pass one, is quite significant. The single pass experiment underestimates the clearance that could be expected clinically (assuming that blood can be approximated by aqueous solution). Therefore, in certain instances, (i.e. where CAP has an intermediate value) a recirculation experiment may give a more realistic prediction of clinical performance. This is especially true if blood is used instead of an aqueous blood substitute.

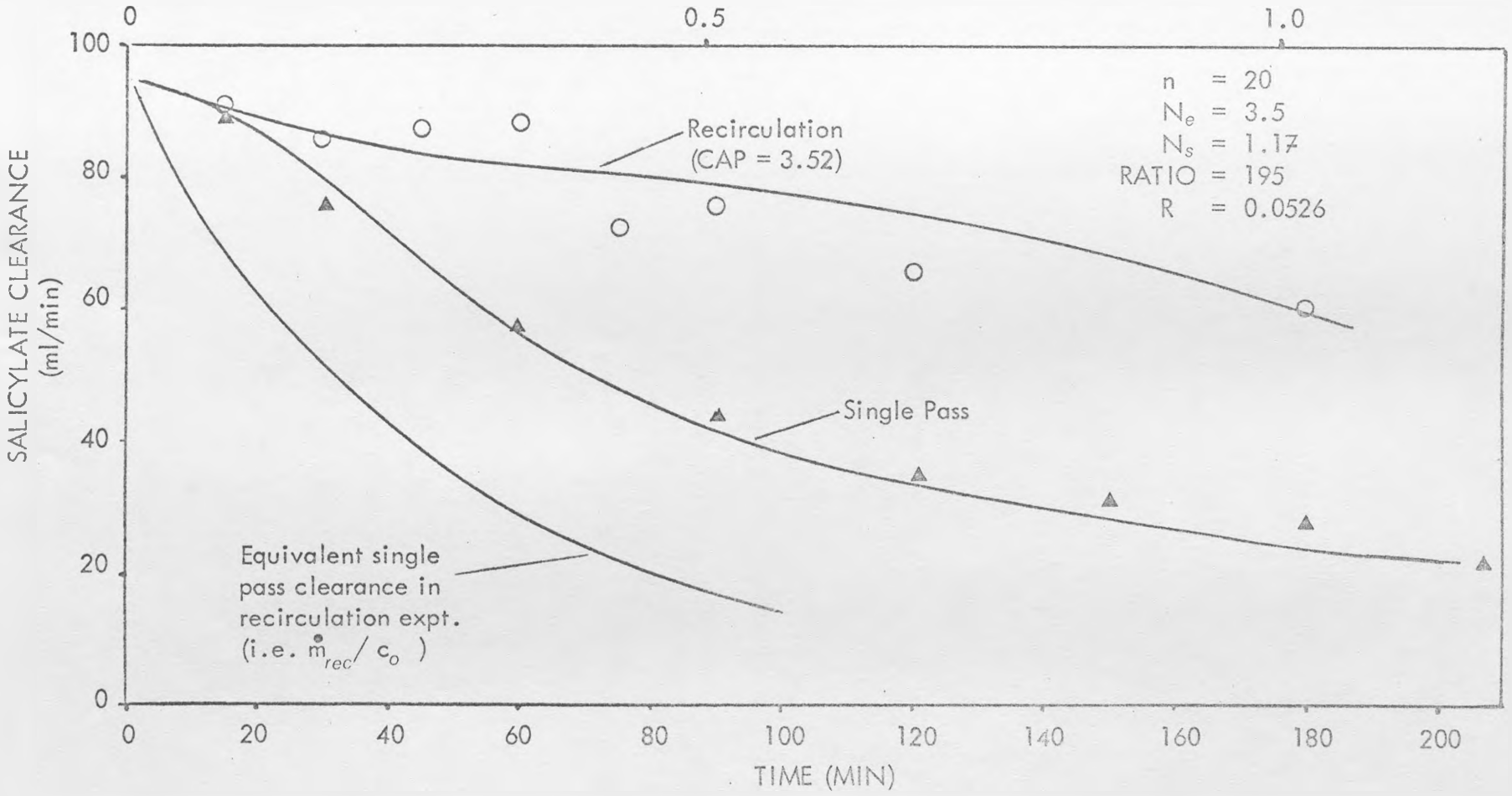

Figure 6.3.4 Comparison of Single Pass and Recirculation Performance of 100 gm Norit RBX-1 filled Column (Data from Walker (1974) and Edwards (1975)

6.4 Influence of Protein Binding

The preceding discussion in this chapter refers to the clearance performance of perfusion columns where the toxin is in simple aqueous solution. As such it is useful for the interpretation and understanding of aqueous, *in vitro* experiments for testing such columns. However, it is clear from Chapter 2 that blood is a heterogeneous fluid in which aqueous solution in the accessible fluid, the plasma, is merely one of several mechanisms for the storage of toxin. The influence of this heterogeneity on perfusion column performance must be taken into account when extrapolating *in vitro* data to clinical applications. With respect to most drugs involved in overdose cases and to many of the suspected toxins in hepatic failure, a crucial factor is the binding of toxin to the plasma proteins. For example, 50% to 70% of the salicylate in the plasma may be bound to protein. It is therefore essential that the influence of protein binding be delineated.

6.4.1 Data on protein binding

Protein binding is described by functional models similar to those used for adsorption isotherms, i.e. Langmuir type equations. Experiments are normally conducted with whole blood or plasma, *in vitro*, although Grib (1973) performed *in vivo* experiments with a special dialysis technique. The binding constants associated with the Langmuir type equations are identified using a Scatchard plot (Chapter 4). It is possible to use this technique to 'peel off' several binding equations from the one set of data i.e. two or more binding equations are needed to fully describe the experimental data. The general form of these equations is

$$c_b = \sum_{i=1}^{n} \frac{n_i K_i c_f}{1 + K_i c_f} \qquad \text{EQ.6.6}$$

where n = no. of binding sites

K_i = association constant (moles/l)

Although Equation 6.6 appears highly non-linear, in practice the values of the constants n_i and K_i are such that the binding is approximately linear. This

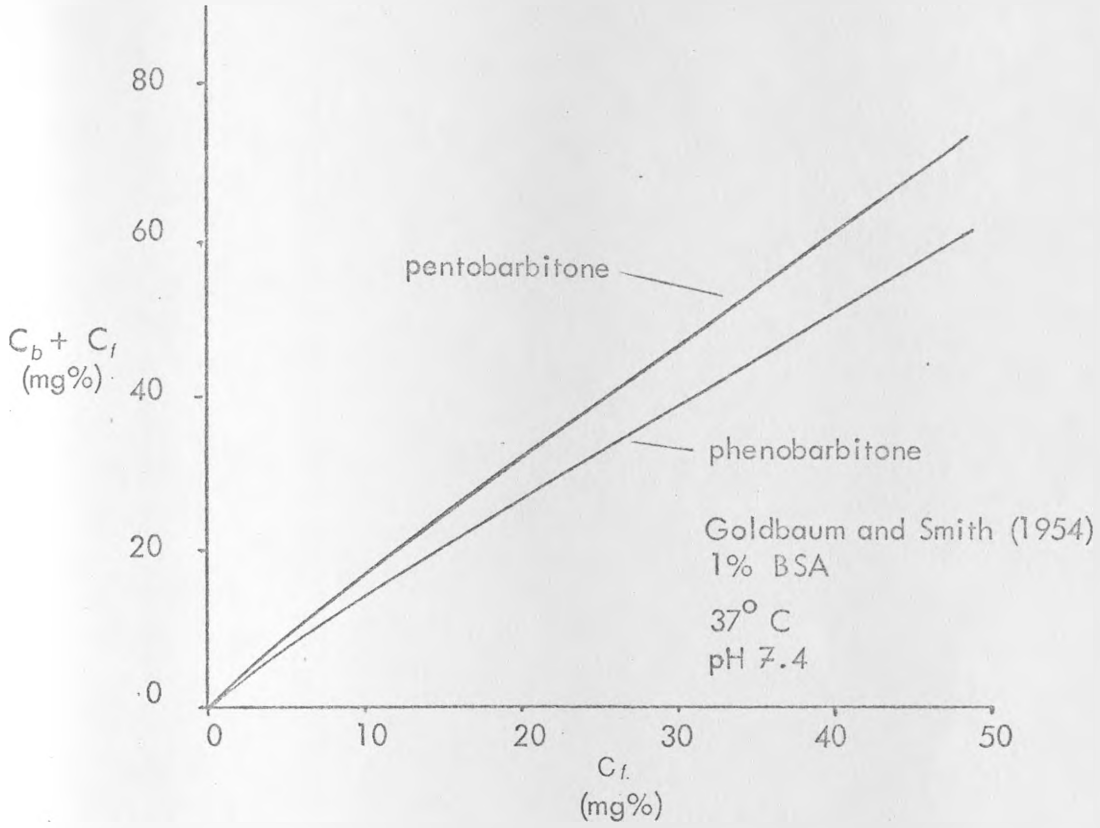

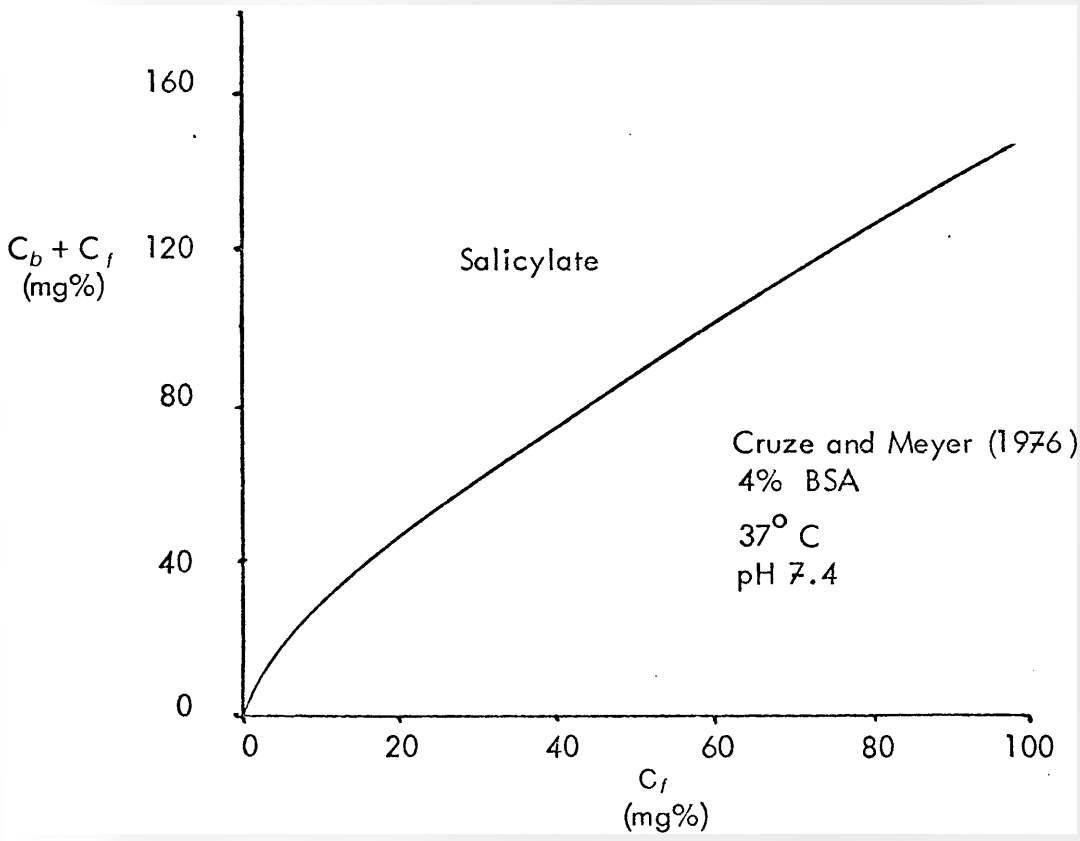

Figure 6.4.1 Protein Binding Data for Phenobarbitone, Pentobarbitane and Salicylate

is illustrated in Figure 6.4.1 by the respective binding curves for phenobarbitone, pentobarbitone and salicylate.

These curves perhaps give an oversimplified view of protein binding data. Firstly the data in the literature, relevant to the toxins of interest in this thesis, is very sparse. Although some studies have produced sufficient data to estimate the coefficients in the binding equation, most consist of only a few isolated binding values. (Meyer and Guttman, 1968 and Vallner, 1977). For example, with barbiturate binding the most significant paper remains that of Goldbaum and Smith (1954) with relatively little work having been done since. However, Goldbaum and Smith used 1% bovine serum albumin (BSA), so the applicability of this data to clinical practice is very questionable. The form of the results is probably similar although the absolute values will be different.

Secondly, there are large variations between values in different papers. This is due partly to the different experimental techniques used and partly to differences in experimental conditions (i.e. type of albumin, pH, temperature). The possible presence of free fatty acids provides a source of uncontrolled variability between different studies. Natural variations between different samples of plasma or albumin solution also contribute to the scatter of data, although these effects are probably secondary compared to those listed above.

Within the limitations of the existing data in the literature it is reasonable to assume that at least some examples of protein binding in the plasma are approximately linear, over the range of concentrations of interest.

6.4.2 Effect of linear protein binding

The influence of linear protein binding on the single pass clearance was investigated using a modified form of the perfusion column model. The equations in Figure 3.7.2 apply to the case of linear protein binding if the values of the normalized parameters N_e, N_s, R and RATIO are modified. The binding is defined by the following equality.

$$c_t \equiv \Delta_1 \; c_f$$

where c_t = total toxin conc.$\frac{n}{-}$ per unit blood vol.

c_f = free (unbound) conc.$\frac{n}{-}$ per unit water vol.

Δ_1 = true binding coefficient.

The binding is introduced into the basic, aqueous column model on the assumption that the total inlet concentration remains constant at c_o, independent of Δ_1. On this basis the expressions for the normalized parameters are,

$$R \equiv 1/(1 + (1/R_o - 1)/\Delta_1))$$
$$N_e \equiv N_{e_o} / \Delta_1$$
$$N_s \equiv N_{s_o} \times R/\Delta_1$$
$$RATIO \equiv RATIO_o \times R / \Delta_1$$
$$T \equiv T_o \times \Delta_1 / R$$

where R ; N_{e_o} ; N_{s_o} ; $RATIO_o$; T_o refer to the respective values of the parameters R, N_e, N_s and T when $\Delta_1 = 1$ (i.e. no binding) and an inlet concentration of c_o. The deviation of these formulae is in Appendix 7.

Therefore, linear binding causes the effective value of N_e to decrease and hence the breakthrough clearance to be smaller than that in the case of no binding, i.e. for no axial dispersion

$$C l_{bt} = Q_b \; (1 - \exp(-\frac{N_e}{\Delta_1})) \qquad \text{EQ.6.7}$$

where bt refers to breakthrough.

Equation 6.7 can be derived from the distributed model of a perfusion column in Appendix 2 as per Equations 3.28 and 3.29, using the previous equality to define the total concentration. Alternatively, Equation 6.7 can be derived from

the equivalent haemodialyser formulae for linear binding in the blood. Therefore, the equivalent haemodialyser also describes the initial breakthrough for the case of linear protein binding.

Linear binding causes the effective number of intraparticle diffusion, mass transfer units, N_s, to decrease and the slope factor of the isotherm to increase. Both these effects make the decline in clearance relatively faster.

The net effect of Δ_1 on the clearance in the standard perfusion column is illustrated in Figure 6.4.2. The abscissa is real time, t, not through--put capacity, $\bar{T}$, as in the simulations in the previous sections. In those simulations the value of RATIO was in each instance, constant. Therefore, t was a constant multiple of $\bar{T}$. With linear binding however, the value of RATIO varies with Δ_1. That is, for each value of Δ_1, $\bar{T}$ is a different multiple of t. It was, therefore, convenient to assume a particular size of column (V_p = 300ml) and convert all $\bar{T}$ values into real time.

In addition, to linear protein binding the results in Figure 6.4.1 assume that only a fraction of the total blood volume is aqueous solution i.e. account is taken of the volume of the protein and the volume of formed elements in the blood. Assuming that the fraction of the blood that is water is μ and that the binding coefficient is ρ, then

$$\Delta_1 = \mu (1 + \rho)$$

where $c_b = \rho c_f$ and $c_t = (1 + \rho) c_f$

with c_b = bound conc. per unit total blood volume

c_t = total conc. per unit total blood volume

c_f = free conc. per unit total blood volume

and $c_{f,true} = \frac{c_f}{\mu}$ = true free conc. (per unit water vol.)

In Figure 6.4.2, $\mu = 0.8$ and the values of the 'percentage bound' equal $100 / (1 + \rho)$. Hence for 50% bound the value of Δ_1 is 1.6 and not 2.0 as would be the case for $\mu = 1.0$. For values μ other than 0.8, the

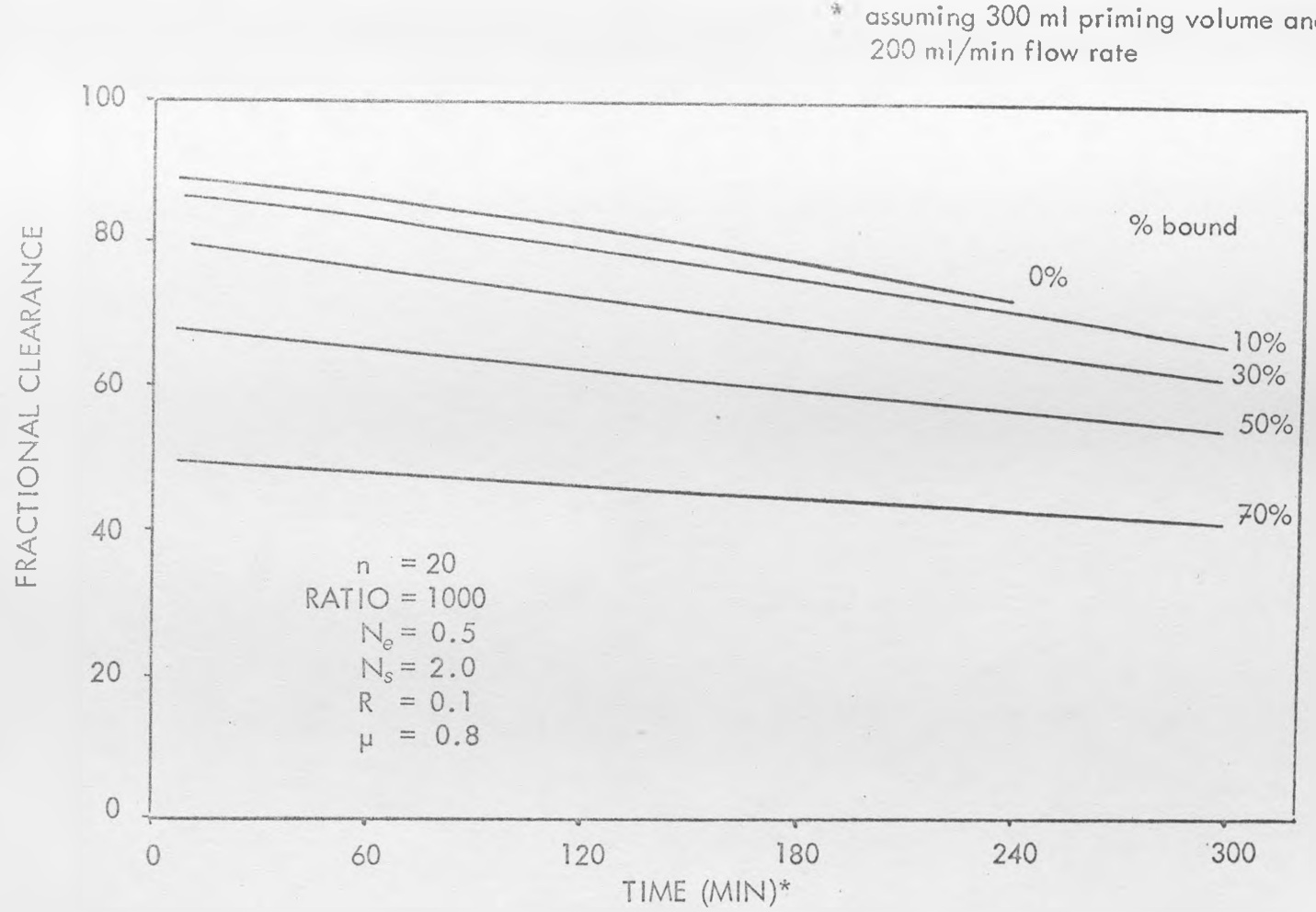

Figure 6.4.2 Effect of Protein Binding on the Single Pass Clearance in a Perfusion Column

value of the percentage bound can be altered accordingly.

The crucial feature of Figure 6.4.2 and Equation 6.7 is that as with sorption from aqueous solution, the clearance of a (linearly) protein bound toxin by a perfusion column is dependent primarily on dialytic mass transfer and not on any property of the sorbent. That is, the initial clearance is defined by performance of the equivalent haemodialyser. Sorption properties such as the intraparticle diffusivity or the isotherm shape, R, merely control how closely the perfusion column performance approaches that of the equivalent dialyser. As with the aqueous solution case, the performance of the equivalent dialyser is superior to that of most commerical haemodialysers because of reduced external diffusion resistance, in particular a reduced membrane resistance.

6.5 Effect of Cellular Distribution

The other major factor contributing to the heterogeneity of blood, is the cellular distribution of solutes. A large fraction of the blood volume is contained within the cells and other formed elements. On average, 40% of the blood volume in man is taken up by red cells, i.e. a haematocrit of 40%. In uraemic patients it falls to 20% to 25%. Since all blood detoxification devices only have direct access to toxins in simple aqueous solution outwith the cells, the distribution of toxin in the cells is very important. The key factor is the rate of transport of toxin between the intracellular and extracellular fluids. For the purposes of this thesis the two extreme cases are considered.

In the first, the toxin is assumed to be rapidly equilibrated across the cell membrane, with a partition coefficient of 1. Hence the blood acts as an aqueous solution with volume equal to the total water volume of the blood. Protein binding may be included as discussed in Section 6.4. The water volume of the blood is only 75% to 80% of the total volume, the rest being taken up with proteins, cellular membranes, etc. This first model is in fact that which was used in Section 6.4 where $\Delta_1 = \mu (1 + \rho)$. Note that with zero protein binding the fractional clearance is higher than that for a simple aqueous solution. (Compare Figures 6.4.2 and 6.2.4). This is because the effective aqueous flow rate in blood is lower due to the blood volume taken up by cellular membranes, proteins etc. Conversely, the absolute clearance is smaller because the decrease in the effective flow rate is larger than the increase in the fractional clearance. This effect applies equally to haemodialysers.

At the other extreme, it may be assumed that equilibration across the cellular membrane is much slower than the transit time through the column. Therefore, toxin in the cells does not enter the plasma during a single transit. However, intracellular and extracellular toxin are assumed to equilibrate as the cells circulate through the body before re-entering the column. This is equivalent to separating the cells from the plasma through the column and re-uniting the cells and plasma at the outlet. Under these conditions the flow rate F is effectively reduced, although all other parameters retain the same

values. The effect on performance is the same as that in the case of rapid equilibration, except that the magnitude of the changes are greater. The effective flow rate decreases as does the absolute initial clearance. The change in F increases N_s and t (for a given T). Therefore, although the initial clearance falls, the rate of decline in clearance thereafter is less than that for perfusion with a simple aqueous solution.

6.6 Effect of Computational Parameters

The effect of changes in various computational parameters on the simulations of the perfusion column model was investigated.

6.6.1 Choice of integration routine

CSMP offers seven integration routines; rectangular, Adams-second order, trapezoidal, Simpsons' Rule and fourth order Runge Kutta (all fixed step) plus two variable step routines, a fourth order Runge Kutta and a fifth order Milne. Fixed step routines were adopted for the column model as the variable step methods often caused instabilities. These may have been partly due to the IMPLICIT LOOPS. In most cases Simpsons' Rule was used. This was selected as a compromise between complexity (cost) and accuracy.

6.6.2 Effect of integration step size

The effect of changing the integration step size (Δ_t) was tested using the standard set of parameters. Provided the step size was sufficiently small a stable solution was achieved. Decreasing the step size (by up to 2 decades) below the stable limit did not significantly alter the clearance values in the simulation. A stable solution is generally achieved for $\Delta_t < 1/(20 \times \text{RATIO})$, i.e. for RATIO $= 1000$, $\Delta_t = 5 \times 10$.

6.6.3 Effect of Y_{oo} and error

Y_{oo} is the parameter introduced into the quadratic driving force equation (Equation 3.5.1), to avoid division by zero at $t = o$. Effects due to changes in its value are closely related to changes in ERROR, the error criterion in the IMPLICIT LOOP. To ensure stability, Y_{oo} should be at least ten times greater than ERROR. If Y_{oo} is decreased from 10^{-3} to 10^{-6}, with ERROR equal to 10^{-7} then the maximum change in the fractional clearance, with the standard set of parameter values, is less than 0.001. There was no evidence of there being more than one stable solution for a given set of parameter values.

6.7 Summary

It is pointless to summarize in detail every facet of column performance introduced in this Chapter. However, there is one overriding feature which should be re-iterated here, i.e. a haemoperfusion column is merely a specialized type of haemodialyser. The primary mass transfer mechanism is dialytic and not sorptive. This applies equally to perfusions where either protein binding or cellular distribution are factors, as to those with a purely aqueous 'blood' solution. In all cases the basic performance is established by the equivalent haemodialyser i.e. a dialyser with the same number of external mass transfer units as the perfusion column under consideration.

The sorptive properties only make a minor contribution to the clearance of the equivalent dialyser, in that they maintain the dialysate side concentration at zero. This is equivalent to making the dialysate flow rate infinite. For an equivalent counter flow dialyser the increase in the clearance is less than 10% for all values of N_e.

The principal reason for the higher clearance in most haemoperfusion columns as compared to haemodialysers, is the larger number of external mass transfer units, i.e. N_e. This appears to be due primarily to the smaller combined blood film and membrane resistances in perfusion columns. Further work is required to delineate the exact contributions of the two mass transfer resistances (and possibly the external area) to this improvement in performance.

CHAPTER 7

MASS TRANSFER IN DIALYSATE AND ULTRAFILTRATE PERFUSION DEVICES

CHAPTER 7

MASS TRANSFER IN DIALYSATE AND ULTRAFILTRATE PERFUSION DEVICES

7.1 Introduction

Various dialysate and ultrafiltrate perfusion devices were introduced in Chapter 1. Although only a few of these are either commercially available or have received widespread application, current interest in several of the devices makes it appropriate that their performance be discussed here. The recent papers by Merino et al. (1977) and Denti et al (1977), and to a lesser extent that by Malchesky et al. (1977) illustrate the empirical nature of the design of such devices (in common with all perfusion devices). Sorbents such as activated carbon are often treated as 'black magic' and devices are designed and evaluated with little apparent understanding of the contribution of the sorbent to the overall mass transfer performance. These comments are especially applicable to the paper by Merino and co-workers. In many instances authors seem to be interested more in developing a "novel device or technique" than in applying mass transfer principles to the problem of the efficient use of sorbents in extracorporeal detoxification. The reverse is true of this chapter. Although some of the results may appear trivial, the literature reveals that even the trivial is often overlooked or misunderstood, and therefore needs restating.

The various discussions assume the ideal performance of the haemodialyser or ultrafilter. For instance the dialysance of a dialyser is, in theory, constant with time. In practice, however, the dialysance gradually decreases due to membrane creep effects which alter the flow geometry and to deposition of proteins and formed elements on the membrane. In the case of hollow fibre dialysers, plugging of the fibres by thrombus formation further reduces the dialysance. Likewise, ultrafilters are essentially constant clearance devices. However, protein and cellular deposition cause a steady reduction in performance (Quellhorst, 1977).

7.2 Dialysate Perfusion Devices

The dialysate perfusion devices that require most attention are those where the sorbent is placed in the dialysate compartment of the dialyser, i.e. sorbent augmented dialysate and integral sorbent/dialysis membranes. The role of the sorbent in these applications has not been clearly stated. Conversely, the basic role of dialysate regeneration cartridges is well understood, although detailed analyses of this type of device do not appear in the literature. Accordingly, these devices are only discussed briefly.

7.2.1 Dialysate regeneration

The contribution of dialysate regeneration to haemodialysis is the reduction of dialysate volume from several hundred litres to just a few litres. Provided the effluent concentration from the regeneration cartridge is zero and the haemodialyser operates in a single pass, dialysate mode, the clearance will equal the dialysance i.e. the clearance is at its maximum value. The basic performance of the dialyser is not improved by the regeneration cartridge. In fact, poor design of the cartridge will cause the clearance to decline. The REDY cartridge maintains very low concentrations in the dialysate, thereby maintaining a near maximum clearance value. (Gordon et al., 1969). Comparable data is not available on other regeneration systems.

Dialysate regeneration cartridges can be designed with the aid of the constant pattern, breakthrough curves in Fleck et al. (1973) and Hall et al. (1966). Small scale single pass experiments together with sorption isotherm studies establish the basic mass transfer properties. Scale up or design changes can then be made on the basis of these and the above theoretical results. It is assumed that the pilot studies are conducted with a constant inlet concentration equal to the initial steady state dialysate concentration. As the concentration in the patient declines, so the outlet dialysate concentration declines (for constant dialysance). Therefore, the throughput capacity, T , and hence the volume of dialysate required to cause breakthrough increases with time. Hence the design based on the initial c_{d_o} is conservative.

$$c_{d_o}\Big|_{t=0} = \frac{DI}{Q_d}(c_{b_i} - c_{d_i}) + c_{d_i} = \frac{CI}{Q_d} \times c_{b_i} \text{ for } c_{d_i} = 0 \qquad \text{EQ. 7.1}$$

7.2.2 Sorbent augmented dialysate

The use of sorbent slurries and lipids in place of conventional dialysate is known to improve the performance of a haemodialyser although the reasons for this improvement have not been stated concisely in the literature. In essence, the slurry or lipid alters the concentration profiles on the dialysate side of the membrane. Ideally, it causes the dialysate concentration to be zero along the entire length of the dialyser, thereby increasing the concentration gradients across the membrane and hence the mass transfer. The effects of dialysate slurries or lipid-based dialysates can be investigated by examination of the formulae for haemodialyser dialysance.

The formulae in Figure 2.2.1 (Chapter 2) describe the performance for single pass, dialysate flow and no protein binding in the blood. Farrell (1972) included linear protein binding for the case of a counter-current haemodialyser, i,e,

$$DI = Q_b \left[\frac{e^{\frac{N_o}{\Delta_1}(1 - \Delta_1 \not{Z})} - 1}{e^{\frac{N_o}{\Delta_1}(1 - \Delta_1 \not{Z})} - \Delta_1 \not{Z}} \right] \qquad \text{EQ. 7.2}$$

where $N_o = k_o A / Q$

$\Delta_1 = \mu (1 + \rho)$

$\not{Z} = Q_b / Q_d$

ρ = linear, binding coefficient

This expression can be extended further to cover the general case of finite blood and dialysate pools with linear binding in the blood and in the dialysate. In the case of a lipid dialysate the partition coefficient takes the place of the binding coefficient in the dialysate side. As the dialysate concentrations are usually small, the assumption of a linear isotherm for the

dialysate sorbent is a reasonable one.

Figure 7.2.1 presents these general formulae for counter current and well mixed dialysate, dialysers. These formulae assume a quasi-steady state operating condition, i.e. transients caused by changes in the inlet blood and dialysate concentrations are negligible.

The effect of the sorbent or the lipid on the dialysate side is demonstrated by examining the formulae as Δ is made very small (i.e. Δ is very large). In both instances

$$\underset{\Delta \to 0}{CI} = \underset{\Delta \to 0}{DI} = Q_b (1 - e^{-N_o}) \qquad \text{EQ. 7.4}$$

This is equivalent to having an infinite dialysate flow ($\mathcal{Z} = 0$) in the case with no sorbent or lipid on the dialysate side. This effect is illustrated in Figure 7.2.2 for single pass, dialysate flow. Clearly the largest improvement occurs in dialysers with a well-mixed, dialysate compartment (i.e. coil dialysers) especially for large values of N_o. It should be noted that in both types of dialyser when N_o is small (i.e. fractional clearances are less than about 0.4) the percentage improvement in performance is negligible. Thus if the clearance is small with single pass, aqueous dialysate, then little improvement should be expected on the basis of the equivalent, infinite dialysate flow rate alone. However, if a finite volume of dialysate is being recirculated through the dialyser, then naturally an improvement occurs due to the effective increase in dialysate volume resulting from the inclusion of the sorbent or lipid.

In addition to modifying the mode of operation of a dialyser, sorbents in the dialysate may affect the basic mass transfer properties of the dialyser. Slurries of activated carbon may increase local mixing on the dialysate side and therefore decrease the dialysate side, film resistance. Conversely a viscous lipid-based dialysate will increase the dialysate resistance in comparison to the aqueous dialysate. However, if the membrane is partly lipophilic, and lipid is

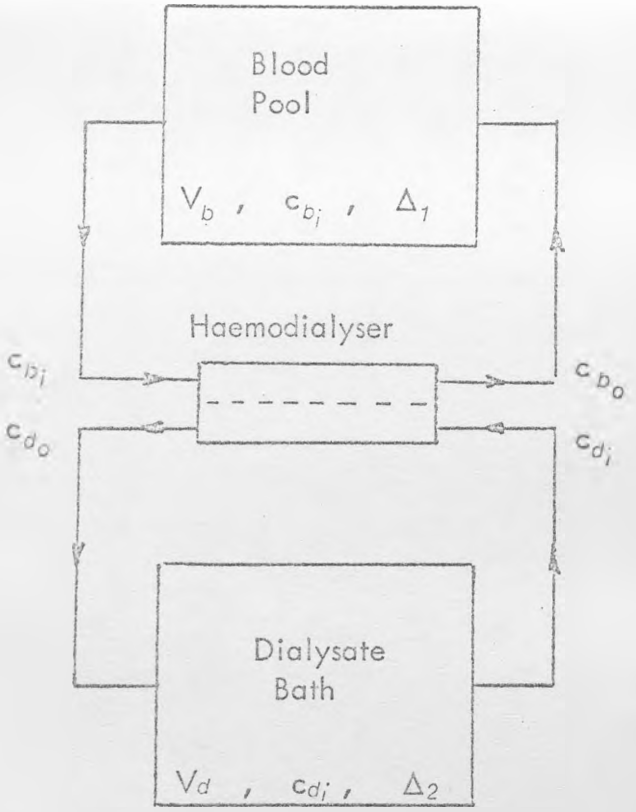

$$\text{Clearance} = \frac{DI \times e^{-DI\,\gamma_1 t}}{(\gamma_2 e^{-DI\,\gamma_1 t} + \gamma_3)} \qquad \text{EQ. 7.2}$$

$$\text{where } DI \equiv \frac{Q_b\,(e^{+N_o(1-\Delta Z)} - 1)}{(e^{+N_o(1-\Delta Z)} - \Delta Z)} \quad \text{for counter current dialysers}$$

$$= \frac{Q_b\,(1 - e^{-N_o})}{(1 + Z\,(1 - e^{-N_o}))} \quad \text{for dialysers with well mixed dialysate compartment}$$

$$N_o \equiv \frac{K_o A}{Q_b \Delta_1} = \text{no. of mass transfer units}$$

$$\gamma_1 \equiv \frac{V_d + \Delta V_b}{V_d V_b} \qquad \Delta \equiv \frac{\Delta_1}{\Delta_2} \quad \text{and} \quad Z = \frac{Q_b}{Q_d}$$

$$\gamma_2 \equiv \frac{V_d}{\Delta V_b + V_d} \qquad \Delta_1 \equiv \frac{c_{b,\,\text{total}}}{c_{b,\,\text{free}}} = \mu\,(1+\rho) \text{ in Farrell's terminology}$$

$$\gamma_3 \equiv \frac{\Delta V_b}{V_d + \Delta V_b} \qquad \Delta_2 \equiv \frac{c_{d,\,\text{total}}}{c_{d,\,\text{free}}} = \text{partition coefficient for lipids}$$

Figure 7.2.1 General Expressions for Clearance in Dialysers

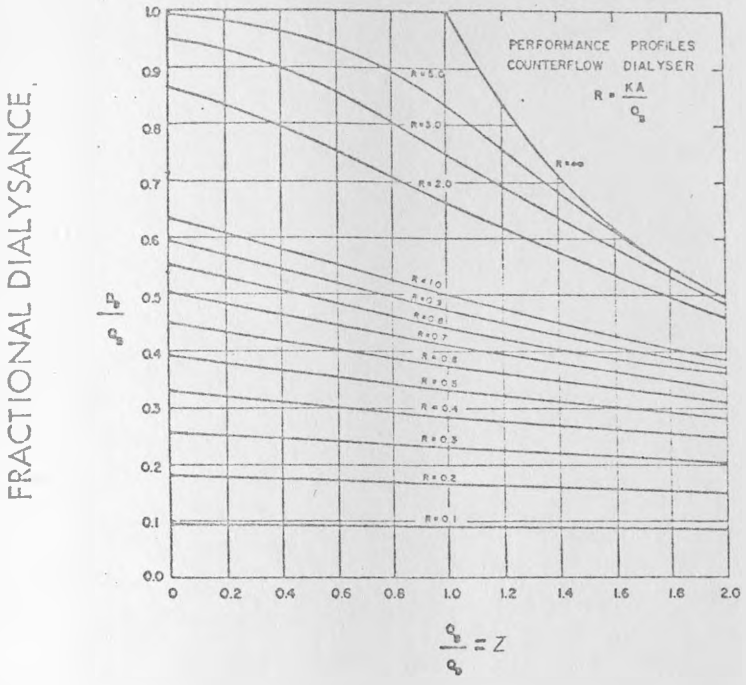

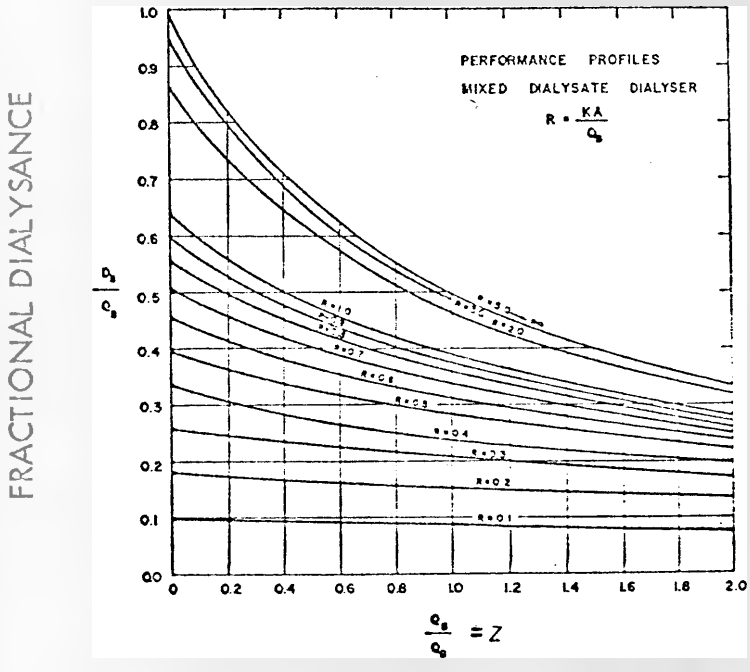

Figure 7.2.2 Effect of Flow Ratio (Z) on Dialyser Performance (after Micheals, 1966)
(Note: In the notation used in this thesis R in the diagrams equals N_o)

absorbed into the membrane, then the membrane resistance to lipophilic toxins will be decreased. Hence the net effect may be to decrease the overall mass transfer resistance. Neither of the phenomena discussed above have been quantified, experimentally in the literature.

In fact, experimental data on dialysers with sorbent augmented dialysate is very limited. Most reviews on toxin removal by dialysis refer to the paper by Decker et al. (1971). However, this in vitro study only utilized a small dialysis test cell and the very nature of the experiments make the results largely irrelevant to clinical practice. The only conclusion that can be drawn is the obvious one that activated carbon increases the capacity of aqueous dialysate to hold toxins at a given 'free' concentration. The paper does not relate the presence of activated carbon in the dialysate to the rate of mass transfer.

Merino et al. (1977) recently compared the performance of a hollow fibre haemodialyser (Cordis Dow Model 5) using an aqueous dialysate and an activated carbon slurry. In vivo experiments in dogs with surgically induced hepatic failure showed only minor (and in all but three cases, statistically insignificant) differences between the blood concentrations of various amino acids following treatment with the respective techniques. In vitro experiments, however, showed marked differences in the clearances of creatinine and L-phenylalanil-Lphenylalanine. Details of the in vitro experimental conditions are not given in the paper, in particular the composition of the 'blood' solution was not defined. On the assumption that the blood and dialysate flow rates are the same as those in the in vivo experiments, namely 150 ml/min and 300 ml/min, it is possible to analyse the in vitro data based on the previous discussion. Figure 7.2.3 presents Merino's creatinine clearance data for aqueous and slurried dialysate together with two theoretical curves based on that data. The first theoretical curve predicts the dialyser performance for an infinite dialysate flow (or Δ, equals zero) on the basis of the values of N_o for aqueous dialysate experiment. This suggests an increase in clearance of about 12% as compared to the 25% improvement in practice with the dialysate slurry. The second theoretical curve shows the performance if the number of mass transfer units (N_o) is increased by 30%, i.e.

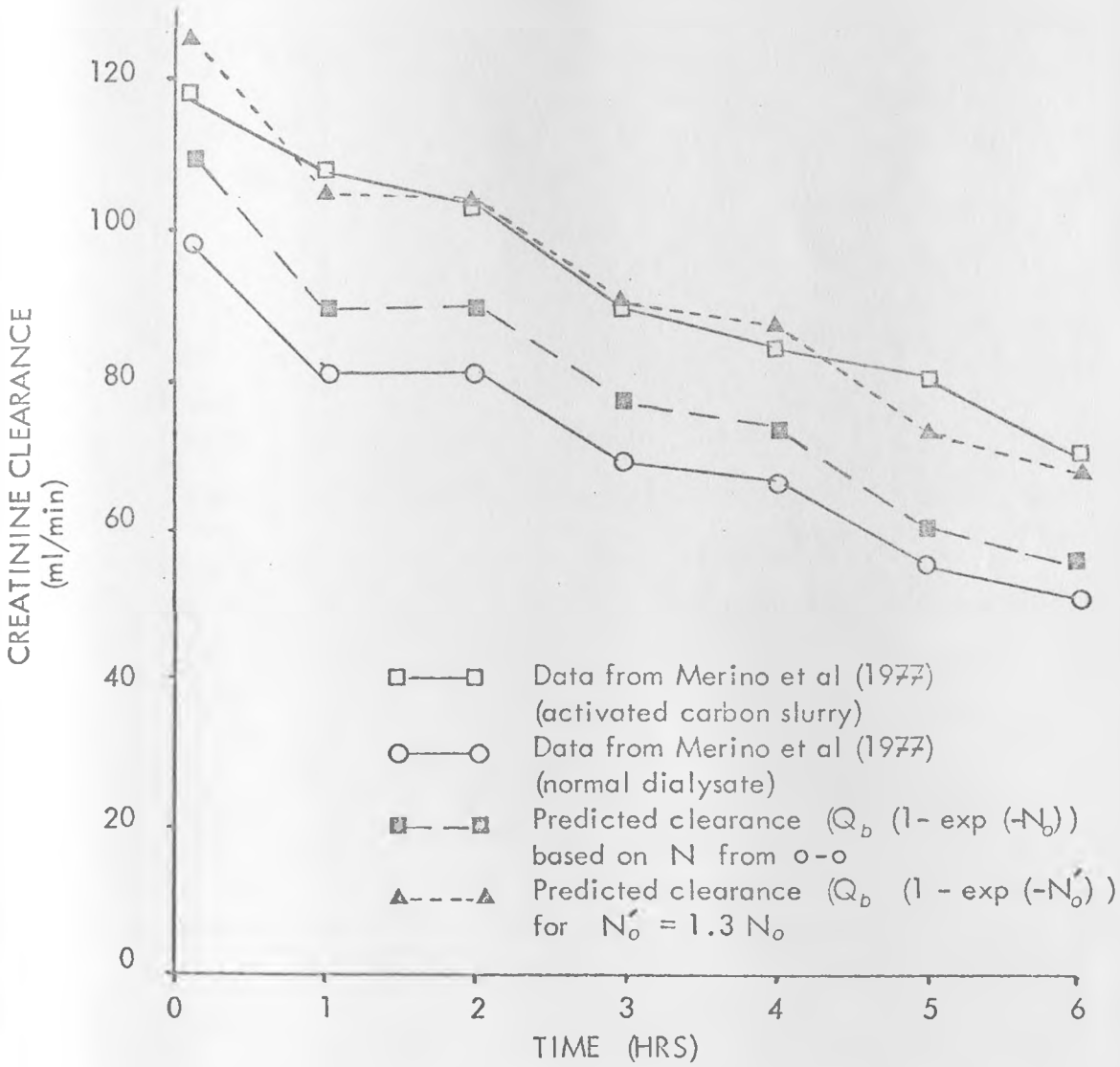

Figure 7.2.3 Comparison of Theoretical and In Vitro Data on the Performance of Dialysers Using Activated Carbon/Dialysate Slurries

a decrease in the total mass transfer resistance of 23%. Calculations based on the physical properties and the performance of the Cordis Dow Model 5 dialyser suggest that the dialysate side resistance contributes 20% or less of the total resistance. Therefore, it may be concluded that if all the dialysate resistance is eliminated by the presence of the slurry, then the theoretical performance based on Equation 7.4 provides a good prediction of the actual in vitro performance using dialysate slurry.

Analysis of the comparative performances for L-phenylalanil-L-phenylalanine do not provide the same measure of agreement between predicted and actual performance. The number of mass transfer units would have to be increased by a factor of 2.5 for the two to be similar. There is no feasible explanation for such an increase being attributed to the presence of the slurry. In fact it is unlikely in the creatinine case that the slurry would completely eliminate the dialysate side resistance. Therefore, for both solutes the theory does not correspond precisely to the experimental data. However, considering the unexplained fall in creatinine clearance with time, the lack of detail regarding the in vitro experiments, in particular data on the respective ultra-filtration rates, firm conclusions cannot be drawn from the above comparisons. Clearly a series of controlled experiments need to be conducted to quantify all aspects of dialyser mass transfer using sorbent dialysate slurries.

For the case of dialysis against lipids more in vitro data is available for comparison of theory and practice. Fletcher and Koplin (1970), Leitzell (1971) and King (1970) all found that lipid-based dialysate did not alter the clearance of toxins with moderate to high oil/water partition coefficients, i.e. gluthethimide, secobarbital and phenobarbital. This suggests that the expected increase in clearance due to the equivalent, dialysate flow rate becoming infinite (i.e. $\Delta Z \rightarrow 0$) is balanced by increases in the dialysate side, mass transfer resistance and possible increases in the membrane permeability.

Contrary to the in vitro evidence, the limited in vivo data suggest an increase in performance due to the presence of the lipid. Shinaberger et al.

(1965) compared the clearance of gluthethimide from dogs using a coil dialyser with aqueous and lipid-based dialysate. Although their data is complicated by the fact that the dialysate volume is finite, differences between the initial clearances (i.e. dialysances) for aqueous and lipid dialysate are greater than would be expected on the basis of differences in Δ, alone (assuming constant N_o). It is possible that the membrane permeability has been increased by the lipid, although there is no way to check this. The in vivo data of von Hartitzsch et al. (1973), based on gluthethimide poisoning in a single patient, also indicates that the clearance in a coil dialyser using a finite bath of lipid dialysate is superior to that of a similar coil using an aqueous dialysate in a recirculation, single pass, dialysate flow mode. Clearances were only measured at the initiation and completion of treatment; serial data was not taken in the interim. Initially the clearances were 63 ml/min for the lipid dialysate and 17 ml/min for the aqueous dialysate. After three hours both clearances were 20 ml/min. Therefore, the possibility of an error in the first clearance reading puts the whole result in jeopardy. The total amount of gluthethimide removed by the lipid-based dialyser was calculated on the basis of the two clearances and not by direct measurement of concentrations in the lipid dialysate bath. Therefore, there is no independent mass balance check on the clearances. Unfortunately, of all the in vitro and in vivo results with lipid-based dialysate, the emphasis in the major review on treatment of acute poisoning by Winchester et al. (1977) is on the results of von Hartitzch and co-workers. The implication is that lipid-based dialysates definitely increase the clearance of lipid soluble toxins in haemodialysers. Based on all the evidence no definitive statement can be made, although it appears there is only a minimal improvement. As with the dialysate slurries more controlled experiments are required to clarify the position.

It should be noted that lipid soluble toxins are distributed largely in the adipose tissue. Consequently, blood concentrations are low and the amount of toxin removed even at high clearance rates is only a small fraction of the total dose. Therefore, the purpose of extracorporeal detoxification must be questioned along the lines of the criteria of Schreiner et al. (1958).

7.2.3 Integral sorbent/dialysis membranes

Inclusion of a sorbent in a tubular dialysis membrane has the same effect as employing a sorbent slurry as the dialysate, in that the dialysate concentration is reduced to zero throughout the dialysate compartment. As the sorbent is on the dialysate side of the membrane, toxin removal from the blood is controlled entirely by dialytic mass transfer across the membrane.

However, if the sorbent is on the blood side, as in the hollow fibre devices produced by Malchesky and co-workers, then the dialytic transport may be augmented by direct sorption from the blood. If initially the system acts as a haemoperfusion device, then the clearance may be much higher than the final, dialytic clearance value when the sorbent has been exhausted. This higher clearance results from the lower mass transfer resistance between the bulk fluid and the sorbent as compared to that between the bulk fluid and the dialysate solution. For both forms of integral sorbent/dialysis membrane a detailed analysis is required to predict the rate of decline of dialysance (or clearance) from the initial high value to the steady state dialytic value.

The only data in the literature for dialysers based on an integral sorbent/dialysis membrane is that of Malchesky et al. (1977). The in vitro performance of a coil dialyser with a tubular membrane was tested for urea, creatinine and uric acid. Unfortunately the performance of the equivalent dialyser with a conventional membrane was not included for comparison. However, a similar conventional dialyser tested by Surovy et al. (1973) had urea and creatinine dialyances equal to or greater than those for the sorbent/dialysis membrane dialyser. In the case of uric acid, the dialysance in the sorbent/dialysis membrane dialyser was initially greater than that in conventional dialyser although after four hours it had approached this value. However, a direct comparison using the same dialyser and the two membranes is required before firm conclusions can be drawn. With such a comparison it is crucial that changes in the dialysance of the sorbent/dialysis membrane dialyser do not occur as a result of differences in the properties of the membrane or differences in the construction of the dialysers. Changes should be attributable to the presence of the sorbent

per se. However, with only 16 gm of sorbent being incorporated in the tubular membrane it is unlikely that marked changes in performance will occur.

7.3 Ultrafiltrate Perfusion

Ultrafiltration perfusion devices are one of two types; ultrafiltration regeneration and plasma filtration.

7.3.1 Ultrafiltrate regeneration

In theory an ultrafilter is a constant clearance device, i.e. the clearance is independent of the inlet concentration. Molecules up to a particular (threshold) molecular size are not rejected (to any degree) by the ultrafiltration membrane. Therefore, the clearance equals the hydrodynamic flux through the membrane. Molecules larger than the threshold are partially or totally rejected by the membrane. Hence, the clearance spectrum in an ultrafilter is quite different to that in a dialyser. It is this difference in the clearance spectrum that justifies current interest in ultrafilters for use in chronic renal failure. In fact the operation of an ultrafilter is quite similar to that of the filtration element in the human kidney, the glomerulus.

Excess water and essential solutes and ions that are lost with the ultrafiltrate must be replaced. This is done by infusing saline solution of appropriate composition into the patient, usually upstream of the ultrafilter. Alternatively, the ultrafiltrate can be cleaned of toxins using a sorbent cartridge and returned directly to the patient. Obviously this simplifies the ultrafiltration process enormously. As with dialysate regeneration the design objective in ultrafiltrate regeneration is to avoid breakthrough in the sorbent cartridge. A similar technique to that outlined in Section 7.2.2 for dialysate regeneration may be used to design the sorbent cartridge. It must be emphasised that the regeneration cartridge merely simplifies operation of the ultrafilter. It does not increase the mass transfer. If incorrectly designed, however, it may modify the clearance spectrum by allowing the breakthrough of certain solutes to occur before the cartridge is judged to be saturated and hence replaced.

7.3.2 Plasma filtration

A conventional ultrafilter does not have direct access to protein

bound molecules. As the free concentration in the retentate is the same as that in the filtrate (for a sieving coefficient of one) the bound toxin is not released. The plasma filtration devices under development by Maini et al. (1977) and Nose et al. (1977) overcome this limitation by allowing plasma proteins to pass into the ultrafiltrate. Bound toxin can then be removed by the sorbent (regeneration) cartridge as per a conventional perfusion column (Section 6.4). The protein is returned to the patient. In addition, Maini's device involves dialytic transport which has a limited access to bound toxin. The two types of devices are illustrated in Figure 7.3.1. Neither has had its performance well documented. A detailed analysis of these devices is beyond the scope of this thesis. However, it is possible to obtain some insight into their operation. Maini's device can operate at one of two extremes, i.e. either as a ultrafilter or as a dialyser. Although the former mode is emphasised, dialytic transport may be more important for small to medium molecules. The real advantages of this device is in the removal of highly protein bound molecules. If the sorbent cartridge is suitably designed then all the ultra--filtrate can be cleaned of toxin. Therefore clearances of 100 ml/min (or more) for a blood flow of 200 ml/min should be feasible. These are considerably in excess of the comparative clearances with a conventional haemodialyser. It is possible to achieve similar clearances with direct haemoperfusion. However, a further advantage of Maini's device is its usefulness for long perfusions. The sorbent cartridge can be easily changed while the device is still attached to the patient. Hence providing cellular deposition and clogging does not drastically reduce the ultrafiltration rate, extremely long perfusions may be conducted in the hepatic failure cases. In addition, the problems of blood compatibility associated with sorbent perfusion in hepatic failure are largely eliminated.

Nose's device is more complex to analyse. In essence, it is a number of macroporous ultrafilters plus regeneration cartridges, in series. Unless there is predilution of the blood the degree of ultrafiltration in each cell will be severely limited and very high pressure drops will be required to maintain both flow and ultrafiltration. The efficiency of the sorbent is limited by the transit time of the plasma passing across each sorbent layer. As in a haemoperfusion column, the critical parameters are the external mass transfer coefficient, the

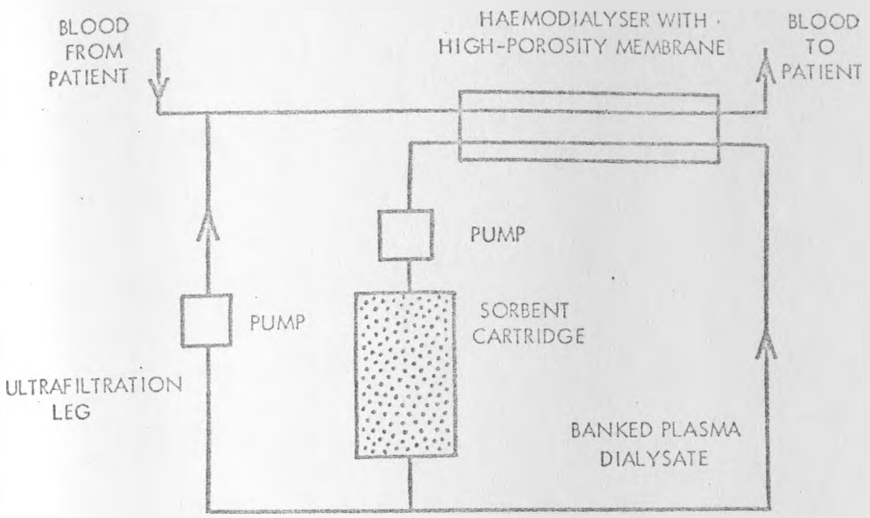

Plasma Filtration Device Designed by Maini (1975)

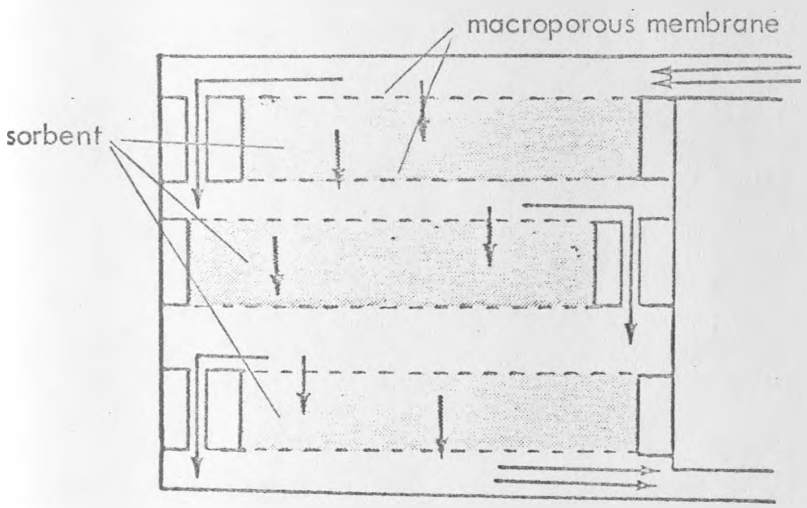

Plasma Filtration Device Designed by Nose et al. (1975)

Figure 7.3.1 Plasma Filtration Devices

external surface area of the particles and the flow rate. However, an increase in the surface area normally involves a decrease in particle size and hence an increase in pressure drop. A decrease in flow rate may increase the fractional clearance across the sorbent layer although the absolute rate of removal will decrease. Therefore, there is a practical limit to the extent to which mass transfer in the sorbent can be increased.

Nose's device can also remove toxins by diffusive transport (dialysis). However, this process is limited by the very small membrane areas involved, i.e. each layer or plate containing 50 gm of activated carbon has a membrane surface area of only 56 cm . The principal diffusion resistance is offered by the blood film at the surface of the membrane. For an average resistance of 20 min/cm and a flow rate of 200 ml/min the clearance due to diffusion (assuming negligible ultrafiltration) is about 2.6 ml/min. From the data in Nose et al. (1977) it appears that most of the clearance for creatinine ($\simeq$ 3.5 ml/min per plate at 200 ml/min) is due to dialysis. For removal of the larger bilirubin molecules however, the transport is presumably dictated by convection.

In conclusion, the potential of Nose's device is limited by the high pressure drops needed to maintain ultrafiltration plus the small membrane area for diffusive transport. Neither of these limitations is associated with Maini's plasma filtration device. Although Maini's device does not offer any major improvement in the mass transfer of protein bound toxins (compared to haemoperfusion), it does offer practical improvements re long term blood detoxification.

CHAPTER 8

CONCLUSIONS

CHAPTER 8

CONCLUSIONS

The following conclusions are drawn from the results in the preceding chapters. Sections 8.3 and 8.4 relate specifically to the thesis aim, i.e. to improve our understanding of the mass transfer processes controlling perfusion devices, with particular emphasis on haemoperfusion columns.

8.1 In Vitro Experiments to Estimate Parameter Values

1. Relatively simple batch experiments provide reproducible data for estimating the adsorption isotherm and intraparticle diffusion parameters. However, in certain circumstances, in addition to being adsorbed, the sorbate undergoes a reaction in the presence of the sorbent. In this regard activated carbon is well documented as a catalyst, especially of oxidation reactions. Therefore, it is important that the possible existence of a sorbate reaction be taken into account when quantifying the adsorption or mass transfer properties from a batch experiment.

2. The quadratic driving force (QDF) approximation provides an adequate description of the intraparticle diffusivity for spherical, cylindrical and irregular particle shapes. However, the values of diffusivity are not necessarily identical to those using the homogeneous solid diffusion model. Nevertheless, the QDF model and associated diffusivity provides an equally valid description of the kinetics. The solution of the QDF model is much simpler than that for the homogeneous model. When simulated with a standard modelling package (i.e. CSMP) the QDF model represents an expedient method of measuring the solid diffusivity in sorbent particles.

3. The particle diameter is a critical parameter in determining the intraparticle diffusion kinetics. If a wide range of particle sizes is used then the kinetics fall between the extreme kinetics controlled by the maximum and minimum particle sizes. In such cases, the model kinetics based on the mean

diameter do not provide an adequate description of the data. For convenience of data analysis, it is best to use a narrow range of particle sizes, i.e. less than a 10% difference between the maximum and the minimum diameters. This is narrower than the range of mesh sizes normally adopted.

4. The hydrodynamic characteristics of commercial haemoperfusion columns suggest that there are regions of partial stagnation involving up to 10% of the volume of the column. However, this effect is relatively minor and to a first approximation the flow can be described by an axial dispersed, plug flow model. Alternatively, a mixing-cell or tanks-in-series model can be used. A multiparameter, mixing-cell model provides a more exact solution by taking into account the apparent partial stagnation.

5. The external mass transfer coefficient in a perfusion column can be estimated from the initial breakthrough. A finite initial breakthrough occurs if the number of external mass transfer units, N_e is sufficiently small. That is, if the rate of sorbate mass transfer across the blood film and coating membrane is less than the rate of sorbate entering the column. Experimental columns can be designed to satisfy this condition. This technique offers a simple experimental method for evaluating the relative contributions of the blood film resistance and the coating resistance to the overall external mass transfer coefficient.

8.2 Perfusion Column Model

1. The lumped parameter, perfusion column model developed in Chapter 3 provides a valid description of perfusion column performance. The computer simulations of the model, using the CSMP package, are very stable. Therefore, the model and its simulation represent a suitable vehicle with which to investigate and interpret the performance of perfusion columns.

8.3 Perfusion Column Performance

Paragraphs (1) to (6) in this subsection refer to perfusion with an aqueous solution.

1. The number of external mass transfer units, N_e , control the upper limit of performance of a perfusion column. In particular, it sets the initial clearance of a perfusion column; the initial clearance increases with N_e . The external diffusion limited performance is best described in terms of an equivalent haemodialyser, i.e. a haemodialyser with the same number of mass transfer units. The basic concept of the equivalent haemodialyser emphasises the fact that the controlling mass transfer process in a perfusion column is dialytic. The reason for the superior initial clearance in most perfusion columns (as compared to commercial haemodialysers), is the larger value of N_e . This is caused by a decrease in the external diffusion resistance (especially the membrane resistance). The sorbent merely facilitates the construction of this special design of dialyser (the perfusion column) where the external resistance can be significantly reduced. In the limit, it can be reduced to the blood film resistance alone.

2. The number of intraparticle mass transfer units, N_s , controls the rate of decline of perfusion column clearance with time. Large values of N_s signify a slow decline and visa versa. As sorbate accumulates in the sorbent, the concentration gradient decreases as does the flux into the particles. This is analogous to an increase in the dialysate side resistance in the equivalent haemodialyser. The sensitivity of the clearance to changes in N_s depends upon the relative magnitude of N_s . For intermediate values the sensitivity is high, i.e. as control of the kinetics after the initial breakthrough changes from the external diffusion resistance to the intraparticle diffusion resistance. Over the sensitive range of N_s ,values the intraparticle diffusion and particle diameter have a critical bearing on the value of the clearance.

3. As expected, the membrane coating in haemoperfusion columns effects the external diffusion mass transfer coefficient. However, it also increases the intraparticle diffusion resistance. This is due presumably to

partial filling of pores in the sorbent particles. The apparent increase ranges from a factor of 3 up to a factor of 40. The latter value may be overestimated due to a loss of effective sorbent capacity caused by the coating.

4. The shape of the isotherm has only a small effect on the performance of a perfusion column. The greater the non-linearity, the flatter the clearance curve and hence the higher the clearance at any time (for throughput values < 0.5).

5. The axial dispersion coefficient, or n in the mixing cell model, alters the shape of the initial breakthrough. The apparent initial breakthrough increases with increasing axial dispersion, i.e. the apparent number of external mass transfer units, N_e' , decreases with increasing axial dispersion. This effect must be considered when measuring external mass transfer coefficients.

6. A steady fall in the inlet concentration to a perfusion column (as occurs in clinical practice) causes the rate of decline in clearance, with time, to decrease. Hence the clearance is generally greater than that in single pass operation. However, the initial value is the same, and as the inlet concentration approaches zero the clearance falls off sharply. The paradox is that despite the increase in clearance, the rate of mass transfer in the column is always lower than that in the single pass mode .

7. The removal of protein bound sorbates by a haemoperfusion column is limited by the performance of the equivalent haemodialyser, i.e. dialysis is the controlling mass transfer process. Again the superior initial clearance in perfusion columns (as compared to commercial haemodialysers) is due to an increase in N_e .

8. The existence of formed elements in blood causes the effective aqueous flow rate to decline. This results in a fall in the initial clearance of a perfusion column (as compared to the clearance with an aqueous solution). If some of the toxin is contained within the cells and if it is only transported slowly through the cell wall, then there is a further decline in clearance.

8.4 Other Sorbent-Based Detoxification Devices

1. In general, when sorbents are used in conjunction with other detoxification devices or techniques (i.e. dialysis and ultrafiltration), the sorbent does not radically alter the performance of the basic device. Rather it complements the basic device by simplifying its mode of operation. Hence, there is no justification for regarding sorbents, such as activated carbon, as a type of 'black magic' that intrinsically improves the mass transfer performance of every novel device in which it is incorporated. It would be instructive to conduct controlled *in vitro* experiments to quantify the contributions of the sorbent in all new detoxification devices that incorporate sorbents.

8.5 Future Work

1. The relative contribution of the blood film and the membrane resistance to the overall external diffusion resistance in haemoperfusion columns needs to be evaluated. The influence of sorbate molecular size and coating type, weight and method should be quantified. A technique for measuring the resistances was outlined in Section 6.2. It involves accurate measurement of the external area of the particles. Suitable methods of determining this area are still to be devised.

2. The contribution of the membrane coating to the intraparticle diffusion resistance should be investigated further. In particular, the influence of the pore structure of the sorbent particles should be examined. The effect of sorbate molecular size plus coating type, weight and method should be assessed in this regard.

3. Standard techniques should be devised for the evaluation and presentation of mass transfer data from haemoperfusion columns, i.e. along similar lines to those for haemodialysers. This will facilitate the *rational* comparison of haemoperfusion columns with other columns or with other detoxification devices. It is envisaged that these techniques will be developed in conjunction with the understanding of mass transfer in perfusion columns gained in Chapter 6.

4. The equivalent haemodialyser concept provides a rationale for understanding and interpreting the clinical performance of haemoperfusion columns. However, the pressing clinical problem remains the specification of blood detoxification therapy. A deeper appreciation of the pharmacokinetics, and in some instances, the molecular etiology, of exogenous and endogenous toxicity is essential for the efficient use of haemoperfusion columns (and other blood detoxification devices). To some extent, the knowledge gained in this thesis will be useful in developing this appreciation.

BIBLIOGRAPHY

BIBLIOGRAPHY

ABBRECHT, P.H., and Prodany, N.W. A model of the patient-artificial kidney system. IEEE Trans. Bio. Med. Eng. 18 : 257, 1971.

ABOUNA, G.M., Barabas, A.Z., Boyd, N., Todd, J.K., et al. Resin and charcoal haemoperfusion in the treatment of hepatic coma. in Kenedi et al., (Eds.) Artificial Organs, Macmillan Press, p. 363, 1977.

AMANO, I., Iwatsuki, S., Saito, A., Manji, T., et al. Microencapsulated bead-type petroleum charcoal in artificial liver assist. Abstr. ASAIO. 5 : 3, 1976.

ANDRADE, J.D., von Wagenen, R., Chen, C., Ghavamian, M., et al. Coated adsorbents for direct blood perfusion II. Trans. ASAIO. 18 : 473, 1972.

ARIS, R. On the dispersion of linear kinematic waves. Proc. Roy. Soc. A 245 : 268, 1958.

BABB, A L., Popovich, R.P., Christopher, T.G., Schribner, B.H. The genesis of the square meter-hour hypothesis. Trans. ASAIO. 17 : 81, 1971.

BABB, A.L., Farrell, P.C., Strand, M.J., Uvelli, D.A., et al. Residual function and chronic haemodialysis therapy. Proc. Dialysis Transplant Forum. 2 : 142, 1972.

BASS, O.E., Nolph, K.D., and Maher, J.F. Dialysance and clearance measurements during clinical dialysis - A plea for standardization. J. Lab. Clin. Med. 86 : 385, 1975.

BELL, R.L., Curtis, F.K., and Bable, A.S. Analogue simulation of patient-artificial kidney system. Trans. ASAIO. 11 : 183, 1965.

BENHAMOU, J.P., Reuff, B., and Sicot, C. Severe hepatic failure : A critical study of current therapy. in Orlandi, F., and Jezequel, A.M. (Eds.) Liver and Drugs, Academic Press, p. 213, 1972.

BERGSTROM, J. Uraemic toxicity . Proc. EDTA. 12 : 579, 1975.

BERGSTROM, J., Furst, P., and Zummermann, C. A study of uraemic toxicity. Proc. 10th Annual Contractors Conference, Artificial Kidney Program. NIAMDD, US Dept., Health, Education and Welfare. p.43, 1977.

BERTHIER, G. Problemes theoriques lies a la determination des coefficients d'autodiffusion dons les solides par la methode des echanges isotopiques retrogenes. J. Chim. Phys. 49 : 527, 1952.

BISCHOFF, K.B., and Brown, R.G. Drug distribution in mammals. Chem. Eng. Progr. Symp. Series. 62 (66) : 33, 1966.

BISCHOFF, K.B. General solution of equations representing effects of catalyst deactivation in fixed bed reactors. Ind. Eng. Chem. Fundam. 8 (4) : 665, 1969.

BLANEY, T.C., Lindan, O., and Sparks, R.E. Cyclic adsorption of urea from artificial kidney dialysing fluid. Chem. Eng. Progr. Symp. Series. 64 (84) : 112, 1968.

BRADLEY, W.G., and Sweed, N.H. Rate controlled constant pattern fixed-bed sorption with axial dispersion and nonlinear multicomponent equilibria. Chem. Eng. Progr. Symp. Series. 71 (152) : 59, 1975.

BRAUCH, V., and Schlunder, E.U. The sale up of activated carbon columns for water purifications, based on results from batch tests - II Theoretical and experimental determination of breakthrough curves for activated carbon columns. Chem. Eng. Sci. 30 (5/6) : 539, 1975.

BRIAN, P.L.T., Hales, H.B., and Sherward, T.K. Transport of heat and mass between liquids and spherical particles in an agitated tank. AIChE J. 15: 727, 1969.

BRUNNER, F.P., Giesecki, B., Gurland, H.J., Jacobs, C., et al. Combined report on regular dialysis and transplantation in Europe, V. 1974. Proc. EDTA. 12: 3. 1975.

BRODIE, B.B. Physico-chemical factors in drug desorption. in Binns, T.B. (Ed.) Adsorption and Distribution of Drugs, E. & S. Livingstone Ltd., 1964.

CARBERRY, J.J. A boundary layer model of fluid particle mass transfer in fixed beds. AIChE J. 6 : 460, 1960.

CHANG, F.H.I., Tan, K.S., and Spinner, I.H. Fixed bed sorption with recycle : Analytic solutions for linear models. AIChE. J. 19 (1) : 88, 1973.

CHANG, T.M.S. Semipermeable aqueous microcapsules (artificial cells) with emphasis on experiments in an extracorporeal shunt system. Trans. ASAIO. 12 : 13, 1966.

CHANG, T.M.S. Removal of endogenous and exogenous toxins by a microcapsulated adsorbent. Can. J. Physiol. Pharm. 47 : 1043, 1969.

CHANG, T.M.S., and Malave, N. The development and first clinical use of semipermeable microcapsules (artificial cells) as a compact artificial kidney. Trans. ASAIO. 16 : 141, 1970.

CHANG, T.M.S., Coffey, J.E., Lister, C., Stark, R., and Taroy, E. The clearance of the ACAC microcapsule artificial kidney for gluthethimide, methprylon and methaqualone : In vitro and in patients. Trans. ASAIO. 19: 87, 1973.

CHANG, T.M.S., Migchelsen, M., Coffey, J.F., and Stark, R. Serum middle molecule level in ureamia during long term intermittent haemoperfusion with the ACAC (coated charcoal microcapsule artificial kidney). Trans. ASAIO. 20: 364, 1974.

CHANG, T.M.S. Protective effect of microencapsulation (coating) on platelet depletion and particulate embolism in the clinical applications of charcoal haemoperfusion. in Kenedi, et al. (Eds.) Artificial Organs, Macmillan Press, p. 164, 1977.

CHEN, C.N., and Andrade, J.D. Pharmacokinetic model for simultaneous determination of drug levels in organs and tissues. J. Pharm. Sci. 65 (5) : 717, 1976.

CHEN, C.N., Coleman, D.L., Andrade, J.D., and Temple, A.R. A pharmacokinetic model for salicylate in CSF, blood, organs and tissues. J. Pharm Sci. (in press). 1977.

CLEMMENSON, C., and Nilssen, E. The theraputic trends in treatment of barbiturate poisoning. Clin. Pharmacol. Ther. 2 :220, 1961.

COLWELL, C.J., and Dranoff, J.S. Nonlinear equilibrium and axial mixing effects in intraparticle diffusion controlled sorption by ion exchange resin beds: Computer analysis. Ind. Eng. Chem. Fundam. 8 (2) : 193, 1969.

COLWELL, C.J., and Dranoff, J.S. Nonlinear equilibrium and axial mixing effects in intraparticle diffusion controlled sorption by ion exchange resin beds: Experimental study. Ind. Eng. Chem. Fundam. 10 (1) : 65, 1971.

COONEY, D.O., and Shieh, D.F. Fixed bed sorption with recycle. AIChE. J. 18 : 145, 1972.

COONEY, D.O. Biomedical Engineering Principles - An Introduction to Fluid, Heat and Mass Transfer Processes. Biomed. Eng. & Instrumentation Series. 2 : Marcel Pekker Inc., 1976.

COOPER, R.S., and Libermann, P.A. Fixed bed adsorption kinetics with pore diffusion control. Ind. Engng. Chem. Fundam. 9 (4) : 620, 1970.

COUGHLIN, R.W. Carbon as adsorbent and catalyst. I.E.C. Prod. Res. Dev. 8 (1) : 12, 1969.

COURTNEY, J.M., Fairweather, I.A., Gilchrist, T., Hood, R.G., et al. The design of a polymer coating for activated carbon. in Kenedi, et al. (Eds.) Artificial Organs, Macmillan Press, p. 133, 1977.

CRANK, J. The Mathematics of Diffusion. 2nd Ed., Clarendon Press, (414p.) 1975.

CRUZE, C.A., and Meyer, M.C. Binding of salicylate and sulfathiazole by whole blood constituents. J. Pharm. Sci. 65 (1) : 33, 1976.

CURRY, S.H. Drug Disposition and Pharmacokinetics. Blackwell Scientific Publications, (214 p.), 1974.

DAVIS, T.A., Cowsar, D.R., Harrison, S.D., and Tanquary, A.C. Activated carbon fibres for haemoperfusion. Trans. ASAIO. 20 : 353, 1974.

DAVIS, T.A., Cowsar, D.R., and Harrison, S.D. Activated carbon fibres for artificial kidney devices. Proc. 7th Annual Contractors Conference, Artificial Kidney Program. NIAMDD, US Dept. Health, Education & Welfare, p.111, 1974.

DAVIS, T.A., Cowsar, D.R., Miller, D.R., Bower, J.D., et al. Activated carbon fibres for artificial kidney devices. Proc. 10th Annual Contractors Conference, Artificial Kidney Program. NIAMDD, US Dept. Health, Education & Welfare, p. 64, 1977.

DECKER, W.J., Combs, H.F., Treutine, J.J., and Branex, R.J. Dialysis of drugs against activated charcoal. Clin. Appl. Pharm. 18 : 573, 1971.

DEDRICK, R.L., and Beckman, R.B. Kinetics of adsorption by activated carbon from dilute aqueous solution. Chen. Eng. Progr. Symp. Series. 63 : 74, 1967.

DEDRICK, R.L., Vantoch, P., Gambos, E.A., and Moore, R. Kinetics of activated carbon kidney. Trans. ASAIO. 13 : 236, 1967.

DEDRICK, R.L., Gabelnick, H.L., and Bischoff, K.B. Kinetics of urea distribution. Proc. Ann. Conf. Eng. Med. Biol. 21: 36, 1971.

DEDRICK, R.L., and Bischoff, K.B. Pharmacokinetics in applications of the artificial kidney. Chem. Eng. Prog. Symp. Series. 64 (84) : 32, 1967.

DELORME, M.L., Rapin, J.R., Black, P., Boschat, M., and Opolon, P. Reversible modifications of brain neurotransmitters in experimental acute hepatic coma. Abstr. ESAO. 3 : 46, 1976.

DENTI, E., Tessore, V., Luboz, M.P., and Malinverni, A. Haemocompatibility problems in blood detoxification by activated carbon. Proc. ESAO. 2 : 215, 1975.

DENTI, E., and Biagini, M. Dialysate regeneration. in Kenedi, et al. (Eds.), Artificial Organs, Macmillan Press, p. 311, 1977.

DENTI, E., Walker, J.M., Lugoz, M.P., Tessore, V., et al. A new concept: The haemocarbodialyser. Abstr. ASAIO. 6 : 18, 1977.

DI GIANO, F.A., and Weber, W.J. Sorption kinetics in finite-bath systems. ASCE. J. Sanit. Eng. Div. 98 (SA 6) : 1021, 1972.

DI GIANO, F.A., and Weber, W.J. Sorption kinetics in infinite bath experiments. J. Water. Poll. Control. Fed. 45 (4) : 713, 1973.

DOMBECK, D.H., Klein, E., and Wendt, R.P. Evaluation of two pool model for predicting serum creatinine levels during intra- and inter-dialytic periods. Trans. ASAIO. 21 : 117, 1975.

DRASUK, J.H., and Smith, J.M. Mass transfer in a packed, pulsed column. AIChE. J. 10 (5) :759, 1964.

DUNEA, G., and Kolff, W.J. Clinical experience with the Yatzidis Charcoal Artificial Kidney. Trans. ASAIO. 11 : 178, 1965.

DUNEA, G., Rizvi, Z.H., Mandani, B.H., Anicama, H.J., and Mahurkar, S.D. Charcoal haemoperfusion and combined dialysis-haemoperfusion in chronic renal failure. Abstr. ASAIO. 5 : 22, 1976.

DUNLOP, E.H., Weston, M.J., Gazzard, B.G., Langley, P.G., and Williams, R. Design features of haemoperfusion columns using activated charcoal. Med. Biol. Eng. 14 (2) : 220, 1976.

EDWARDS, R.O. Blood detoxification devices. PhD. Thesis, University of Strathclyde, 1975.

FARRELL, P.C. Solute protein binding and membrane transport characteristics in haemodialysis. PhD. Thesis, University of Washington, 1972.

FENNIMORE, J., Watson, P.A., Munro, G.D., and Kolthammer, J.C. The design and evaluation of a convenient haemoperfusion system. Proc. ESAO. 1 : 90, 1974.

FENNIMORE, J., and Munro, G.D. Design problems. in R. Williams and I.M. Murray-Lyons (Eds.), Artificial Liver Support, Pitman Medical, p.330, 1975.

FLECK, R.D., Kirwan, D.J., and Hall, K.R. Mixed-resistance diffusion kinetics in fixed-bed adsorption under constant pattern conditions. Ind. Eng. Chem. Fundam. 12 (1): 95, 1973.

FLETCHER, G., and Koplin, N.S. In vitro comparison of aqueous and lipid dialysate in haemodialysers for gluthethimide, secobarbital and phenobarbital. Amer. Soc. Neph. Abstr. p. 25, 1970.

FRANZ, H.E. European experience with haemofiltration. Proc. 10th Annual Contractors Conference, Artificial Kidney Program. NIAMDD, US Dept. Health, Education & Welfare, p. 145, 1977.

FURUSAWA, T., and Smith, J.M. Fluid-particle and intraparticle mass transport rates in slurries. Ind. Eng. Chem. Fundam. 12 (2) : 197, 1973.

FURUSAWA, T., and Smith, J.M. Intraparticle mass transport in slurries by dynamic adsorption studies. AIChE J. 20 (1) : 88, 1974.

GANONG, W.F. Review of Medical Physiology. 6th Ed. Lange Medical Publications, (577 p.) , 1973.

GARTEN, V.A., and Weiss, D.E. The ion and electron exchange properties of activated carbon in relation to its behavious as a catalyst and adsorbent. Rev. Pure. Appl. Chem. 7 (2) : 69, 1957.

GAYLOR, J.D.S., Muir, W.M., and Allan, W.T. Kinetics of solute transfer from whole blood in a haemodialyser. Med. Biol. Eng. 8 (1) : 1, 1970.

GAYLOR, J.D.S. Experimental verification of a two-compartment mass-transfer model for whole blood in a haemodialyser. Med. Biol. Eng. 12 (1) : 90, 1974.

GAZZARD, B.G., Weston, M.J., Murray-Lyon, I.M., Flax, H. et al. Charcoal haemoperfusion in the treatment of filminant hepatic failure. Lancet 1 : 1301, 1974.

GILCHRIST, T., Jonsson, E., Martin, A.M., Nauler, L., et al. Development of the Strathclyde haemoperfusion system. in Williams, R., and Murray-Lyon, I.M. (Eds.), Artificial Liver Support, Pitman Medical, p. 319, 1975.

GILLETTE, J.R. The importance of tissue distribution in pharmacokinetics. in Teorell, T., Dedrick, R.L. & Condliffe, P.G. (Eds.) Pharmacology & Pharmacokinetics, p. 209, 1973.

GIORDANO, C. Uraemia. Kidney Int., 7 (2) : Supplement 3, 1975.

GLEUCKAUF, E., and Coates, J.I. Theory of chromatography. Part IV. The influence of incomplete equilibrium on the front boundary of chromatograms and on the effectiveness of separation. J. Chem. Soc. p. 1315, 1947.

GLUECKAUF, E. Theory of chromatography- Part 10. Trans. Faraday. Soc. 51: 1540, 1955.

GOLDBAUM, L.R. and Smith, P.K. The interaction of barbiturates with serum albumin and its possible relation to their deposition and pharmacological actions. J. Pharmacol. Exp. Therap. 111 : 197, 1954.

GORDON, A., Popovtzer, M., Greenbaum, M., Marantz, L. et al. A potentially useful adsorbent in the treatment of chronic renal failure. Proc. EDTA. 5 : 86, 1968.

GORDON, A., Greenbaum, M.A., Marantz, L.B., McArthur, M.J., and Maxwell, M.H. A sorbent-based low volume recirculating dialysate system. Trans. ASAIO. 15 : 347, 1969.

GORMLEY, W.T., and Bell, R.L. The dynamics of urea transfer and cerebral pressure during rapidly changing urea levels in the blood. Chem. Eng. Progr. Symp. Series. 66 (99) : 1, 1970.

GOTCH, F.A., and Krueger, K.K. (Eds.) Adequacy of Dialysis. Kidney Internat. 7 (1) : Supplement, 2, 1975.

GOTCH, F.A., Sargent, J.A., Keen, M.L., Seid, M., and Lee, M. Relationships of uraemic abnormalities to variable molecular weight dialysis therapy and residual renal function. Proc. 8th Annual Contractors Conference, Artificial Kidney Program. NIAMDD, US Dept. Health Education & Welfare, p. 100, 1975.

GRIB, N.L. In vivo and in vitro solute protein binding and diffusivity studies with applications to haemodialysis. PhD. Thesis, University of Washington, 1973.

HAGSTAM, K.E., Larsson, L.E. and Thysell, H. Charcoal deposition in internal organs after haemoperfusion with the Yatzidis technique in rabbits. Proc. EDTA. 3 : 352, 1966.

HALL, K.R., Eagleton, L.C., Acrivos, A., and Vermeulen, T. Pore and solid diffusion kinetics in fixed bed adsorption under constant pattern conditions. Ind. Eng. Chem. Fundam. 5 : 212, 1966.

HARTITZSCH, von, B., Pinto, M.H., Mauer, S.M., Casali, R.G., et al. Treatment of gluthethimide intoxication : an in vivo comparison of lipid, aqueous, and peritoneal dialysis with albumin. Proc. Clin. Dialysis & Transplantation Forum. 3 : 102, 1973.

HASHIMOTO, K., Miura, K., and Nagata, S. Intraparticle diffusivities in liquid-phase adsorption with nonlinear isotherms. J. Chem. Eng. Japan. 8 (5) : 367, 1975.

HASHIMOTO, K., Miura, K., and Tsukano, M. Experimental verification of design methods for liquid phase fixed-bed adsorbers. J. Chem. Eng. Japan. 10 (1) : 27, 1977.

HENDERSON, L.W., Bersarab, A., Michaels, A., and Bluemle, L.W. Blood purification by ultrafiltration and fluid replacement (diafiltration). Trans. ASAIO. 13 : 216, 1967.

HENDERSON, L.W. Development of a convective blood cleansing technique. Proc. 10th Annual Contractors Conference, Artificial Kidney Program. NIAMDD, US Dept. Health Education & Welfare, p. 130, 1977.

HILL, J.B., Palaia, F.L., and Horres, C.R. The design of charcoal haemoperfusion system. in Kenedi, et al. (Eds.), Artificial Organs, Macmillan Press, p. 123, 1977.

HIMMELBLAU, D.M. Process analysis by statistical methods. Wiley. 1970.

HOLLAND, F.F., Donnaud, A., Gidden, H.K., and Klein, E. Methods of measurement of mass transfer rates and capacities of haemoperfusion cartridges. Trans. ASAIO. 23 : 573, 1977.

HOUGEN, O.A., and Watson, K.M. Chemical Process Principles : Part 3. Kinetics and Catalysis. Wiley, 1947.

HOW, T.V. Haemodynamic characteristics of parallel flow artificial kidneys. PhD. Thesis, University of Strathclyde, 1977.

HSIEH, J.S.C., Turian, R.M., and Tien, C. Multicomponent liquid phase adsorption in fixed bed. AIChE. J. 23 (3) : 263, 1977.

HUANG, W. Microencapsulation to control adsorption on activated carbon. PhD. Thesis, Washington University, 1974.

HUGHES, R.D., Ton, H.Y., Langley, P.G., Silk, D.B.A., and Williams R. Blood compatibility of albumin coated XAD-7 resin for use in artificial liver support systems. Abstrs. EASO. 4 : 61, 1977.

JAIN, J.S., and Snoeyink, V.L. Adsorption from bisolute systems on active carbon. J. Water. Poll. Control. Fed. 45 (12) : 2463, 1973.

JONG, de, J.C.F., Sibinga, C.T.S., and Wildevuur, C.R.H. Thrombocytopenia in extracorporeal circulation (ECC). II Bubble oxygenator versus artificial kidney. Trans. ASAIO. 21 : 40, 1975.

KATAOKA, T., Yoshida, H., and Ueyama, K. Mass transfer in laminar region between liquid and packing material surface in the packed bed. J. Chem. Eng. Japan. 5 (2), 132, 1972.

KENEDI, R.M.K., Courtney, J.M., Gaylor, J.D.S., and Gilchrist, T. (Eds.) Artificial Organs, Macmillan Press, (450 p.) 1977.

KENNEDY, A.C., Linton, A.L., Luke, R.G., Renfrew, S., and Dinivoodie, A. The pathogenesis and prevention of cerebral dysfunction during dialysis. Lancet 1 : 790, 1964.

KING, L.H., Decherd, J.F., and Newton, J.L. A clinically efficient and economic lipid dialyser. JAMA. 211 : 652, 1970.

KING, P.H., Baker, W.R., Ginn, H.E., and Frost, A.B. Computer optimization of haemodialysis. Trans. ASAIO. 14 : 389, 1968.

KLEIN, E. (Ed). Evaluation of haemodialysers and dialysis membranes. Artificial Kidney - Chronic Uraemia Program. NIAMDD, National Institute of Health, 1976.

KLEIN, G., Tondeur, D., and Vermeulen, T. Multicomponent ion exchange in fixed beds : General properties of equilibrium systems. Ind. Eng. Chem. Fundam. 6 (3) : 339, 1967.

KNEPSHIELD, J.H., Schreiner, G.E., Lowenthal, D.T., and Gelfand, M.C. Dialysis of poisons and drugs - annual review. Trans. ASAIO. 19 : 590, 1973.

KOLOBOW, T., and Dedrick R.L. Dialysate capacity augmentation at ultra-low flow rates with activated carbon slurry. Trans. ASAIO. 12 :, 1, 1966.

KRUGER-THIEMER, E. Chpt. 2 Pharmacokinetics. in van Rossum, J.M. (Ed.) Kinetics of Drug Action, 47th Handbook of Experimental Pharmacology, Springer-Verlag, 1977.

LANGLEY, P.G., Hughes, R.D., Ton, H.Y., Silk, D.B.A., and Williams R. Studies in vitro of the use of Prostaglandin E, to protect against adverse platelet reactions to charcoal haemoperfusion. Abstrs. ESAO. 4 : 82, 1977.

LEITZELL, B.J., Barton, L.H., Wilcox, H.G., and Bloomer, H.A. Comparison of aqueous and lipid dialysis for removing gluthethimide from plasma. Clin. Res. (abstr.) 19: 152, 1971.

LETTERMAN, R.D., Quon, J.E., and Gemmell, R.S. Film transport coefficient in agitated suspensions of activated carbon. J. Water. Poll. Control. Fed. 46 (11) : 2536, 1974.

LEVENSPIEL, O. Comparison of the tanks-in-series and the dispersion models for non-ideal flow of fluid. Chem. Eng. Sci. 17 : 575, 1962.

LEVENSPIEL, O., and Bischoff, K.B. Patterns of flow in chemical process vessels. Advances in Chemical Engineering . 4 : 95, 1963.

LEVENSPIEL, O. Chemical Reaction Engineering. 2nd Ed. Wiley, 1972.

LEVINS, D.M. and Glastonbury, J.R. Application of Kolmogoroff's Theory to particle-liquid mass transfer in agitated vessels. Chem. Eng. Sci. 27: 537, 1972.

LEVY, G. Pharmacokinetics of salicylate elimination in man. J. Pharm. Sci. 54: 959, 1965.

LEVY, G., Tsuchiya, T., and Amsel, L.P. Limited capacity for salicyl phenolic glucuronide formation and its effects on the kinetics of salicylate elimination in man. Clin. Pharmacol. Ther. 13: 258, 1972.

LINDSAY, R.M. Personal communication, 1977.

McCLURE, D. Adsorbents for gastrointestinal use. PhD. Thesis, University of Strathclyde, 1977.

MAEDA, K., Kawaguchi, S., Manji, T., Kobayashi, K., et al. Portable artificial kidney system with adsorbents. Proc. EDTA. 10 : 298, 1973.

MAEDA, K., Kawaguchi, S., Shimizu, K., Manji, T., et al. Ten-litre dialysate supply system with adsorbents. Proc. EDTA. 11 : 180, 1974.

MAINI, R., and Winchester, J.R. Removal of paraquat from blood by haemoperfusion over sorbent materials. Brit. Med. J. 3 : 281, 1975.

MAINI, R. Toxin removal by ion exchange and adsorption. PhD. Thesis, University of Strathclyde, 1975.

MAINI, R., Baillie, H., and Stark, M. Hepatic support system utilizing high porosity protein-permeable membranes in conjunction with dialysate regeneration. in Kenedi, et al. (Eds.) Artificial Organs, Macmillan Press, p. 395, 1977.

MALCHESKY, P.S., Nokoff, R., Varnes, W., and Nose, Y. The charcoal capillary haemoperfusion system. Proc. EDTA. 13 : 242, 1976.

MALCHESKY, P.S., Varnes, W., Pialkiewicz, W., and Nose, Y. Membranes containing sorbents for blood detoxification. Trans. ASAIO. 23 : 659, 1977.

MARTIN, A.M., Gibbins, J.K., Jonsson, E., and Trinder, P. The clinical use of a carbon haemoperfusion column. in Kenedi, et al. (Eds.), Artificial Organs, Macmillan Press, p. 196, 1977.

MATHEWS, A.P. Mathematical modelling of multicomponent adsorption in batch reactors. PhD. University of Michigan, 1975.

MATTHEW, H., and Lawson, A.A.H. Treatment of acute poisoning. 3rd Ed. Churchill Livingston, (202p.), 1975.

MEIER, P. Adsorption control and kinetic model for microencapsulated carbon. PhD. Thesis, Case Western Reserve, University, 1972.

MERINO, G.E., Jetzer, T., Buselmeier, J.J., and Najarian, J.S. Haemodialysis against activated charcoal suspension as a treatment of hepatic encephalopathy. Trans. ASAIO. 23 : 591, 1977.

MEYER, M.C., and Guttman, D.E. The binding of drugs by plasma proteins. J. Pharm. Sci. 57 (6) : 895, 1968.

MICHAELS, A.S. Operating parameters and performance criteria for haemodialysers and other membrane separation devices. Trans. ASAIO. 12: 387, 1966.

MITCHELL, D.C. Haemodetoxification : a clinical introduction. PhD. Thesis, University of Strathclyde, 1975.

MIYAUCHI, T. Film coefficients of mass transfer of dilute sphere-packed beds in low flow rate regime. J. Chem. Eng. Japan. 4 (3) : 238, 1971.

MIYAUCHI, T., and Kikuchi, T. Axial dispersion in packed beds. Chem. Eng. Sci. 343, 1975.

MYTTENAERE, de, M.H., Maher, J.F., and Schreiner, G.E. Haemoperfusion through a charcoal column for gluthethimide poisoning. Trans. ASAIO. 13 : 190, 1967.

NERETNIEKS, I. Adsorption in finite bath and countercurrent flow with systems having non linear isotherm. Chem. Eng. Sci. 31 (2) 107, 1976 (a).

NERETNIEKS, I. Analysis of some adsorption experiments with activated carbon. Chem. Eng. Sci. 31 (11) : 1029, 1976 (b).

NOSE, Y., Malchesky, P.S., Castino, F., Koshino, I. et al. Improved haemoperfusion system for renal-hepatic support.in Sorbents in Ureamia and Hepatic Failure, Kidney Int. Suppl. (in press) 1975.

NOSE, Y., Malchesky, P.S., Koshino, I., Castino, F., and Scheucher, K. Hepatic assist : Devices for use with sorbents and biological reactors. in Kenedi, et al. (Eds.) Artificial Organs, Macmillan Press, p. 378, 1977.

PERRY, R.H., and Chilton, C.H. Chemical Engineer' Handbook, 5th Ed. McGraw Hill, 1973.

PETRELLA, E., Orlandini, G.C., and Bigi, L. Regeneration of dialysis fluid. Proc. EDTA. 11: 173, 1974.

POPOVICH, R.P., Hlavinka, D.J., Bomar, I B., Moncrief, I.W., and Decherd, J.F. The consequence of physiological resistance in metabolite removal from the patient-artificial kidney system. Trans. ASAIO. 21: 108, 1975.

QUELLHORT, E. Haemofiltration - a new method for the treatment of end stage renal failure. Proc. 10th Annual Contractors Conference, Artificial Kidney Program, NIAMDD, US Dept. Health, Education & Welfare, p. 181, 1977.

RAMIREZ, W.F., Lewis, D.W., and Mickley, M.C. Optimal control of the artificial kidney patient system. Med. Biol. Eng. 11 : 743, 1973.

RASTOGI, S.P., Frost, T., Anderson, J. Ashcroft, R., and Kerr, D.N.S. The significance of desequilibrium between body compartments in the treatment of chronic renal failure by haemodialysis. Proc. EDTA. 5 : 102, 1968.

ROSEN, J.B. Kinetics of a fixed bed system for solid diffusion into spherical particles. J. Chem. Phys. 20: 387, 1952.

ROSENBAUM, J.L., Ronquillo, E., and Argyres, S.N. Column haemoperfusion and haemodialysis techniques to treat barbiturate intoxication in dogs. J. Albert Einstein Med. Centre. 16 : 67, 1968.

ROSENBAUM, J.L., Winsten, S., Kramer, M.S., Moros, J., and Raja, R. Resin haemoperfusion in the treatment of drug intoxication Trans. ASAIO. 16: 134, 1970.

ROSENBAUM, J.L., Kramer, M.S., Raja, R., and Boreyko, C. Resin haemoperfusion : a new treatment for acute drug intoxication. New Engl. J. Med. 284 : 874, 1971.

ROSENBAUM, J.L. Resin haemoperfusion in the treatment of acute drug intoxication. Ind. Eng. Chem. Res. Devel. 14 : 99, 1975.

ROSENBAUM, J.L Haemoperfusion in the treatment of acute poisoning. in Kenedi et al. (Eds.), Artificial Organs, Macmillan Press, p. 203, 1977.

ROSSUM, van , J.M. Kinetics of drug action. 47th Handbook of Experimental Pharmocology, Springer-Verlang, 1977.

SAITO, S., Naotsuka, T., Manji, T., Kawaguchi, S., et al. Change in nitrogen metabolism in dialysis patients treated with 10 - dialysate supply system with adsorbents. Proc. EDTA. 12 : 534, 1975.

SANFELIPPO, M.L., Hall, D.A., Walker, W.E., and Swenson, R.S. Quantitative evaluation of haemodialysis therapy using a simple mathematical model and a programmable pocket calculator. Trans. ASAIO. 21 : 125, 1975.

SARGEANT, J.A., and Gotch, F.A. The analysis of concentration dependence of uraemic lesions in clinical studies. Kidney Int. 7 (1) : Suppl. 2 : 35, 1975.

SAUSSE, A., Man, N.K., and Funck-Brentano, J.L. A mathematical approach to haemodialysis therapy. Proc. ESAO. 1 : 81, 1974.

SCHREINER, G.E. The role of haemodialysis in acute poisoning. Arch. Intern. Med. 102: 896, 1958.

SHERWOOD, T.K., Pigford, R.L., and Wilke, C.R. Mass Transfer. McGraw Hill, 1975.

SHETTIGAR, V.R., and Deepak, D. Analysis of haemoperfusion through fixed bed adsorber. Med. & Biol. Eng. & Comput. 15 : 589, 1977.

SHINABERGER, J.H., Shear, L., Clayton, L.E., Barry, K.G., et al. Dialysis for intoxication with lipid soluable drugs : Enhancement of gluthethimide extraction with lipid dialysate. Trans. ASAIO. 11: 173, 1965.

SILK, D.B.A., Chase, R.A., Trewby, P.N., Wheeler, P., et al. Use of the Rhone-Poulenc Polyacrylinitrile membrane in fulminant hepatic failure and its effect on plasma amino acid levels. Abstr. EASO. 3 : 142, 1976.

SKELLARD, A.H.P. Diffusional mass transfer. Wiley, 1974.

SMISEK, M., and Cerney, S. Active Carbon. Elservier (479 p.) , 1970.

SMITH, E.M. Personal communication, 1976.

SMITH, E.M., Affrossman, S., and Courtney, J.M. The catalytic oxidation of creatinine by activated carbon. Carbon (in press), 1978.

SMITH, R.B., Dittert, L.W., Griffen, W.O. and Dolvisio, J.T. Pharmacokinetics of pentobarbital after intraveneous and oral administration. J. Pharmacokinetics & Biopharmacentics. 1 (1) : 5, 1973.

SPAHN, H., and Schlunder, E.U. The scale up of activated carbon columns for water purification based on results from batch tests - 1. Theoretical and experimental determination of adsorption rates of single solute organic batch tests. Chem. Eng. Sci. 30 (5/6) : 529, 1975.

SPARKS, R.E., Blaney, T.L. and Lindan, O. Adsorption of nitrogeneous waste metabolites from artificial kidney dialysing fluid. Chem. Eng. Prog. Symp. Series. 62 (66) : 2, 1966.

SPARKS, R.E., Lindan, O., and Mason, N.S. Annual Report to NIAMMD, Contract No. PH-43-67-1349, 1969.

SPARKS, R.E., Gupta, D.V.S., and Mason, N.S. Adsorption of barbiturates from buffers, blood and intestinal fluids. in Kenedi, et al. (Eds.), Artificial Organs, Macmillan Press, p. 300, 1977.

SPECKHART, F.H., and Green, W.L. A guide to using CSMP - the continuous system modelling program. Prentic Hall, 1976.

STEVENS, F. General Information on the REDY Dialysis System. Organon Teknika, 1974.

STEPHAN, R.L., Jacobsen, S.C., Atkin-Thor, E., and Kolff, W.J. Portable/wearable artificial kidney (WAK) - Initial evaluation. Proc. EDTA. 12: 511, 1975.

SUROVY, R.M., Malchesky, P.S., Kiraly, R.J., Cause, C.M., and Nose, Y. Winding tension - a critical factor in coil dialyser performance. Proc. 26th Ann. Conf. on Eng. In Med. & Biol. p. 265, 1973.

SUZUKI, M., and Kawazoe, K. Batch measurement of adsorption rate in agitated rank. J. Chem. Eng. Japan. 7 (5) : 346, 1974.

SUZUKI, M., Kawazoe, K., Particle-to-lipid mass transfer in a stirred tank with a basket impellar. J. Chem. Eng. Japan. 8 (1) : 79, 1975.

TESTIN, R.F., and Stuart, E.B. Diffusion coefficients measured for gas-solid adsorption rate experiments. Chem. Eng. Progr. Symp. Series. 63 (74) : 10, 1967.

THYSELL, H., Lindkolm, T., Heinegard, D., Henrikson, H., and Jonsson, E. A haemoperfusion column using cellophane coated charcoal. Proc. EASO. 2: 212, 1975.

TOWNSEND, W.B. Microencapsulation of activated carbon for haemoperfusion. PhD. Thesis, University of Strathclyde, 1977.

TIJSSEN, J., Kaptein, M.J.F.M. and Feyin, J. Conversion of creatinine in the presence of activated carbon. in Kenedi et al. (Eds.), Artificial Organs, Macmillan Press, p. 158, 1977.

TWISS, E.E., and Paulsen, M.M.P. Dialysis system incorporating the use of activated carbon. Proc. EDTA 3, 262, 1966.

UPADHYAY, S.N., and Tripathi, G. Liquid phase mass transfer in fixed bed and fluidized beds of large particles. J. Chem. Eng. Data. 20 (1) : 20, 1975.

VALLNER, J.J. Binding of drugs by albumin and plasma protein. J. Pharm. Sci. 66 (4) : 447, 1977.

VERMEULEN, T., and Hiester, N.K. Saturation performance of ion exchange and adsorption columns. Chem. Eng. Progr. 48 (10) : 505, 1952.

VERMEULEN, T. Theory of irreversible and constant pattern solid diffusion. Ind. Eng. Chem. 45 (8) : 1664, 1953.

VERMEULEN, T. Separation by adsorption methods. Adv. Chem. Eng. 2 : 147, 1958.

VERMEULEN, T., and Quilici, R.E. Analytic driving force relation for pore diffusion kinetics in fixed bed adsorption. Ind. Eng. Chem. Fund. 9 (1) : 179, 1970.

VOLANS, G.N., Vale, J.A., Crome, P., Widdop, B., and Goulding, R. The role of charcoal haemoperfusion in the management of acute poisoning by drugs. in Kenedi et al. (Eds.), Artificial Organs, Macmillan Press, p. 178, 1977.

WALKER, J.M. Evaluation of carbon haemoperfusion and urea removal systems. PhD. Thesis, University of Strathclyde, 1974.

WALKER, J.M., Jacobsen, S.C., Stephen, R.L., Kolf, W.J., and Rose, D. The role of adsorbents in the wearable artificial kidney. in Kenedi, et al. (Eds.) Artificial Organs, Macmillan Press, p. 139, 1977.

WEBER, W.J., and Morris, J.C. Kinetics of adsorption on carbon from solution. Proc. ASCE. J. Sanit. Eng. Div. 89 (SA 2) : 31, 1963.

WEBER, W.J., and Morris, J.C. Equilibria and capacities for adsorption on carbon. Proc. ASCE, J. Sanit. Eng. Div. 90 (SA 3): 79, 1964.

WEBER, W.J., and Rumer, R.R. Intraparticle transport of sulfonated alkylbenzenes in a porous solid diffusion with nonlinear adsorption. Water Resources Res. 1 (3) : 361, 1965.

WEBER, T.W., and Chakravorti, R.K. Pore and solid diffusion models for fixed bed adsorbers. AIChE J. 20 (2) : 228, 1974.

WEBER, W.J. and Crittenden, J.C. Madam 1 - A numeric method for design of adsorption systems. J. WPCF. J. Water. Poll. Control. Fed. 47 (5) : 924, 1975.

WEIZ, P.B. Sorption - diffusion in heterogeneous sytems. Part 1. - General sorptive behaviour. Trans. Faraday. Soc. 63 : 1801, 1967.

WEIZ, P.B., and Hicks, J.S. Sorption - Diffusion in heterogeneous systems Part 2. - Quantitative solutions for uptake rates. Trans. Faraday. Soc. 63 : 1807, 1967.

WEIZ,P.B., and Zolleringer. Sorption - diffusion in heterogeneous systems Part 3. Experimental models of dye sorption. Trans. Faraday. Soc. 63 :1815, 1967.

WELT, L.G., Black, H.R., and Kruger, K.K. Symposium on Uraemic Toxins. Arch. Intern. Med. 126 (5) : 1970.

WESTERMARK, M. Kinetics of activated carbon adsorption. J. Water. Poll. Control. Fed. 47 (4) : 1975.

WIDDOP, B., Medd., R.K., Braithwaite, R.A., and Vale, J.A. Haemoperfusion in the treatment of paraquat poisoning. Proc. EASO. 2 : 244, 1975.

WIDEROE, T.E., Grimsrud, L., Berg, K.J., Godal, A., et al. A mathematical single pool model for short time haemodialysis. Proc. EDTA. 11 : 136, 1974.

WILLIAMS, R. The need for artificial liver support. in Williams R., and Murray-Lyon, I.M. (Eds.), Artificial Liver Support, Pitman Medical, p. 3, 1975.

WILLIAMS, R. Approaches to the development of artificial liver support. in Kenedi, et al. (Eds.), Artificial Organs, Macmillan Press, p. 403, 1977.

WILSON, E.J., and Geankoplis, G.J. Liquid mass transfer at very low Reynolds number in packed beds. Ind. Chem. Eng. Fundam. 5 : 9, 1966.

WINCHESTER, J.F., Tilstone, W.J., Edwards, R.O., Gilchrist, T., and Kennedy, A.C. Haemoperfusion for enhanced drug elimination - a kinetic analysis in paracetamol poisoning. Trans. ASAIO. 20 : 358, 1974.

WINCHESTER, J.F., Apiliga, M.T., Mackay, J.M., and Kennedy, A.C. Haemodialysis with charcoal haemoperfusion. Proc. EDTA. 12 : 526, 1975.

WINCHESTER, J.F. Clinical application of haemoperfusion in uraemia. in Kenedi, et al. (Eds.), Artificial Organs, Macmillan Press, p. 188, 1977.

WINCHESTER, J.F., Gelfand, M.C., Knepshield, J.H., and Schreiner, G.E. Dialysis and haemoperfusion of poisons and drugs - up date. Trans. ASAIO. 23: 762. 1977.

WINEMAN, R.J. Status of the national co-operative dialysis study. Proc. 10th Annual Contractors Conference Artificial Kidney Program. NIAMDD, US Dept. Health Education & Welfare, p. 197, 1977.

WOLF, A.V., Remp, D.G., Kiley, J.E., Currie, G.D. Artificial Kidney Function: Kinetics of Haemodialysis. J. Clin. Invest. 30 : 1062, 1951.

WOLF, M.B., Watson, P.D., Barbour, B.H. Theoretical evaluation of patient-artificial kidney system using the Kiil dialyser. Math. Biosciences. 6 : 367, 1970.

YATZIDIS, H. A convenient haemoperfusion microapparatus over charcoal for the treatment of endogenous and exogenous intoxications. Proc. EDTA. 1 : 83, 1964.

YATZIDIS, H., Oreopoulous, D., Triantaphyllidis, D., Voudiclaris, S., et al. Treatment of severebarbiturate poisoning. Lancet 2 : 216, 1965.

YATZIDIS, H. Further experience with the charcoal artificial kidney. Abstr. 3rd Int. Cong. Neph. p. 299, 1966.

YATZIDIS, H., and Oreopoulous, D. Early clinical trials with sorbents. Kidney. Int. 10 (7) : 215, 1976.

YATZIDIS, H., Yulis, G., and Digenis, P. Haemocarboperfusion -haemodialysis treatment in terminal renal failure. Kidney Int. 10 (7): 312, 1976.

ZIEVE, L. Pathogenesis of hepatic coma. Ann. Review Med. 26. 143, 1975.

ZUTPHEN, van, P. The film adsorber - a new artificial organ to remove exogenous and endogenous poisons from blood. PhD. Thesis, Technical University, Eindhoven, 1975.

APPENDICES

APPENDIX 1

Continuity Equation for a Perfusion Column

The development of the continuity equation (Eq. 3.26) for the distributed description of a perfusion column is outlined in this Appendix. This equation is then normalized and in Appendix 2 it is solved for small times.

Consider the mass balance on a thin cross-sectional element in an ideal perfusion column.

(Rate of Solute in) - (Rate of Solute out) = (Rate of Solute Accumulation)

$$\text{i.e. } \varepsilon_b S U_i (c - (c + \delta c)) \delta t - \varepsilon_b S \left(D_a \left.\frac{\partial c}{\partial z}\right|_z - D_a \left.\frac{\partial c}{\partial z}\right|_{z+\delta z} \right) \delta t = S \delta z (\varepsilon_b \delta c + \rho_b \delta q) \qquad \text{EQ. A.1.1}$$

where
- ε_b = column void fraction
- S = cross-sectional area of column
- z = axial co-ordinate
- U_i = interstitial velocity
- D_a = axial dispersion coefficient
- ρ_b = bulk density of sorbent
- c = concentration of sorbate in fluid phase
- q = concentration of sorbate in sorbent phase

In the limit Equation A1.1 reduces to

$$\varepsilon_b \left(\frac{\partial c}{\partial t}\right)_z + \rho_b \left(\frac{\partial q}{\partial t}\right)_z + U_s \left(\frac{\partial c}{\partial z}\right)_t = \varepsilon_b D_a \left(\frac{\partial^2 c}{\partial z^2}\right)_t \qquad \text{EQ. A1.2}$$

where U_s = superficial velocity ($\equiv \varepsilon_b U_i$)

Normalized continuity equation

The following normalized variables are introduced

$$\theta = t/\bar{t} \; ; \; Z = z/L \; ; \; X = c/c_0 \; ; \; Y = q/q_0$$

where $\bar{t}$ = mean residence time ($= L/U_i$)

L = length of column

c_0 = inlet fluid phase concentration

q_0 = solid phase concentration in equilibrium with c

Substituting these variables Equation A1.2 becomes

$$\left(\frac{\partial X}{\partial \theta}\right)_Z + \left(\frac{\partial Y}{\partial \theta}\right)_Z + \left(\frac{\partial X}{\partial Z}\right)_\theta = \frac{1}{Pe_L}\left(\frac{\partial^2 X}{\partial Z^2}\right)_\theta \qquad \text{EQ. A1.3}$$

where $Pe_L = (U_i L / D_a)$

and $\Lambda = (\rho_b q_0 / c_0)$

APPENDIX 2

Initial Breakthrough in a Perfusion Column

The term describing the accumulation of sorbate in the solid phase in Equations A1.2 and A1.3 can be rewritten for small times, assuming that the fluid phase concentration adjacent to the sorbent is negligible, the external diffusion flux is driven by the bulk fluid phase concentration, c , alone, i.e.

$$\rho_b \left(\frac{\partial q}{\partial t}\right)_z = (k_e\, a_p (1 - \varepsilon_b))\, c \qquad \text{EQ. A2.1}$$

where k_e = external diffusion coefficient

a_p = specific external surface area of sorbent

Equation A2.2 is normalized to give

$$\frac{\Lambda}{\varepsilon_b}\left(\frac{\partial Y}{\partial \theta}\right)_z = \left(\frac{k_e\, A_p}{F}\right) X \qquad \text{EQ. A2.2}$$

where A_p = total surface area of sorbent

The term $(k_e\, A_p / F)$ is the number of external mass transfer units N_e. Hence Equation A1.3 becomes

$$\left(\frac{\partial X}{\partial \theta}\right)_Z + N_e X + \left(\frac{\partial X}{\partial Z}\right)_\theta = \frac{1}{Pe_L}\left(\frac{\partial^2 X}{\partial Z^2}\right)_\theta \qquad \text{EQ. A2.3}$$

for small times.

Initial breakthrough

Typical initial breakthrough are depicted in Figure A2.1

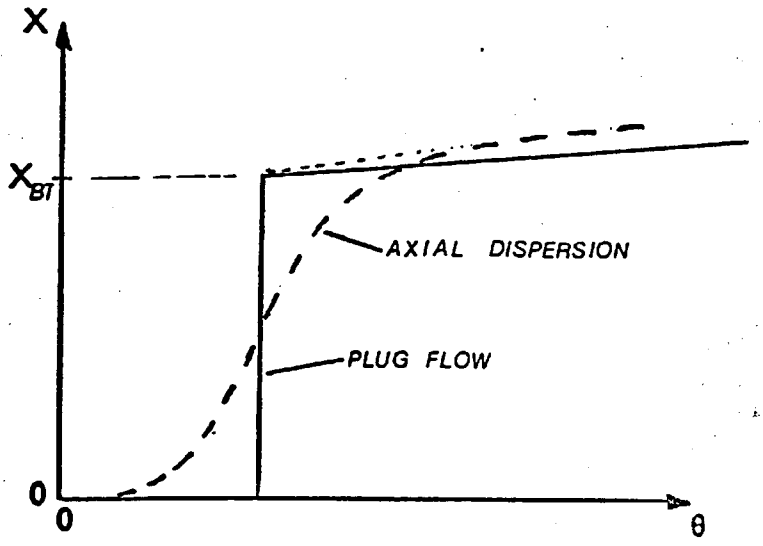

If the axial dispersion term is retained in Equation A2.3, then the solution for X is continuous with θ. With plug flow (no axial dispersion) there is a discontinuity at one mean residence time. The initial breakthrough is defined by X_{BT}, the normalized effluent concentration at one mean residence time. With axial dispersion this definition is modified such that X is the projection of the breakthrough back to one mean residence time (MRT). Assuming the slope after about two MRT's is small, then the breakthrough is roughly equal to X at this value θ.

Initial breakthrough with axial dispersion

Assuming the slope of the breakthrough curve is small at $\theta \simeq 2$, i.e. $\left(\frac{\partial X}{\partial \theta}\right)_Z \simeq 0$; Equation A2.3 reduces to

$$\frac{1}{Pe_L} \frac{d^2 X_{BT}}{d Z^2} - \frac{d X_{BT}}{d Z} + N_e X_{BT} = 0 \qquad \text{EQ. A2.4}$$

The solution of Equation A2.4 is of the form

$$X_{BT} = X_1 e^{m_1 Z} + X_2 e^{m_2 Z} \qquad \text{EQ. A2.5}$$

$$\text{where} \quad m_{1,2} = \frac{1 \pm \sqrt{1 + (4\,N_e / Pe_L)}}{(2 / Pe_L)}$$

Let m_2 be the positive root. For a positive m, Equation A2.5 is not bounded, yet phyically X_{BT} must be bounded; therefore X_2 is zero. From the initial conditions $X_1 = 1$, hence for axial dispersed plug flow,

$$X_{BT} = e^{-N'_e} \qquad \text{EQ. A2.6}$$

$$\text{where} \quad N'_e = \frac{Pe_L}{2} - \left(1 + 4\,\frac{N_e}{Pe_L}\right)^{1/2} - 1 \Big)$$

Initial breakthrough with no axial dispersion (i.e. plug flow)

With no axial dispersion, the initial breakthrough consists of a step increase in outlet concentration at one mean residence time. In order to solve Equation A2.3 a further change of time variability is necessary, i.e.

$$\theta' \equiv \theta - Z$$

From the definition of the partial derivative of a function of a function we have

$$\left(\frac{\partial X}{\partial Z}\right)_\theta = \left(\frac{\partial X}{\partial \theta'}\right)_Z + \left(\frac{\partial X}{\partial Z}\right)_{\theta'} \quad \text{and} \quad \left(\frac{\partial X}{\partial \theta}\right)_Z = \left(\frac{\partial X}{\partial \theta'}\right)_Z$$

$$\text{hence} \quad \left(\frac{\partial X}{\partial Z}\right)_\theta = -\left(\frac{\partial X}{\partial \theta}\right)_Z + \left(\frac{\partial X}{\partial Z}\right)_{\theta'}$$

Substitution into Equation A2.3 gives

$$\left(\frac{\partial X}{\partial Z}\right)_{\theta'} + N_e\,X = \frac{1}{Pe_L}\left(\frac{\partial X}{\partial Z}\right)_\theta \qquad \text{EQ. A2.7}$$

$$= 0 \text{ for plug flow}$$

Hence the breakthrough is defined by

$$\frac{d X_{BT}}{d Z} + N_e X_{BT} = 0 \qquad \text{Eq. A2.8}$$

The solution of Equation A2.8, with appropriate initial conditions is,

$$X_{BT} = e^{-N_e} \qquad \text{Eq. A2.9}$$

This result can also be obtained by taking the limit of Equation A2.6 as $Pe_L \rightarrow \infty$, i.e.

$$(1 + 4N_e/Pe_L)^{1/2} \simeq 1 + 2 N_e/Pe_L$$

$$\therefore \quad N_e' \rightarrow N_e \quad \text{as} \quad Pe \rightarrow \infty$$

APPENDIX 3

Computer Listings of Models

Computer listings for the batch equations, the external diffusion, the multiparameter mixing cell model, limited perfusion column model and the complete perfusion column model are listed on the subsequent pages. In most instances the symbolic names adopted for the computer implementation of the models are obvious. However, there are several exceptions. These are listed below.

$$\text{n DOT} = \frac{d\,n}{d\,t}$$

$$\text{FQ} = \psi_q$$

$$\text{NSS} = N_s$$

$$\text{NS} = \psi_q N_s$$

$$\text{NF} = N_e$$ (originally N_f, the number of fluid film mass transfer units)

```
      TITLE    BATCH KINETIC MODEL

*      SALICYLATE ADSORPTION ON SS610 CARBON

PARAMETER   A=3950.00, B=19.0
PARAMETER   DENSE=0.634
PARAMETER   DP=0.18

PARAMETER   D=5.6E-08
PARAMETER   KF=1.0E-03

PARAMETER   C0=0.9
PARAMETER   V=400, M=2.0

PARAMETER   Q0=0.0
PARAMETER   ERROR=1.0E-04
PARAMETER   QS0=1.0E-03

INITIAL
      R=1/(1+B*C0)
      FQ=1/(R**1.5+1.688*(1-R))
      COEFF1=FQ*60*D/(DP**2)
      AP=6.0/DP
      KF1=KF*AP/DENSE

DYNAMIC
      MV=M/V

      QSTAR=IMPL(QS0,ERROR,DUMIE)
      FQS=QSTAR/(A-B*QSTAR)
      DUMIE=SQRT(((2*Q+QS0)*KF1*(C-FQS)/COEFF1)+Q**2)
      QDOT=COEFF1*(QSTAR**2-Q**2)/(2*Q+QS0)
      Q=INTGRL(Q0,QDOT)
      CDOT=-MV*QDOT
      C=INTGRL(C0,CDOT)
      TIMEM=TIME/60.0

TERMINAL
      PRINT  C,TIMEM,Q,CDOT,MV

*       OUTPUT SEQUENCE TO ACCOUNT FOR SAMPLE VOLUME LOSS

      METHOD SIMP
      TIMER  FINTIM=300, PRDEL=10.0, DELT=1.0
      CONTINUE
PARAMETER  V=398
      TIMER  FINTIM=600, PRDEL=10, DELT=1.0
      CONTINUE
```

```
PARAMETER  V=396
     TIMER  FINTIM=1200, PRDEL=20, DELT=2.0
     CONTINUE
PARAMETER  V=394
     METHOD RKS
     TIMER  FINTIM=1800, PRDEL=20.0
     CONTINUE
PARAMETER  V=392
     TIMER  FINTIM=3000.0, PRDEL=60.0
     CONTINUE
PARAMETER  V=390
     TIMER  FINTIM=4500.0, PRDEL=60.0
     CONTINUE
PARAMETER  V=388
     TIMER  FINTIM=7200.0, PRDEL=60.0
     CONTINUE
PARAMETER  V=386
      TIMER  FINTIM=10800.0, PRDEL=120
     CONTINUE
PARAMETER  V=384
     TIMER  FINTIM=18000.0, PRDEL=120.0, DELT=10.0
     END
STOP
```

```
      TITLE  MULTIPARAMETER MIXING CELL MODEL

*        RUNS 22 & 23

/      DIMENSION C(50),CI(50),CDOT(50),S(50),SI(50),SDOT(50)

/      EQUIVALENCE (CE,C(1)),(CDOTE,CDOT(1)),(CIE,CI(1))
/     5 ,(SE,S(1)),(SDOTE,SDOT(1)),(SIE,SI(1))

INITIAL
PARAMETER  N=35
PARAMETER  ALPHA=0.88
PARAMETER  BETA=0.015
PARAMETER  TBAR=160.0
PARAMETER  F=1.70
PARAMETER  TOTALC=50000.0
PARAMETER  T1=0.0
PARAMETER  T2=0.5

      K=BETA*F
      VT=TBAR*F
      V1=VT/N
      V2=V1/ALPHA-V1

DYNAMIC
      CE=INTGRL(CIE,CDOTE,50)
      SE=INTGRL(SIE,SDOTE,50)
NOSORT

      C0=(STEP(T1)-STEP(T2))*TOTALC/(T2-T1)

      CDOT(1)=F*(C0-C(1))/V1-K*(C(1)-S(1))/V1
      SDOT(1)=K*(C(1)-S(1))/V2
      DO 2 I=2,50
      CDOT(I)=F*(C(I-1)-C(I))/V1-K*(C(I)-S(I))/V1
      SDOT(I)=K*(C(I)-S(I))/V2

      C35=C(35)

TERMINAL
      PRINT  C0,C35
      TIMER  FINTIM=500.0, PRDEL=10.0
      END
STOP
```

```
      TITLE  EXTERNAL DIFFUSION LIMITED COLUMN MODEL

*       STANDARD COLUMN VARIABLES

/      DIMENSION XDOT(50),XI(50),X(50),YDOT(50),YI(50)
/     3 ,Y(50),XSTAR(50)
/      EQUIVALENCE (XDOTE,XDOT(1)),(XIE,XI(1)),(XE,X(1))
/     4 ,(YDOTE,YDOT(1)),(YIE,YI(1)),(YE,Y(1))
/     9 , (YIE,YI(1)),(YE,Y(1))

PARAMETER   NF=0.5
PARAMETER   N=20
PARAMETER   R=0.1
PARAMETER   RATIO=1000.0
PARAMETER   VOL1=300000.0
PARAMETER   FLOW=200.0
PARAMETER   X0=1.0

      FIXED I

INITIAL
NOSORT
      DO 1 I=1,20
      YI(I)=0.0
      XI(I)=0.0

DYNAMIC
      XE=INTGRL(XIE,XDOTE,20)
      YE=INTGRL(YIE,YDOTE,20)

NOSORT

*      FIRST CELL

      XSTAR(1)=R*Y(1)/(1-(1-R)*Y(1))
      XDOT(1)=RATIO*(N*(X0-X(1))-NF*(X(1)-XSTAR(1)))
      YDOT(1)=NF*(X(1)-XSTAR(1))

*       REMAINING CELLS

      DO 2  I=2,20
      XSTAR(I)=R*Y(I)/(1-(1-R)*Y(I))
      XDOT(I)=RATIO*(N*(X(I-1)-X(I))-NF*(X(I)-XSTAR(I)))

      YDOT(I)=NF*(X(I)-XSTAR(I))

      X20=X(20)
      XDOT20=XDOT(20)
      Y20=Y(20)
      VOL=VOL1*TIME
```

```
      TIMEM=VOL/FLOW
      CL20=FLOW*(X0-X20)/X0

TERMINAL
      PRINT  TIMEM,CL20,X20,XDOT20,Y20
      METHOD SIMP
      TIMER  FINTIM=1.0, PRDEL=0.01, DELT=5.0E-05
      END
STOP
```

```
      TITLE  SINGLE PASS / RECIRCULATION COLUNM MODEL  20
CELLS

*       STANDARD COLUMN VALUES

*       COLUMN / RECIRCULATION PARAMETERS

PARAMETER  FLOW=200.0
PARAMETER  N=20
PARAMETER  NF=2.0
PARAMETER  NSS=0.5
PARAMETER  R=0.1
PARAMETER  RATIO=1000.0
PARAMETER  VOL1=300000.0
PARAMETER  CAP=0.0

*       COMPUTATIONAL AND INITIAL VALUES

PARAMETER  XS0=0.0
PARAMETER  Y0=0.0
PARAMETER  Y00=0.001
PARAMETER  ERROR=1.0E-05

INITIAL

      FQ=10(R**1.5+1.688*(1-R))
      NS=NSS*FQ
*       NSS IS N SUBSCRIPT S ; FQ IS FOR SPHERICAL PARTICLES


DYNAMIC

*       RECIRCULATION MASS BALANCE EQUATIONS

      X0DOT=CAP*(X40-X0)
      X0=INTGRL(1.0,X0DOT)

*       COLUMN CELL EQUATIONS

      XS1=IMPL(XS0,ERROR,DUME1)
      FXS1=XS1/(R+(1-R)*XS1)
      DUME1=X1-NS*(FXS1**2-Y1**2)/((2*Y1+Y00)*NF)
      YDOT1=NF*(X1-XS1)
      Y1=INTGRL(Y0,YDOT1)
      XDOT1=RATIO*(N*(X0-X1)-YDOT1)
      X1=INTGRL(0.0,XDOT1)

      XS2=IMPL(XS0,ERROR,DUME2)
```

```
FXS2=XS2/(R+(1-R)*XS2)
DUME2=X2-NS*(FXS2**2-Y2**2)/((2*Y2+Y00)*NF)
YDOT2=NF*(X2-XS2)
Y2=INTGRL(Y0,YDOT2)
XDOT2=RATIO*(N*(X1-X2)-YDOT2)
X2=INTGRL(0.0,XDOT2)

XS3=IMPL(XS0,ERROR,DUME3)
FXS3=XS3/(R+(1-R)*XS3)
DUME3=X3-NS*(FXS3**2-Y3**2)/((2*Y3+Y00)*NF)
YDOT3=NF*(X3-XS3)
Y3=INTGRL(Y0,YDOT3)
XDOT3=RATIO*(N*(X2-X3)-YDOT3)
X3=INTGRL(0.0,XDOT3)

XS4=IMPL(XS0,ERROR,DUME4)
FXS4=XS4/(R+(1-R)*XS4)
DUME4=X4-NS*(FXS4**2-Y4**2)/((2*Y4+Y00)*NF)
YDOT4=NF*(X4-XS4)
Y4=INTGRL(Y0,YDOT4)
XDOT4=RATIO*(N*(X3-X4)-YDOT4)
X4=INTGRL(0.0,XDOT4)

XS5=IMPL(XS0,ERROR,DUME5)
FXS5=XS5/(R+(1-R)*XS5)
DUME5=X5-NS*(FXS5**2-Y5**2)/((2*Y5+Y00)*NF)
YDOT5=NF*(X5-XS5)
Y5=INTGRL(Y0,YDOT5)
XDOT5=RATIO*(N*(X4-X5)-YDOT5)
X5=INTGRL(0.0,XDOT5)

XS6=IMPL(XS0,ERROR,DUME6)
FXS6=XS6/(R+(1-R)*XS6)
DUME6=X6-NS*(FXS6**2-Y6**2)/((2*Y6+Y00)*NF)
YDOT6=NF*(X6-XS6)
Y6=INTGRL(Y0,YDOT6)
XDOT6=RATIO*(N*(X5-X6)-YDOT6)
X6=INTGRL(0.0,XDOT6)

XS7=IMPL(XS0,ERROR,DUME7)
FXS7=XS7/(R+(1-R)*XS7)
DUME7=X7-NS*(FXS7**2-Y7**2)/((2*Y7+Y00)*NF)
YDOT7=NF*(X7-XS7)
Y7=INTGRL(Y0,YDOT7)
XDOT7=RATIO*(N*(X6-X7)-YDOT7)
X7=INTGRL(0.0,XDOT7)

XS8=IMPL(XS0,ERROR,DUME8)
```

```
FXS8=XS8/(R+(1-R)*XS8)
DUME8=X8-NS*(FXS8**2-Y8**2)/((2*Y8+Y00)*NF)
YDOT8=NF*(X8-XS8)
Y8=INTGRL(Y0,YDOT8)
XDOT8=RATIO*(N*(X7-X8)-YDOT8)
X8=INTGRL(0.0,XDOT8)

XS9=IMPL(XS0,ERROR,DUME9)
FXS9=XS9/(R+(1-R)*XS9)
DUME9=X9-NS*(FXS9**2-Y9**2)/((2*Y9+Y00)*NF)
YDOT9=NF*(X9-XS9)
Y9=INTGRL(Y0,YDOT9)
XDOT9=RATIO*(N*(X8-X9)-YDOT9)
X9=INTGRL(0.0,XDOT9)

XS10=IMPL(XS0,ERROR,DUME10)
FXS10=XS10/(R+(1-R)*XS10)
DUME10=X10-NS*(FXS10**2-Y10**2)/((2*Y10+Y00)*NF)
YDOT10=NF*(X10-XS10)
Y10=INTGRL(Y0,YDOT10)
XDOT10=RATIO*(N*(X9-X10)-YDOT10)
X10=INTGRL(0.0,XDOT10)

XS11=IMPL(XS0,ERROR,DUME11)
FXS11=XS11/(R+(1-R)*XS11)
DUME11=X11-NS*(FXS11**2-Y11**2)/((2*Y11+Y00)*NF)
YDOT11=NF*(X11-XS11)
Y11=INTGRL(Y0,YDOT11)
XDOT11=RATIO*(N*(X10-X11)-YDOT11)
X11=INTGRL(0.0,XDOT11)

XS12=IMPL(XS0,ERROR,DUME12)
FXS12=XS12/(R+(1-R)*XS12)
DUME12=X12-NS*(FXS12**2-Y12**2)/((2*Y12+Y00)*NF)
YDOT12=NF*(X12-XS12)
Y12=INTGRL(Y0,YDOT12)
XDOT12=RATIO*(N*(X11-X12)-YDOT12)
X12=INTGRL(0.0,XDOT12)

XS13=IMPL(XS0,ERROR,DUME13)
FXS13=XS13/(R+(1-R)*XS13)
DUME13=X13-NS*(FXS13**2-Y13**2)/((2*Y13+Y00)*NF)
YDOT13=NF*(X13-XS13)
Y13=INTGRL(Y0,YDOT13)
XDOT13=RATIO*(N*(X12-X13)-YDOT13)
X13=INTGRL(0.0,XDOT13)

XS14=IMPL(XS0,ERROR,DUME14)
```

```
FXS14=XS14/(R+(1-R)*XS14)
DUME14=X14-NS*(FXS14**2-Y14**2)/((2*Y14+Y00)*NF)
YDOT14=NF*(X14-XS14)
Y14=INTGRL(Y0,YDOT14)
XDOT14=RATIO*(N*(X13-X14)-YDOT14)
X14=INTGRL(0.0,XDOT14)

XS15=IMPL(XS0,ERROR,DUME15)
FXS15=XS15/(R+(1-R)*XS15)
DUME15=X15-NS*(FXS15**2-Y15**2)/((2*Y15+Y00)*NF)
YDOT15=NF*(X15-XS15)
Y15=INTGRL(Y0,YDOT15)
XDOT15=RATIO*(N*(X14-X15)-YDOT15)
X15=INTGRL(0.0,XDOT15)

XS16=IMPL(XS0,ERROR,DUME16)
FXS16=XS16/(R+(1-R)*XS16)
DUME16=X16-NS*(FXS16**2-Y16**2)/((2*Y16+Y00)*NF)
YDOT16=NF*(X16-XS16)
Y16=INTGRL(Y0,YDOT16)
XDOT16=RATIO*(N*(X15-X16)-YDOT16)
X16=INTGRL(0.0,XDOT16)

XS17=IMPL(XS0,ERROR,DUME17)
FXS17=XS17/(R+(1-R)*XS17)
DUME17=X17-NS*(FXS17**2-Y17**2)/((2*Y17+Y00)*NF)
YDOT17=NF*(X17-XS17)
Y17=INTGRL(Y0,YDOT17)
XDOT17=RATIO*(N*(X16-X17)-YDOT17)
X17=INTGRL(0.0,XDOT17)

XS18=IMPL(XS0,ERROR,DUME18)
FXS18=XS18/(R+(1-R)*XS18)
DUME18=X18-NS*(FXS18**2-Y18**2)/((2*Y18+Y00)*NF)
YDOT18=NF*(X18-XS18)
Y18=INTGRL(Y0,YDOT18)
XDOT18=RATIO*(N*(X17-X18)-YDOT18)
X18=INTGRL(0.0,XDOT18)

XS19=IMPL(XS0,ERROR,DUME19)
FXS19=XS19/(R+(1-R)*XS19)
DUME19=X19-NS*(FXS19**2-Y19**2)/((2*Y19+Y00)*NF)
YDOT19=NF*(X19-XS19)
Y19=INTGRL(Y0,YDOT19)
XDOT19=RATIO*(N*(X18-X19)-YDOT19)
X19=INTGRL(0.0,XDOT19)

XS20=IMPL(XS0,ERROR,DUME20)
```

```
      FXS20=XS20/(R+(1-R)*XS20)
      DUME20=X20-NS*(FXS20**2-Y20**2)/((2*Y20+Y00)*NF)
      YDOT20=NF*(X20-XS20)
      Y20=INTGRL(Y0,YDOT20)
      XDOT20=RATIO*(N*(X19-X20)-YDOT20)
      X20=INTGRL(0.0,XDOT20)

      VOL=VOL1*TIME
      TIMEM=VOL/FLOW
      CL20=FLOW*(X0-X20)/X0
TERMINAL
      PRINT  TIMEM,CL20,X20,X0,XDOT20,X1
      METHOD  SIMP
      TIMER  FINTIM=5.0E-03, PRDEL=1.0E-04, DELT=5.0E-05
      CONTINUE
      METHOD SIMP
      TIMER  FINTIM=1.0, PRDEL=5.0E-05, DELT=5.0E-05
      END
```

APPENDIX 4

Analytical Techniques

Solute	Measurement Technique
Creatinine	Technicon Acute-Analyser Clinical Method 11
Sodium Salicylate	Unicam Sp 800 UV Spectrophotometer Peak wavelength 296 millimicrons Max. Conc.$\frac{n}{-}$ 9 mg%
Sodium Phenobarbitone	Unicam SP 800 UV Spectrophotometer Peak wavelength 239 millimicrons Max. Conc.$\frac{n}{-}$ 7 mg%
Paracetamol	Unicam SP 800 UV Spectrophotometer Peak wavelength 243 millimicrons Max. Conc.$\frac{n}{-}$ 7 mg%

APPENDIX 5

Errors due to Measurement

The principal measurement errors are those associated with toxin concentrations. All concentrations, except creatinine, were measured on a Unicam SP 800 spectrophotometer. The probably error with the SP 800 was assumed to be ± 1 division on the output. This was estimated on the basis of the scatter in standards used for calibration. The spectrophotometer was calibrated on each occasion it was used. The dilution ratio was adjusted for each series of samples, such that the highest concentration corresponded to 0.8 or 0.9 of full scale on the output. Therefore, as there are 200 divisions full scale, the error in each set of samples is approximately 1% of the maximum concentration. The absolute errors for each type of solute and experiment are listed below. The approximate errors in measuring creatinine concentration on the Autoanalyser are included.

Toxin	Experiment and Max. Concentration (mg %)	Error (mg %)
Sodium Salicylate	Batch (90)	$\pm$ 1
	Column Inlet (90)	$\pm$ 1
	Column Inlet (50)	$\pm$ 0.5
	Column Outlet (0 - 10)	$\pm$ 0.2
Sodium Phenobarbitone	Batch (50)	$\pm$ 0.5
	Column Inlet (50)	$\pm$ 0.5
	Column Inlet (20)	$\pm$ 0.2
	Column Outlet (0 - 5)	$\pm$ 0.1
Paracetamol	Batch (50)	$\pm$ 0.5
Creatinine (Auto analyser)	Batch (20)	$\pm$ 0.1

Other sources of measurement error	
Batch Volume (V_b)	$\pm$ 1%
Mass of Sorbent (M)	1 %
Flow Rate (F)	$\pm$ 1%

Compound errors

When quantities such as clearance or quantity adsorbed are calculated, the errors associated with each variable in the formula is compounded, to give an overall error. This compounding of errors is expressed in its most general form below.

$$\text{If } X = F(n_1, n_2, n_3, \ldots\ldots n_i, \ldots) \qquad \text{A 5.1}$$

then the fractional expected error associated with the value of X is given by

$$\left(\frac{\Delta X}{X}\right) = \sum \left(\frac{\partial X}{\partial n}\right) \left(\frac{n}{X}\right) \left(\frac{\Delta n}{n}\right) \qquad \text{A 5.2}$$

For the examples in this thesis, the right hand side of A 5.2 reduces to the sum of the squares of the fractional errors associated with each quantity. Listed below are the compound errors associated with the data in the thesis.

Batch isotherms

The quantity adsorbed is given by

$$q_\infty = V_b (c_o - c_\infty) / M$$

The expected errors for q , in percentage terms, are listed below for adsorption for sodium salicylate and sodium phenobarbitone.

For salicylate, c_o - 90 mg%

c	80	70	60	50	40	30	20	10
Δ q (%)	20	10	6.7	5.1	4.1	3.5	3.0	2.7

Note, for BDH/salicylate isotherms, c_o = 100 mg%, hence the % error for each c is proportionately smaller.

For phenobarbitone, c_o = 50 mg%

c	40	30	20	10
Δ q(%)	10	5.1	3.5	2.7

The corresponding error bars are presented on the isotherms in the text.

Batch kinetic studies

The batch kinetic data is depicted as fractional or normalized concentrations. The errors in (c/c_o) are listed below.

For salicylate, c_o = 90 mg%

c/c_o	1.0	0.8	0.6	0.4	0.2
Δ c	0.016	0.014	0.013	0.012	0.011

For phenobarbitone, c_o = 50 mg%

c/c_o	1.0	0.8	0.6	0.4	0.2
Δ c	0.014	0.013	0.012	0.011	0.010

For all batch kinetics, the data points are 0.02 units in diameter, i.e. they indicate the minimum possible error range.

Single pass clearance

With the single pass clearance results (i.e. validation in Chapter 5) the fractional, rather than the absolute clearance is plotted, as the former is compatible with the output of the normalized model. The values of absolute clearance on the left hand axis are merely the fractional clearances multiplied by the nominal flow rate. The errors are approximately the same for salicylate and phenobarbitone, i.e.

Fractional Clearance	1.0	0.8	0.6	0.4	0.2
Error	0.017	0.016	0.015	0.014	0.013

The data points in all clearance curves have a diameter of 0.02, i.e. they span approximately 2/3 of the probable measurement error for each point.

Recirculation clearance (Haemocol)

With recirculation, the decline in the inlet concentration causes the concentration difference between inlet and outlet to fall rapidly. Hence the percentage error in the clearance increase rapidly. This is illustrated below.

Time	Salicylate, c_o = 50 mg%			Phenobarbitone, c_o = 20 mg%		
	c	Fractional Clearance	Error	c	Fractional Clearance	Error
0	50.5	0.99	0.017	20	0.99	0.022
5	43.5	0.88	0.018	16.8	0.81	0.015
10	37.5	0.89	0.026	14.2	0.76	0.030
20	24.0	0.87	0.034	10.0	0.79	0.043
40	11.5	0.84	0.070	5.4	0.79	0.079
60	5.5	0.85	0.150	2.9	0.62	0.144
80	2.5	0.76	0.32	2.4	0.71	0.18
100	1.0	0.7	0.80	1.0	0.5	0.41

APPENDIX 6

Equivalent Haemodialyser with Piecewise Linear Sorption Isotherm in Dialysate

When the dialysate of a conventional haemodialyser is replaced by a sorbent slurry, the sorption isotherm associated with that slurry is typically non-linear. In order to simplify the solution of the equations governing such a dialyser it is convenient to approximate the isotherm by a piecewise linear representation. This is illustrated below.

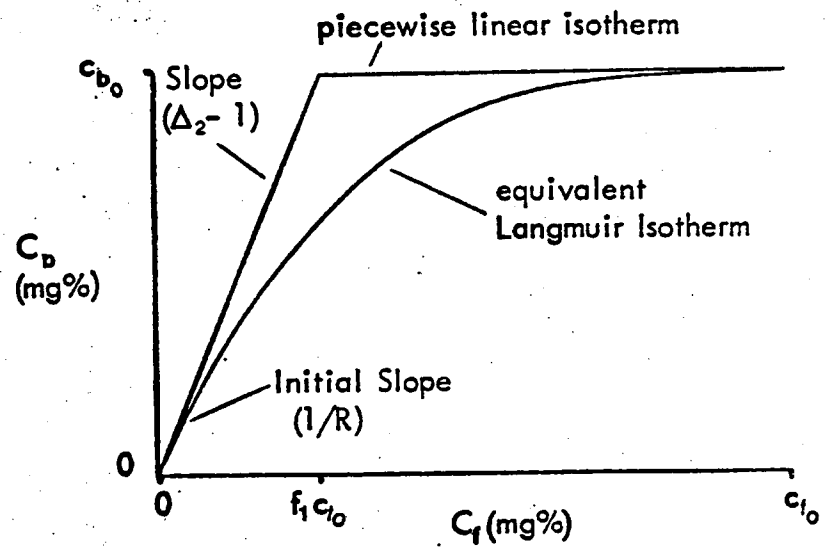

The following simplified analysis of a dialyser with a sorbent slurry, is based on the additional assumption that although the dialysate concentration is steadily increasing, a quasi-steady state exists, i.e. the boundary layers have developed and the dialysance is constant. This analysis is an extension of the results given in Figure 7.2.1

Clearance formula as the free dialysate concentration rises from zero to $f_1 c_0$ (i.e. section A)

Over this section the dialyser acts as if these were a sorbent with a linear isotherm in the dialysate. Hence from Figure 7.2.1 for single

pass operation ($V_b \rightarrow \infty$), we have

$$Cl_A = DI \; e^{-\frac{DI\,\Delta\, t}{V_d}} \quad . \qquad \text{EQ. A6.1}$$

where $DI^{\circ} = Q_b \left[\dfrac{e^{N_o(1-\Delta Z)} - 1}{e^{N_o(1-\Delta Z)} - \Delta Z} \right]$ for a counter current dialyser

$$\simeq Q_b \left[1 - e^{N_o} \right] \quad \text{for } \Delta \ll 1$$

Equation A6.1 can be normalized in a similar manner to that of the perfusion column equations in Chapter 3, i.e.

$$T = \frac{\text{rate of sorbate entering}}{\text{equilibrium capacity of sorbent slurry}} = \frac{Q_b\, c_o\, t}{V_d\, c_d}$$

where $c_{d_{i\,final}} = \dfrac{c_o}{\Delta_1} \cdot \left\{ f_1 \, (\Delta_2 - 1.) + 1 \right\}$

It is assumed that the total inlet blood concentration is c_o, free plus bound. Section A of the solution is operative until the free concentration in the dialysate equals a fraction, f_1, of the final (equilibrium) free concentration in the blood, i.e.

$$\frac{c_{d_i}}{\Delta_2} = f_1 \left(\frac{c_o}{\Delta_1} \right) \qquad \text{EQ. A6.2}$$

From the definitions of dialysance and clearance we have that,

$$\frac{Cl}{DI} = 1 - \frac{c_{d_i}}{c_o} \qquad \text{EQ. A6.3}$$

Substituting from Equations A6.1 and A6.2 into A6.3 gives

$$\frac{c_{d_1}}{c_o} = \frac{1}{\Delta} \cdot \left(1 - e^{-\frac{DI\,\Delta}{V_d}}\right) = \frac{f_1}{\Delta} \qquad \text{EQ. A6.4}$$

$$\text{or} \quad \left(\frac{Dl\ \Delta}{V_d}\ t\right)_A = \ln\left(\frac{1}{1 - f_1}\right) \qquad \text{EQ. A6.5}$$

at the end of Section A.

Substitution of Equation A6.5 into the definition of the throughput parameter T gives

$$\left(\frac{Dl\ \Delta\ t}{V_d}\right)_A = \frac{Dl\ (f_1\ (\Delta_2 - 1) + 1)\ T}{\Delta_2}$$

or for $\Delta_1 \gg 1$ and $\Delta_2 \gg 1$,

$$\left(\frac{Dl\ \Delta\ t}{V_d}\right)_A = (1 - e^{N_o})\ f_1\ T \qquad \text{EQ. A6.6}$$

If the piece wise linear isotherm is normalized with c_{f_0} and c_{b_0} equal to 1, then $1/f_1$ equals the slope of the isotherm over Section A. The initial slope of a continuous Langmuir type isotherm is $1/R$, hence it is convenient to let $f_1 = R$.

Hence Equation A6.6 plus A6.1 reduce to Equation 6.1 in Chapter 6, i.e.

$$Cl_A = Q_b\ (1 - e^{-N_o})\ e^{-(1 - e^{N_o})RT} \qquad \text{EQ. 6.1}$$

Clearance formula as the free dialysate concentration rises from $f_1\ c_{f_0}$ to c_{f_0} (i.e. section B)

After the free dialysate concentration reaches $f_1\ c_{f_0}$, the sorbent in the dialysate is saturated. Hence the free concentration rises rapidly in Section B. Using the appropriate initial conditions the clearance in Section B is given by

$$Cl_B = (1 - f_1)\, Dl_B\, e^{-\frac{Dl\,\Delta_1}{V_d}(t-\tau)} \qquad \text{EQ. A6.7}$$

where $$Dl_B = Q_b \left[\frac{e^{N_0(1-\Delta_1 Z)} - 1}{e^{N_0(1-\Delta_1 Z)} - \Delta Z} \right]$$

and $$\tau = \frac{V_d}{Dl\,\Delta} \ln\left(\frac{1}{1-f_1}\right)$$

Although Equation A6.7 can be normalized using T it is more convenient to use it with t as the dependent variable.

A typical clearance curve (Section A plus Section B) for a haemodialyser, with a sorbent slurry instead of conventional dialysate is shown below.

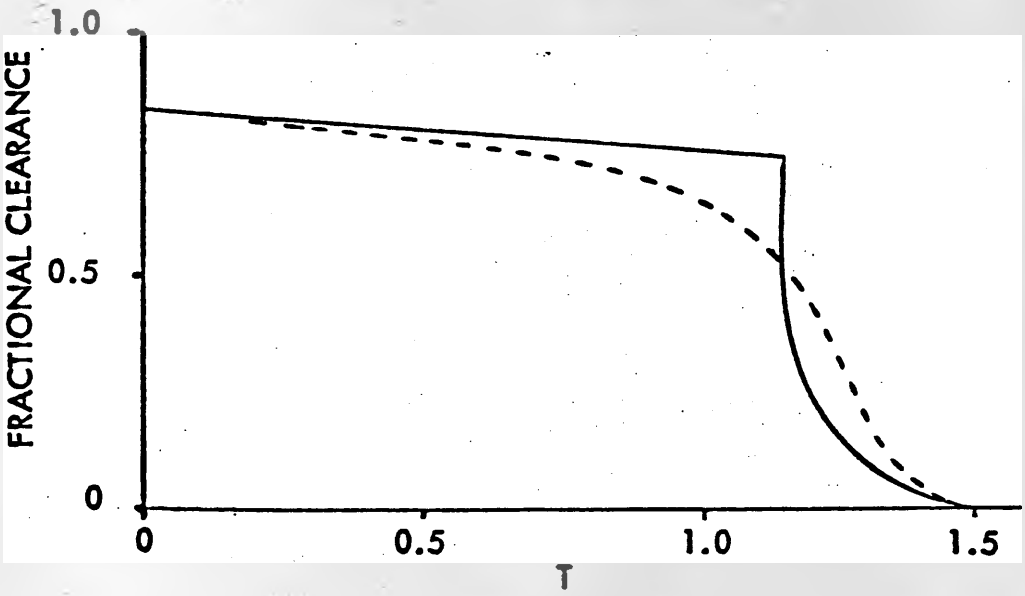

APPENDIX 7

List of Symbols

a	geometric constant in Eqn. 3.9 to 3.11
a_p	specific external area (cm^2/cm^3)
A	constant in Langmuir equation (ml/gm)
A_p	total external area of particles (cm^2)
B	constant in Langmuir isotherm (ml/mg)
c	fluid phase concentration (mg/ml)
CAP	(Mq_o/Vc_o) - capacity ratio in recirculation expt. (-)
Cl	clearance (ml/min)
d_p	particle diameter (cm)
Dl	dialysance (ml/min)
D_a	axial dispersion coefficient(cm^2/sec)
D_l	diffusivity of sorbate in solvent (cm^2/sec)
D_p	pore diffusivity (cm^2/sec)
D_{pore}	apparent pore diffusivity $(= \varepsilon_b D_p)$ (cm^2/sec)
D_s	solid diffusivity (cm^2/sec)
F	flow rate (ml/min)
k_e	total external mass transfer coefficient (cm/sec)
k_f	fluid film mass transfer coefficient (cm/sec)
k_l	empirical constant in LDF equation (-)
k_m	membrane mass transfer coefficient (cm/sec)
K	ion exchange selectivity coefficient
n	number of cells in mixing cell model (-)
N_e	$\left(\frac{k_e A_p}{F}\right)$ - number of external mass transfer units (-)
N_e'	(Eqn. 3.29) - apparent no. of external mass transfer units (-)
N_s	$\left(\frac{60\, D_s}{d_p^2}\right)\left(\frac{n\, v\Lambda}{F}\right)$ - number of intraparticle mass transfer units (-)
Pe_l	$\left(\frac{U_l L}{D_a}\right)$ - Peclet No. (rel. length of column)

q solid phase (adsorbed) conc. $\underline{n}$ (mg/gm)

Q_b blood flow rate (ml/min)

r_p radius of particle

R $(1/(1 + B\, c_o)$ - isotherm shape factor (-)

Re $\left(\frac{\rho U_s\, d_p}{\mu}\right)$ - Reynold No. (-)

RATIO $\left(\frac{\Lambda}{\varepsilon}\right)$ - ratio of capacity to MRT of column (-)

Sc $\left(\frac{\mu}{\rho D_l}\right)$ - Schmidt No. (-)

t time (sec)

$\bar{t}$ mean residence time (MRT) (Figure 3.6.1)

T $\left(\frac{F}{n\, v\Lambda}\right) t$ - throughput parameter (-)

U_s superficial velocity (cm/sec)

U_i interstitial $(= U_s / \varepsilon)$ (cm/sec)

v total volume in column (ml)

V_b volume in batch experiment (ml)

X normalized fluid phase conc. $\underline{n}$ (-)

X_{BT} normalized breakthrough conc. $\underline{n}$ (-)

Y normalized solid phase conc. $\underline{n}$ (-)

$\bar{z}$ normalized axial co-ordinate in column

z axial co-ordinate in column (cm)

β exponent on Freundlich isotherm (-)

Δ_1 binding ratio in blood $(= c_{b_{total}} / c_{b_{free}})$ (-)

Δ_2 binding ratio in dialysate $(= c_{d_{total}} / c_{d_{free}})$ (-)

Δ (Δ_1 / Δ_2)

$\Delta\mu$ differential mean of normalized c-curve (Figure 3.6.1)

$\Delta\sigma^2$ differential variance of normalized c-curve (Figure 3.6.1)

ε porosity (b - in bed, p - in particle) (-)

η coefficient in Freundlich isotherm (mg/gm)

μ viscosity (gm/cm sec)

or fraction water in blood (-)

or mean of normalized c-curve (Figure 3.6.1)

Λ	($\rho_b \, q_o / c_o$) - capacity ratio (-)
ρ	density (b - bed, p - particle) (mg/ml)
σ	variance of normalized c-curve (Figure 3.6.1)
ψ	empirical factor in driving force expressions (q - quadratic- 1 - linear)
α	volume ratio in multiparameter mixing cell model (Figure 3.6.4)
β	cross flow ratio in multiparameter mixing cell model (Figure 3.6.4)
	or exponent in Freundlich isotherm